Final Report

Determination of the Rate of Formation of Hydroceramic Waste Forms made with INEEL Calcined Wastes

Contract # DE-FG07-98ID13649

01 August 1998 through 31 July 2001

Submitted by

Barry E. Scheetz and Johnson Olanrewaju

Room 107

Materials Research Laboratory

Materials Research Institute

The Pennsylvania State University

University Park, PA 16802

15 October 2001

Executive Summary

A "hydroceramic" nuclear waste form, developed especially to address the immobilization of the reprocessing wastes from the Idaho National Engineering and Environmental Laboratory, has been demonstrated to possess superior chemical and mechanincal properties. Furthermore, the processing requirements of hydroceramic waste forms are simple, less costly and offer greater safety to INEEL personnel than other waste form preparation systems.

The objective of this research was two fold. The initial phase of the study was to systematically survey the suitability of readily available pozzolanic additions as raw materials for hydroceramic formulations in order to identify a source material that would be compatible with the established processing requirements for the waste form i.e., no excessive water demand, proper mineralogical composition of the waste form, low leachability, waste loadings greater than 20 weight percent calcine and also readily available to INEEL in large quantities once the pozzolan(s) selection was made. Pozzolanic materials are normally finely divided substances that contain either glassy or crystalline sources of silica that are chemically reactive enough to combine with lime and water at room temperature to form cementitious material. The primary objective of the research program was to establish the final processing parameters for the preparation of hydroceramic waste forms form INEEL wastes i.e., the rate at which hydroceramic is formed, the phases that formed and the optimum temperature needed to minimize leachability.

A total of 20 pozzolanic materials were surveyed. These included a number of different fly ash sample, natural and thermally altered clays, reactive aluminas and even finely ground bottle glass. The survey resulted in the selection of a natural, thermally altered clay (metakaolinite) that has found extensive use in the manufacture of blended Portland cement and currently mined in Troy Idaho.

A "host" matix formulation was initially developed using Troy metakaolinite and all processing parameters and chemical and mineralogical characterization was conducted on these samples. Once developed, the host matrix was used to subsequently prepare waste forms based on fluorinel and zirconia simulated calcines supplied by INEEL. A waste loading study was conducted in order to determine the maximum loading that could be sustained and still exibit the leaching characteristics and mechanical properties of the laboratory specimens. The "host" matrix samples and the two waste forms were processed at 75, 85, 95, 125, 150, 175 and 200°C at 100% relative humidity for times often exceeding 500 hours. Two sets of mineralogy were observed for the "host" samples and "waste loaded" samples. The "host" samples crystallized upon hydration to a zeolite calssified as Type A in the temperature range of 75 to 150°C and to another zeolite classifed as NaP1 from 175 to 200°C. Both sample sets contained minor amount of quartz derived from the meta-kaolin used as the pozzolan. In the waste form specimens, a mixture of predominantly Type A zeolite and minor hydroxysodalite were observed between 75 and 95°C. These gradually transformed into a mixture of hydroxysodalite with minor

Type A zeolite between 125 and 150°C which in turn transformed to hydroxysodalite above 175-200°C. In all samples, minor to trace amounts of quartz from the meta-kaolin were detected.

The waste loading study optimized the hydroceramic waste form at 30% by weight for both fluorinel and zirconia waste calcines.

The hydration rate studies conducted as a function of time and temperature determined that both the "host" matrix formulation and the fluorinel and zirconia waste loaded formulations followed a first-order kinetic reaction that can be summarized as follows:

Waste Form	**Temperature range**	**Crystalline form**	**Rate constant**	**Activation energy**
Host hydroceramic	75-150 ^{o}C	Type A zeolite	-	16.10 kJ/mol
	175-200 ^{o}C	NaP1	-	13.03 kJ/mol
30wt% fluorinel waste form	75-95 ^{o}C	Type A zeolite	-	49.57 kJ/mol
	125 ^{o}C	Type A zeolite + hydroxysodalite	5.5×10^{-4}/s	-
	150 ^{o}C	Type A zeolite + hydroxysodalite	7.8×10^{-4}/s	-
	175-200 ^{o}C	Hydroxysodalite	-	6.16 kJ/mol
30wt% zirconia waste form	75-95 ^{o}C	Type A zeolite	-	28.642 kJ/mol
	125 ^{o}C	Type A zeolite + hydroxysodalite	5×10^{-4}/s	-
	150 ^{o}C	Type A zeolite + hydroxysodalite	9.1×10^{-4}/s	-
	175-200 ^{o}C	Hydroxysodalite	-	12.081 kJ/mol

From the data collected in this study, it is recommended that a processing regiment be developed that utilizes the addition of calcined Troy clay with a waste loading of 30% by weight and processed at 200°C for 8 to 10 hours.

ABSTRACT

The formulation, synthesis, characterization and hydration kinetics of hydroceramic waste forms designed as potential hosts for exisiting INEEL calcine high-level wastes have been established as functions of temperature and processing time. Initial experimentations were conducted with several aluminosilicate pozzolanic materials, ranging from fly ash obtained from various power generating coal and other combustion industries to reactive alumina, natural clays and ground bottled glass powders. The final selection criteria were based on the ease of processing, excellent physical properties and chemical durability (low-leaching) determined from the PCT test produced in hydroceramic. The formulation contains vermiculite, $Sr(NO_3)_2$, CsCl, NaOH, thermally altered (calcined) natural clay and INEEL simulated calcine high-level nuclear wastes and 30 weight percent of fluorinel blend calcine and zirconia calcine. Syntheses were carried out at 75-200°C at autogeneous water pressure (100% relative humidity) at various time intervals. The resulting monolithic compact products were hard and resisted breaking when dropped from a 5 ft height. Hydroceramic host mixed with fluorinel blend calcine and processed at 75°C crumbled into rice hull-size grains or developed scaly flakes. However, the samples equally possessed the same chemical durability as their unbroken counterparts.

Phase identification by XRD revealed that hydroceramic host crystallized type A zeolite at 75-150°C and NaP1 at 175-200°C in addition to the presence of quartz phase originating from the clay reactant. Hydroceramic host mixed with either fluorinel blend calcine or zirconia calcine crystallized type A zeolite at 75-95°C,

formed a mixture of type A zeolite and hydroxysodalite at 125-150°C and hydroxysodalite at 175-200°C. Quartz, calcium fluoride and zirconia phases from the clay reactant and the two calcine wastes were also detected

The PCT test solution conductivity, pH and analytical concentration measured as a function of time decrease exponentially. In some cases nitrate, sulfate, chloride and fluoride ion concentrations increased with time and processing temperature with respect to the reference sample. The increasing concentration of these ions was due to the lack of formation of crystalline phases that can incorporate them in their structures, especially cancrinite. Another plausible explanations for their increase was due to the continuous withdrawal of cations with time, for example sodium to form zeolites, thereby increase their concentrations.

Hydration rates of the host and the host waste forms as a function of temperature followed a first-order reaction kinetics. The activation energy of type A zeolite crystallization in hydroceramic host at 75-150°C was calculated to be 16.10 kJ/mol and the formation of the NaP1 at 175-200°C was 13.03 kJ/mol. Type A zeolite crystallization in hydroceramic host mixed with 30 weight percent of fluorinel blend calcine was 49.57 kJ/mol; the rate constants of type A zeolite and hydroxysodalite formation at 125°C and 150°C sample were 5.5×10^{-4}/s and 7.8×10^{-4}/s; and the calculated activation energy of hydroxysodalite formation at 175-200°C was 6.16 kJ/mol. Hydroceramic-zirconia calcined waste forms processed at 75-95°C crystallized type A zeolite with an estimated activation energy of 28.642 kJ/mol.

Traces of hydroxysodalite was detected in the 95°C samples. The 125°C and 150°C crystallized mixed phases of type A zeolite and hydroxysodalite with rate constants of $5x10^{-4}$/s and $9.1x10^{-4}$/s, respectively. The activation energy of the 175-200°C samples crystallized only hydroxysodalite with an activation energy of 12.081 kJ/mol.

Hydration reaction was completed in hydroceramic host waste form at 6-8 hours of processing time at 200°C and 100% relative humidity. From the combined characterization results and chemical analysis data, the recommended processing temperature and time for the host mixed with 30 weight percent simulated fluorinel and zirconia calcines are 200°C at 8-10 hours processing time and 100% relative humidity.

TABLE OF CONTENTS

LIST OF FIGURES ..... **xi**

LIST OF TABLES ..... **xx**

ACKNOWLEDGEMENTS ..... **xxiii**

CHAPTER I INTRODUCTION AND LITERATURE REVIEW **1**

1.0 Introduction 2
1.1 Zeolites 4
1.1.1 Introduction 4
1.1.2 Composition 5
1.1.3 Structure 6
1.1.3.1 Zeolites 6
1.1.3.2 Feldsparthoids 9
1.1.3.3 Phases Found in this Study 9

1.2 Research Objective 11

1.3 Literature Review: Waste Form Description 11
1.3.1 Cement 12
1.3.2 Composition of Cement Waste Forms 13
1.3.3 Limitations of Cementitious Waste Forms 16

1.4 FUETAP Concretes 16
1.4.1 Limitations of FUETAP Concretes 20

1.5 Alkali-Activated Cements 21

1.6 Hydroceramic Host Waste Forms 24

1.6.1 Introduction 24
1.6.1.1 Fly Ash 25
1.6.1.2 Blast Furnace Slag 28
1.6.1.3 Silica 29
1.6.1.4 NaturalAluminosilicate Pozzolans 29
1.6.1.5 Reactive Alumina Pozzolans 31

1.7 Nature of the INEEL Calcined High-Level Radioactive Wastes 35
1.7.1 Uniqueness of the INEEL Radioactive Wastes 40

1.8 Research to Date in Hydroceramic 41
1.8.1 Preliminary Work 42
1.8.2 Fly Ash Pozzolan Experiments 43
1.8.3 Behavior of the Simulated INEEL Waste in Hydroceramic Prepared with Various Pozzolanic Media 49
1.8.4 Experiments with Simulated Zirconia Calcined Waste 49
1.8.5 Pozzolan Substitution of Alumina Experiments .. 52
1.8.6 Fluorinel Blend Calcined Experiments 53
1.8.7 Pozzolanic Study: Ground Bottle Glass Experiments 55
1.8.8 Fluorinel Blend Calcine Experiments with NaOH and Na_2S 57
1.8.9 Additional Pozzolan Experiments 59

1.9 Summary 65

CHAPTER II EXPERIMENTAL PROCEDURES 69

2.0 Introduction 70
2.1 Materials 70
2.1.1 Troy Clay: Pozzolanic Matrix 70
2.1.2 Vermiculite: Cesium Getter 74
2.1.3 Chemicals 75
2.1.4 Simulated Waste from Fluidized Bed 75

2.2 Sample Preparation 76
2.2.1 Stoichiometry Calculations of Hydroceramic Components 76
2.2.2 Bulk Waste Form Calculations 80
2.2.3 Paste Preparation 80

2.3 Hydrothermal Processing 83

2.4 Characterization 85
2.4.1 Specimen Preparation for Characterization 86
2.4.2 X-ray Diffraction 86
2.4.3 SEM 87
2.4.4 Product Consistency Test (PCT) 87
2.4.5 Bulk Chemical Analysis 88

CHAPTER III RESULTS OF SYNTHESIS, CHARACTERIZATION AND KINETICS OF HYDROCERAMIC HOST 91

3.0 Introduction 92
3.1 Results 93
3.1.1 Results of Conductivity and pH Measurements... 93
3.1.2 Xray Results 101
3.1.3 Microstructural Analysis with SEM 111

3.2 Chemical Analysis and Estimation of Sodium Concentrations 114

3.3 Kinetic Results of Hydroceramic Host Waste Form..... 120
3.3.1 Kinetic Model 120
3.3.2 Temperature Dependence of Rate Constants 121
3.3.3 Comparison of Hydroceramic Host Kinetics Results with Literature Data..... 124

3.4 General Theory of Crystal Growth and Dissolution..... 126

3.5 Mechanisms of Zeolite Transformation 127

3.6 Mechanisms of Hydroceramic Formation 130

3.7 Evaluation of Process Variables 132
3.7.1 Effects of Precuring Sample on Hydroceramic Synthesis 132
3.7.2 Stability of the Crystalline Phases in Hydroceramic Waste Form..... 134
3.7.3 Effects of Varying Reactants 136
3.7.4 Effect of Water 136

3.8 Recommendations 140

CHAPTER IV RESULTS OF SYNTHESIS, CHARACTERIZATION AND KINETICS OF HYDROCERAMIC HOST MIXED WITH 30 WEIGHT PERCENT SOLID OF ZIRCONIA SIMULATED CALCINED RADIOCTIVE WASTE 142

4.0 Introduction 143
4.1 Results 144
4.1.1 Conductivity and pH Measurements 144
4.1.2 Chemical Analysis 152
4.1.2.1 Chromium Results 152

4.1.3 Anions 154
4.1.3.1 Results of Nitrate and Sulfate 154
4.1.3.2 Results of Fluoride and Chloride..... 155

4.1.4 Results of Surrogate Strontium and Cesium Radionuclides..... 157

4.1.5 XRD Results..... 158

4.2 Hydration Kinetics..... 166

4.3 SEM..... 176

4.4 Evaluation of Process Variables..... 179
4.4.1 Effect of Water 179
4.4.2 PCT Test Residues..... 181

4.5 Recommendations 181

CHAPTER V RESULTS OF SYNTHESIS, CHARACTERIZATION AND KINETICS OF HYDROCERAMIC HOST MIXED WITH 30 WEIGHT PERCENT SOLID OF FLUORINEL BLEND SIMULATED CALCINED RADIOCTIVE WASTE..... 186

5.0 Introduction..... 187

5.1 Results 187
5.1.1 Conductivity and pH Measurements..... 187
5.1.2 Chemical Analysis 188
5.1.2.1 Chromium Results..... 188
5.1.3 Anions 197
5.1.3.1 Nitrate and Sulfate 197
5.1.3.2 Fluoride and Chloride..... 198

5.1.4 Surrogate Strontium and Cesium Radionuclides . 200

5.1.5 XRD Results..... 201

5.2 Interpretation of Kinetic Data as a Function of Temperature 201

5.3 Evaluation of the Effect of Water on the Hydration of the Host Mixed with Simulated Fluorinel Blend Calcine Waste..... 209
5.3.1 Effect of Water on the Synthesis of Host-Waste Form ... 219
5.3.2 PCT Test Residues 219

5.4 Recommendations..... 221

CHAPTER VI SUMMARY, CONCLUSION AND FUTRE WORK..... 225

6.0 Summary..... 226

6.1 Conclusion 232

6.2 Suggestion for Future Work 235

REFERENCES 237

APPENDIX A QBASIC Computer Program Codes **..... 251**

APPENDIX B Derivation of Equation 3.1 used to calculate rate constants for hydroceramic waste forms. **..... 260**

APPENDIX C Elemental Analysis of the PCT Test Solutions Obtained from Hydroceramic Host Mixed with 30 Weight Percent of Simulated Zirconia Calcined Waste. **..... 263**

APPENDIX D Elemental Analysis of the PCT Test Solutions Obtained from Hydroceramic Host Mixed with 30 Weight Percent of Simulated Fluorinel Blend Calcined Waste. **..... 271**

APPENDIX E Bibliography of Vitrifiable, Hydroceramic Chemically Bonded Ceramic Waste Forms. **..... 279**

LIST OF FIGURES

Figure 2.1. XRD of the three different strata, white, brown and yellow found in the Troy Clay. K = Kaolinite ($Si_2Al_2O_5(OH)_4$) and Q = quartz (SiO_2, 46-1045) as the two major crystalline phases. Similarity in the peak positions in the spectra patterns attested to the lack of impurity in the clay 72

Figure 2.2. XRD pattern of calcined Troy Clay (dehydroxylated Metakaolinite) showing Q = quartz (SiO_2, 46-1045) and M = mullite as the only persistent crystalline phases. The broad diffraction maxima between 15 and 40° 2? is an indication of the amorphous phase 73

Figure 2.3. X-ray diffraction pattern of zirconia calcined simulated waste showing CA = calcium aluminum oxide ($CaAl_4O_7$, 07-0082), F = calcium fluoride (CaF_2, 35-0816) and Z = zirconia (ZrO_2, 50-1089) as the major crystalline phases present in the simulated waste 77

Figure 2.4. X-ray diffraction pattern of simulated fluorinel blend calcined showing M = mullite ($Al_{2.35}Si_{0.84}O_{4.82}$, 73-1253), CA = calcium aluminum ($CaAl_4O_7$, 07-0082), F = calcium fluoride (CaF_2, 35-0816) and Z = zirconia oxide (ZrO_2, 50-1089) as the major crystalline phases present in the simulated waste..... 78

Figure 2.5. Disassembled hydrothermal Parr bomb (Parr Instrument, IL, USA) used in the hydrothermal syntheses of hydroceramic waste forms 84

Figure 3.1. Conductivity-pH-time plot of hydroceramic host processed at 75°C 94

Figure 3.2. Conductivity-pH-time plot of hydroceramic host processed at 85°C 95

Figure 3.3. Conductivity-pH-time plot of hydroceramic host processed at 95°C 96

Figure 3.4. Conductivity-pH-time plot of hydroceramic host processed at 125°C..... 97

Figure 3.5. Conductivity-pH-time plot of hydroceramic host processed at 150°C..... 98

Figure 3.6. Conductivity-pH-time plot of hydroceramic host processed at 175°C..... 99

Figure 3.7. Conductivity-pH-time plot of hydroceramic host processed at 200°C..... 100

Figure 3.8. Representative x-ray diffraction patterns of hydroceramic host waste form processed at 75-150°C at various times. Letter Q represents quartz phase two-major peaks and the remaining unmarked peaks belong to the type A zeolite..... 102

Figure 3.9. Representative x-ray diffraction patterns of hydroceramic host waste form processed at 175-200°C at various times. Letter Q represents quartz phase two-major peaks and the remaining unmarked peaks belong to the type Na-P1 zeolite..... 103

Figure 3.10. Crystallization of type A zeolite in hydroceramic waste form at 75°C as a function of time. Intensity versus time of the most intense peak located at (hkl, 200) indicates the extent of crystallization as determined by x-ray powder method 104

Figure 3.11. Crystallization of type A zeolite in hydroceramic waste form at 85°C as a function of time. Intensity versus time of the most intense peak located at (hkl, 200) indicates the extent of crystallization as determined by x-ray powder method 105

Figure 3.12. Crystallization of type A zeolite in hydroceramic waste form at 95°C as a function of time. Intensity versus time of the most intense peak located at (hkl, 200) indicates the extent of crystallization as determined by x-ray powder method 106

Figure 3.13. Crystallization of type A zeolite in hydroceramic waste form at 125°C as a function of time. Intensity versus time of the most intense peak located at (hkl, 200) indicates the extent of crystallization as determined by x-ray powder method 107

Figure 3.14. Crystallization of type A zeolite in hydroceramic waste form at 150°C as a function of time. Intensity versus time of the most intense peak located at (hkl, 200) indicates the extent of crystallization as determined by x-ray powder method 108

Figure 3.15. Crystallization of type Na-P1 zeolite in hydroceramic waste form at 175°C as a function of time. Intensity versus time of the most intense peak located at (hkl, 3 0 1/3) indicates the extent of crystallization as determined by x-ray powder method 109

Figure 3.16. Crystallization of type Na-P1 zeolite in hydroceramic waste form at 200°C as a function of time. Intensity versus time of the most intense peak located at (hkl, 3 0 1/3) indicates the extent of crystallization as determined by x-ray powder method 110

Figure 3.17 SEM euhedra cubes of type A zeolite formed in hydroceramic host synthesized at 95°C for 480 hours 112

Figure 3.18. The SEM micrograph of NaP1 zeolite formed in hydroceramic host synthesized at 200°C for 60 hours 113

Figure 3.19 Concentration-conductivity curve of KCl standard solutions..... 116

Figure 3.20. Sodium concentration-time of hydroceramic host waste forms hydrothermally processed at 75-95°C at various time intervals 118

Figure 3.21. Sodium concentration-time of hydroceramic host waste forms hydrothermally processed at 125-200°C at various time intervals..... 119

Figure 3.22. Linear plot of the rate constant calculation of the hydroceramic host synthesized at 75-150°C and at various reaction times 123

Figure 3.23. Concentration-time plot of hydroceramic. Comparison between uncured and precured at 90°C for 24 hours of hydroceramic samples synthesized at 200°C at various times 133

Figure 3.24. pH-time plot of hydroceramic host waste form. Comparison between uncured and precured at 90°C for 24 hours of hydroceramic samples synthesized at 200°C at various times 135

Figure 3.25. X-ray diffraction patterns of vermiculite-based hydroceramic host waste form processed at 125°C for 64 hours. In the legend letter codes, C = cesium, M = metakolinite, N = sodium hydroxide, S = strontium and V = vermiculite. Letter Q represents quartz phase two-major peaks and the remaining unmarked peaks belong to the type A zeolite..... 137

Figure 3.26. X-ray diffraction patterns of nonvermiculite-based hydroceramic host waste form processed at 125°C for 64 hours. In the legend letter codes, C = cesium, M = metakolinite and N = sodium hydroxide. Letter Q represents quartz phase two-major peaks and the remaining unmarked peaks belong to the type A zeolite..... 138

Figure 3.27. X-ray diffraction patterns of hydroceramic host waste form processed at 125°C for 120 hours. In the legend letter codes, X = factor representing the quantity of extra distilled water added to sample. Letter Q represents quartz phase two-major peaks and the remaining unmarked peaks belong to the type A zeolite..... 141

Figure 4.1. Conductivity-pH-time plot of hydroceramic host mixed with 30 weight percent of zirconia calcined simulated radioactive waste and hydrothermally autoclaved at 75°C as a function processing time 145

Figure 4.2. Conductivity-pH-time plot of hydroceramic host mixed with 30 weight percent of zirconia calcined simulated radioactive waste and hydrothermally autoclaved at 85°C as a function processing time 146

Figure 4.3. Conductivity-pH-time plot of hydroceramic host mixed with 30 weight percent of zirconia calcined simulated radioactive waste and hydrothermally autoclaved at 95°C as a function processing time 147

Figure 4.4. Conductivity-pH-time plot of hydroceramic host mixed with 30 weight percent of zirconia calcined simulated radioactive waste and hydrothermally autoclaved at 125°C as a function processing time..... 148

Figure 4.5. Conductivity-pH-time plot of hydroceramic host mixed with 30 weight percent of zirconia calcined simulated radioactive waste and hydrothermally autoclaved at 150°C as a function processing time..... 149

Figure 4.6. Conductivity-pH-time plot of hydroceramic host mixed with 30 weight percent of zirconia calcined simulated radioactive waste and hydrothermally autoclaved at 175°C as a function processing time..... 150

Figure 4.7. Conductivity-pH-time plot of hydroceramic host mixed with 30 weight percent of zirconia calcined simulated radioactive waste and hydrothermally autoclaved at 200°C as a function processing time..... 151

Figure 4.8. Representative XRD patterns of hydroceramic host mixed with 30 (solid) weight percent of simulated zirconia calcined radioactive waste hydrothermally synthesized at 75°C at various time intervals. A = type A zeolite ($Na_{96}Al_{96}Si_{96}O_{384}.2H_2O$, 39-0222); Z = zirconia (ZrO_2, 37-1484); C = calcium fluoride (CaF_2, 35-0816); Q = (SiO_2, 46-1045); and x unidentified poorly crystalline phase, possibly calcium compounds 159

Figure 4.9. Representative XRD patterns of hydroceramic host mixed with 30 (solid) weight percent of simulated zirconia calcined radioactive waste hydrothermally synthesized at 85°C at various time intervals. A = type A zeolite ($Na_{96}Al_{96}Si_{96}O_{384}.2H_2O$, 39-0222); Z = zirconia (ZrO_2, 37-1484); C = calcium fluoride (CaF_2, 35-0816); Q = (SiO_2, 46-1045); and x unidentified poorly crystalline phase, possibly calcium compounds 160

Figure 4.10. Representative XRD patterns of hydroceramic host mixed with 30 (solid) weight percent of simulated zirconia calcined radioactive waste hydrothermally synthesized at 95°C at various time intervals. A = type A zeolite ($Na_{96}Al_{96}Si_{96}O_{384}.2H_2O$, 39-0222); H = hydroxysodalite ($Na_4Al_3Si_3O_{12}(OH)$, 11-0401); Z = zirconia (ZrO_2, 37-1484); C = calcium fluoride (CaF_2, 35-0816); Q = (SiO_2, 46-1045); V = unreacted vermiculite and X = unidentified poorly crystalline phase, possibly calcium compounds 161

Figure 4.11. Representative XRD patterns of hydroceramic host mixed with 30 (solid) weight percent of simulated zirconia calcine radioactive waste hydrothermally synthesized at 125°C at various time intervals. A = type A zeolite ($NA_{96}Al_{96}Si_{96}O_{384}.2H_2O$, 39-0222); H = hydroxysodalite ($Na_4Al_3Si_3O_{12}(OH)$, 11-0401); Z = zirconia (ZrO_2, 37-1484); C = calcium fluoride (CaF_2, 35-0816); Q = (SiO_2, 46-1045); and x unidentified poorly crystalline phase, possibly calcium compounds 162

Figure 4.12. Representative XRD patterns of hydroceramic host mixed with 30 (solid) weight percent of simulated zirconia calcined radioactive waste hydrothermally synthesized at 150°C at various time intervals. A = type A zeolite ($NA_{96}Al_{96}Si_{96}O_{384}.2H_2O$, 39-0222); H = hydroxysodalite ($Na_4Al_3Si_3O_{12}(OH)$, 11-0401); Z = zirconia (ZrO_2, 37-1484); C = calcium fluoride (CaF_2, 35-0816); Q = (SiO_2, 46-1045); and x unidentified poorly crystalline phase, possibly calcium compounds 163

Figure 4.13. Representative XRD patterns of hydroceramic host mixed with 30 (solid) weight percent of simulated zirconia calcined radioactive waste hydrothermally synthesized at 175°C at various time intervals. H = hydroxysodalite ($Na_4Al_3Si_3O_{12}(OH)$, 11-0401); Z = zirconia (ZrO_2, 37-1484); C = calcium fluoride (CaF_2, 35-0816); Q = (SiO_2, 46-1045); and X = unidentified poorly crystalline phase, possibly calcium compound..... 164

Figure 4.14. Representative XRD patterns of hydroceramic host mixed with 30 (solid) weight percent of simulated zirconia calcined radioactive waste hydrothermally synthesized at 200°C at various time intervals. H = hydroxysodalite ($Na_4Al_3Si_3O_{12}(OH)$, 11-0401); Z = zirconia (ZrO_2, 37-1484); C = calcium fluoride (CaF_2, 35-0816); Q = (SiO_2, 46-1045); and V unidentified crystalline phase, possibly unreacted vermiculite..... 165

Figure 4.15. Sodium concentration as a function of time of hydroceramic host mixed with 30 weight percent of zirconia calcined simulated radioactive waste and hydrothermally autoclaved at 75°C..... 167

Figure 4.16. Sodium concentration as a function of time of hydroceramic host mixed with 30 weight percent of zirconia calcined simulated radioactive waste and hydrothermally autoclaved at 85°C..... 168

Figure 4.17. Sodium concentration as a function of time of hydroceramic host mixed with 30 weight percent of zirconia calcined simulated radioactive waste and hydrothermally autoclaved at 95°C..... 169

Figure 4.18. Sodium concentration as a function of time of hydroceramic host mixed with 30 weight percent of zirconia calcined simulated radioactive waste and hydrothermally autoclaved at 125°C..... 170

Figure 4.19. Sodium concentration as a function of time of hydroceramic host mixed with 30 weight percent of zirconia calcined simulated radioactive waste and hydrothermally autoclaved at 150°C..... 171

Figure 4.20. Sodium concentration as a function of time of hydroceramic host mixed with 30 weight percent of zirconia calcined simulated radioactive waste and hydrothermally autoclaved at 175°C..... 172

Figure 4.21. Sodium concentration as a function of time of hydroceramic host mixed with 30 weight percent of zirconia calcined simulated radioactive waste and hydrothermally autoclaved at 200°C..... 173

Figure 4.22. Linear plot of the rate constant of the hydroceramic host mixed with 30 weight percent of zirconia calcined simulated radioactive waste hydrothermally synthesized at 75-95°C and at various reaction times..... 175

Figure 4.23. SEM of euhedral cubes of unreacted CaF_2 crystal in the matrix of type A zeolite in hydroceramic host mixed with 30 weight percent solid of simulated zirconia calcined radioactive waste and hydrothermally processed at 75°C for 527 hours 177

Figure 4.24. SEM of euhedral cubes of type A zeolite crystallized in hydroceramic mixed with 30 weight percent solid of simulated zirconia calcined radioactive waste and hydrothermally processed at 75°C for 527 hour 178

Figure 4.25. XRD patterns showing the effect of varying water content in comparison with an untreated sample of hydroceramic host mixed with 30 (solid) weight percent of simulated zirconia calcined radioactive waste hydrothermally processed at 125°C for 120 hours. X represents the factor of water added to each sample; A = type A zeolite ($NA_{96}Al_{96}Si_{96}O_{384}.2H_2O$, 39-0222); H = hydroxysodalite ($Na_4Al_3Si_3O_{12}$ (OH), 11-0401); Z = zirconia (ZrO_2, 37-1484); C = calcium fluoride (CaF_2, 35-0816); Q = (SiO_2, 46-1045); V = unreacted vermiculite 180

Figure 4.26. XRD patterns of selected PCT test residues compared with an untreated hydroceramic host mixed with 30 (solid) weight percent simulated zirconia radioactive waste hydrothermally synthesized at 75°C at various time intervals. A = type A zeolite ($NA_{96}Al_{96}Si_{96}O_{384}.2H_2O$, 39-0222); Z = zirconia (ZrO_2, 37-1484); C = calcium fluoride (CaF_2, 35-0816); Q = (SiO_2, 46-1045); x = unidentified poorly crystalline phase, possibly calcium compounds 182

Figure 4.27. XRD patterns of selected PCT test residues compared with an untreated hydroceramic host mixed with 30 (solid) weight percent simulated zirconia calcined radioactive waste hydrothermally synthesized at 125°C at various time intervals. A = type A zeolite ($NA_{96}Al_{96}Si_{96}O_{384}.2H_2O$, 39-0222); Q = quartz ($SiO_2$, 46-1045); H = hydroxysodalite ($Na_4Al_3Si_3O_{12}$(OH), 11-0401); Z = zirconia (ZrO_2, 37-1484); C = calcium fluoride (CaF_2, 35-0816); and V unidentified crystalline phase, possibly vermiculite 183

Figure 4.28. XRD patterns of selected PCT test residues compared with an untreated hydroceramic host mixed with 30 (solid) weight percent simulated zirconia calcined radioactive waste hydrothermally synthesized at 200°C at various time intervals. Q = quartz (SiO2, 46-1045); H = hydroxysodalite ($Na_4Al_3Si_3O_{12}$(OH), 110401); Z = zirconia (ZrO_2, 37-1484); C = calcium fluoride (CaF_2, 35-0816); and V unidentified crystalline phase, possibly vermiculite 184

Figure 5.1. Conductivity-pH-time plot of hydroceramic host mixed with 30 weight percent of fluorinel blend calcined simulated radioactive waste and hydrothermally autoclaved at 75°C as a function of processing time 189

Figure 5.2. Conductivity-pH-time plot of hydroceramic host mixed with 30 weight percent of fluorinel blend calcined simulated radioactive waste and hydrothermally autoclaved at 85°C as a function of processing time 190

Figure 5.3. Conductivity-pH-time plot of hydroceramic host mixed with 30 weight percent of fluorinel blend calcined simulated radioactive waste and hydrothermally autoclaved at 95°C as a function of processing time 191

Figure 5.4. Conductivity-pH-time plot of hydroceramic host mixed with 30 weight percent of fluorinel blend calcined simulated radioactive waste and hydrothermally autoclaved at 125°C as a function of processing time 192

Figure 5.5. Conductivity-pH-time plot of hydroceramic host mixed with 30 weight percent of fluorinel blend calcined simulated radioactive waste and hydrothermally autoclaved at 150°C as a function of processing time 193

Figure 5.6. Conductivity-pH-time plot of hydroceramic host mixed with 30 weight percent of fluorinel blend calcined simulated radioactive waste and hydrothermally autoclaved at 175°C as a function of processing time 194

Figure 5.7. Conductivity-pH-time plot of hydroceramic host mixed with 30 weight percent of fluorinel blend calcined simulated radioactive waste and hydrothermally autoclaved at 200°C as a function of processing time 195

Figure 5.8. Representative XRD patterns of hydroceramic host mixed with 30 (solid) weight percent of simulated fluorinel blend calcined simulated radioactive waste hydrothermally synthesized at 75°C at various time intervals. A = type A zeolite ($NA_{96}Al_{96}Si_{96}O_{384}.2H_2O$, 39-0222); Z = zirconia (ZrO_2, 37-1484); C = calcium fluoride (CaF_2, 35-0816); Q = (SiO_2, 46-1045); and x unidentified poorly crystalline phase, possibly calcium compounds 202

Figure 5.9. Representative XRD patterns of hydroceramic host mixed with 30 (solid) weight percent of simulated fluorinel blend calcined simulated radioactive waste hydrothermally synthesized at 85°C at various time intervals. A = type A zeolite ($NA_{96}Al_{96}Si_{96}O_{384}.2H_2O$, 39-0222); Z = zirconia (ZrO_2, 37-1484); C = calcium fluoride (CaF_2, 35-0816); Q = (SiO_2, 46-1045); and x unidentified poorly crystalline phase, possibly calcium compounds 203

Figure 5.10. Representative XRD patterns of hydroceramic host mixed with 30 (solid) weight percent of simulated fluorinel blend calcined simulated radioactive waste hydrothermally synthesized at 95°C at various time intervals. A = type A zeolite ($NA_{96}Al_{96}Si_{96}O_{384}.2H_2O$, 39-0222); Z = zirconia (ZrO_2, 37-1484); C = calcium fluoride (CaF_2, 35-0816); Q = (SiO_2, 46-1045); H = hydroxysodalite ($Na_4Al_3Si_3O_{12}(OH)$, 11-0401) and x unidentified poorly crystalline phase, possibly calcium compounds 204

Figure 5.11. Representative XRD patterns of hydroceramic host mixed with 30 (solid) weight percent of simulated fluorinel blend calcined simulated radioactive waste hydrothermally synthesized at 125°C at various time intervals. A = type A

zeolite ($NA_{96}Al_{96}Si_{96}O_{384}.2H_2O$, 39-0222); z = zirconia (ZrO_2, 37-1484); C = calcium fluoride (CaF_2, 35-0816); Q = (SiO_2, 46-1045); H = hydroxysodalite ($Na_4Al_3Si_3O_{12}$ (OH), 11-0401) and x unidentified poorly crystalline phase, possibly calcium compounds 205

Figure 5.12. Representative XRD patterns of hydroceramic host mixed with 30 (solid) weight percent of simulated fluorinel blend calcined simulated radioactive waste hydrothermally synthesized at 150°C at various time intervals. A = type A zeolite ($NA_{96}Al_{96}Si_{96}O_{384}.2H_2O$, 39-0222); Z = zirconia (ZrO_2, 37-1484); C = calcium fluoride (CaF_2, 35-0816); Q = (SiO_2, 46-1045); H = hydroxysodalite ($Na_4Al_3Si_3O_{12}$(OH), 11-0401) and x unidentified poorly crystalline phase, possibly calcium compounds 206

Figure 5.13. Representative XRD patterns of hydroceramic host mixed with 30 (solid) weight percent of simulated fluorinel blend calcined simulated radioactive waste hydrothermally synthesized at 175°C at various time intervals. Z = zirconia (ZrO_2, 37-1484); C = calcium fluoride (CaF_2, 35-0816); Q = (SiO_2, 46-1045); H = hydroxysodalite ($Na_4Al_3Si_3O_{12}$ (OH), 11-0401) and x unidentified poorly crystalline phase, possibly calcium compounds 207

Figure 5.14. Representative XRD patterns of hydroceramic host mixed with 30 (solid) weight percent of simulated fluorinel blend calcined simulated radioactive waste hydrothermally synthesized at 200°C at various time intervals. A = type A zeolite ($NA_{96}Al_{96}Si_{96}O_{384}.2H_2O$, 39-0222); Z = zirconia (ZrO_2, 37-1484); C = calcium fluoride (CaF_2, 35-0816); Q = (SiO_2, 46-1045); H = hydroxysodalite ($Na_4Al_3Si_3O_{12}$(OH), 11-0401) and x unidentified poorly crystalline phase, possibly calcium compounds 208

Figure 5.15. Sodium concentration as a function of time of hydroceramic host mixed with 30 weight percent of fluorinel blend calcined simulated radioactive waste and hydrothermally autoclaved at 75°C..... 210

Figure 5.16. Sodium concentration as a function of time of hydroceramic host mixed with 30 weight percent of fluorinel blend calcined simulated radioactive waste and hydrothermally autoclaved at 85°C..... 211

Figure 5.17. Sodium concentration as a function of time of hydroceramic host mixed with 30 weight percent of fluorinel blend calcined simulated radioactive waste and hydrothermally autoclaved at 95°C..... 212

Figure 5.18. Sodium concentration as a function of time of hydroceramic host mixed with 30 weight percent of fluorinel blend calcined simulated radioactive waste and hydrothermally autoclaved at 125°C..... 213

Figure 5.19. Sodium concentration as a function of time of hydroceramic host mixed with 30 weight percent of fluorinel blend calcined simulated radioactive waste and hydrothermally autoclaved at 150°C 214

Figure 5.20. Sodium concentration as a function of time of hydroceramic host mixed with 30 weight percent of fluorinel blend calcined simulated radioactive waste and hydrothermally autoclaved at 175°C 215

Figure 5.21. Sodium concentration as a function of time of hydroceramic host mixed with 30 weight percent of fluorinel blend calcined simulated radioactive waste and hydrothermally autoclaved at 200°C 216

Figure 5.22. Linear plot of the rate constant of the hydroceramic host mixed with 30 weight percent of fluorinel blend calcined simulated radioactive waste hydrothermally synthesized at 75-95°C and at various reaction times 218

Figure 5.23. XRD patterns showing the effect of varying water content of hydroceramic host mixed with 30 (solid) weight percent of simulated fluorinel blend radioactive waste hydrothermally processed at 125°C for 120 hours. X represents the factor of water added to each sample. A = type A zeolite ($NA_{96}Al_{96}Si_{96}O_{384}.2H_2O$, 39-0222); z = zirconia (ZrO_2, 37-1484); C = calcium fluoride (CaF_2, 35-0816); Q = (SiO_2, 46-1045); and x unidentified poorly crystalline phase, possibly calcium compounds 220

Figure 5.24. XRD patterns of selected PCT test residues compared with an untreated hydroceramic host mixed with 30 (solid) weight percent simulated fluorinel blend calcined radioactive waste hydrothermally synthesized at 75°C at various time intervals. A = type A zeolite ($NA_{96}Al_{96}Si_{96}O_{384}.2H_2O$, 39-0222); z = = zirconia (ZrO_2, 37-1484); C = calcium fluoride (CaF_2, 35-0816); Q = (SiO_2, 46-1045); and x unidentified poorly crystalline phase, possibly calcium compounds 222

Figure 5.25. XRD patterns of selected PCT test residues compared with an untreated hydroceramic host mixed with 30 (solid) weight percent simulated fluorinel blend calcined radioactive waste hydrothermally synthesized at 150°C at various time intervals. A = type A zeolite ($NA_{96}Al_{96}Si_{96}O_{384}.2H_2O$, 39-0222); Z = zirconia (ZrO_2, 37-1484); C = calcium fluoride (CaF_2, 35-0816); Q = (SiO_2, 46-1045); and x unidentified poorly crystalline phase, possibly calcium compounds 223

Figure 5.26. XRD patterns of selected PCT test residues compared with an untreated hydroceramic host mixed with 30 (solid) weight percent simulated fluorinel blend calcined radioactive waste hydrothermally synthesized at 200°C at various time intervals. A = type A zeolite ($NA_{96}Al_{96}Si_{96}O_{384}.2H_2O$, 39-0222); z = = zirconia (ZrO_2, 37-1484); C = calcium fluoride (CaF_2, 35-0816); Q = (SiO_2, 46-1045); and x unidentified poorly crystalline phase, possibly calcium compounds 224

LIST OF TABLES

Table 1.1. Coordination of Cations with Oxygen in Silicate Structures 8

Table 1.2. Major Minerals of the Feldspathoid Group 10

Table 1.3. Reference formulation for FUETAP concrete hosts for Savannah River High-level waste 18

Table 1.4a. Mineral admixtures by weight percent of typical Class F and Class C fly ashes..... 26

Table 1.4b. Comparison of typical Calss F and Class C fly ashes 26

Table 1.5. Fly ashes and their sources 27

Table 1.6. Bulk composition of Troy Creek metakaolinite was made from kaolinite by calcining it at 750°C for 2-3 hours 30

Table 1.7. Characteristics of the calcined high-level nuclear waste at the INEEL 37

Table 1.8. Simulated zirconia calcined high-level radioactive waste 38

Table 1.9. Simulated fluorinel blend calcined high-level radioactive waste containing cadmium 39

Table 1.10. Analytical results of the leachates from Hydroceramic made from Hatfield and Holtwood fly ashes 46

Table 1.11. Major components of liquid waste simulant 48

Table 1.12. Major composition of Ashgrove Troy clay..... 48

Table 1.13. Percent of sodium and nitrate leached from the three alumina sources..... 54

Table 1.14. Table showing variable NaOH concentrations with their corresponding alkali:calcium:alumina:silica leached..... 56

Table 1.15. Percent of sodium and nitrate released with respect to NaOH concentration in the grouts..... 56

Table 1.16. Percentage of sodium and nitrate leached in Fluorinel blend experiments with NaOH and Na_2S..... 60

Table 1.17. Percentage and concentrations of sodium, nitrate and cesium leached in Fluorinel blend calcined experiments with pozzolans 63

Table 1.18. Percentage and concentrations of sodium, nitrate and cesium leached in Fluorinel blend calcined experiments with mixture of fly ashes and calcined clays 66

Table 2.1. Hydroceramic host formulation 79

Table 2.2. Table of results of the computer calculation of the percentage of the hydroceramic formulation plus 30 weight percent (solid) simulated waste containing oxides, oxide ratios, fraction of solid-water, non-bridging oxygens and hydration energy 79

Table 2.3. Hydroceramic host plus 30 weight percent (solid) waste (fluorinel blend or zirconia calcine) formulation 81

Table 2.4. Results of the computer calculation of the percentage of the host-waste (fluorinel blend calcine) formulation containing oxides; oxide, solid-water ratios, non-bridging oxygens and hydration energy 82

Table 2.5. Detection limits for the bulk chemical analysis for the major anions and cations 90

Table 3.1. Concentrations of the major species in the PCT test solutions conducted at 90°C for 24 hours for Hydroceramic host forms hydrothermally synthesized at various temperatures and times 115

Table 3.2. Summary of the rate constant calculations for the first-order hydration kinetics of hydroceramic host waste form..... 122

Table 3.3. The formulation used in probing the effect of water on the crystallization of hydroceramic waste form..... 139

Table 4.8. Ranges of concentrations of selected ions for each temperature summarized from tables 4.1-4.7 in comparison with the reference sample (room temperature). The maximum processing time for each temperature are indicated below the temperature 153

Table 4.9. Summary of the rate constant calculations for the first-order hydration kinetics of hydroceramic host mixed with 30 weight percent of zirconia simulated calcined solid waste 174

Table 5.8. Summary of the rate constant calculations for the first-order hydration kinetics of hydroceramic host mixed with 30 weight percent of fluorinel blend simulated calcined solid waste..... 217

Table 6.1. Summary of the hydration kinetic results for the hydroceramic host and host mixed with 30 weight percent of simulated fluorinel blend and zirconia calcined wastes 231

CHAPTER I

INTRODUCTION AND LITERATURE REVIEW

CHAPTER I

INTRODUCTION AND LITERATURE REVIEW

1.0 Introduction

The late 70s and 80s witnessed intensive efforts in the development of a wide variety of waste forms (Lutze and Ewing, 1988). Notable among the waste forms developed during this golden age are borosilicate glass developed at Savannah River Laboratory, Aiken, SC; Synroc ceramic development at Lucas Heights, Australia (Ringwood et al., 1988); Formed Under Elevated Temperature and High Pressure (FUETAP) concretes, Oakridge National Laboratory, Oak ridge, TN (McDaniel and Delzer, 1988); tailored ceramic, The Pennsylvania State University, University Park, PA and Rockwell International, Costa Mesa, CA (Harker, 1988); and High-silica Glass, Catholic University of America, Washignton, DC (Macedo et al., 1979), and more recently, Hydroceramic waste forms at INEEL, Idaho Falls, ID and Pennsylvania State University, University Park, PA (Xi et al., 1995; Siemer et al., 1995). Hydroceramic is formed by the activation of pozzolanic materials such as thermally treated clay by alkali and temperature as provided by mild hydrothermal conditions. The hydroceramic synthesis process is a combination of the Hanford's clay reaction process (Barney, 1976) and Oak Ridge National Laboratory's (ORNL's) FUETAP technology (Moore et al., 1982). Among all the waste forms developed, borosilicate glass was chosen as the desired waste form and as the benchmark waste form against which the chemical and physical durabilities of other waste forms must be compared.

Vitrification (glass) has been the preferred solidification technology favored by the Department of Energy (DOE) (Hench, 1995; Lutze and Ewing, 1988). Improvements in the areas of processing technologies and fundamental knowledge of nuclear wastes and expected repository conditions have lead to the development of other waste forms which have chemical and mechanical durablities, heat and radiation resistant. The vitrification option (glass) may not be the ultimate immobilization medium for some aqueous radioactive wastes due to the presence of high concentrations of alkali ions, small volume, low-radiation and in liquid state; that is, the so-called sodium bearing waste (SBW). For example, the INEEL spent fuel high-level radioactive wastes originating from the same nuclear activities have different physical properties (calcined and sodium-bearing wastes) and however, the same chemical compositions.

A very attractive scientific approach is to design a waste form specifically tailored to convert the alkali/alkaline containing defense reprocessing nuclear waste (SBW) into assemblages of aluminosilicate containing waste forms. The immobilization of the reprocessed nuclear waste (SBW) can be achieved through hydrothermal solidification processes at relatively low-temperature by combining appropriate amounts of pozzolanic materials which will in turn be activated by the existing alkali (sodium hydroxide) in the waste. Alternatively, the natural heat generated by the waste itself would be as high as 90°C could be used as the driving force for the process if the waste canisters were stored in temperature controlled buildings. This would eliminate the need for hydrothermal process. The resulting product will consist of mainly chemically bonded ceramic mostly aluminosilicate minerals with

zeolitic bulk chemistry which posses the requisite chemical durability, mechanical integrity and thermodynamic stability common to ceramic materials. Thus these waste forms are herein referred to as “hydroceramics”.

1.1 Zeolites

1.1.1 Introduction

The use of zeolites in countless technological and industrial settings has been credited to three properties: capacity to sorb liquids (gases, vapors and liquids); catalyze chemical reactions; and act as ion exchangers (Barrer, 1978). The sorption capabilities of zeolites to selectively take up guest molecules in place of water are based on the molecular dimensions. This property is utilized in petrochemical industries to separate n-paraffins from other hydrocarbons (Severin and Gupta, 1999), in odor control materials in poultry farm houses (Amon et al., 1997; Koelliker et al., 1978), removal of toxic industrial gases (Kopac et al., 1998; Srinivasan and Grutzeck, 1999) and the removal of strontium from contaminated waters (Baxter and Berghauser, 1986; Sylvester and Clearfield, 1998). Ion exchange capacity is by far the most important property of zeolite materials applicable to the immobilzation of radioactive wastes. The mole sieving behavior, selectivity of sorbents and the synthesis of zeolite-based catalysts are all determined by the ion exchange capacity. High selectivity for certain cations can aid in the sequestration and concentration of such ions. Therefore, high affinity for certain ions during ion exchange processes and

the ability to lock them up in cages qualified zeolites as potential nuclear waste forms.

Zeolitic materials have been utilized in the immobilization of radionulides and toxic metals (McFarlane et al., 1997). Their application is due to their sufficient latitude to accept high proportion of radioactive and nonradioactive elements such as major alkali and alkaline-earth metal cations (Cs, Na, Rb, Sr) and various heavy metals for example, Pb, Ag, Hg, and Cd, Cr. Exchange is due in part to the fact that most zeolites are Na or K based and that these ions are mobile and can be replaced by smaller ions with higher charge densities.

1.1.2 Composition

Zeolites generally are tectosilicates consisting of three-dimensional framework of SiO_4^{-4} and AlO^{-5} tetrahedra in which all oxygen atoms of each tetrhedron are shared with adjacent tetrahedrons, giving rise to an O/Si ratio of 2:1. The 2:1 arrangement of O and Si will give rise to quartz, an electrically neutral molecule. However, in zeolite structures, some of the central quadrivalent Si^{+4} in the tetrahedral site is substituted by trivalent Al^{3+}, leading to deficiency in negative charge in the framework (Ming and Mumpton, 1989; Szostak, 1998). The shortage of charge positive in the structure is balanced by mono- and divalent cations notably, Na^+ and K^+, and Li^+, and less commonly Rb^+, Ca^{2+}, Ba^{2+}, Mg^{2+} and Sr^{2+}. Gottardi (1978), suggested a general formula for a zeolite:

$$\left[M_x^{+}, M_y^{2+}\right]\left[Al_{(x+2y)}Si_{n-(x+2y)}O_{2n}\right] \cdot mH_2O \qquad (1.1)$$

where M^+ and M^{2+} are monovalent and divalent cations, respectively. They involve an ordered arrangement of SiO_4 and AlO_4 tetrahedra interconnected via shared oxygen atoms. As a result of this arrangement, open channels and cages of molecular dimensions are formed. Cation exchange processes are limited to the ions occurring in the first parentheses; while the cations and oxygen ions in the second parentheses are responsible for the structural framework. The critical ratio of Al/Si is usually 1:1 but not less. Furthermore, the ratio of Al + Si/O of 1:2 is usually maintained in a zeolite; and the sum of exchangeable positive charges of cations is equal to the number of Al ions in the tetrahedral site. The extent of hydration is reported with respect to the *m* coefficient.

1.1.3 Structure

1.1.3.1 Zeolites

Zeolites are complex aluminosilicate materials that possess various chemical constituents and a variety of structures. Structural information is usually obtained from x-ray diffraction (XRD) patterns (Pilter et al., 2000; Johnson et al., 1999; Walton et al., 2001), Fourier transform infrared (FTIR) spectroscopy spectra, and solid-state nuclear magnetic resonance (NMR) [Klinowski, 1989; Bell et al., 1986;

Yang et al., 1988; Pellegrino et al., 1990). The chemical compositions of these structures are based on electronegativity rules of ionic crystal systems (Bragg and Claringbull, 1965). Various major cations substituting in zeolite structures are listed in Table 1.1.

The structure of zeolites consist of low-density three dimensional extended structures constructed from corner sharing SiO_4 and AlO_4 tetrahedra (primary building blocks) linked together to form simple geometrical forms known as secondary building units. The resulting secondary building units range from simple 4 or 6 tetrahedra units (4- or 6-rings) to complex (cubo-octahedra) sodalite units. Different zeolites result from changes in the spatial combination of tetrahedra in one-, two, or three-dimensional space and/or changes in chemistry that result in isomorphic substitution. The linkages of tetrahedral may form infinite chains to form needle-like crystal, two- or three-dimensional arrangement through a mutual sharing of oxygen to form a framework structures. For example, an ion or a water molecule may move through a three-dimensional channel system of a zeolite and reach any other place within the crystal. On the other hand, a movement that is constrained to a plane, or an unidirectional geometry movement is termed a two dimensional or one dimensional channel. The low-density and porous nature of zeolite is demonstrated by the way molecular water of hydration is held within the intracrysatalline of the framework (Barrer, 1978). This water is easily removed upon heating zeolite up to $350^{o}C$.

Table 1.1. Coordination of cations with oxygen in silicate structures (Bragg and Claringbull, 1965).

Ion	Radius (Å)	Radius Ratio	Coordination Number	Bond Strengths
B^{3+}	0.20	0.20	3, 4	1 or 3/4
Be^{2+}	0.31	0.25	4	1/2
Li^{+}	0.60	0.34	4	1/4
Si^{4+}	0.41	0.37	4,6	1
P^{5+}	0.34	0.34	4, 6	5/4 or 5/6
Al^{3+}	0.50	0.41	4, 5, 6	¾ or 1/2
Ge^{4+}	0.44	0.43	4, 6	1 or 2/3
Ga^{3+}	0.62	0.46	4, 6	¾ or 1/2
Mg^{2+}	0.65	0.47	6	1/3
Na^{+}	0.95	0.54	6, 8	1/6 or 1/8
Ca^{2+}	0.99	0.67	7, 8, 9	1/4
K^{+}	1.33	0.75	6, 7, 8, 9, 10, 12	1/9

1.1.3.2 Feldspathoids

Feldspathoids also have open-channel structures as a result of large open cavity which may house cations or sometimes anions. In many ways they are similar to zeolites, but senso stricto they are not zeolites, that is, they do not contain water molecules. Minerals that constitute felspathoid group are listed in Table 1.2. Their framework is composed of 4-ring or 6-ring ($Al_2Si_2O_8$ or $Al_3Si_3O_{12}$) groups. Anions such as Cl^-, SO_4^{-2} resides in the center of the cubo-octahedron sodalite cage. Sodalite may be classified as hydroxy or basic sodalite due to the presence of additional Na and OH- and water molecules.

1.1.3.3 Phases Found in this Study

Zeolite phases found in this study are Type A zeolite, hydroxysodalite and NaP1. Type A zeolite is composed of truncated octahedron of sodalite cages linked together by double four-membered rings that form 11.40 Å diameter cavity. The structural formula is $[Na_{96}[(AlO_2)_{96}(SiO_2)_{96}].wH_2O$, corresponding to Si/Al = 1.0. Zeolite Type A has a cubic structure with space group $Fm\overset{?}{3}c$ and a unit-cell constant, ? = b = c = 24.64 Å. Sodalite is cubic with space group Im-3m with ABC-ABC layer packing. NaP1 is pseudocubic with the unit cell constant, ? = b = c = 10 Å and intracrystalline pore volume, (as cm^3 liquid H_2O per cm^3 of crystal) of 0.47.

Table 1.2. Major minerals of the feldspathoid group (Breck, 1984).

Mineral	Formula/unit cell	Crsytallographic Data
Sodalite	$Na_8[(AlO_2)_6(SiO_2)_6]Cl_2$	Cubic, a = 8.87 Å
Nosean	$Na_8[(AlO_2)_6(SiO_2)_6]SO_4$	Cubic, a = 9.03 Å
Nepheline	$Na_6K_2[(AlO_2)_8(SiO_2)_8$	Hexagonal, a = 10 Å, c = 8.4 Å
Cancrinite	$(Na, Ca, K)_{6\text{-}8}[(AlO_2)_6(SiO_2)_6]$ $(CO_3, SO_4, Cl)_{1\text{-}2}$	Hexagonal, a = 12.6Å, c= 5.18 Å
Scapolite (Marialite)	$Na_8[(Al_2O)_6(SiO_2)_{18}]Cl_2$	Tetragonal, a =12.06 Å, c=7.57Å

1.2 Research Objective

The dual objectives of this investigation were to formulate hydroceramic waste forms for INEEL calcines having optimal chemical durability and excellent physical properties; followed by a detailed study to elucidate the hydration kinetics of the selected hydroceramic waste forms within glass compositional regions as a function of temperature, time and constant waste loading percent. Dissolution rates ultimately determine the chemical durability of a nuclear waste form. Hydration kinetic data combined with various analytical results will be used to establish processing limits that will be utilized in engineering durable waste forms capable of immobilizing the calcined high-level radioactive waste in storage at the INEEL.

1.3 Literature Review: Waste Form Description

The period between 1977 and 1982 witnessed the proliferation of the development of different types of nuclear waste forms (Lutze and Ewing, 1988). Since then several solidification technologies ranging from the complex to the relatively simple- have been developed or adapted mainly to simultaneously immobilize radioactive wastes and heavy metals (Ringwood et al., 1988; McDaniel and Delzer, 1988; Macedo et al., 1979; Xi et al., 1995; Siemer et al., 1995). Concept waste forms were developed based on ease of processing, high strength, high resistance to chemical attack (Roy and Burns, 1982; Burns, 1971; Roy, 1978; Glasser, 1992; Langton and Roy, 1980a; Langton and Roy, 1981). These technologies involve mixing waste with a

solidification agent to augment the resulting chemical and physical properties. Ions in the resulting waste forms posses low mobilities and toxicities due to high degree of structural integrity.

1.3.1 Cement

Cementitious materials have been investigated as potential waste form candidates in several areas of radioactive waste management. Cements have been used as physical barriers in order to isolate waste (walls, grouted walls, etc) [Roy and Burns, 1982], in engineered structures such as vaults, supports, barriers, backfill and encapsulation (Burns, 1971; Roy, 1978; Glasser, 1992); and as both chemical and physical solidification/stabilization of low- to high-level radioactive wastes. Tailored concrete or concrete-based waste forms such as the grout sheets injected in shale fractures deep underground (Morgan et al., 1983; Langton et al., 1983; Malek et al., 1986), the concretes mixed mixed with soil in trenches (Langton, 1987), or the concrete monoliths buried in low-level waste sites have been utilized for many decades for the immobilization of various levels of radioactive wastes.

The popularity of cement in the treatment of radioactive waste can be credited to its ease of processing at relatively low-temperatures, low or overall cost due to lower equipment and capital cost requirements, thermodynamic stability (Roy, 1990), and ability to encapsulate various levels of radioactive wastes (Scheetz et al., 1985). A reflection of these inherent advantages of cement materials is in the worldwide

applications such as in the United Kingdom, France, Belgium and the United States (Glasser and Atkins, 1994).

1.3.2 Composition of Cement Waste Forms

Generally, ordinary portland cement (OPC) is used in radioactive management (Roy, 1990). The chemical makeup of OPC consists of four major phases: two calcium silicates (Ca_3SiO_5 and Ca_2SiO_4), an aluminate ($Ca_3Al_2O_3$) and an aluminoferrite solid solution ($Ca_2(Fe,Al)_2O_5$). The calcium silicates amount to 70-80 weight percent of the total clinker. The formation of a clinker results when limestone and shale are heated at 1450°C until partial fusion occurs. The final product is milled to a high specific surface area, normally 3000-5000 cm^2/g (Glasser and Atkins, 1994). The mechanism of immobilizing radionuclides in cement waste forms involves compositional manipulation of OPC cements resulting from physical interactions and chemical reactions to achieve desired chemical, physical and mechanical properties. In some instances, precipitation of insoluble compounds in the high pH environment occurs in the pore space and/or crystal chemical substitution in crystalline phases in the cement matrix structures.

Cement additives have been supplemented to enhance specific chemical/physical properties in the bulk chemistry of OPC cement for radioactive waste immobilization. The addition of pozzolanic components (30-70% fly ashes, up to 90% slags, silica fumes) to cement provides an increase in sorption and a decrease in permeability in

the cement matrix on a short-term basis (Glasser, 1992; Glasser and Atkins, 1994; Scheetz et al., 1993). Flyash and slag with sufficient Fe^{III} and sulfur readily reduce Cr^{VI} mobility and toxicity to a less toxic and less mobile Cr^{III} (Lee et al., 1995; Bajt et al., 1993). Finally, the incorporation of 0.2-2% superplasticizers (sulfonated melamine, naphthaline formaldehyde polymers, or lignoslphonates) in cement improves permeability because of less water content needed (Malhotra, 1986).

Chemicals have been added to promote specific chemical reactions. Calcium hydroxide, sodium hydroxide and sodium silicate (Izumida et al., 1987) have been added to neutralize acidic wastes and precipitate borates. Xi et al., (1995) obtained improved strength and reduced pore structures of OPC by the addition of highly reactive silica fume. The improvement was credited to lack of formation of a-C_2SH, slower hydration of slag, and the pore filling characteristics of silica fume particles.

Getters and organic polymers have been added to specifically reduce the solubility of certain radionuclides (Glasser, 1992). Zeolite getters have been incorporated in cement-based formulations to control cesium dissolution from the cement matrix (Glasser, et al., 1982). Hardened cement has been impregnated by various liquid organic polymers and heat-treated to form polymer impregnated concrete, polymer cement concrete and polymer concretes (Grosskurth, 1991). The cross-linked polymers retard the ingress and egress of water or other leaching agents. Organic polymer cement matrices are excellent for tritium immobilization (Lamberger and Rogers, 1981).

NonOPC cements are commonly utilized in the construction sector but are less popular in the nuclear waste management. Some considerations have been given to the calcium aluminate cements as, potential radioactive hosts for certain radioactive waste because of their thermodynamic compatibility (Scheetz et al., 1985; Roy and Burns, 1982; Roy et al., 1980; Barnes et al., 1982). Sorrel cements, a group of hydraulic cements based on acid/base reactions which, when set, comprise mainly magnesium oxychloride, have been proposed as potential hosts for radioactive wastes (Wilson and Nicolson, 1993). A subclass of sorrel cement group, consisting of different types of metal oxide/phosphoric acid cements have been less investigated as a potential waste form.

Regardless of a cement formulation, the water content (water/cement ratio) determines the ultimate chemical and physical immobilization mechanisms in operation in a cement waste form. The role of water is to give fluidity in accordance to the application, however, the minimum theoretical water content to achieve full hydration and low-permeability concrete corresponds to water/cement ratio of ~0.24 (Glasser, 1992; Glasser and Atkins, 1994). Excess water tends to accumulate as pore water which consists mainly of alkali ions such as Na^+, K^+ and radionuclides. The presence of such pores increase porosity, prolong the setting time and reduce compressive strength (Scheetz et al., 1993; Roy and Scheetz, 1993; Roy, 1978).

1.3.3 Limitations of Cementitious Waste Forms

The major shortcomings of OPC based waste forms are their inherent high porosity due to the large surface area of the particles and their incompatibility with alkali ions, nitrates and sulfates (Berner et al., 1987; Glasser and Atkins, 1994; Glasser, 1992; Colombo and Neilson 1977).

1.4 FUEATAP Concretes

In the early 1970s, Roy and her colleagues at The Pennsylvania State University developed the first "hot-pressed concrete" by combining various cement-types, fly ash, clays and simulated radioactive wastes (Roy and Gouda, 1978). The formulation was processed at 150-400°C and pressure ranging from 178-345 Mpa (25-100 kpsi). The capability of the concrete to serve as a nuclear waste host was tested by the introduction of simulated wastes containing 60.5 weight percent sodium as sodium nitrate. The resulting waste forms, which contains no coarse aggregates had densities of 2.65-2.8 g/cm^3 and permeabilities of less than 10^{-3} darcy, and high compressive strengths of >690 Mpa (100 kpsi). Sodium nitrate had deleterious effects on the mechanical properties of the final product. However, by calcining the waste the mechanical properties improved tremendously even with 50 weight percent calcine in the matrix.

Since early 1960s under the direction of Moore, Tamura, McDaniel, and others (De Laguna et al., 1968; Moore et al., 1977; Moore, 1981), Oak Ridge National Laboratory has actively been engaging in cement-based waste form research for the immobilization of it's radioactive waste. Their experiences combined with that of Roy's research results led to the development of tailored formulations of FUETAP concretes processed at 250°C and 4.10 Mpa or 600 psi, suitable for high-level radioactive wastes (Moore et al., 1982). Following a series of experiments, a reference formulation was developed for the Savannah River high-level wastes, (Table 1.3). The resulting FUETAP concretes have excellent mechanical properties with compressive strengths of ~100 Mpa, densities of 2 g/cm^3, and porosities of 22-26%. Leach rates for TRU, Cs, and Sr showed better results than borosilicate glass. Other properties of FUETAP concretes include thermal stability up to 900°C (Stone, 1977; Dole et al., 1983), and radiation stability (Bibler, 1978).

High-level radioactive species naturally generate high activity during their incorporation into the cement matrix which may lead to gas-pressure build-up from pore water radiolysis (McDaniel and Delzer, 1988). Consequently, expansion and thermal cracking of the waste form may occur. However, the thermal generating power of radioactive species was utilized by FUETAP concretes for accelerated curing (McDaniel and Delzer, 1988).

Dole et al. (1982) studied a slightly different FUETAP concrete formulation made with 22% OPC, 11% fly ash, 28% sand, 29% Savannah River Project solids and 10% water. The constituent mixture was stirred and mixed, solidified and cured for 24

Table 1.3. Reference formulation for FUETAP concrete hosts for Savannah River High-level waste (Stone et al., 1979).

Component	Weight Percent
Cement	26.80
Fly ash	21.90
Clay	8.70
Suspending Agent	0.40
Waste (hydrated)	15.0
Water	27.20

hours at 100-250°C. Optical microscope and SEM with EDX analytical methods revealed the presence of up to ten phases consisting of different combinations of Al, Si, Cs, Sr, Fe, Na, K, T, Mn, Gd, Ti, Ce, and Ca in the final product. Cs was located in the cement phase rich in Si and Al or in a zeolite, and Sr was found exclusively with Mn. However, the type of zeolite was not specified. Effects of several variables on the physical and chemical properties of the final product were investigated. Different cement types had no noticeable affect on the performance of the waste form (Roy and Gouda, 1978). The addition of Indian red pottery clay to the formulation reduced the initial Cs washout by as much as a factor of two. The effects of silica, water, deionized water, and salt brine on the release rate of Cs, Sr, U, Ce and Nd were tested at 40 and 90°C. Only silica saturated water showed a slight increase in the concentration of Cs from 37 g/m^2 at 40°C to 46 g/m^2 at 90°C. Also, different Materials Characterization Center (MCC) tests were carried out on the samples. It was concluded that the tests were not good enough to ascertain the long-term performance of the FUETAP concretes.

FUETAP concrete-based waste forms possesses some special advantages over conventional concrete such as high strength, excellent leaching resistance of contained radionuclear species especially (Cs and Sr) and other nonradionuclear species, high tolerance for nitrate, and a minute amount of free water. Furthermore, the problems of hydrogen-oxygen radiolysis that can lead to pressure buildup, and the build up of nitrogen, a radiolysis product from nitrate containing water-saturated waste are eliminated via calcination (Katz, 1980; Kazanjian and Killion, 1981). The

equipment is simple and easy to operate at <350°C, a temperature much less than that required for glass operation or other ceramic waste forms. Since it operates under a closed system, loss of volatile and hazardous species by evaporation is eliminated. The waste form produced will be expected to be in thermodynamic equilibrium with the repository geological environments.

1.4.1 Limitations of FUETAP Concretes

The resulting product FUETAP process was praised as a potential nuclear waste form however, with some reservations. The main disadvantages of FUETP concrete is the presence of up to 24% porosity which may result in high initial leach rate due to initial washout through the porous structure of the waste forms. Following the development of FUETAP concretes, their performances against other waste forms such as borosilicate glass, tailored ceramic, synroc, high silica glass, coated sol-gel particles, and glass marbles in lead matrix were compared. The criteria “figure of merit” used were data obtained from leach resistance, impact resistance, waste-loading percent and processing conditions (Stone et al., 1979). FUETAP concrete waste forms were rated last, having the lowest score among the seven waste forms compared (Bernadzikowski et al., 1983).

Several processing conditions with time under various conditions such as the mix density, curing-dewatering cycle time and waste loading percentage were not known. A waste loading of 20 weight percent was suggested but not tested.

The final optimum concrete composition was not known. Suitable cement type and optimum cement/fly ash ratio was not known. Clay additive in the formulation serve the purpose of retaining cesium however, the need for both clay and zeolite in the mixture was not clear. The roles of water at optimum water/cement ratio of 0.24 were previously emphasized as the driving force for the physical and chemical processes controlling cement based waste forms. An examination of Table 1.2 revealed that that there was excess water, 0.272 present in the FUETAP formulation. This translates to cement:water ratio of ~1. As a result the product probably had high-permeability (high porosity) which caused it to fail the test.

1.5 Alkali-Activated Cements

Several investigations have been conducted on alkali-activated cement concretes with different pozzolans using FUETAP techniques with the purpose of improving strength and chemical durability. It was observed by many researchers that prolonged hydrothermal treatment of Portland cement paste lead to decreases in strength and coarsening of pore structures (Verbeck and Helmuth, 1968; Kjellsen et al., 1990; Taylor, 1997; Menzel, 1934).

Wang et al., (1993) used ash-slag-cement as a matrix for nuclear waste. Fly ash and lime were first heated at 60°C for 4 hours and then hydrothermally treated at 200°C for 6 additional hours. Appropriate amounts of Class F fly ash were then mixed with

Ordinary Portland Cement (OPC), the fly ash + lime mixture, slag, alkali, and nuclear waste. The final mixture was also subjected to the hydrothermal solidification process. Their result showed better compressive strength and lower Cs leach rates compared with an OPC matrix. However, the research did not show that the end products via x-ray diffraction or the morphology of the crystalline phases using scanning electron microscopy. It is not clear where the Cs ion was residing in the matrix.. In another alkali-activated slag cement (AASC) study conducted by Xuequan et al. (1991), designed to absorb cesium, their experimental results demonstrated that AASC had low porosity and lower Cs leach rates than OPC, high alumina cement, and macro defect free cements. Nonetheless, it suffered high Cs leachability at 373°C. Also, the potential of forming zeolites was mentioned but the possibility was not confirmed. Therefore, AASC might have better physical and chemical properties than other cements, but it may not be a suitable host for the immobilization of high-level radioactive waste.

Jantzen et al. 1984 I and Jantzen, 1984 II proposed a waste form based on Portland cement plus radioactive waste produced during heat treatment at 1000-1200°C by single-phase substitutions of Cs and Sr for Ca, Si, and other cations. Several crystalline phases compatible with cement phases were identified, notably Ca zirconate, $CaMO_6$, and other major phases common to cement reaction. Leach testing indicated that the cement-based waste form was a potential candidate for high-level radioactive waste. However, incomplete reaction occurred at 1000°C and volitilization of Cs was noted at 1200°C. Incomplete reaction may cause phase

separation and volitilization will result in loss of radioactive Cs and corrosion of process equipment.

Hydrothermal hot-pressing of concrete-based high-level radioactive waste forms was suggested by Yanagisawa, et al. (1985). A high-level radioactive waste form containing silica was produced by the alkali (3-10N NaOH) activation of ?-quartz (70 wt%) and amorphous aluminosilicates (30 wt%). The composition of the waste was dominated by Fe_2O_3 oxide (40 wt%); and ~8 wt% each of MoO_3, Nd_2O_3 and ZrO_2. Other minor oxides of Sr, Cr, Ag, Cd, Sb and the rare earth elements were part of the waste. X-ray diffraction patterns revealed the presence of sodium aluminosilicates such as analcime ($NaAlSi_2O_6.H_2O$), ?-quartz, MoO_3, Nd_2O_3 and ZrO_2. The waste form produced in 30 minutes possessed excellent compressive strength and low-leach rate. The effects of NaOH concentration, reaction temperature and pressure and reaction time on the compressive strength, density, and weight-loss of the waste form were tested. It was concluded that the optimum condition resulted from the addition of 10 wt% $Al(OH)_3$ and 10N NaOH solution and processing at 350°C, 66 Mpa for 6 hours. In similar hydrothermal experiments, a mixture of strontium, ?-quartz and NaOH solution resulted in the formation of strontium silicates Yanagisawa et al, 1984, whereas a mixture of cesium, amorphous aluminosilicate with NaOH solution yielded pollucite ($CaAlSi_2O_6$) (Yanagisawa et al. 1984). Stone et al., (1979) summarized the pros and cons of alternative waste forms including hot-pressed concretes. The major advantage is their excellent long-term stability. Unfortunately, they have high-leachability and require large and costly hot-press equipment.

1.6 Hydroceramic Host Waste Forms

1.6.1 Introduction

The development of a potential host for the incorporation of any radioactive waste requires the development of an appropriate formulation, synthesis of the formulation and characterization of the resulting products to determine their chemical durability and physical and mechanical properties. Each component of the formulation is chosen so as to impact certain physical properties and/or chemical reactivity. The combined results of the preliminary study can then be used to arrive at the final formulation and the optimum levels of waste loading.

In an effort to develop an appropriate formulation for the immobilization of the INEEL calcine high-level nuclear wastes, several pozzolanic materials and other reactants were screened as potential starting materials for the proposed hydroceramic. A pozzolan is defined as a finely divided natural or man-made material that reacts with calcium hydroxide or alkali hydroxides to form compounds possessing cementitious properties. Examples of natural pozzolans include diatomaceous earth, volcanic ash, opaline shale, and tuff. Fly ashes originating from coal generating power plants are examples of man-made pozzolans. Information regarding their definitions, sources and bulk chemical compositions will be given in this section.

1.6.1.1 Fly Ash

Fly ashes are a finely segregated residue captured from the flue gas produced during the combustion of powdered coal. The clay, quartz and feldspar fraction of the coal melts in the combustion process and the small droplets solidify in the moving air stream as it exits the plants. This gives approximately 60% of the fly ash particles a spherical shape and amorphous character. The chemical composition of fly ash is as complex as the sources of the coal they are obtained from. Because this variability in chemical composition exists, only representative chemical composition of a few samples will be furnished, however information about their sources will be given.

Fly ashes are classified into two major types as specified in the ASTM C 618 on the basis of their chemical composition resulting from the type of coal burned; these are designated as Class F or Class C. Class F fly ash results from the burning of anthracite or bituminous coal. Class C fly ash is normally obtained from lignite or subituminous coal. Lime and SiO_2 + Al_2O_3 + Fe_2O_3 contents of Class C fly ash are typically higher than class F fly ash. The presence of free lime in Class C fly ash gives it cementitious properties in addition to pozzolanic characteristics. Representative chemical data and comparison for both Class F and Class C Fly ashes are listed in Tables 14. Table 1.5 lists the fly ashes and their sources used in the evaluation of the preliminary hydroceramic waste forms.

Table 1.4 Mineral admixtures by weight percent of typical Class F and Class C fly ashes [ASTM C 618].

Mineral Admixtures (%)	Class C Fly Ash	Class F Fly Ash
SiO_2 + Al_2O_3 + Fe_2O_3, minimum	>70	>50
SiO_3, maximum	5	5
Moisture content, Maximum	3	3
Loss on ignition, maximum	6	6
Available alkali as Na_2O	1.50	1.50
Calcium content	>10%	<10%
LOI	Very low LOI of < 1%	Typically contain > 3%
Major crystalline phases	Quartz, mullite ($3Al_2.2SiO_2$), and hematite	Anhydrite, tricalcium aluminate, lime, quartz, periclase (MgO), mullite, merwinite (Ca3Mg[Si2O8], and ferrite

Table 1.5. Fly ashes and their sources

Fly Ash	Source
Jim Bridger Fly Ash	Power Plant in Point of Rocks, WY
Riveside Fly Ash	Rivesville Power Plant, PA
Armstrong Fly Ash	Allegheny Power, PA
Riverside Fly Ash	MidAmerican Energy Co., Des-Moines, IA
Sherco Fly Ash	Northern States Power, Minneapolis, MN
Holtwood Fly Ash	PA Power and Light Co., Allentown, PA
Montour Fly Ash	PA Power and Light Co., Allentown, PA
Springerville Fly Ash	Tucson Electric Power, Tucson, AZ
Hatfield Fly Ash	Allegheny Electric, Greensburg, PA

1.6.1.2 Blast Furnace Slag

Ground granulated blast-furnace slag (from iron making industries) is defined as the granular material that is formed when molten iron blast furnace slag is rapidly air quenched by spraying it with water. It is a granular product that contains very limited crystal formation. It is highly cementitious in nature, it hydrates like cementitious material when ground to cement fineness (Mehta, 1980; Mehta, 1983; Lewis 1981; Virtanen, 1983). ASTM C 989-82 is one of the major specifications covering ground granulated blast furnace slag for use in concrete and mortar. The main advantages of using slag in hydroceramic formulations are: to provide reactive sources of silica and alumina, to decrease the water demand for mixing due to the increase in paste volume provided by the lower relative density of the slag (Hinczak, 1990), and to reduce permeability via the tranformation of large pores to smaller pores in the paste (Malhotra, 1987). All the aforementioned benefits increase with decreasing particle sizes. The three blast furnace slags used in this study are Reclime, NewCem and Koch slags. Reclime was obtained from Recmix of PA, Canosburg, PA; Koch slag was obtained from the Koch Mineral Company, Wichita, KS, with an approximately particle size of 8?m. NewCem was generously supplied by Blue Circle/LaFarge, Baltimore, MD.

1.6.1.3 Silica

MIN-U-SIL and silica fume silica sources provided the reactive quartz needed in the preliminary hydroceramic investigations. The MIN-U-SIL was obtained from the U.S. Silica Company (Berkley Springs, WV). It consists of 1.1?m particle size quartz particles, while CAB-O-SIL fumed silica is a fumed-silica obtained from Cabot Corporation, IL. Silica fume is normally a by-product of manufacturing silicon metal or ferrosilicon alloys. Silicon metal and alloys are produced in electric furnaces from quartz, coal and wood chips. The resulting vapor from this process is (SiO gas) which oxidizes at the top of the furnace and is then collected as silica fume. Silica fume consists mainly of amorphous (non-crystalline) SiO_2 with an average particle size of 10^{-2} times less than an average cement particle. Due to its fine particles, large surface area, and the high silica content, silica fume is a chemically reactive pozzolan. The CAB-O-SIL used is equivalent to silica fume but produced by flash calcinations of $SiCl_4$. It was used because it is purer, but for large-scale applications either fume could be used.

1.6.1.4 Natural Aluminosilicate Pozzolans

Three natural sources of aluminosilicate minerals used in this study were Engelhard kaolinite (Engelhard Corporation, Engelhard, GA), Wyoming bentonite (Wyo-Ben, Billings, MT) and Ashgrove troy Creek clay (Ashgrove Cement Co., Kansas City, A). The bulk composition of the calcined Troy clay is listed in Table 1.6. Wyoming

Table 1.6. Bulk composition of Troy Creek metakaolinite was made from kaolinite by calcining it at 750°C for 2-3 hours.

Major Component	Weight Percentage
Al_2O_3	33.10
CaO	0.20
Fe_2O_3	1.10
K_2O	0.60
MgO	0.20
Na_2O	1.20
SiO_2	49
LOI	14.50
Total	**99.00**

Bentonite is a swelling type clay. The degree of swelling in a clay is normally determined by the percent of the presence of smectite, cation-exchange capacity, and exchangeable sodium percentage.

1.6.1.5 Reactive Alumina Pozzolans

Three reactive alumina pozzolans used in this study were bohmite, Rhône Poulenc and Colloidal Alumina. Bohmite alumina (Cata? Pal D Alumina) contains 99.99% alumina and was obtained from Vista Chemical Company, Houston, Texas. Rhône Poulenc Alumina is a flash calcined alumina (Amorphous Alumina) obtained from Minerale Fine, France. Colloidal Alumina contains ~99% Al_2O_3 and was obtained from Pace Technologies, Northbrook, IL.

Following the establishment of the chemical reactivities and physical characteristics of several pozzolans, studies were conducted targeting the formation of aluminosilicates from these pozzolans. Siemer et al. (1998) combined the clay reaction process with FUETAP technology to form a mixture of zeolite minerals. Ashgrove Troy clay was mixed with various pozzolans. Aluminum metal was dissolved in concentrated NaOH solution to obtain Na:Al ratio of 3:1, the same ratio present in the INEEL as yet uncalcined sodium-bearing waste. In order to gauge the effects of common ion effects, Na_2CO_3 and/or $NaNO_3$ were sometimes substituted for NaOH. Nitrate salts of (Na, K, Ca, Fe, Al & Zr) were added to nitric and hydrofluoric acids and used in the formulations of other simulants. The chemical

compositions were similar to both INEEL radioactive liquid waste stored in tanks and calcined wastes stored in silos. These simulants were sugar-calcined at 500°C to destroy the majority of the nitrate present in the formulation. Sugar facilitates low-temperature calcinations and the conversion of most of the sodium nitrates in the waste to sodium carbonates. A minimum amount of water was added to the mixture of calcine and/or Sodium Bearing Waste and calcined Troy clay (metakaolinite) as needed to enable grouts to settle into molds at atmospheric and under steam pressure. The formulations were such that enable zeolite formation.

The mixture was put in a custom fabricated autoclave made from steel pipe (37 mm ID) and two 76 mm flanges along with a small amount of water. The molds holding the samples were held above water (i.e., not immersed in it) and processed at 200°C for several hours. At the end of reaction, the molds were removed from the autoclave and put back into the oven to remove unreacted water (dry the sample).

X-ray analysis of the sample processed at 2 hours revealed the presence of hydroxysodalite [$Na_8Al_6Si_6O_{24}(OH)_2.4H_2O$], Type A zeolite [$Na_{12}Al_{12}Si_{12}O_{48}(OH)_2.27H_2O$] zeolites and quartz ($SiO_2$). Quartz was present in the metakaolinite and as such persisted throughout the reaction. Cancrinite and quartz phases were obtained with specimens made from Na_2CO_3 and processed for 3.5 hours. The reaction of metakaolinite was determined to be incomplete because the x-ray diffraction pattern contained a noticeable amorphous hump scattering centered at ~20° 2T.

Results of several investigations were used to establish the physical and chemical properties and the rule of thumb for hydroceramic waste forms components in the glass-forming regions: the ratio of [MO-M_2O-M_2O_3-SiO_2 (1:1:1.1:1.8) [Gougar-Dunzik et al., 1998]. The reasons for maintaining glass regions in the hydroceramic formulation are two fold: to synthesize zeolite containing waste products for interim storage or direct burial in the proposed Nevada repository site; or the waste forms can be vitrified, converted to glass. The formulation contains less calcium than glass composition. The resulting products are zeolites that are chemically and physically compatible with the repository mineral assemblages. Consequently, hydoceramics are most unlikely to experience any long-term adverse chemical reactions once placed in a storage facility such as Yucca Mountain. Several advantages have been noted from hydroceramics as wasteform compared with the Environmental Assessment (EA) benchmark glass:

- converts ions to zeolites
- low water solubility
- compressive strength 4000-6000 psi
- waste loading from 25-45%
- always pass TCLP and PCT, for metals
- potentially self-curing under the radiation heat (90^oC) generated by the wastes
- presents dual options: hydroceramic-waste can be stored as is or HIPped into glass if the need arises

Hydroceramic is a concrete-like solid that owes its physical properties to the interlocking of hydrated feldspathoid mineral assemblages (cancrinite and sodalites) and zeolites (natural analogs). The properties of hydroceramic waste forms include: compressive strengths of 4000 to 6000 psi, potential for high waste loading of 25-45%, passing Toxicity Charactersitic Leaching Procedure (TCLP) for toxic metals such as cadmium and hexavalent chromium that are not easily retained by encapsulated ceramic and glass; (ASTM E: 1908-97) easy to pass 28 MCC-1 for MO, M_2O_3, MO_2 metals (ASTM C: 1220-98); and surpassed the Product Consistency Test (PCT) tests requirements (ASTM C: 1285-97). The PCT was developed by the Department of Energy's Savannah River site to provide quality control to the operator of high-level waste glass making facilities. The PCT is used to determine the hot water solubility of crushed and sieved particle sizes between 74 and 150 ?m size powders of a sample in the ratio of 10:1 sample to distilled water, at 90°C for seven days. The data can be compared with similarly treated Environmental Assessment (EA) benchmark glass. The rate of dissolution is determined by measuring the concentrations of the major component ions in the leachate. For intra- and intercomparisons of samples, specific conductance of the leachate is monitored. A sample is acceptable if its solubility is lower than that of the standard EA glass (Document WSRC-TR-92-346, Revision 1, June 1, 1993). The PCT is designed to simulate the release of species present in a waste into the groundwater system at elevated temperature similar to those expected in a repository.

The main disadvantage of a hydroceramic waste form is that it is unable to accommodate large amount of nitrate, sulfur, or chloride ions. However, this should not necessarily be considered a disadvantage because the INEEL waste contains very small amount these ions and SBW can be calcined and used as a source of NaOH to activate the reaction.

1.7 Nature of the INEEL Calcined High-Level Radioactive Wastes

The Idaho National Engineering and Environmental Laboratories (INEEL) has long been known to engage in nuclear research which include designing and testing prototype nuclear reactors for military and commercial applications (Gougar-Dunzik, 1997). These reactors produced spent fuel, which were reprocessed to extract fissionable uranium (Mann and Todd, 2000). Concentrated nitric acid was used to dissolve the spent fuels and claddings. Uranium and plutonium were extracted from the solution resulting from the dissolution of spent fuels originating from these experimental reactors alongside those that result from military activities. The liquid waste consists of oxides and fluorides of cladding elements primarily aluminum and zirconium and nonradioactive elements added as processing agents notably Al, B, Cd, and Na (Siemer. 1995).

Ninety percent of the mixture was then calcined at 500°C into sand-like powders to reduce volume for interim storage in binsets until proper immobilization/disposal methods are available. The remaining uncalcined 10% is termed sodium-bearing

waste (SBW). The main reason for not calcining the sodium-bearing waste is due to its high content of sodium that limits calcination efficiency. Agglomeration occurs at the bottom of the reactor (Gougar-Dunzik, 1997). It should be noted that both calcines and the SBW wastes are similar in the concentrations of their toxics, fission products and transuranic elements (TRU). They are both classified as mixed wastes due to the presence of nonfission RCRA toxic metals such as hexavalent chromium, mercury, cadmium and lead (Siemer et al., 2000). Table 1.7 shows the composition, chemical and physical characteristics of the calcines. The color of the calcine ranged from white to yellow or brown and contains mainly poorly soluble inorganic phases (Siemer, 1995).

The calcined wastes are of three major types: alumina calcine consisting of predominantly 90% alumina; zirconia calcine containing ~50% CaF_2 and CaO balanced mostly by alumina and zirconia; and fluorinel-blend calcine originated mainly from zirconia calcine diluted with sodium nitrate and ß-alumina. Tables 1.8 and 1.9 represent the bulk chemical components of fluorinel blend calcine and zirconia calcine. Examination of the two tables revealed that the compositions of the wastes are similar except that fluorinel belend calcine contains substantial amount of cadmium. These calcines generate approximately 0.033 watt/kg in comparison with the British/French high-level waste with 10-35 watts/kg being vitrified (Siemer, 1995). In this study, fluorinel and zirconia calcines were used as two representative wastes. Aluminum content was varied over a wide range representing the possibility of blending these calcinations with the third (nearly pure Al_2O_3).

Table 1.7. Characteristics of the calcined high-level nuclear waste at the INEEL.

	(Dry Calcine)
Quantity	~3800 m^3 or ~5100 tons
Composition	Mostly CaF_2, Al_2O_3, ZrO_2, CaO, etc.
^{90}Sr	? 3800 Ci/m^3 (25 Watts/m^3)
^{137}Cs	? 4200 Ci/m^3 (21 Watts/m^3)
TRU	3000 nCi/g (~27 kg Pu)
Toxics	some Cr as Cr^{VI} ~1.5×10^5 kg Cd, Hg (?)

Table 1.8. Simulated zirconia calcined high-level radioactive waste. (Adapted from the MSDS sheet for Run 64, Run 74, and Run 17, Pilot Plant Calcine. V.C. Maio (208) 526-3696.

Principal components	Approximate weight percent
Al_3O_3	6-90
B_2O_3	0.5-3.5
CaO	3.5-13.5
CaF_2	38-55
Cr_2O_3	1-1.4
Fe_2O_3	0.03-10
Gd_2O_3	0-6
Hg	0-3
PO_4^{-3}	0-0.5
KNO_3	0-6
K_2O	0.5-1.5
$NaNO_3$	0-6
Na_2O	3-6
SO_4^{-2}	0.3-6
ZrO_2	17-26

Physical Data

Boiling point = N/A; Vapor pressure = N/A; Vapor density = N/A
Melting point = 1000°C
Density (specific gravity) = 1.4 g/mL
Evaporation rate = N/A
Solubility = 50% in water

Table 1.9. Simulated fluorinel blend calcined high-level radioactive waste containing cadmium. (Adapted from the MSDS sheet for Run 20 and Run 17, Pilot Plant Calcine (Cadmium). V.C. Maio (208) 526-3696.

Principal components	Approximate weight percent
Al_2O_3	6-90
B_2O_3	0.5-3.5
CdO	5.8
CaO	3.5-13.5
CaF_2	38-55
Cr_2O_3	1-1.4
Fe_2O_3	0.03-10
Gd_2O_3	0-6
Hg	0-3
PO_4^{-3}	0-0.5
KNO_3	0-6
K_2O	0.5-1.5
$NaNO_3$	0-6
Na_2O	3-6
SO_4^{-2}	0.3-13
ZrO_2	17-26

Physical Data

Boiling point = N/A; Vapor pressure = N/A; Vapor density = N/A
Melting point = 1000°C
Density (specific gravity) = 1.4 g/mL
Evaporation rate = N/A
Solubility = 50% in water

1.7.1 Uniqueness of the INEEL high-level Radioactive Wastes

Of major concern is the isolation of high-level radioactive waste containing cesium and strontium from the biosphere by both physical solidification and chemical stabilization (Flynn et al., 1979). The reason for the difficulty in the isolation of Cs and Sr ions is their mobility and, in addition, their activity. This translates to waste forms/packages characterized by high leaching rate and highly mobile ions. The activity of the fission products ^{137}Cs and ^{90}Sr are of major concern during the first century of burial because of the serious damaging effects associated with their high activity, heat, and radiations (Odoj et al., 1979; Haggerty, 1983). Consequently, their isolation presents immediate problem and future challenge.

From the environmental and health perspectives, nonradioactive elements that are included in the radioactive wastes could pose some risks if injested beyond a certain concentration limit, for example, chromium, mercury and cadmium. The hexavalent, Cr^{VI} chromium is highly toxic (Bajt et al., 1993; Lee et al., 1995; USEPA 1985a; USEPA 1991e), producing liver and kidney damage, internal hemorrhage and respiratory disorder. Cadmium has been a major health concern since many people had suffered adverse health effects on kidney and bone diseases from consuming rice grown from contaminated rice paddies (Kobayashi, 1978; Tsuchiya, 1978; Nogawa, 1984; Nogawa et al., 1987; EPA 1985a). Inorganic mercury if injested above 2 µg/L can cause stomach tumors (Schoeny, 1996).

The INEEL radioactive wastes are mixed wastes containing radionuclides notably ^{137}Cs and ^{90}Sr, nonradioactive and regulated RCRA metals such as Hg, Cd, and Cr^{VI}, and anions NO_3^-, SO_4^{2-}, Cl^-, F^- that need to be simultaneously immobilized in waste forms. The radionuclides are subject to the Nuclear Regulatory Commission regulations and the toxic metals to the Environmental Protection Agency (EPA) regulations. The wastes are laden with sodium, a nonregulated element in the form of $NaNO_3$.

The reason sodium may be of concern is its high dissolution rate in most natural minerals and the subsequently destruction of their chemical structures once Na is leached. Therefore, the main problem of the INEEL wastes is finding host waste forms that will chemically stabilize and physically contain all the cations and anions at the same time. The waste forms must in effect satisfy both the Nuclear Regulatory Commission regulations and the EPA guidelines.

1.8 Research to Date in Hydroceramic

Research involving different grout compositions to develop an appropriate formulation to synthesized rock-like monoliths have been undertaken at the Materials Research Institute, The Pennsylvania State University.

A hydroceramic is a chemically bonded ceramic, more specifically, it is an alkali-activated cementitious material prepared by the action of alkali, nominally sodium,

with aluminosilicate pozzolans. It is designed to form zeolitic monoliths by the proper selection of pozzolanic materials to form a low-soluble cryptocrystalline-mineral assemblage waste form consisting of aluminosilicates or zeolites notably NaP1, canrinite and sodalite that are capable of being hydrothermally synthesized at relatively low-temperatures (Siemer, 2000).

A hydroceramic waste form possesses all of the inherent mechanical, chemical and physical properties of FUETAP concrete-based waste forms. A hydroceramic formulation is specifically targeted within the glass compositional regions (Gougar, 1997) to form aluminosilicates of which are thermodynamically stable in anticipated repository geological environments. Vermiculite and dehydroxylated metakaolinite were introduced to specifically adsorb Cs and Sr by ion exchange processes.

1.8.1 Preliminary Work

The concept of hydroceramic has been used by the British Nuclear Fuel (BNF) for the solidification of low- to high-level nuclear waste since 1950. To date they have processed up to 30,000 m^3 by volume, and over 140 distinguishable waste streams with radioactive heat generation rate of 500 watts/m^3 (Palmer, 1990). Progressions of experiments with improvements have been conducted in the U.S. for the acceptability and efficacy of the technology to safely dispose of the INEEL waste (Roy and Gouda, 1978; Moore, 1979; Xi et al., 1995; and Siemer et al., 1995, Siemer et al., 2000).

Previous research has demonstrated the viability of transforming the INEEL calcine waste into a solid monolithic body by the addition of selected pozzolanic materials to the calcines and processing the mixtures under relatively low-temperature hydrothermal conditions (Siemer et al., 1998; Gougar-Dunzik et al., 1996; Grutzeck and Siemer, 1997). Several pozzolanic materials ranging from simple to quite complex were tested in an effort to develop optimum formulation that will yield durable waste form for the INEEL wastes.

1.8.2 Fly Ash Pozzolan Experiments

Fly ashes are an inexpensive and readily available source of amorphous silica and alumina that can be made chemically reactive with alkali activation. Origins of different fly ashes used in this preliminary study have previously been given. Each fly ash was mixed with the same chemical components. The main purpose of using different fly ashes was to compare the properties of the resulting grouts with respect to their physical characteristics (density and porosity) and chemical durability (low or high leachability).

Fly ash pozzolan experiments were performed by mixing 25 g of the pozzolan with 11 g (13M) NaOH with waste simulant solution containing 11.5M NaOH, 1.50M $NaNO_3$ and 0.069M CsCl. Sodium concentration in the mixture was equivalent to 6.5% by weight. The “as prepared” mixture was thoroughly kneaded to produce a dough-like paste, put into an autoclave, cured at 70°C for 10 minutes to stiffen the

grout prior to autoclaving. As prepared implied that a grout was not dewatered even if excess water was present before autoclaving. The grout was put in a preheated oven at 200°C and processed for 7 hours. The modified PCT test (5 hours) was conducted on the resulting sample.

The results of the experiment showed that Riveside fly ash and Reclime slag were unsuitable because they formed, or contained high percentage of sand-size particles. The final products exhibited higher porosites, lower density and possibly higher leachability due to the presence of large particles in the matrix. They failed to form stiff doughs even after precured at 70°C.

The Hatfield and Holtwood fly ashes (both from Allegheny Electric Co., PA) produced physically desirable grouts which became hard and dense hydroceramics after curing. However, large amounts of water were required to make the grouts. The results of PCT testing yielded a conductivity of 81 ? S/cm for both samples. Since sodium is the most easily leached ion, it tend to come out of the hydroceramic rather easily, conductivity of the leachate was often used to screen results. This value corresponds to the loss of 24% of the original 6.5% sodium in the original hydroceramic grout and a mean conductivity of 120 ? S/cm.

The PCT test solutions obtained were all analyzed using ICAP. About 1200-1300 ppm of sodium leached out of these grouts. The percent of sodium leached out was calculated using the initial sodium concentration as a reference as follows: (1200 or

(1300 ppm)/(0.0065)*1x10^{-6} = 18.5% sodium leached The ICAP analytical results are summarized in Table 1.10.

The concentration of sodium and cesium leached from both samples were similar. Cesium may have been converted to aluminosilicate or possibly pollucite as indicated by the low concentration. Hatfield fly ash containing grout leached about 14 times more sulfate than the equivalent Holtwood grout. In conclusion, both hydroceramic samples containing Hatfield and Holtwood fly ashes were rejected from further investigation because their large water demand.

Other fly ashes tested were Springerville fly ash, the Riverside fly ash, the Montour and Sherco fly ash. The Springerville fly ash grout hardened during precuring at 70°C resulting in a moderately hard final product. The conductivity of the PCT solution of the specimen was 8.10 mS/cm or 36% (0.103M) of 0.028M leached Na.

Riverside fly ash is a Class C fly ash and hardening began before it was put in a pre-curing bath at 70°C. It had a similar leaching characteristic as that of the Springerville fly ash. The Montour fly ash grout did not hardened during initial precuring process however, it resulted in a hard rock-like material at the end of the processing time. The conductivity of the PCT solution of the specimen was 5.20 mS/cm or 13% leached Na. The Sherco fly ash containing grout showed considerable hardening before putting it into the precuring bath where hardening proceeded very rapidly. However, the resulting final product failed to harden adequately. The final product had a very poor leachability of 16.7 mS/cm.

Table 1.10. Analytical results of the leachates from Hydroceramic made from Hatfield and Holtwood fly ashes.

Ions	Hatfield Power Percent & Concentration Leached (ppm)	Holtwood Percent & Concentration Leached (ppm)
Na	1200 ppm	1200 ppm
Nitrate	20% (470 ppm)	25% (500 ppm)
Cs	0.35% (0.70 ppm)	0.35% (0.70 ppm)
Sulfate	760 ppm	55 ppm

Riverside fly ash is a Class C fly ash and hardening began before it was put in a pre-curing bath at 70°C. It had a similar leaching characteristic as that of the Springerville fly ash. The Montour fly ash grout did not hardened during initial precuring process however, it resulted in a hard rock-like material at the end of the processing time. The conductivity of the PCT solution of the specimen was 5.20 mS/cm or 13% leached Na. The Sherco fly ash containing grout showed considerable hardening before putting it into the precuring bath where hardening proceeded very rapidly. However, the resulting final product failed to harden adequately. The final product had a very poor leachability of 16.7 mS/cm.

The above physical and chemical results of the five fly ashes showed that none of the grouts made with them was durable enough to be a good host for the INEEL high-level radioactive waste. Some are physically weak and/or chemically unsuitable due to leaching of high Na concentrations.

A sample was made using the same formulation using Troy clay (metakaolinite) instead of fly ash. The bulk composition of the liquid waste simulants and clay are listed in Tables 1.11 and 1.12, respectively. The conductivity measurement of the PCT solution was 41 ? S/cm, corresponding to 12% of the initial sodium.

Hydroceramics made from Montour and Riveside fly ashes were among the best. They yielded compact monolithic and chemically durable hydroceramics as did the calcined Troy clay containing products. Armstrong and Riveside fly ashes contained

Table 1.11. Major components of liquid waste simulant (Siemer et al., 1998).

Component	Molarity
H^+	0.77
Al	0.337
Ca	0.028
Sulfate	0.026
F	0.036
Fe	0.012
K	.0108
Na	1.10
Nitrate	2.98

Table 1.12. Major composition of Ashgrove Troy clay (Siemer et al., 1998).

Component	Weight %
Al_2O_3	28.20
SiO_2	42.70
Na_2O	12.60
K_2O	2.51
Carbonate	6.87
CaO	2.21
MgO	0.62
B_2O_3	0.13
Sulfate	1.16

large proportion of unburned carbon requiring extra water to make grouts. Overall, the fly ashes containing hydroceramics were rejected because their products requires large amount of water, contained so much unburnt carbon as to make their chemistry inconsistent and potentially troublesome to establish on a day-to-day basis.

1.8.3 Behavior of the Simulated INEEL Waste in Hydroceramic Prepared with Various Pozzolanic Media

The aim of these experiments was to understand the dissolution and transportation of the major components of cacined wastes, notably CaF_2, ZrO_2, Al_2O_3 and CaO from the zirconia, alumina and fluorined calcine waste. All the three waste types were dissolved in water and the conductivities of their leachate solution measure to determine how many ions will be released. Three experiments were performed to gauge the behavior of these calcines under hydroceramic processing conditions.

1.8.4 Experiments with Simulated Zirconia Calcine Waste

Experiment I. About 0.50 g of “as received calcined” zirconia calcined waste with particle size ~0.20-0.50 mm in diameter was added to 20 mL of distilled water and stirred for 5 hours. The as received experiment was geared toward determining how many ions will be released in comparison with particle sizes less than as received calcines.

Experiment II. One-half gram of ground and sieved calcine waste (75µm size) was added to 20 mL of cold water and stirred with a magnetic stirrer for 5 hours. A 6M concentration of HCl was used to dissolve the same amount and particle size. These two experiments were meant to compare "as received" with ground and sieved particles with larger surface areas.

Experiment III. One-half gram of ground and sieved calcine waste (75µm size) was added to 20 mL of 90°C water and stirred with a magnetic stirrer for 5 hours. A 2M concentration of NaOH was used to dissolve the same amount and particle size at 90°C. This particular experiment was aimed at understanding the chemical processes that may be taking place in a hydroceramic cured or processed at 90°C. A 6M concentration of HCl (20 mL) at 90°C was used to dissolve the same amount and particle size.

At the end of reaction times (5 hours), the leachates from each sample were analyzed and compared with those obtained from the HCl experiments. The results showed that the leachates analyzed from cold and 90°C water for both "as received" and ground experiments did solubilize very small aluminum concentrations. The amount of aluminum released from cold and hot water experiments were normalized to those of the HCl in each experimental category to arrive at 0.004, 0.005 and 0.028M, respectively.

The hot NaOH solubilize about 10% of the aluminum probably due to the presence of a high concentration of calcium in the calcine. As for the 6M HCl experiments, only 25% of the initial sodium concentration was released in both experiment numbers II and III. Sodium was absent (below detection level) in the experiment conducted at room temperature.

The fraction of the total calcium released increased from experiment I to III. They were 2, 4, and 11% of the total calcium. The concentrations of the strontium fractional release (10%, 20%, 35%) from the three water-experiments were more than the calcium. Only 25% of the initial total nitrate was released from the cold-water and as received calcine and hot-water mixed with the 75µm size experiments.

The analytical results of the other leachant tests showed that all of the nitrate had been released. Sulfate ions tend to dissolve slowly. However, hot water coupled with smaller particle sizes later facilitates dissolution of it all. Calcium sulfate was the major component that was very soluble in all the three-water experiments. It can be argued that NaOH suppressed the solubilities of Fe, Ca, and Sr with respect to ordinary water. Amazingly, the fractional release of aluminum and zirconium were the same (~10%). All the water experiments leached out only trace amounts of zirconium.

The chemical behaviors of zirconia calcine with waste have been elucidated in different media under different experimental conditions. Zirconia was thought to be

an inert and refractory compound. However, a small fraction of it can be released in alkaline solutions at 90°C and perhaps more during hydroceramic processing at higher autoclaving temperatures and times.

1.8.5 Pozzolan Substitution of Alumina Experiments

This investigation was carried out to gauge the sources of alumina from three alumina samples: coarsely-powdered Rhone Poulenc amorphous alumina (RPAA), colloidal alumina and boehmite alumina. Three experiments each containing 0.973 g of 5µ Minusil mixed with 0.649 g of alumina and 1.012 g of liquid waste simulant were performed. The minusil is a high purity, high quality natural crystalline silica. This white ground silica sand is inherently inert, has low moisture content and is at least 99.2% SiO_2. The gross compositions of the liquid waste used in this experiment were 11.50M NaOH, 1.50M $NaNO_3$ and 0.069M CsCl. Overall, the gross composition of each grout-type was approximately 24% water, 24% alumina, 11% soda oxide and 2.60% nitrate. All the components were mixed together, put in a brass mold, wrapped with tin foil, precured at 70°C and processed at 200°C overnight. Each sample was withdrawn and drilled out of the mold in a powdered form. A PCT test was conducted on the leachate from the 1 part powdered sample to 10 part distilled water at 95°C. The fractional leachate of sodium salts were compared to the standard derived from $NaNO_3$/water solution. Nitrate concentration was analyzed by spectrophotometry via reaction with phenoldisulfonic acid to make yellow dye. The

results of the percent of sodium and nitrate leached from the three different alumina sources are summarized in Table 1.13.

The percentages of sodium and nitrates leached from the three alumina sources were varied. Boehmite alumina source showed low-leachability percentages for both sodium and nitrate. Colloidal alumina performed worst of all. The three alumina sources in terms of nitrate release, however, outperformed Rhone Poulenc alumina source with respect to sodium.

1.8.6 Fluorinel Blend Calcined Experiments

Fluorinel blend calcine waste contains more sodium, cadmium and residual nitrate than the rest of the wastes. Three different grouts were made with fluorinel particles moistened and blended with the back of a mixing spoon. Troy clay, a source of aluminum and silicon was added together with 0.195 g of boehmite alumina. Boehmite alumina was chosen because of its excellent performance in "Zirconia" Pilot Plant in experiments previously described. About 0.032 g of sodium sulfide was added to each of the three specimens to chemically reduce the concentration of chromate present in the calcine. Experience showed that microencapsulation of chromate in the crystallized sodalite and cancrinite phases will not retain all the available chromate. The effects of NaOH, an activator in the reaction processes, was gauged in this experiment by varying its concentrations in the grouts. Specimens were prepared, cured and leached following the procedures previously stated.

Table 1.13. Percent of sodium and nitrate leached from the three hydroceramics made with alumina sources.

Reactive Alumina Source	Percent of Na Leached	Percent of NO_3^- Leached
Rhone Poulenc Alumina	3.80 %	6.10 %
Colloidal Alumina	3.10 %	11.0 %
Boehmite Alumina	2.60 %	2.0 %

The concentrations of NaOH in the mixture ranged from low to high in the ratios of the total alkali:calcium:alumina:silica atoms (Table 1.14).

The resulting products from the three grouts were exceptionally hard samples.

The percentages of sodium and nitrate leached during the PCT tests as a function of NaOH concentration is shown in Table 1.15.

Increasing NaOH concentrations in the grouts resulted in the decreasing percent of sodium leached. One justifiable explanation for the NaOH and sodium correlation is their conversion to feldspathoids in the higher NaOH products. Nitrate did not show any trend with NaOH concentrations. The measured conductivity for all the specimens were similar.

1.8.7 Pozzolanic Study: Ground Bottle Glass Experiments

One grout was prepared with 0.973 of ground bottle glass, 0.324 g of RPAA, and 0.46 mL of sodium bearing liquid waste (11.50M NaOH, 1.50M NaNO3 and 0.069M CsCl). The grout did not have an adequate consistency and therefore lacked the physical attributes of a good pozzolan because the glass frits were too coarse. The PCT test of the leachate solution revealed that 29% and 10% of the initial amount of sodium and nitrate added to the simulant leached out. The reason for using the amount of sodium added to the simulant (as the initial sodium) was that the sodium

Table 1.14. Table showing variable NaOH concentrations with their corresponding alkali:calcium:alumina:silica leached.

Relative NaOH Concentration	Percent of alkali:calcium:alumina:silica leached
Low NaOH Specimen	1.0:0.37:2.70:2.70
Medium NaOH Specimen	1.0:0.22:1.59:1.59
High NaOH Specimen	1.0:0.13:1.13:1.13

Table 1.15. Percent of sodium and nitrate released with respect to NaOH concentration in the grouts.

Relative NaOH Concentration	Percent of Na Leached	Percent of NO_3^- Leached
Low NaOH Specimen	10.30 %	12.0 %
Medium NaOH Specimen	5.80 %	41.0 %
High NaOH Specimen	4.30 %	22.0 %

concentration in the glass was unknown and may not have been sufficiently available for reactions.

1.8.8 Fluorinel Blend Calcine Experiments with NaOH and Na_2S

Seven specimens were made with "Fluorinel" blend calcine waste simulant and the addition of other components. Specimens made from experiment II through experiment VII contained 0.649 g calcine plus extra 0.233 g of NaOH and 0.050M of Na_2S.

Experiment I. Specimen #1 consisted of calcine waste, 0.13 g of soda, 0.973 g of NewChem furnace slag and 0.448 g of distilled water. The ratio of alkali:calcia:alumina:silica was 1.0:2.29:0.69:1.17. The resulting grout was very dense and hard with excellent physical characteristics however, it exhibited poor leaching behavior.

Experiment II. Specimen #2 consisted of calcine waste, NaOH, sodium sulfide, 0.863 g of metakaolinite and 0.668 g of distilled water. The ratio of alkali:calcia:alumina:silica was 1.0:16.0:1.15:1.12. Similar to specimen one, the resulting grout was very dense and hard with excellent physical characteristics but with improved leaching behavior.

Experiment III. Specimen #3 was made from a mixture of calcine waste, NaOH, sodium sulfide, 0.649 g of 5-micron minusil, 0.389 g of RPAA and 0.597 g of

distilled water. The total ratio of alkali:calcia:alumina:silica was 1.0:16.0:1.28:1.51. The product exhibited a fairly hard specimen and a good leaching behavior.

Experiment IV. Specimen #4 contained a mixture of calcine waste, NaOH, sodium sulfide, 0.649 g of 30-micron minusil, 6 grains of RPAA and 0.597 g of distilled water. The total ratio of alkali:calcia:alumina:silica was 1.0:16.0:1.28:1.51. The chemical composition was similar to specimen #3 except that the particle size of the minusil used in experiment IV was larger than that used in experiment III. The product exhibited the same physical and chemical durability as in experiment III.

Experiment V. Specimen #5 formulation consisted of a mixture of calcine waste, NaOH, sodium sulfide, 1.232 g of Troy clay. The total ratio of alkali:calcia:alumina:silica was 1.0:0.24:1.28:1.72. The resulting grout was very hard with fair leachability.

Experiment VI. Specimen #6 contained a mixture of calcine waste, NaOH, sodium sulfide, 1.232 g of Troy Clay. The total ratio of alkali:calcia:alumina:silica was 1.0:0.24:1.52:1.54. The grout was physically hard with improved leachability over specimen #1.

Experiment VII. Specimen #7 was made from a mixture of calcine waste, NaOH, sodium sulfide, 0.649 g of silica fume and 0.389 g of RPAA. The total

atomic ratio of alkali:calcia:alumina:silica was 1.0:16.0:1.28:1.51 with moderate to poor leachability.

Table 1.16 contains the summary of sodium and nitrate percent released from each specimen. Results showed that the specimen made from experiment III exhibited the best chemical durability due to the low percentage of sodium and nitrate leached. On the other hand, specimen 1 possessed the worst chemical durability and would not be a good host for the INEEL wastes.

1.8.9 Additional Pozzolan Experiments

Experiments with a mixture of pozzolans containing the same simulant solution were prepared. The pozzolan formulation was analogous to that of metakaolinite (~40% Al_2O_3). Rhône Poulenc Amorphous Alumina was used as aluminum supplement for the aluminum deficient materials. Waste loading was correspondingly increased to reflect the increase in aluminum concentrations. All but one specimen contained 1.17 g or 1.17g of the 13M simulant and a mixture of 1.621 g of pozzolan powders. The final product resulted in 8.90% Na, 2.80% NO_3^- and 0.27% Cs, assuming no water loss. The alkali/alumina ratio was approximately 1:1, a maximum waste percent loading. The final specimens were precured, autoclaved and leached under the PCT test conditions.

One of the grout specimens did not make it past the precuring stage because it lacked the consistency required to make a hard and dense product. It contained 0.065

Table 1.16. Percentage of sodium and nitrate leached in Fluorinel blend experiments with NaOH and Na_2S.

Specimen Number	Alkali:calcia:alumina:silica	Percent of Na Leached	Percent of Nitrate Leached
I	1.0:2.29:0.69:1.17	33.0 %	55.0 %
II	1.0:16.0:1.15:1.12	4.90 %	23.0 %
III	1.0:16.0:1.28:1.51	4.70 %	9.20 %
IV	1.0:16.0:1.28:1.51	4.70 %	14.0 %
V	1.0:0.24:1.28:1.72	8.80 %	35.0 %
VI	1.0:0.24:1.52:1.54	6.40 %	23.0 %
VII	1.0:16.0:1.28:1.51	12.70 %	52.0 %

g of silica clay (96% SiO_2, 2.8% Al_2O_3) mixed with 0.649 g of Rhône Poulenc amorphous alumina and 1 mL of extra distilled water. The details of the six successful experiments are given below.

Experiment VIII. Specimen #8 was prepared by mixing 1.362 g of Montour fly ash with 0.26 g of Rhône Poulenc amorphous alumina and 1.17 g of waste simulant. The green body was initially sloppy but finally cured into a fairly hard rock with good chemical durability as determined from the PCT leach test.

Experiment IX. Specimen #9 contained 1.17 g of Montour Fly Ash, 0.26 g of Rhône Poulenc amorphous alumina, 0.195 g of condensed silica fume and 1.17 g of waste simulant. Swelling and expansion of the specimen occurred during the precuring processes that resulted in a sloppy product. The specimen was subjected to vibration, autoclaved and then leached.

Experiment X. Specimen #10 was prepared from mixing 0.649 g of Montour Fly Ash, 0.649 g of Rhône Poulenc amorphous alumina, 0.973 g of condensed silica fume and 1.17 g of waste simulant kneaded into a stiff dough-like product. Expansion of the product occurred during both precuring and auctoclaving stages. A significant amount of the sample was lost from the mold during the processing time. Expansion and loss of sample are fatal flaws not needed during a radioactive waste solidification process. The PCT result was very encouraging. However, it may be in part due to loss of sample during the autoclaving step and not to be trusted.

Experiment XI. Specimen #11 had 1.362 g of Troy clay, 0.26 g of Rhône Poulenc amorphous alumina and 1.17 g of waste simulant. The sample was successfully precured and autoclaved.

Experiment XII. Specimen #12 contained 1.621 g of pure Engelhard metakaolinite, 1.17 g of waste siumlant and 0.26 g of water. The mixture was kneaded into a stiff-dough with the addition of distilled-water.

Experiment XIII. Specimen #13 had 0.973 g of silica flour, 0.649 g of Rhône Poulenc amorphous alumina and 0.876 g of waste simulant. Waste simulant of 1.17 g resulted in a sloppy specimen. The specimen did not set during the precuring stage. It was then covered with copper foil and processed. The final product was fairly hard upon inspection.

Table 1.17 showed that no specimen was capable of retaining Na, Cs and NO_3^- simultaneously. Their capability to immobilize sodium was nearly the same. Specimen number 9 was the best at retaining Cs, poor for Na and fair for NO_3^- immobilization. Grout number 13 was best at retaining NO_3^- and Na and good at immobilizing Cs.

The effects of fly ashes mixed with calcine clays were gauged on Fluorinel blend waste. The fraction of the solid part of the formulation include 1.621 g of pozzolan to

Table 1.17. Percentage and concentrations of sodium, nitrate and cesium leached in Fluorinel blend calcined experiments with pozzolans.

Specimen No.	Percent and Concentration (ppm) of Na Leached	Percent and Concentration (ppm) of NO_3^- Leached	Percent and Concentration (ppm) of Cs Leached
IIX	3.60% (330 ppm)	2.20% (61 ppm)	0.11% (0.30 ppm)
IX	3.80% (341 ppm)	5.70% (160 ppm)	0.10% (0.028 ppm)
X	363 ppm	116 ppm	0.22 ppm
XI	3.60% (330 ppm)	4.90% (138 ppm)	0.10% (0.30 ppm)
XII	3.90% (350 ppm)	18% (510 ppm)	0.07% (0.2 ppm)
XII	2.80% (209 ppm)	1.40% (33 ppm)	0.28% (0.64)

1.17 g of 13M sodium-bearing liquid waste. The specimens were mixed, precured for approximately 30 minutes in a 90°C water bath and autoclaved at 200°C for 3 hours. The specimens were leached for approximately 5 hours. The detailed descriptions of the four specimens formulation are given below.

Experiment XIV. Specimen 14 contained 1.362 g of Montour Fly Ash, 0.26 g of Rhône Poulenc amorphous alumina and 1.17 g of waste simulant and resulted in a very sloppy grout.

Experiment XV. Number 15 grout had 1.362 g of Jim Bridge Power Plant Fly ash, 0.26 g of Rhône Poulenc Amorphous Alumina and 1.17 g of waste simulant. Again, it resulted in a very sloppy grout as in specimen 4.

Experiment XVI. The grout #16 contained 1.362 g of Ashgrove's calcine Troy clay, 0.26 g of RPAA and 1.17 g of waste simulant. The final specimen had a wet consistency.

Experiment XVII. The 17th specimen consisted of 1.17 g of calcined Wyoming bentonite, 0.454 g of RPAA and 1.17 g of waste siumulant. The specimen expanded during precuring and autoclaving stages. The phenomena was common to both specimens made from calcined and raw bentonite. Invariably, the resulting products were soft and porous. The PCT of the final product was good.

Tabulated results of the effects of mixing fly ashes with calcined clays showed that no specimen was capable of retaining Na, Cs and NO_3^- simultaneously (Table 1.18). All but specimen #15, have the same capability to immobilize sodium. Cesium was well retained by all the grouts. Specimen number 15 was the best at retaining Cs and worst at immobilizing both Na and NO_3^-.

1.9 Summary

The final selection of pozzolanic materials has a critical impact on the physical properties and chemical durabilities of the resulting hydrated hydroceramic product. The selection of the formulation was based on the ease of processing, consistency of chemistry, physical properties and chemical durability of the final product. These attributes must be met for a pozzolan to qualify as a reactant for hydroceramic formulation.

The fly ashes were rejected based on one or more of the following reasons. Their grouts required a large water demand and had sand-like particles that resulted in low-density and highly porous products. Chemical durability tests via the PCT test showed that high concentration of leachates were released. Ground, bottled glass pozzolan containing hydroceramics were rejected because their products were very weak due to the large particle size of the powder.

The calcined high-silica pozzolans required a large quantity of water. Incomplete oxidation coupled with gas evolution (probably hydrogen) during precuring stage

Table 1.18. Percentage and concentrations of sodium, nitrate and cesium leached in Fluorinel blend calcined experiments with mixture of fly ashes and calcined clays.

Specimen No.	Percent and Concentration (ppm) of Na Leached	Percent and Concentration (ppm) of NO_3^- Leached	Percent and Concentration (ppm) of Cs Leached
14	3.40% (308 ppm)	1.40% (38 ppm)	0.04% (0.11 ppm)
15	16.70% (1496 ppm)	8.60% (240 ppm)	0.03% (0.09 ppm)
16	4.60% (407 ppm)	5.90 (165 ppm)	0.06% (0.18 ppm
17	3.70% (330 ppm)	1.90% (51 ppm)	0.13% (0.34 ppm)

plagued the silica fume products. The advantage of silica fume is that it is very reactive and its flash-setting time is a good factor for accelerating production. Minusil proved to be a good additive because the resulting specimens were easily mixed and became dense. It reacted sufficiently to be an excellent source of silica for a hydroceramic but the presence of Si and Al in the Troy clay rendered it unusable.

The chemical durability, that is, less leachability of monitored ions (Na, Cs, NO_3^-) in the specimens with the RPAA in their formulations was excellent. They also have the capability of accommodating high waste loading percentages. The optimum chemical durability is attained when the atomic ratios of alkali:alumina:silica is 1:1:1. The durability is not as good when the silica:aluminum atomic ratio is greater than 1:1, a quantity required to attain glass composition.

The two natural aluminosilicates investigated were Troy clay and Wyoming bentonite. The hydroceramic products processed from a mixture of bentonite experienced swelling during the precuring stage. The finished products were physically weak and porous. These observations were in contrast to the conclusion drawn by Brownell et al., (1973) of Hanford Researchers that bentonite clay was a good additive for the immobilization of radioactive waste. The physical and chemical durability of hydroceramic specimens made from calcined Troy clay outperformed all other pozzolans during the preliminary experimentation. The ratio of silicon to aluminum was ~1.7:1. There was no need for the addition of other pozzolans to provide either silicon or aluminum. Once Troy clay was thermally transformed

(calcined) and mixed with other components, the grout was chemically reactive upon activation by alkali.

CHAPTER II

EXPERIMENTAL PROCEDURES

CHAPTER II

EXPERIMENTAL PROCEDURES

2.0 Introduction

This chapter addresses sources of the reactant components and the preparation procedures that resulted in the synthesis, physical and chemical property measurements of hydroceramic waste forms. Characterization techniques used to probe the resulting phase composition, morphology of crystalline phases and chemical durability of the final hydroceramic products are described.

2.1 Materials

2.1.1 Troy Clay: Pozzolanic Matrix

Metakaolinite derived from calcined Troy clay (kaolinite) is the major source of aluminum and silicon used for the pozzolanic reaction in hydroceramic waste form (Siemer et al., 1998). It is a dioctahedral kaolinite and belongs to the 1:1 layer (tetrahedral sheet:octerhedral sheet) type sheet silicate with extremely small or no layer charge. Consequently, it possesses very little or no cation exchange capacity. There are no interlayer spacings between the tetrahedral and the octahedral sheets. The tetrahedral and the octahedral layers are held together by hydrogen bonding, electrostatic bonding between H^+ and O^{2-} (Klein and Hurlbut, 1993) or water

molecules as in halloysite (Newman, 1987). The half-cell chemical formula can be represented by $Si_2Al_2O_5(OH)_4$. In kaolinite, there is very little substitution, if any at all, isomorphic substitution.

Thermal transformation of kaolinite to metakaolinite is a crucial process in order to render it amorphous and chemically reactive. The oxide components ($Al_2O_3.2SiO_2.xH_2O$) of metakaolinite are soluble in aqueous caustic and provides SiO_2/Al_2O_3 mole ratio of 2:1 in the absence of additional Al^{3+} and Si^{4+} cations. Metakaolinite derived from Troy clay (kaolinite) used in this study is relatively clean with very little physical contaminant material and very small soluble salts. It is mined in Troy, Idaho, the same locality and deposits as Helmar kaolin (Figure 2.1). The bulk chemical analysis and physical properties of Troy clay are given in Chapter I. It is mostly white and interstratified with iron of a few millimeter-thick of yellow and brown strata. It contains a high percent of water plasticity (26-28%) and LOI with a density of 1.75 g/cm^3 and drying shrinkage of 5-7%. Three centimeter size lumps were crushed into smaller crumbs (~0.5 cm), dried at 110°C in an oven overnight and then calcined for 2-3 hours at 750°C in a muffle furnace (Linberg furnace, WI, USA). The color changed from white to reddish brown due to iron oxidation after calcination. The original crystalline structure of kaolinite (Figure 2.1) collapsed leading to an amorphous metakaolinite and quartz phase (Figure 2.2). Metakaolinite is amorphous to XRD, giving a featureless band with a maximum located at 2T of 22° (Rees and Chandrasekhar, 1993). The chemical transitions taking place when kaolin-type clays are heated in air is represented by Equation 1.

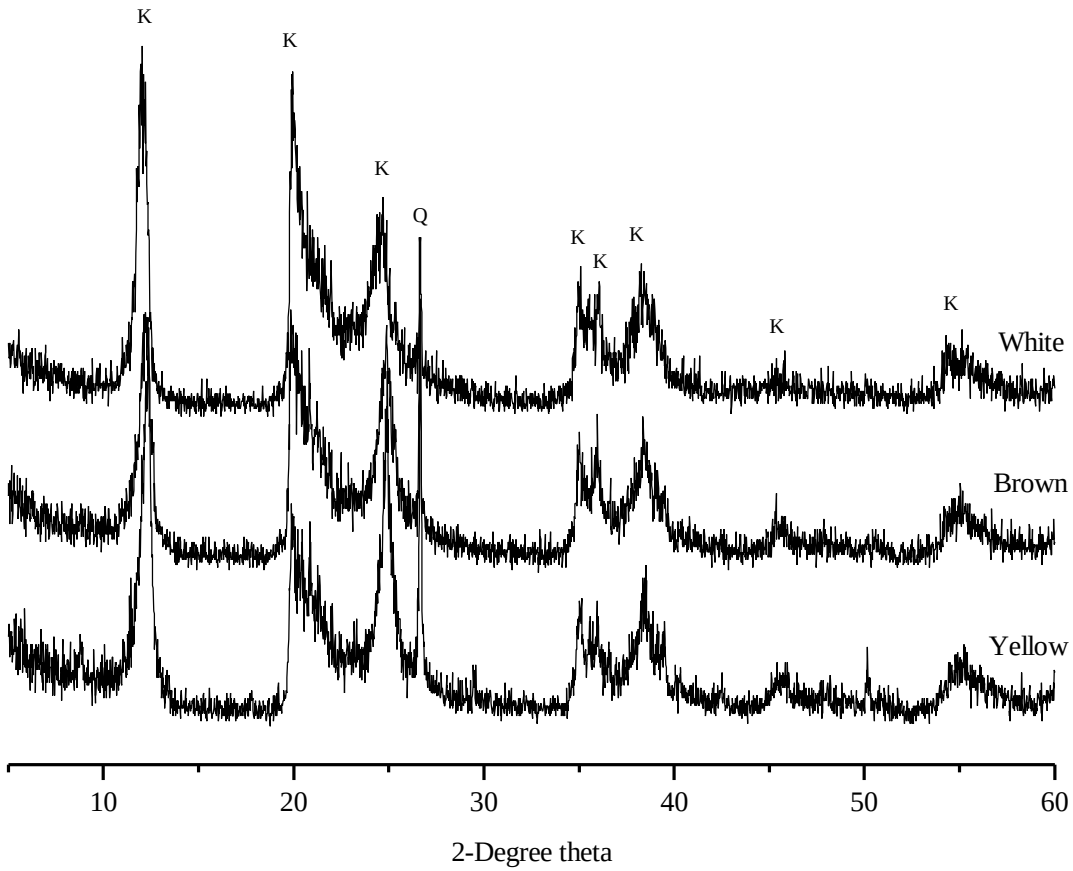

Figure 2.1. XRD of the three different strata, white, brown and yellow found in the Troy Clay. K = Kaolinite ($Si_2Al_2O_5(OH)_4$) and Q = quartz (SiO_2, 46-1045) as the two major crystalline phases. Similarity in the peak positions in the spectra patterns attested to the lack of impurity in the clay.

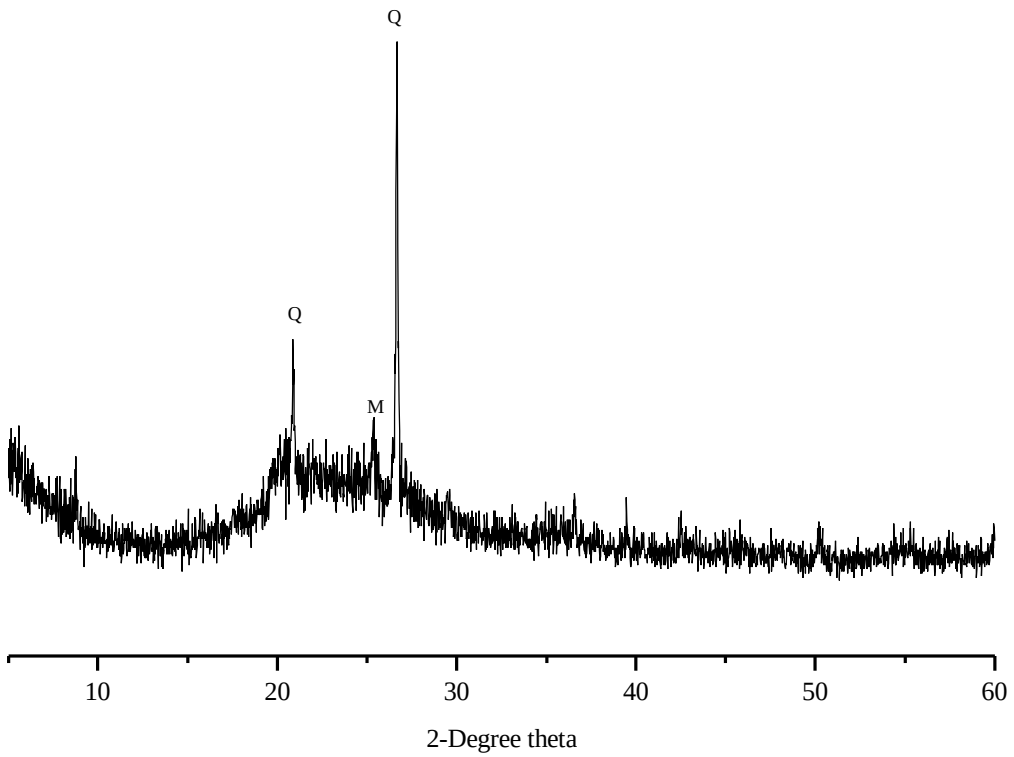

Figure 2.2. XRD pattern of calcined Troy Clay (dehydroxylated Metakaolinite) showing Q = quartz (SiO_2, 46-1045) and M = mullite as the only persistent crystalline phases. The broad diffraction maxima between 15 and 40° 2? is an indication of the amorphous phase.

$$2Al_2Si_2O_5(OH)_4 \longrightarrow 2Al_2Si_2O_7 + 4H_2O \qquad (2.1)$$

Kaolinite Metakaolinite

It has been shown that the optimum calcination temperature for kaolinite transformation to metakaolinte in air ranges from 700-850°C. This claim was supported by NMR spectroscopy, selected area electron diffraction, XRD, TEM (Dion et al., 1995; Dion et al., 1996; Dion et al., 1998; Bergaya et al., 1996) and controlled-transformation by thermal analysis. The kinetics of transformation during the dehydroxylation followed a first-order reaction (Murray and White, 1949; Brindley and Nakhira, 1957; Kissinger, 1957, Toussaint et al., 1963) and diffusion controlled (Holt et al., 1962; Archar et al., 1966; Redfern, 1987; Brindley et al., 1967; Hortvath, 1985; Hancock and Sharp, 1987; Dion et al., 1998). Undercalcined kaolin will produce less chemically reactive metakoalinite. At calcination temperature above 900°C, metakaolinite will decompose to spinel ($Si_3Al_4O_{12}$) and SiO_2 (Brown, 1961). Metakaolinite was ground and sieved to obtain particle sizes passing through 325 mesh (45? size).

2.1.2 Vermiculite: Cesium Getter

Expandable vermiculite was obtained from W. R. Grace and Co., Enoree, South Carolina, for the purpose of exchanging interlayer potassium for strontium cation. The generalized chemical formula (Mg, Ca, K, Fe^{II})$_3$(Si, Al, Fe^{III})$4O_{10}(OH)_2.H_2O$

belongs to the dioctahedral group. The cation exchange capacity ranged from 100-200 (mmol/kg). Vermiculite interlayer-charge balance ranged from 0.6-0.9, and hence possesses a very high ion-exchange capacity (Spark, 1995). Vermiculite flakes were ground and sieved to obtain size fractions passing through a 100 mesh (150? size).

2.1.3 Chemicals

Chemicals used in this study were obtained from various manufacturers. Sodium hydroxide pellets were purchased from J. T. Baker, USA. It neutralizes the acidic capability of added water, dissolves metakaolinte and provides the source of alkaline mineralizer that will activate metakaolinite. $Sr(NO_3)_2$ obtained from Mallinckrodt, Inc., USA and CsCl powders from Alfa-Æser, USA, are the major sources of surrogate strontium and cesium radionuclides. The impurities of the chemicals were taken as the manufactures specifications. Predetermined weights of chemicals were dissolved in de-ionized water prior to being mixed with other solid reactant components.

2.1.4 Simulated Waste from Fluidized Bed

The simulated waste forms were obtained from the INEEL, both of which represented accurate surrogates for the waste type. Simulated wastes were ball-milled with zirconia balls for 24 hours to reduce particle sizes and increase surface areas to

increase chemical reactivity. The physical and chemical data of the wastes have been specified in Chapter I of the introduction. X-rayed spectra of the zirconia calcine (figure 2.3) and fluorinel blend calcine (figure 2.4), the two raw wastes representing chromium and non-chromium wastes were analyzed for their major crystalline phases. The major crystalline phases common to both wastes are calcium fluoride, and zircornium oxide. Mullite was present only in the fluorinel blend calcine. Chromium containing crystalline phase did not show up in the XRD of either of the simulated wastes.

2.2 Sample Preparation

2.2.1 Stoichiometry Calculations of Hydroceramic Components

A computer program specifically written to convert the bulk composition of the reactant of hydroceramic formulation into oxides, is shown in Appendix A. From the formulation determined from the preliminary studies in Chapter I (Table 2.1), the program was used to determine the bulk formulation, that is, the weight percent and ratios of the oxides, solid-water ratio; hydration energies and number of nonbridging oxygens in the hydroceramic host formulation (Table 2.2). Appropriate amount of reactants for a waste form or any of the reactants were entered as inputs, the resulting oxide ratios normalized to that of sodium oxide was generated. The main purpose is to adjust the components to maintain glass compositional regions (Gougar-Dunzik, 1997).

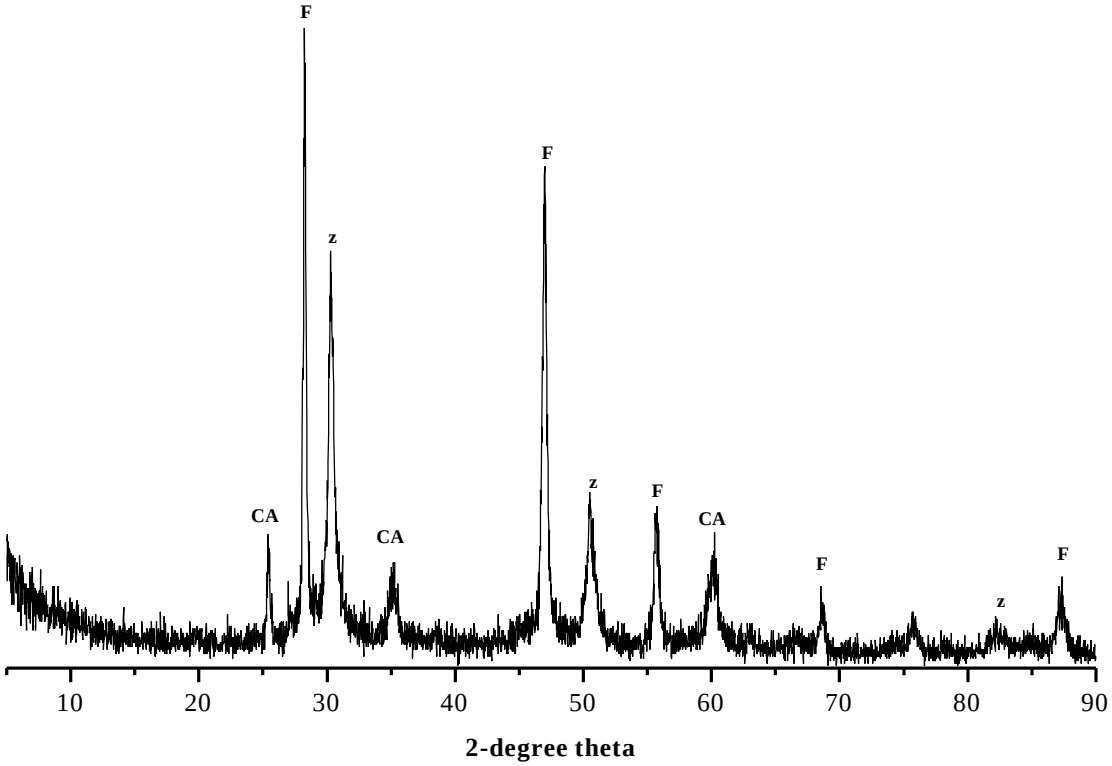

Figure 2.3. X-ray diffraction pattern of zirconia calcined simulated waste showing CA = calcium aluminum oxide ($CaAl_4O_7$, 07-0082), F = calcium fluoride (CaF_2, 35-0816) and Z = zirconia (ZrO_2, 50-1089) as the major crystalline phases present in the simulated waste.

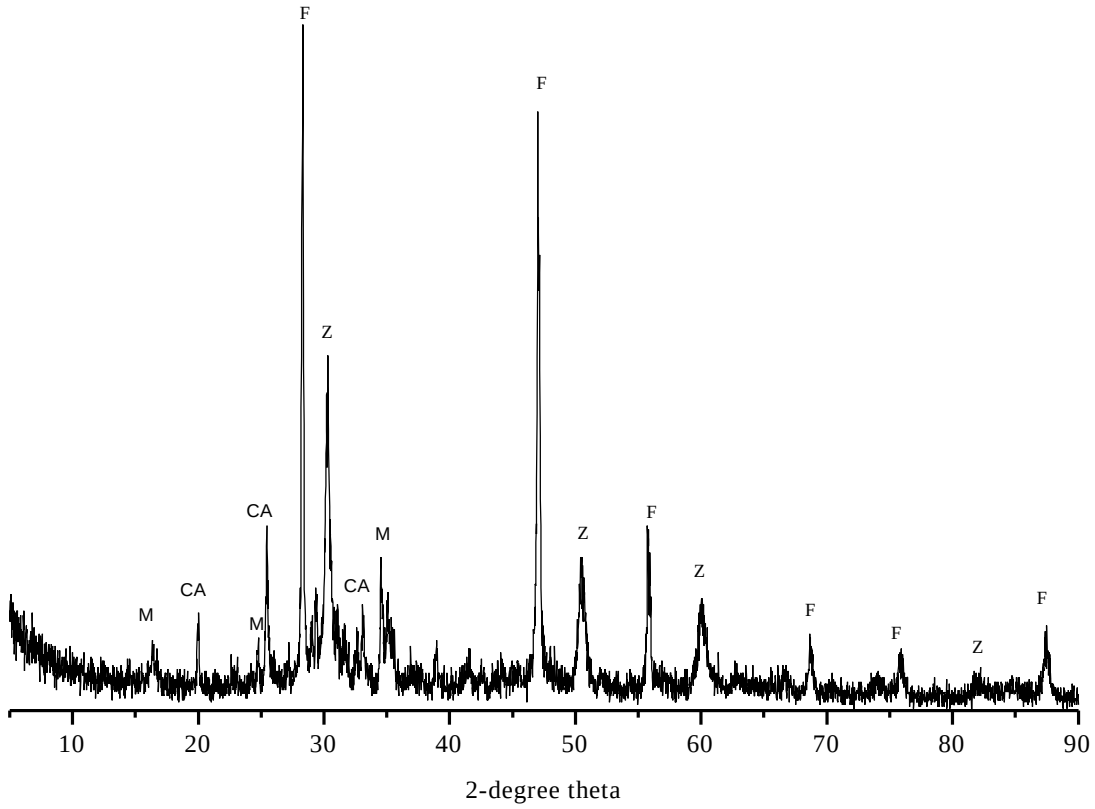

Figure 2.4. X-ray diffraction pattern of simulated fluorinel blend calcined showing M = mullite ($Al_{2.35}Si_{0.84}O_{4.82}$, 73-1253), CA = calcium aluminum ($CaAl_4O_7$, 07-0082), F = calcium fluoride (CaF_2, 35-0816) and Z = zirconia oxide (ZrO_2, 50-1089) as the major crystalline phases present in the simulated waste.

Table 2.1. Hydroceramic host formulation.

	Weight (g)	%
Calcined clay (metakaolinite)	4.33 g	5.62
$Sr(NO_3)_2$	0.0225 g	0.30
CsCl	0.0225 g	0.30
37.5 weight percent NaOH (9.375M)	2.60 g	33.96
DI water	0.25 g	3.27
Total	7.655 g	100.01

Table 2.2. Table of results of the computer calculation of the percentage of the hydroceramic formulation plus 30 weight percent (solid) simulated waste containing oxides, oxide ratios, fraction of solid-water, non-bridging oxygens and hydration energy.

Oxide	Percentage in the formulation
Al_2O_3	17.814
CaO	1.466
Cs_2O	0.240
Fe_2O_3	3.120
H_2O	29.07
K_2O	0.338
MgO	0.964
Na_2O	9.894
SiO_2	36.73
SrO	0.150

NO_3^- from SrCs, calcines, TOXIMix's, $NaNO_3$, and SIM = 0.18
Cl- from SrCs, calcines, TOXIMix's, $NaNO_3$, and SIM = 6.1×10^{-2}

Fraction of dry solids = 0.71
$M_2O/MO/M_2O_3/SiO_2$ = 1:0.1541:1.19:1.876
Number of non-bridging oxygens = 0.0821
? $G^o_{hydration}$ = -4.825 kcal/mole

2.2.2 Bulk Waste Form Calculations

For the host-waste (hydroceramic host + fluorinel blend calcine or zirconia calcine) formulations, the same computer program was used to calculate the weight percent and ratios of the oxides, solid to water ratio, hydration energies and number of nonbridging oxygens in the formulation (Tables 2.3-2.4). The amounts of calcined clay and NaOH solutions in hydroceramic host formulation were increased to compensate for the calcined waste chemistry.

2.2.3 Paste Preparation

Powder components, (including the formulation without simulated waste or formulation plus simulated waste), and vermiculite were blended in a Hobart mixing machine (Model N-50) for 5-10 minutes. Sodium hydroxide solution (37.5 weight percent or 9.375 M) and the solution containing $Sr(NO_3)_2$ and CsCl were combined and added to the mixed powder. All the components were mixed in accordance with the ASTM C 305 standard until the mixture formed a dough-like consistency. The mixture was divided into bits (~ 10.0 g), weighed with Sartorius balance (Brinkmann Instruments Inc., NY, USA) having a precision of up to 100 micrograms.

Table 2.3. Hydroceramic host plus 30 weight percent (solid) waste (fluorinel blend or zirconia calcine) formulation.

Component	Weight (g)
Calcined clay (metakaolinite)	5.33
Vermiculite	0.43
$Sr(NO_3)_2$	0.0225
CsCl	0.0225
37.5 weight percent NaOH (9.375M)	3.50
Fluorinel belnd/zirconia calcine	2.85
DI water	0.25
Total weight	12.655

Table 2.4. Results of the computer calculation of the percentage of the host-waste (fluorinel blend calcine) formulation containing oxides; oxide, solid-water ratios, non-bridging oxygens and hydration energy.

Oxide	Percentage in the formulation
Al_2O_3	22.68
B_2O_3	0.97
CaF_2	6.03
CaO	2.73
CdO	0.44
Cr_2O_3	0.21
Cs_2O	0.15
Fe_2O_3	2.33
H_2O	23.24
K_2O	0.46
MgO	0.59
Na_2O	9.33
SiO_2	27.58
SrO	0.12
ZrO_2	3.00

NO_3^- from SrCs, calcines, TOXIMix's, $NaNO_3$, and SIM = 1.15

Cl- from SrCs, calcines, TOXIMix's, $NaNO_3$, and SIM = 3.76×10^{-2}

Fraction of dry solids = 0.77

Fraction of dry stuff that's waste = 0.30

$M_2O/MO/M_2O_3/SiO_2$ = 1:0.20:1.52:1.48

2.3 Hydrothermal Processing

The green monoliths were put in ~23mL Teflon-lined 316 stainless steel, hydrothermal autoclave vessels obtained from Parr Instrument, Illinois, USA. (Figure 2.5). The sample plus the container was weighed with a Mettler PL1200 (Mettler Instruments Corp., NJ, USA) weighing balance and then put in a preheated oven (Yamato or Fisher). To monitor reaction times and temperatures, one of the vessels was fitted with a J-thermocouple (Omega, USA) to ensure that the sample temperature matched that of the oven set temperature. It took approximately two hours before the sample temperature reaches that of the oven, depending on the number of hydrothermal vessels in the oven. The reason for the long duration of the attainment of the set temperature is ascribed to the high insulating property of the Teflon. Hydrothermal syntheses of samples were conducted under steam pressure at 100% relative humidity ranging from at 75-200°C. At the end of predetermined reaction time dictated by experimental design, the hydrothermal vessel was withdrawn, allowed to be air cooled and then weighed to within ?0.20 g to test for leakage during the run.

Samples were visually inspected for any evidence of deformation, cracking or any other physical developments. The amount of free water expelled from each sample increased with time and temperature. The water also became clearer with increasing temperature and time. This qualitative observation implies increasing degree of

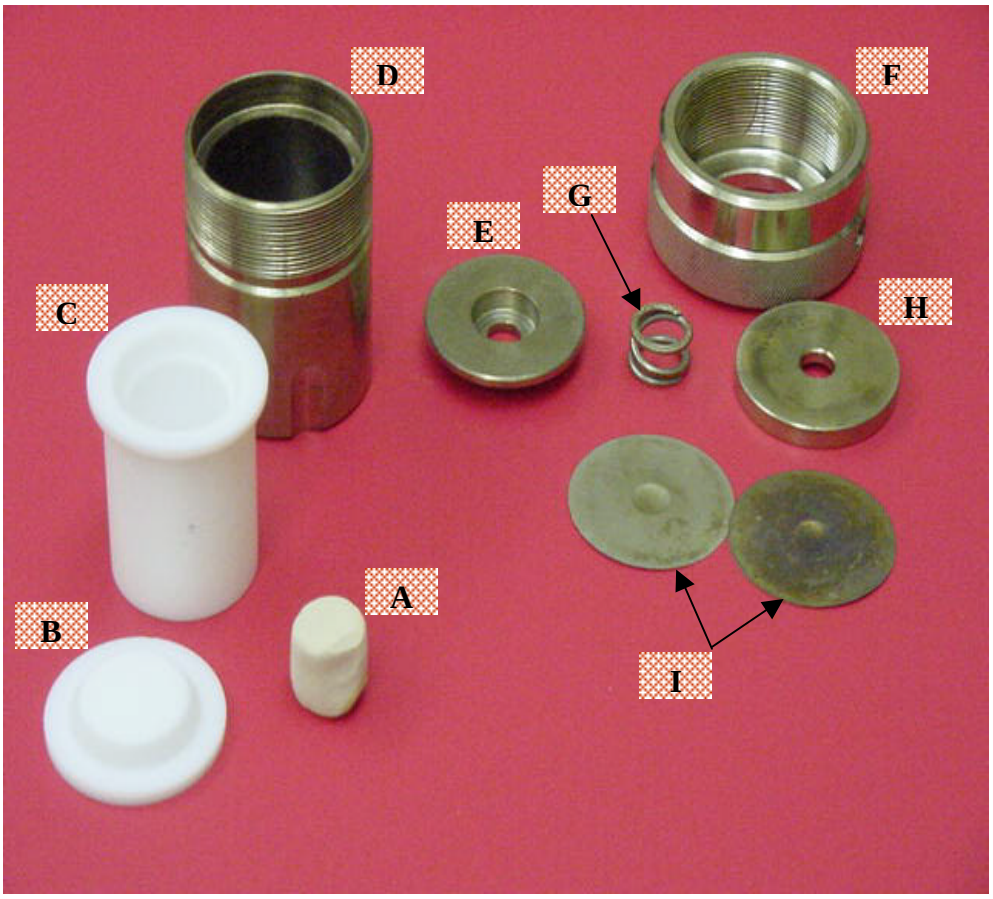

Part Label	Description
A	Hydroceramic monolithic sample
B	PTFE cup cover
C	PTFE cup
D	Parr bomb body
E	Pressure plate, upper
F	Screw cap
G	Spring
H	Pressure plate, lower
I	Rupture discs (0.002” and 0.003”)

Figure 2.5. Disassembled hydrothermal Parr bomb (Parr Instrument, IL, USA) used in the hydrothermal syntheses of hydroceramic waste forms.

reaction during formation of zeolites in hydroceramic waste forms. This phenomenon has also been observed during the solution crystallization of type A zeolite (Hu and Lee, 1990). Monoliths obtained from fluorinel blend calcine at low temperatures (75-95°C) experienced swelling, cracking, and sometimes total crumbling into sand-size grains. Careful observations revealed that samples with their long axes aligned with the Teflon container swell. Samples with less space between the Teflon container or with their long axes perpendicular to that of the Teflon vessel swell and crumble. The 75°C samples suffered all the previously mentioned physical changes, while the 85°C samples only swell with the development of some scally skins. The 95°C sampleswere only coated with a few white granules.

One sample of each formulation was cured at room temperature and served as a reference material. It is this reference sample with which the physical and chemical information obtained from the processed samples were compared, under the same treatment conditions.

2.4 Characterization

The evolution of the physical and chemical development of sample preparation and processing conditions as a functions of time, temperature and waste loading percent described above, were monitored with different characterization techniques. This was done to benchmark them against those of the original starting materials, respective crystalline phases, and the Environmental Assessment (EA) benchmark glass.

2.4.1 Specimen Preparation for Characterization

Samples were immersed in liquid nitrogen for approximately 2 hours. These samples were freeze-dried (Flexi-Dry, FTS Systems, Inc., NY) for 24 hours. The freeze-dried option was chosen to terminate further hydration reactions. At the end of the freeze-dried period, the samples were re-weighed. The ratio of the freeze-dried sample to the green monolith is about 23%. All specimens were crushed, ground, and sieved for physical and chemical analyses.

2.4.2 X-ray Diffraction

The nature and the amount of the crystalline phases present, in the dried and comminuted reactants, and the final monolithic products were determined at room temperature with X-ray powder diffraction. The diffractometer was a Type PadV, Scintag Instrument, U.S.A. It uses CuK? target having a wavelength of 1.540562Å and Si(Li) Peltier detector. The divergence slits were 2mm, the scatter slit was 4mm, and the convergence slits were 0.3mm with the scatter slit at 0.5mm. There are two gonimeters: ? /2? representing sample/detector goniometers and moving at ratio 1:2. The x-ray tube was operated at 30mA and 35kV. A zero background (quartz) and hollowed sample holder was used for powdered samples. The scan speed was 4° per minute between 5° and 40° 2? degree for the hydroceramic host waste-form comprising mainly of zeolites and 5-60° for hydroceramic + 30 weight percent solid

waste. Computerized matching of the peaks in both intensity and location (d-spacing or 2?^{o}) with the JCPDS files was carried out on the data using a computer program DMSNT version 1.37 program.

2.4.3 SEM

Scanning electron microscopy (SEM) [Hitachi Model S-3500N] determined the crystal sizes and morphologies of the crystalline phases present in sample. The accelerating voltage used was 20 kilovolts. Energy dispersive x-ray spectroscopy (EDS) [Princeton Gamma Tech) in conjunction with secondary electron imaging coupled to the SEM detected the major cations (Si, Al, Na, and Ca) in the sample.

2.4.4 Product Consistency Test (PCT)

Samples were crushed, ground, and sieved to obtain the ? 75 ?m < 150 ?m size fraction needed for a modified product consistency test (PCT) [ASTM: C 1285-97]. One gram of sample to 10g of water was put in 316 stainless steel, high-pressure Parr hydrothermal vessels, weighed and put in a preheated oven at 90°C for 24 hours. At the end of the reaction time, vessels were air-cooled and re-weighed. The mixture of solid sample and the solution was separated.

The Product Consistency Test (PCT) [ASTM: C 1285-97] was used to monitor the chemical durability and leachability of the processed samples. The PCT is a

standardized test established to measure the chemical durability of the newly developed waste form against the established performance of the Environmental Assessment (EA) benchmark glass (Document WSRC-TR-92-346, Revision 1, June 1, 1993). The test consists of 10g (10 cc, assuming density of 1 g/cm^3) of water to 1 gram of sample and leached for 7 days at 90°C. The concentration and the conductivity of the leachates released are then measured. A waste form is considered superior to the EA benchmark glass if the values of the conductivities and/or the concentrations of the dissolved leachates measured under the same test conditions, are less than that of the EA benchmark glass.

The specific conductivity and pH of the released cations and anions for the PCT test solutions were measured using Cole Parmer? and YSI? model 3200 conductivity meters and pH (Orion? model 290A) meter. The conductivity meters were calibrated with freshly prepared solutions of KCl (0.1M, 0.01M, and 0.001M) of known conductivities: 12.86, 1.14, and 0.147 mS/cm (The pH and Conductivity Handbook, Omega). The pH meter was calibrated with standard solutions (pH = 4, 7, 10 and 12.45) obtained from VWR chemical company. Both meters have an automatic temperature compensation capability.

2.4.5 Bulk Chemical Analysis

Quantitative chemical analyses of the major cations and anions present in the decanted PCT test solutions were analyzed for the major cations, except cesium,

using Atomic Emission Plasma (AEP) [Spectrametrics, Andover, MA], cesium with Atomic Absorption Spectrometry (AAS) [Perkin Elmer, Norwalk, CT] and anions by Ion Chromatography (IC) [Dionex, Sunnyvale CA]. The detection limits of each characterization technique for different ions are given in Table 2.5.

Table 2.5. Detection limits for the bulk chemical analysis for the major anions and cations.

Analytical Technique	**Cation/Anion**	**Concentration (mg/L)**
AAS	Cs	<0.02
AEP	All cations except cesium	<0.02
IC	Cl^- and NO_3^-	0.01
	SO_4^{-2} and PO_4^{-3}	0.02
	F^-	0.05

CHAPTER III

RESULTS OF SYNTHESIS, CHARACTERIZATION AND KINETICS OF HYDROCERAMIC HOST

CHAPTER III

RESULTS OF SYNTHESIS, CHARACTERIZATION AND KINETICS OF HYDROCERAMIC HOST

3.0 Introduction

The solutions obtained from the Product Consistency Test (PCT) of the hydroceramic host synthesized at 75, 85, 95, 125, 150, 175 and 200°C were measured for their electrical conductivity which was an indication of the total amount of solid materials dissolved in solution. The pH of the solutions were also measured as a function of the processing time. From the conductivity data and standard plot of KCl concentrations versus conductivity, transient equivalent sodium concentrations were estimated for all the samples for all temperatures. Analytical concentrations of a few selected samples were carried out to verify the accuracy of the estimated sodium ion concentrations.

Since sodium from an NaOH solution is several times more conductive than many of the other ions in solution (Omega Environmental Handbook, 1989) and are the dominating cations in the tetrahedral sites of zeolites, Na^{+} ion was used to monitor the degree of chemical durability of the hydroceramic host which was synthesized at different temperatures and times. It should be noted that the hydroceramic host formulations did not contain any of the three calcined simulated wastes: alumina,

zirconia blend or fluorinel blend calcine. The release rates of sodium ion during the PCT were used to interpret the degree, or the rate, of conversion of metakaolinite and sodium hydroxide solution to aluminosilicates (zeolites) crystalline phases. Consequently, the effects of temperature on the reaction rates were determined. Phase identification and morphologies of the crystalline phases in the monolithic samples were carried out. The combined results of phase characterizations, chemical analysis data and kinetics results were used to recommend the appropriate processing limits as a function of temperature, time and relative humidity.

3.1 Results

3.1.1 Results of Conductivity and pH Measurements

The conductivity and pH of the PCT test solutions of samples from each temperature were measured and plotted separately for 75-200°C (Figures 3.1-3.7). The PCT of the reference sample (7.95 mS/cm) was not included in the plots because of the large numerical differences, especially the high-temperatures (150-200°C), between the processed samples and the reference sample. In all cases, the conductivities and the pH of the samples decrease exponentially with increasing temperature and processing time. The time, for the onset of a steady state for the conductivity and pH for each temperature increases as the processing temperature decreases. A steady state is defined as the time at which the conductivity or other dependent variable remains constant with time.

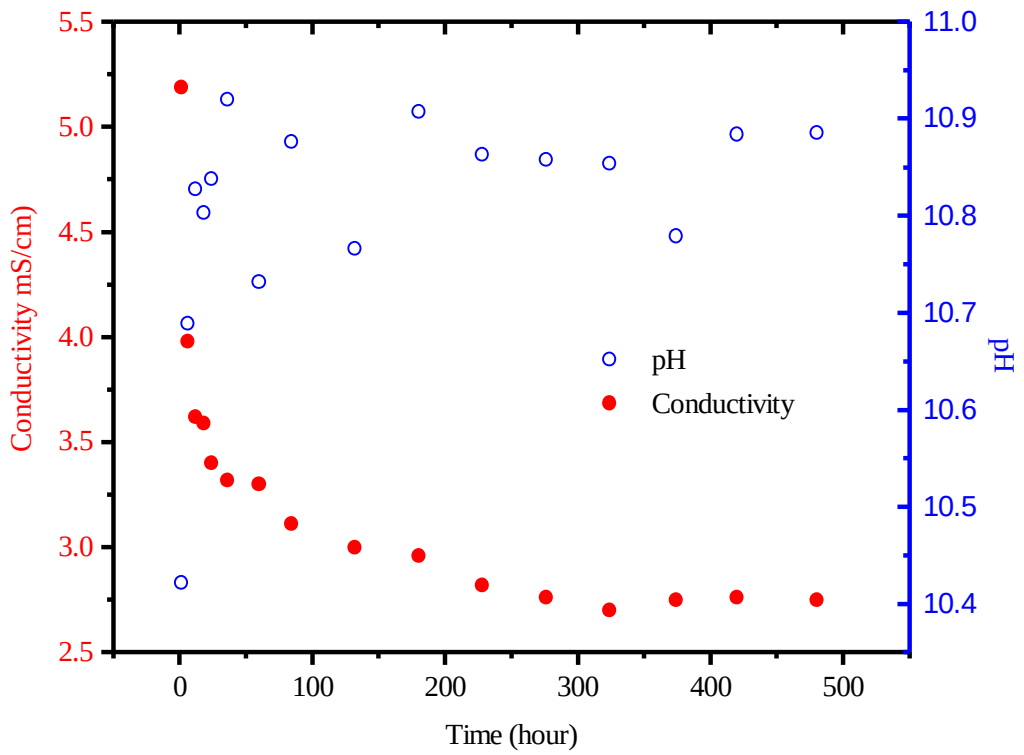

Figure 3.1. Conductivity-pH-time plot of hydroceramic host processed at 75°C.

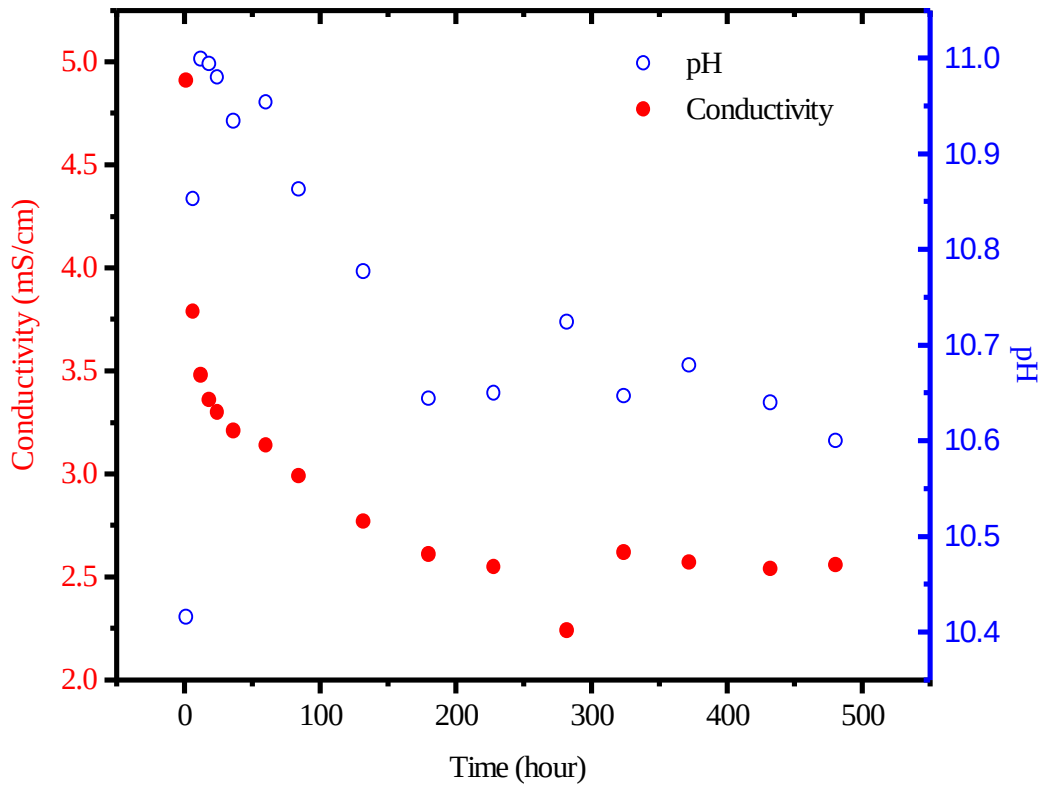

Figure 3.2. Conductivity-pH-time plot of hydroceramic host processed at 85°C.

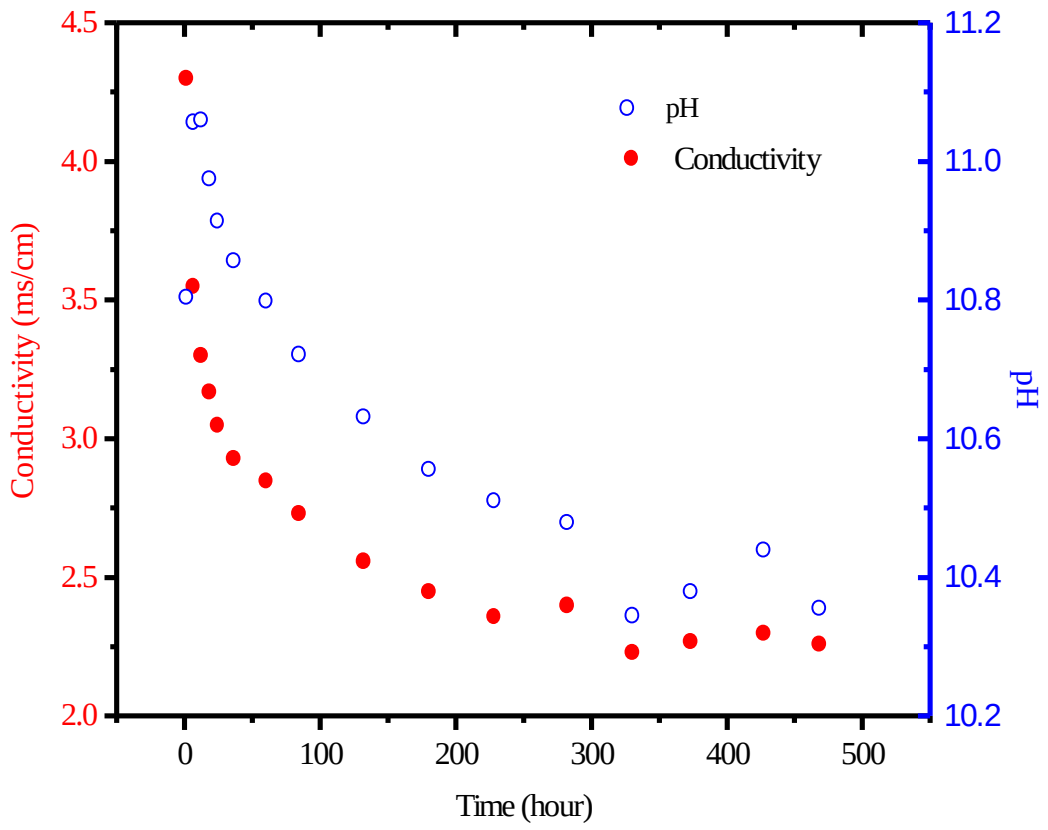

Figure 3.3. Conductivity-pH-time plot of hydroceramic host processed at 95°C.

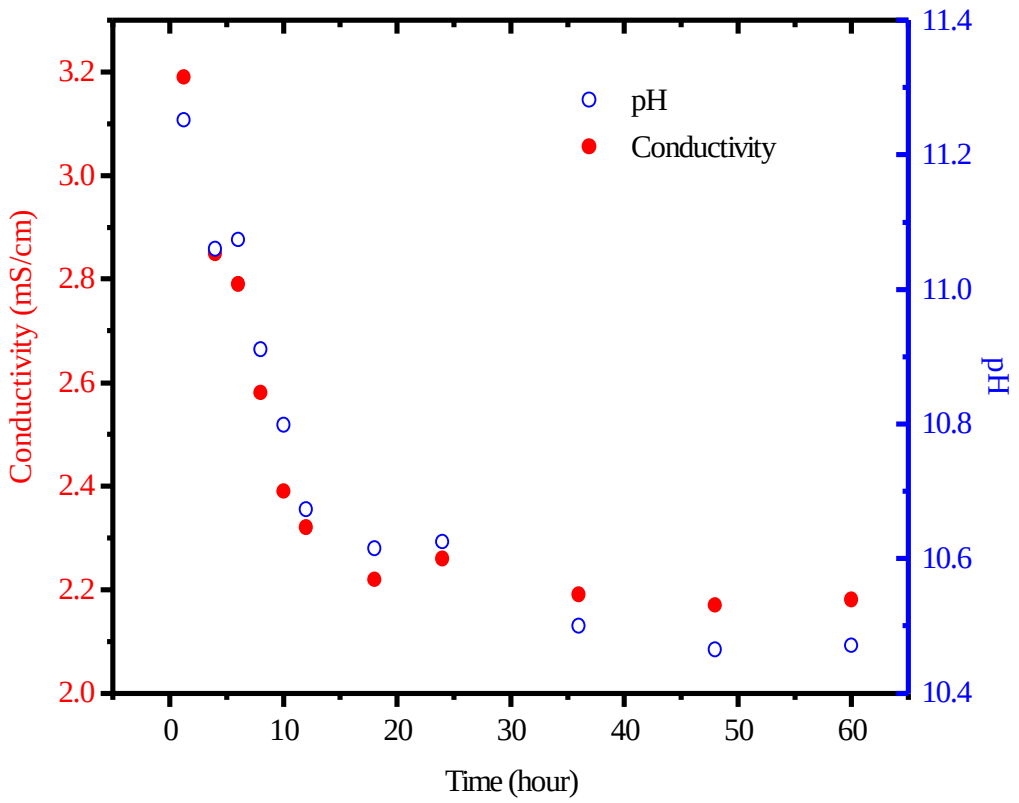

Figure 3.4. Conductivity-pH-time plot of hydroceramic host processed at 125°C.

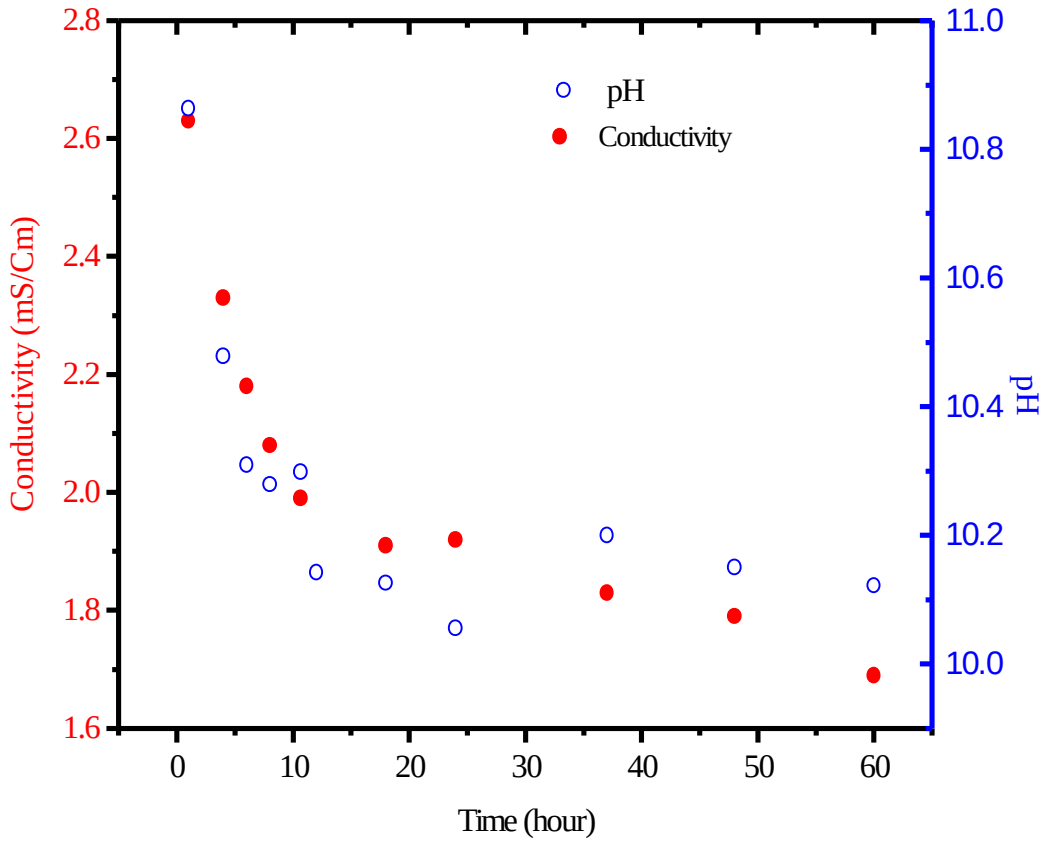

Figure 3.5. Conductivity-pH-time plot of hydroceramic host processed at 150°C.

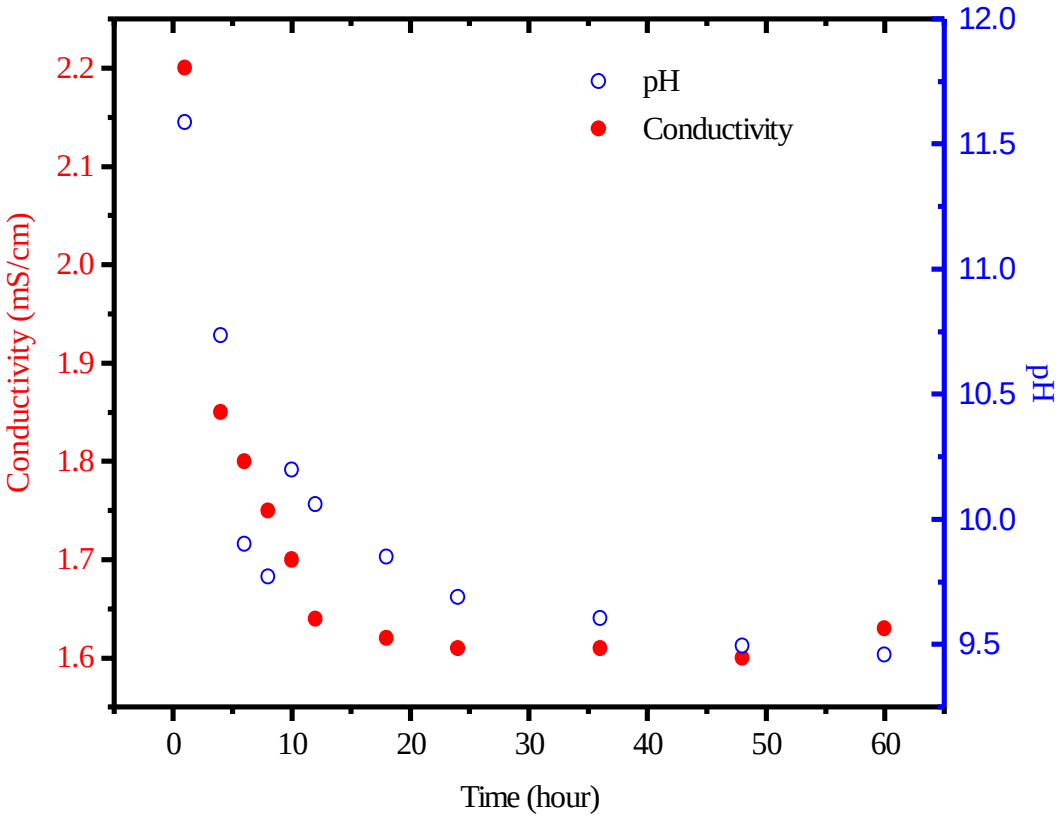

Figure 3.6. Conductivity-pH-time plot of hydroceramic host processed at 175°C.

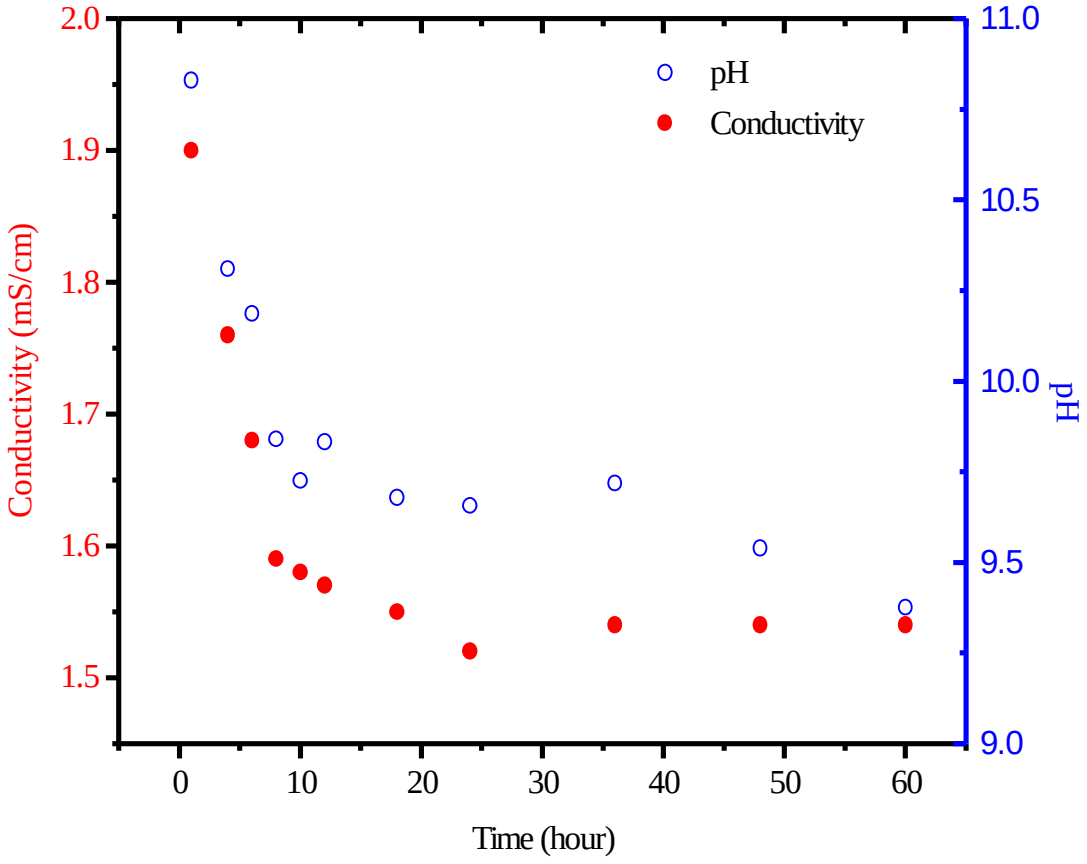

Figure 3.7. Conductivity-pH-time plot of hydroceramic host processed at 200°C.

The plots showed similar trends and similar numerical differences between the reference sample and the processed samples as their conductivity counterparts. Except for the 75°C samples, all the pH-time plots of hydroceramics synthesized at 85-200°C follow the same trend as their concentration-time plot counterparts. The exponential decrease in the pH with increasing processing time is another supporting evidence that sodium ion is being taken out of solution and combined with aluminum to form corresponding zeolites. As a result, the degree of alkalinity decreases with time leading to decrease in the pH.

3.1.2 X- ray Results

X-ray diffraction (XRD) spectra of the hydroceramic synthesized at 75-200°C, at various times, crystallized into two distinctive phases in addition to the already present and persistent quartz crystalline phase. The XRD patterns of the samples processed at 75-150°C showed type A zeolite and quartz (Figure 3.8), and zeolite NaP1 and quartz phases at 175-200°C (Figure 3.9).

Figures 3.10-3.13 and figures 3.14-3.15 show qualitatively, an increase in the intensity with processing time of the most intense peaks of the type A zeolite (hkl, 200) and NaP1 (hkl, 301/3) formed between 75-150°C and 175-200°C samples. The point of inflections of the highest Bragg reflection versus time plots correlate to the end of reaction (nucleation). Thereafter, the crystalline growth reached a maximum probably due to the depletion of reagent source and/or temperature. In most cases,

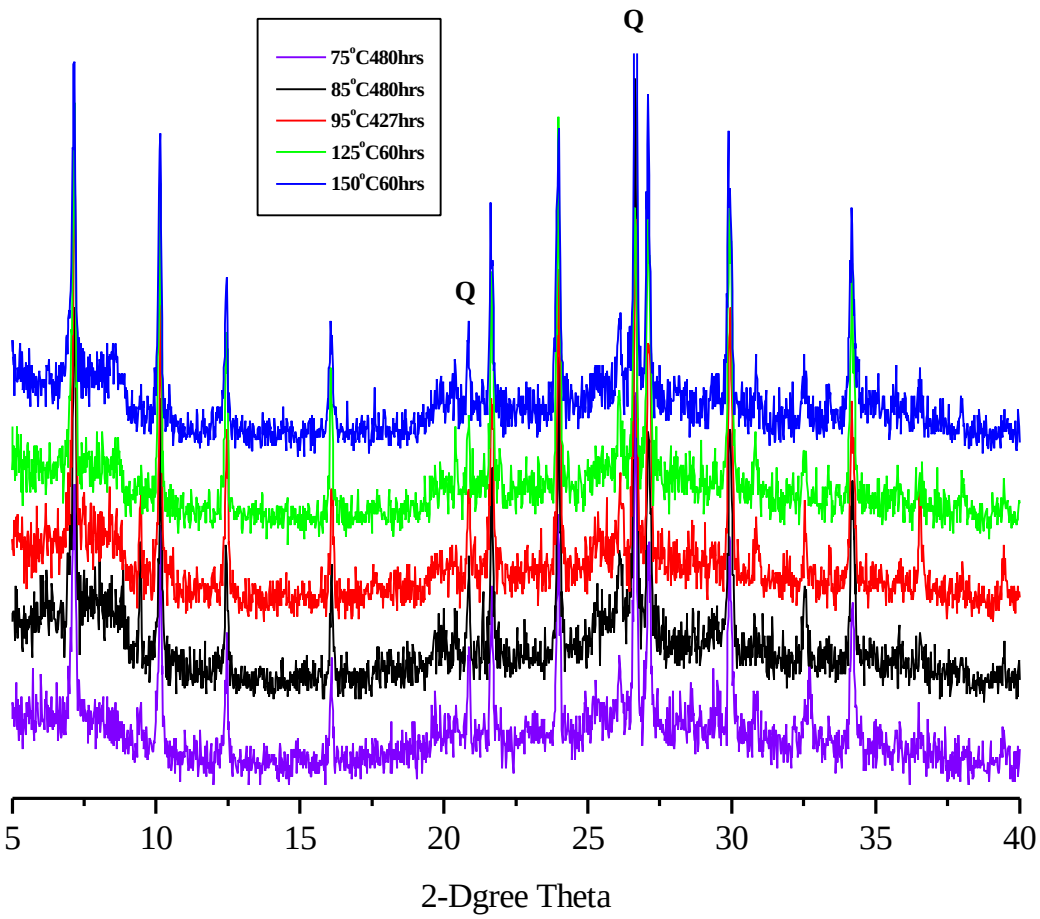

Figure 3.8. Representative x-ray diffraction patterns of hydroceramic host waste form processed at 75-150°C at various times. Letter Q represents quartz phase two-major peaks and the remaining unmarked peaks belong to the type A zeolite.

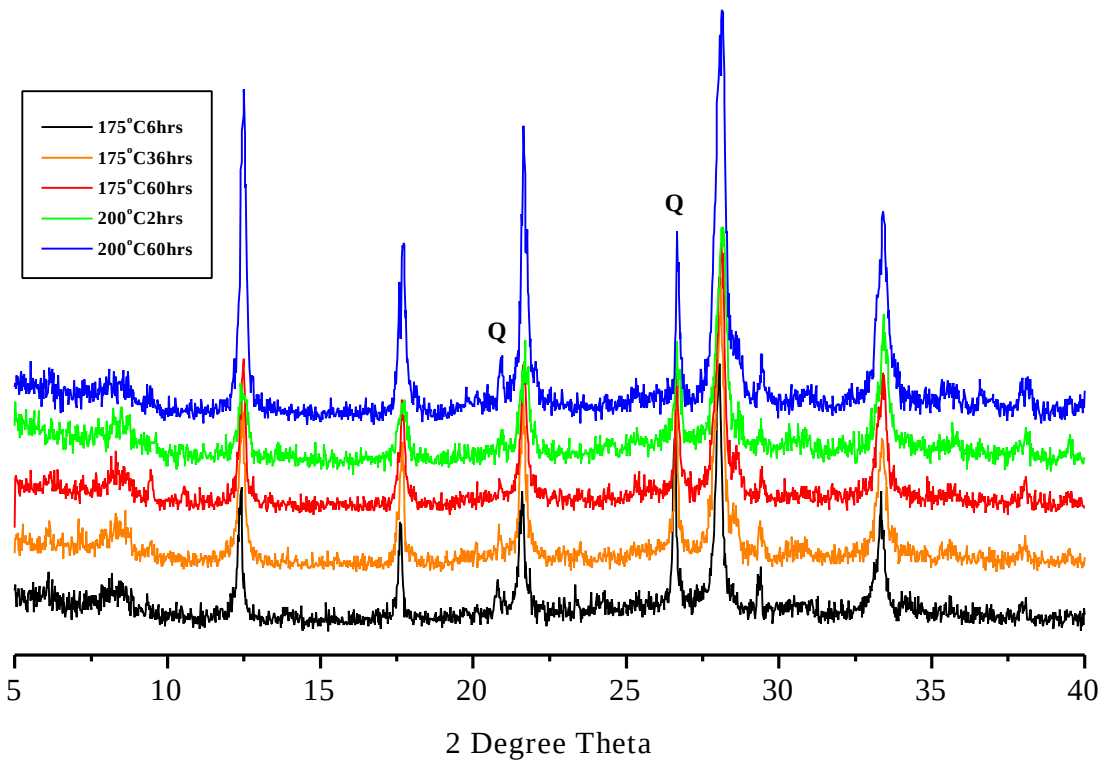

Figure 3.9. Representative x-ray diffraction patterns of hydroceramic host waste form processed at 175-200°C at various times. Letter Q represents quartz phase two-major peaks and the remaining unmarked peaks belong to the type Na-P1 zeolite.

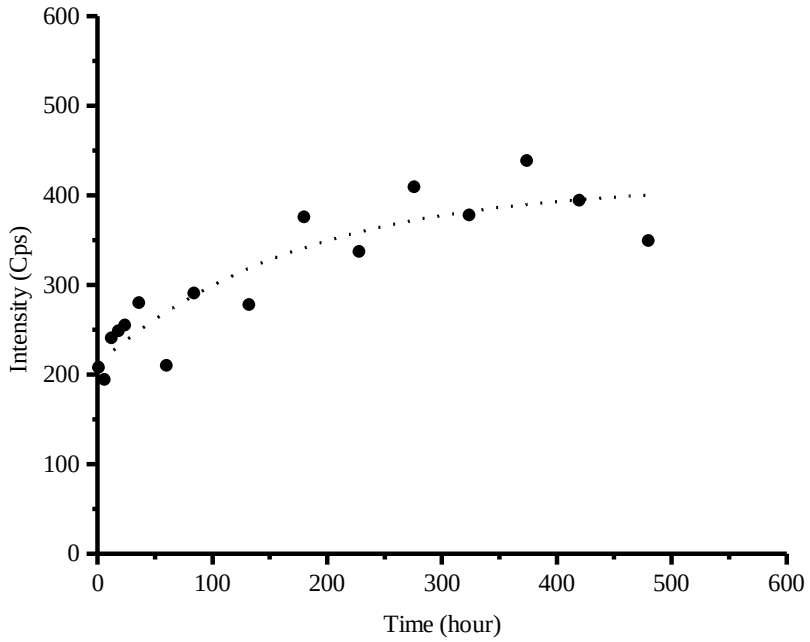

Figure 3.10. Crystallization of type A zeolite in hydroceramic waste form at 75°C as a function of time. Intensity versus time of the most intense peak located at (hkl, 200) indicates the extent of crystallization as determined by x-ray powder method.

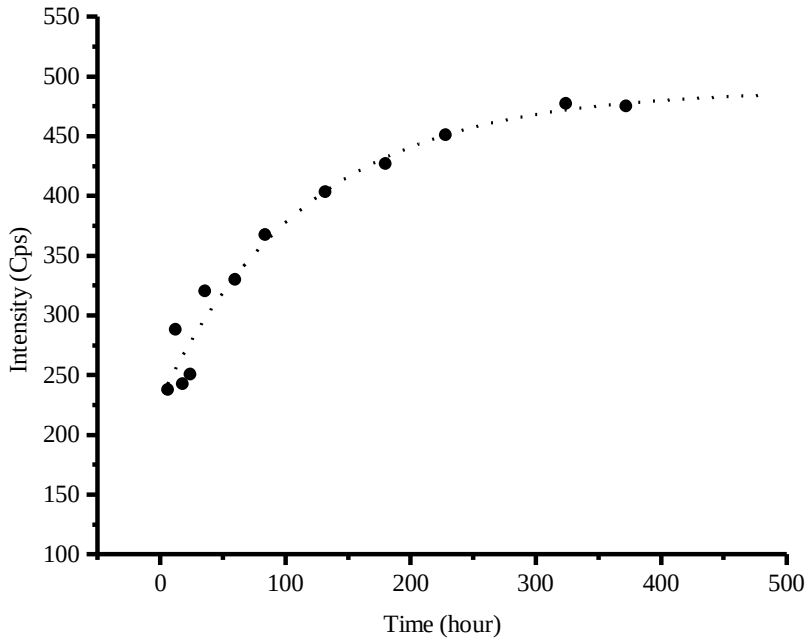

Figure 3.11. Crystallization of type A zeolite in hydroceramic waste form at 85°C as a function of time. Intensity versus time of the most intense peak located at (hkl, 200) indicates the extent of crystallization as determined by x-ray powder method.

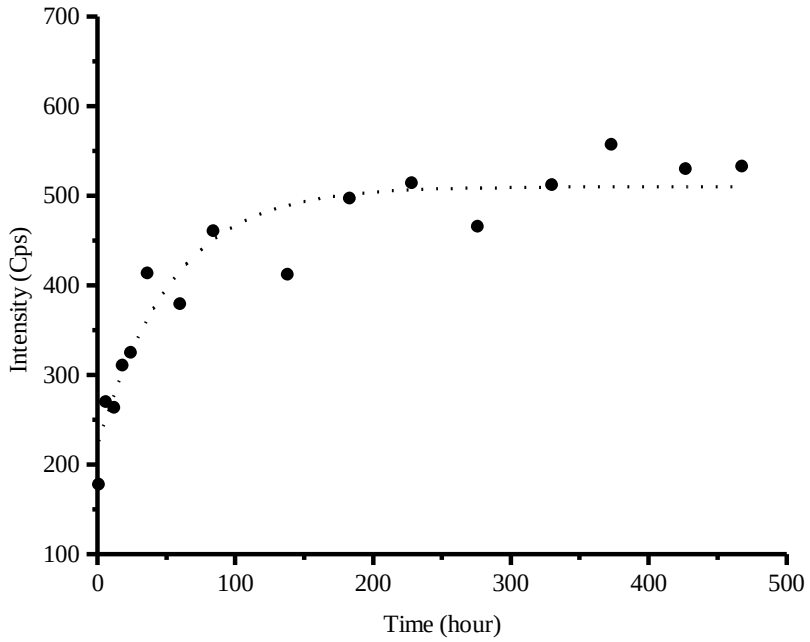

Figure 3.12. Crystallization of type A zeolite in hydroceramic waste form at 95°C as a function of time. Intensity versus time of the most intense peak located at (hkl, 200) indicates the extent of crystallization as determined by x-ray powder method.

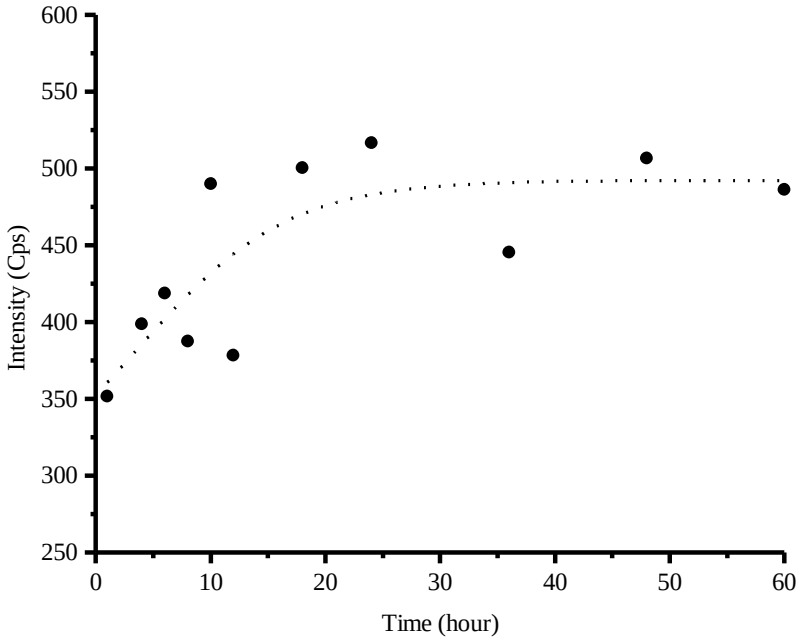

Figure 3.13. Crystallization of type A zeolite in hydroceramic waste form at 125°C as a function of time. Intensity versus time of the most intense peak located at (hkl, 200) indicates the extent of crystallization as determined by x-ray powder method.

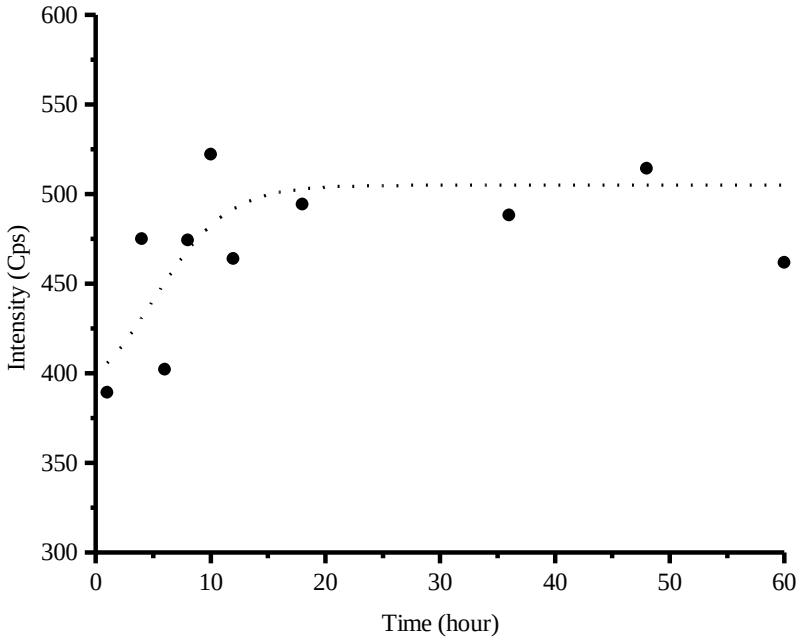

Figure 3.14. Crystallization of type A zeolite in hydroceramic waste form at 150°C as a function of time. Intensity versus time of the most intense peak located at (hkl, 200) indicates the extent of crystallization as determined by x-ray powder method.

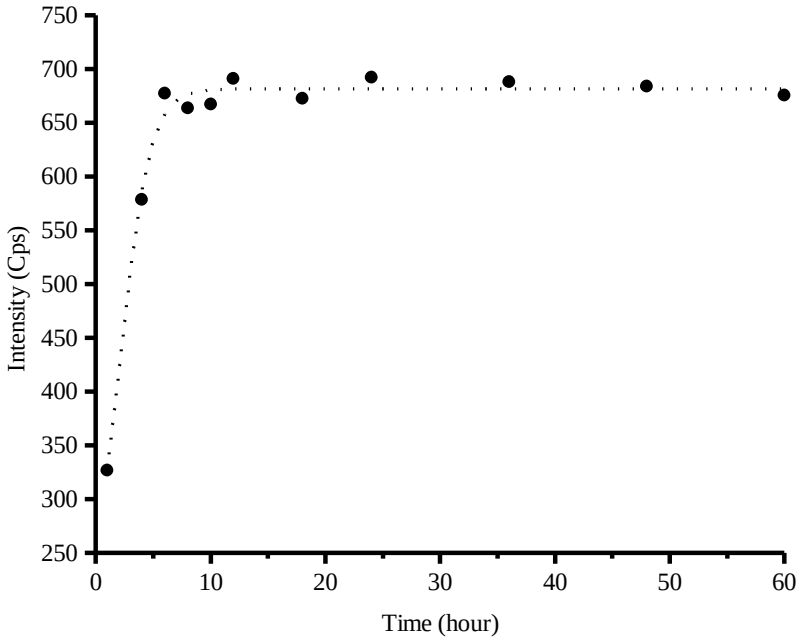

Figure 3.15. Crystallization of type Na-P1 zeolite in hydroceramic waste form at 175°C as a function of time. Intensity versus time of the most intense peak located at (hkl, 3 0 1/3) indicates the extent of crystallization as determined by x-ray powder method.

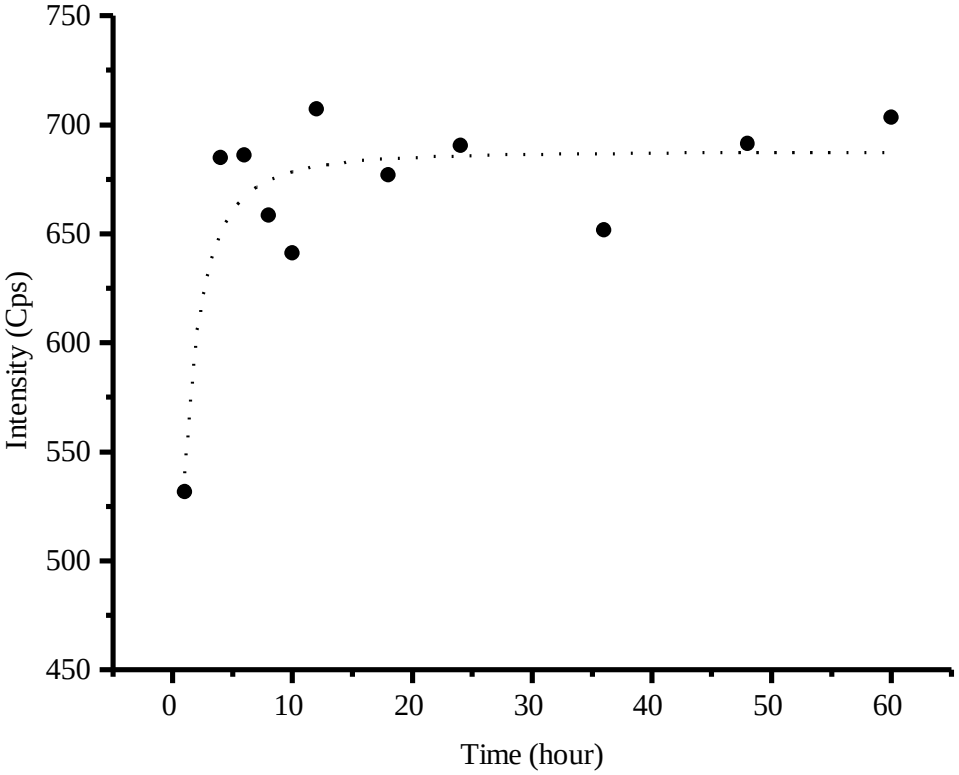

Figure 3.16. Crystallization of type Na-P1 zeolite in hydroceramic waste form at 200°C as a function of time. Intensity versus time of the most intense peak located at (hkl, 3 0 1/3) indicates the extent of crystallization as determined by x-ray powder method.

The inflection points change from round (arc-shaped) to elbow-shaped form as the reaction temperatures increase. The curves mimic the vertical flipping of the conductivity or pH-time curves plotted from the PCT test solutions. Hydroceramic samples processed at 75, 85, 95, 125 and 150°C are characterized by gently rising slopes with no abrupt or sharp changes where the slopes are close to zero (Figures 3.10-3.13). Whereas, hydroceramic hosts synthesized at 175-200°C exhibit somewhat different trends (Figures 3.14-3.16). Their plots rose very sharply within a short time and reached maximum before 12 hours where they remained nearly flat. The fast-rising slopes are indications of fast reactions.

The major difference is that the intensity-time plots follow an increasing trend while those of conductivity/concentration-time data follow a decreasing trend. The implication is that gently or fast risen slopes coupled with abrupt slope changes may be ascribed to the stages of crystallizations of the zeolites formed.

3.1.3 Microstructural Analysis with SEM

The SEM crystalline morphologies and sizes of the type A and NaP1 zeolite phases in support of the XRD patterns are shown in figure 3.1 and figure 3.2, respectively. The two figures represent samples processed at 75-150°C and 175-200°C, respectively.

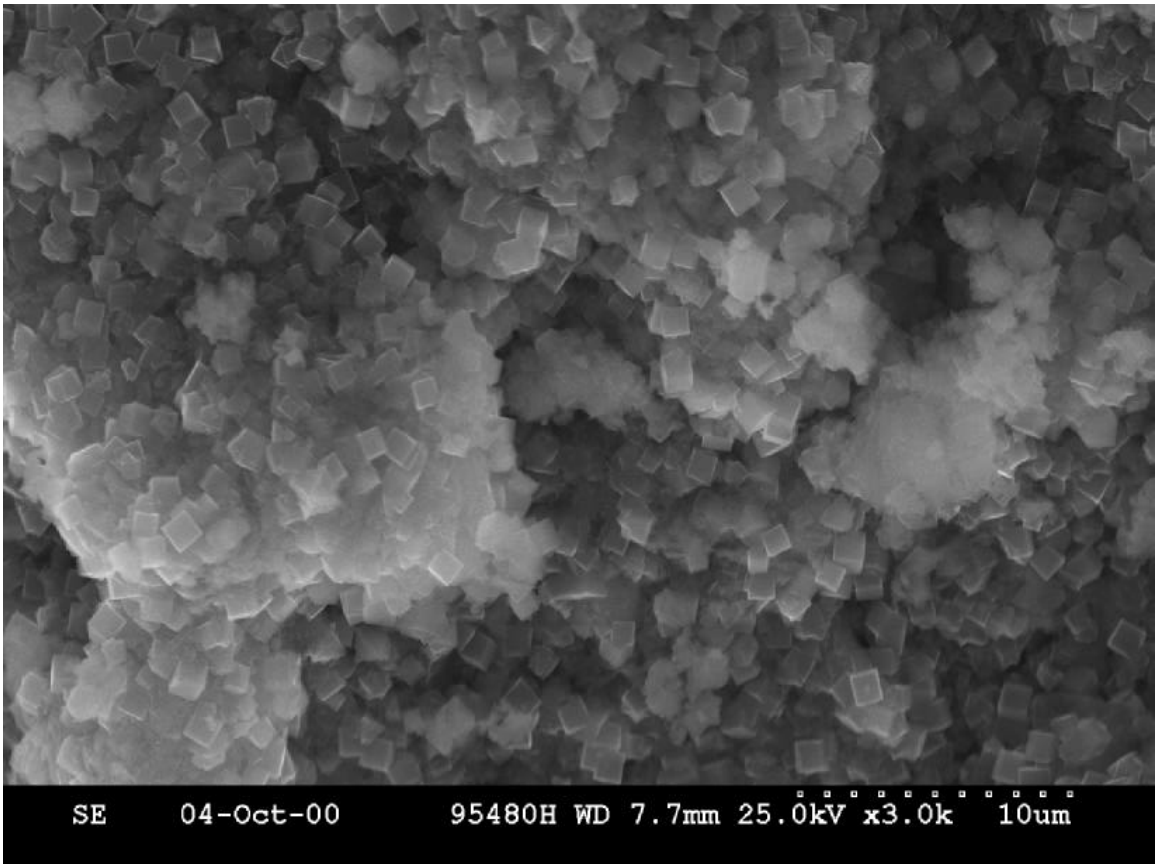

Figure 3.17 SEM euhedra cubes of type A zeolite formed in hydroceramic host synthesized at 95°C for 480 hours.

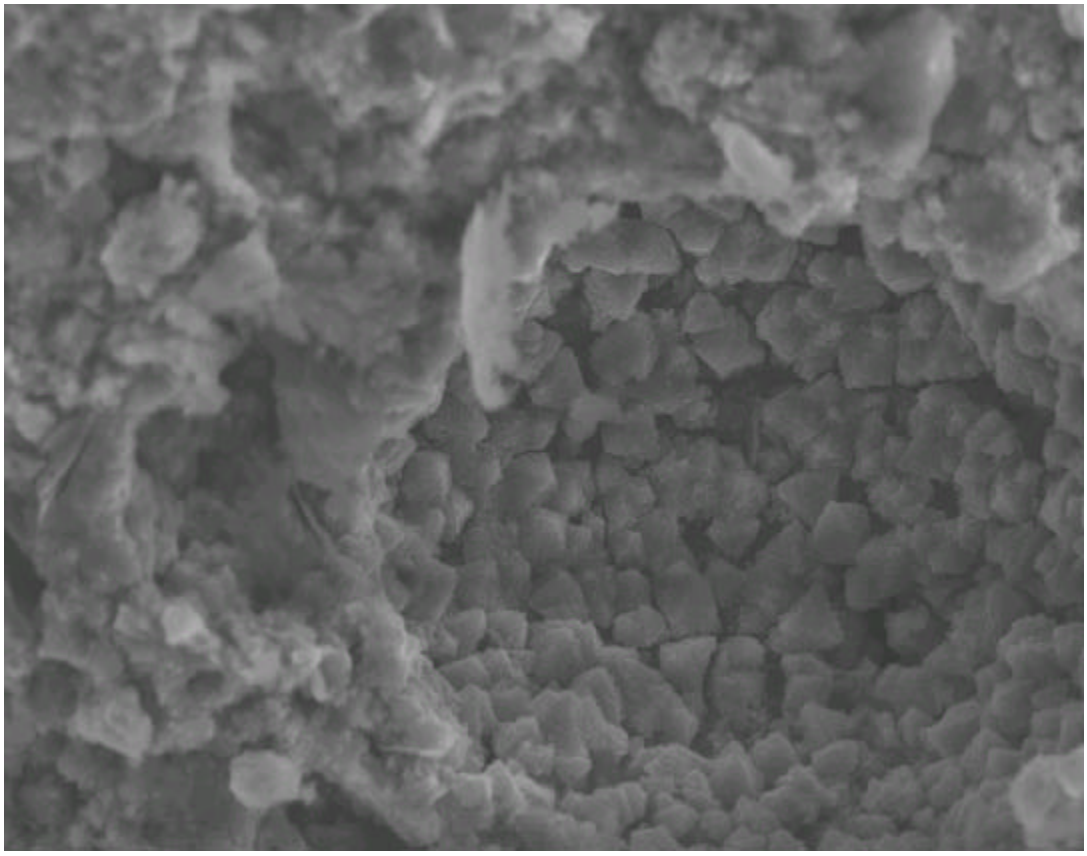

Figure 3.18. The SEM micrograph of NaP1 zeolite formed in hydroceramic host synthesized at 200°C for 60 hours.

3.2 Chemical Analysis and Estimation of Sodium Concentrations

The results of the chemical analysis of selected hydroceramic host sample PCT test solutions are shown in Table 3.1. The table depicts that the concentration of sodium constituted over 80% of the total concentrations of the cations. For the remaining samples, sodium concentrations were estimated from the conductivity-time plots and verified by the results of the selected chemically analyzed solutions.

The transient sodium concentrations of samples not analytically obtained were calculated from the conductivity-time plots and verified by the empirical factor of 230 derived from the AEP and AAS analytical techniques. A standard plot of concentration versus conductivity from the reference solutions of freshly prepared KCl of concentrations 10^{-3}, 10^{-2} and 10^{-1} M and corresponding to 0.147, 1.41 and 12.86 mS/cm (Omega Handbook, 1989) was constructed (Figure 3.19). The slope of the standard plot (0.0079 M/mScm) was used to multiply the values of the specific conductance measured from each sample to obtain sodium equivalent concentration (M) and then converted to mg/L. Alternatively, a factor of approximately 230 can be used to multiply the values of the conductivity values to arrive at the same sodium equivalent concentrations.

Concentration-time data plots were constructed for samples at constant temperature. The concentration-time plots of sodium equivalent concentration released during a 24-hour PCT test of hydroceramics synthesized at 75-200°C as a function of time are

Table 3.1 Concentrations of the major species in the PCT test solutions conducted at 90°C for 24 hours for Hydroceramic host forms hydrothermally synthesized at various temperatures and times.

	125°C			150°C		175°C			200°C		
mg/L	**24Hrs**	**36Hrs**	**60Hrs**	**18Hrs**	**60Hrs**	**12Hrs**	**30Hrs**	**60Hrs**	**6Hrs**	**24Hrs**	**60Hrs**
Al	49	54	37	38	46	75	85	44	61	59	54
B	0.90	0.70	0.60	0.60	0.50	0.40	0.30	0.50	0.40	0.30	0.50
Ba	0.10	0.10	0.10	0.10	0.10	0.10	0.10	0.10	0.10	0.10	0.10
Ca	1.40	0.90	1.40	1.70	1.60	2.10	2	1.60	1.30	1.20	1.70
Co	0.05	0.05	0.05	0.05	0.05	0.30	0.30	0.05	0.05	0.05	0.05
Cr	0.05	0.05	0.05	0.05	0.05	0.05	0.05	0.05	0.05	0.05	0.05
Cs	0.05	0.05	0.05	0.05	0.05	0.05	0.05	0.05	0.05	0.05	0.05
Fe	0.30	0.30	0.20	0.30	0.80	1.50	2.50	0.90	1	0.80	0.90
K	3.50	4.30	5.10	2.50	2.30	4.60	3.90	2.50	3.30	3.10	3
Mg	0.10	0	0	0.10	0.20	0.50	0.80	0.20	0.30	0.20	0.20
Mn	0.05	0.05	0.05	0.05	0.05	0.05	0.05	0.05	0.05	0.05	0.05
Mo	0.10	0.10	0.10	0.10	0.10	0.10	0.10	0.10	0.10	0.10	0.10
Na	500	450	510	400	430	460	400	410	420	360	350
Ni	0.05	0.05	0.05	0.05	0.05	0.05	0.05	0.05	0.05	0.05	0.05
Si	25.30	19.10	11.10	16.50	20.80	47.10	41.30	21.70	37.70	25.40	24.60
Sr	0.20	0.20	0.40	0.20	0.20	0.30	0.30	0.20	0.20	0.20	0.20
Ti	0.05	0.05	0.05	0.05	0.05	0.20	0.30	0.10	0.10	0.05	0.10
V	3.50	3.20	1.20	2.80	2.20	2.30	1.60	1.80	1.90	1.50	1.50
Zn	0.05	0.05	0.05	0.05	0.05	0.05	0.05	0.05	0.05	0.05	0.10

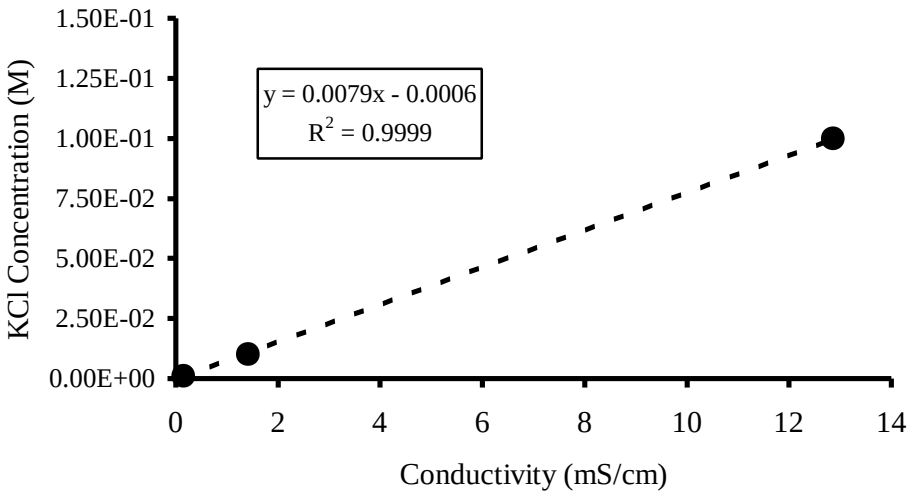

Figure 3.19 Concentration-conductivity curve of KCl standard solutions.

shown in Figures 3.20-3.21, respectively. The concentration of the reference sample is 1828.50 mg/L, a sample with the same formulation but kept at room temperature, was not included in the plots. The difference was so large that it obscured clear correlations between samples from different temperatures.

All the plots displayed similar trends indicating that the same mechanisms govern reactions at all temperatures. The initial higher dissolution rate was due to an insufficient reaction among the reactants and initial washout. In all cases, the concentration of the sodium equivalent decreases exponentially as the processing time increases and increasing temperature from 75-200°C, implying that sodium ion is being combined with the aluminum ion in the tetrahedral sites of the resulting zeolites. The difference in the concentrations of the reference sample (1828.50 mg/L) to the sample processed in one hour at 75°C is (1828.50-1193.67 = 634) and 200°C is (1828.50-436 = 1391.79). The reaction is very fast judging from the fact that the ratio of the first sample processed in one hour at 75°C and 200°C to the initial concentration of the reference sample are 65% and 24%. At the end of the processing times for hydroceramics processed at 75°C and 200°C, only 34.60% and 19.40% of sodium equivalent concentration with respect to the reference sample was released during the PCT test. The ratio of the sodium equivalent concentration between 175 and 200°C at a higher processing time to the reference sample is just over 3% at 12-hour, indicating that the physical and chemical properties of hydroceramics processed at these two temperatures at time >12 hours are expected to be similar.

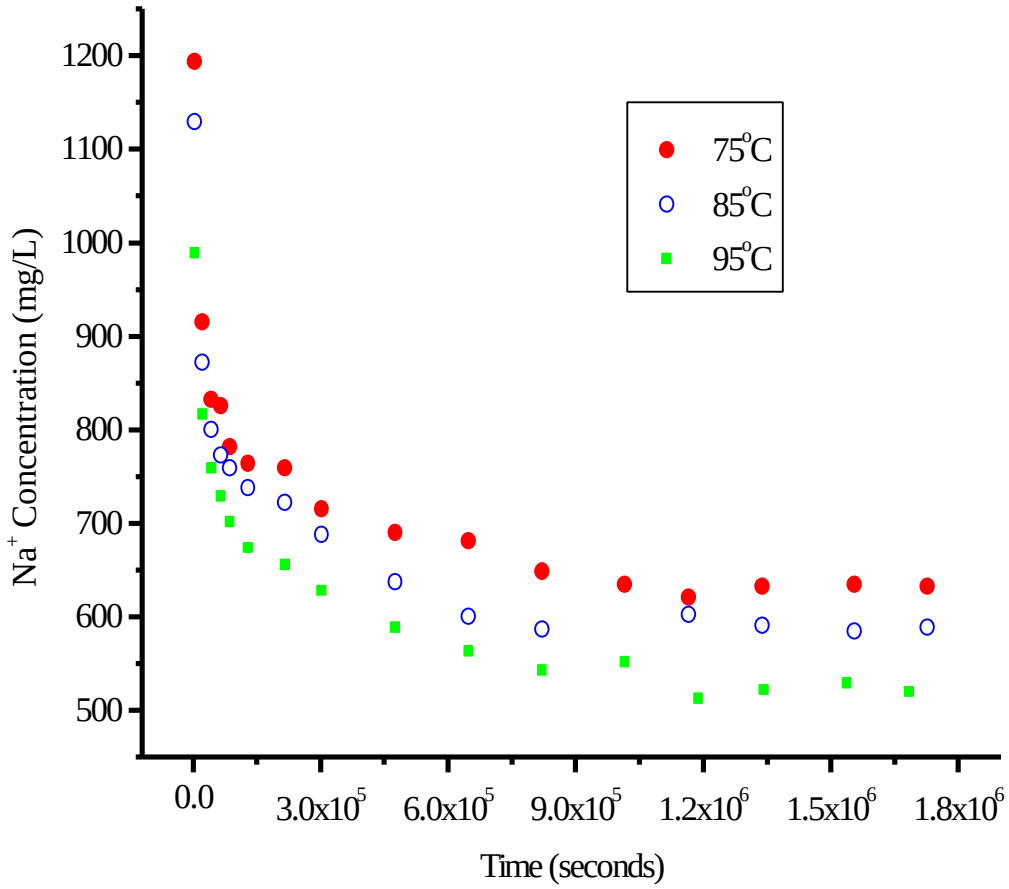

Figure 3.20. Sodium concentration-time of hydroceramic host waste forms hydrothermally processed at 75-95°C at various time intervals.

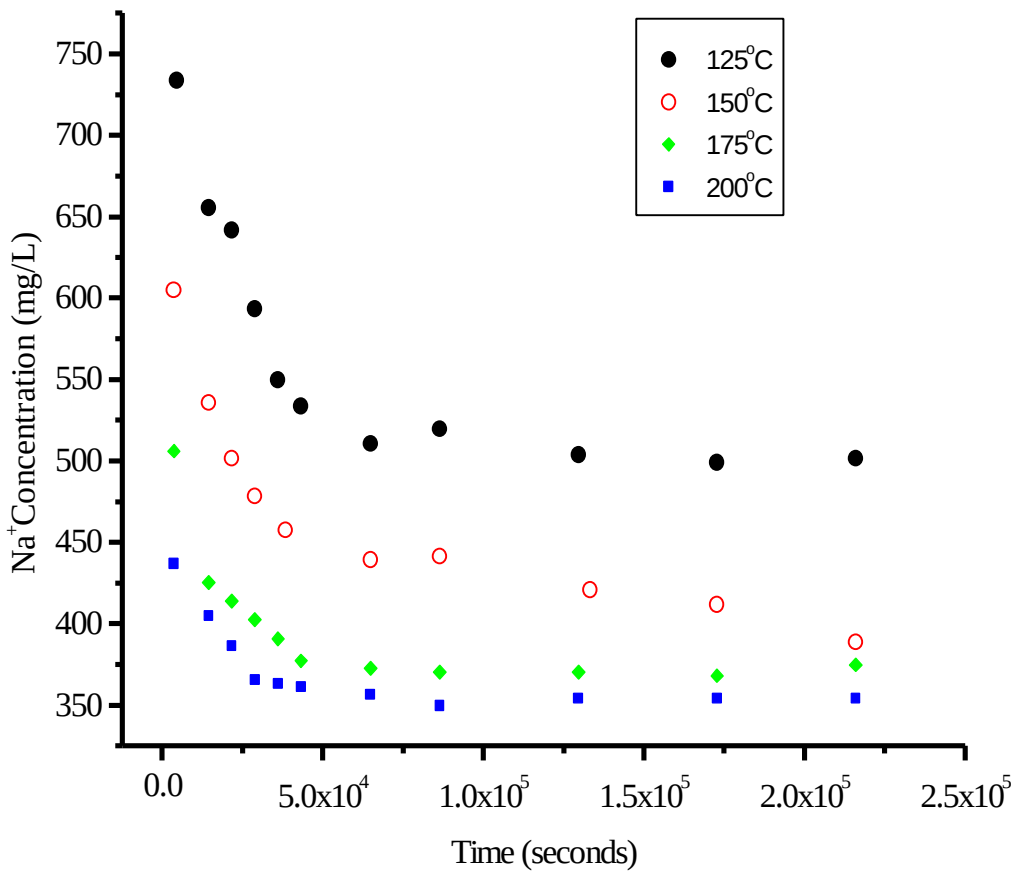

Figure 3.21. Sodium concentration-time of hydroceramic host waste forms hydrothermally processed at 125-200°C at various time intervals.

3.3 Kinetic Results of Hydroceramic Host Waste Form

3.3.1 Kinetic Model

The combined sodium concentrations obtained from chemical analysis and calculated from the conductivity data were used to interpret the hydration kinetics of hydroceramic host waste forms. Data was analyzed using a nonlinear least squares (NLLS) fitting function (Johnson, 1992; Johnson and Fraser, 1985; Johnson and Faunt, 1992; Fogler, 1999; Laidler, 1987; Levenspiel, 1999) expressed in Equation 3.1.,

$$y \; ? \; (y_o \; ? \; y_?)e^{?kt} \; ? \; y_? \qquad (3.1)$$

where y is the concentration at any time, y_o is the initial concentration of the first sample such as the reference sample, y_8 is the concentration at infinite time, t is the time and k is a proportionality or a rate constant. The derivation of Equation 3.1 is shown in Appendix A2.

The choice of nonlinear least square method was based on the assumption that the mechanisms obeyed a first-order irreversible reaction; and that the independent variable (time) was well controlled than the dependent variables (conductivity, concentration, and pH) during the experiment.

The above 3-parameter (k, y_o, and y_8) equation may be difficult to solve analytically. The software Origin 5.0 version by Microcal specifically designed for data analysis and technical graphics was utilized to evaluate k, y_o, and y_8 numerical values. The software uses Levenberg-Marquardt algorithm to evaluate parameters. The reason for the choice of this software lies in its functions for data analysis and graphical construction. More importantly, mathematical expressions written by a user in the user-defined module can be directly solved for various parameters. Iteration of the expression was carried out until the best parameters that minimize the weighted sum of the squares of the deviation between the fitting function and the data were obtained. Results of the numerical values including the deviation from actual data and simulated data of k, y_o, and y_8 are displayed in Table 3.2. The calculated values of the rate constants for the type A zeolite and NaP1 ranged from 2.2×10^{-4} to 6.1×10^{-4}/s and 6.90×10^{-4} to 8.40×10^{-4}/s

3.3.2 Temperature Dependence of Rate Constants

The influence of temperature on the rates of chemical reactions of hydroceramic host computed from the natural logarithms of the rate constants as a function of the reciprocal of temperature (K) is shown in Figure 3.22, for the type A zeolite formed at 75-150°C. A similar method was used for the NaP1 zeolite phase crystallized at 175-200°C. From the slope of the lines, the activation energies for the overall reaction for the type A and NaP1 zeolite phases were calculated to be 16.10 kJ/mol

Table 3.2 Summary of the rate constant calculations for the first-order hydration kinetics of hydroceramic host waste form.

Temperature	Parameter		
	y_o (mg/L)	$y_?$ (mg/L)	K (s^{-1})
75°C	1820.90 ± 362	716.38 ± 23.85	$2.2x10^{-4} \pm 6x10^{-5}$
85°C	1823.82 ± 101.22	669.56 ± 26.22	$2.5x10^{-4} \pm 6x10^{-5}$
95°C	1827.66 ± 97.99	619.389 ± 25.322	$3.30x10^{-4} \pm 8x10^{-5}$
125°C	1827.97 ± 58.38	550.1 ± 18.545	$4.2x10^{-4} \pm 7.0x10^{-5}$
150°C	1828.46 ± 46.15	452.78 ± 15.40	$6.1x10^{-4} \pm 9x10^{-5}$
175°C	1828.5 ± 20.63	386.62 ± 6.524	$6.9x10^{-4} \pm 5x10^{-5}$
200°C	1828.5 ± 17.38	365.01 ± 5.50	$8.40x10^{-4} \pm 7x10^{-5}$

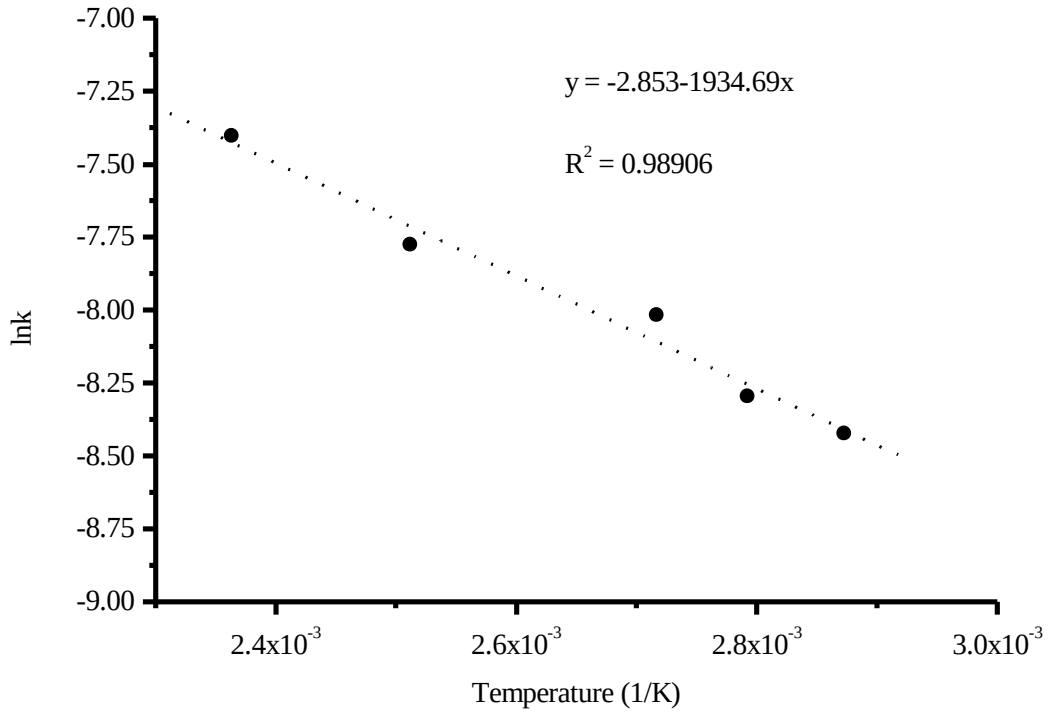

Figure 3.22. Linear plot of the rate constant calculation of the hydroceramic host synthesized at 75-150°C and at various reaction times.

(3.85 kcal/mol) and 13.03 kJ/mole (3.12 kcal/mol), respectively. The difference in activation energy between type A and NaP1 zeolites is only ~3 kJ/mol. These values of the activation energy can be used to decipher the rate-limiting mechanisms of hydroceramic synthesis.

3.3.3 Comparison of Hydroceramic Host Kinetics Results with Literature Data

The values of the rate constants for the type A zeolite, k ($2.2x10^{-4}$ – $6.10x10^{-4}$, table 3.1) or the overall activation energy calculated from the PCT (dissolution) at $90^{o}C$ for 24-hours is comparable with or sometimes less than the literature data. Walton et al., (2001) obtained $3.27x10^{-4}$ and $5.34x10^{-4}$/s rate constants for type A zeolite transformation to sodalite at 80 and $90^{o}C$ using an in situ energy-dispersive x-ray methods. The rate constants were directly obtained by taking the double logarithms of the Avrami-Erofe's equation (Avrami, 1939; Avrami, 1940; Avrami, 1941). Various values of the activation energies for the nucleation and growth of zeolite A have been quoted in the literature. Hu and Lee (1990) obtained 62.7 and 45.6 kJ/mol, Culfaz and Sand (1973) 50.16 and 79.42 kJ/mol. Breck and Flannigen (1968) and Zhdanov (1971) obtained 45.98 and 43.89 kJ/mol for the activation energy of zeolite A crystallization. All the values, including this study, were based on first-order kinetic rate laws. The moderate overall activation energy (14-80 kJ/mol) for the nucleation and growth of zeolite A in hydroceramic waste form implies that the controlling mechanism is mass transfer (Lasaga 1998; Lasaga et al.; 1994; Berner 1978).

Higher values of rate constants and hence the overall activation energy between hydroceramics' and the literature values may be ascribed to varieties in the different sources and concentrations of precursors (Chapter I), physical state of precursors (solid or liquid) and processing conditions. For example, high sodium hydroxide solution concentration may result in fast crystallization rate with very little induction period (Kerr, 1966). Several of the kinetic data in the literature are case specific and caution must be exercised when making comparisons. Type A zeolite is usually carried out in solution synthesis and the products washed and thermally post-treated (Ciric, 1968; Hu and Lee, 1990).

Kinetics data for NaP1 zeolite is very scarce in the literature.

One experimental practice that is questionable among some workers is the syntheses of samples quenched at lower temperatures to terminate further reactions and then post-treat them at much higher temperatures. Many variables including temperature can in fact influence the crystallization of zeolite phases. Ciric (1968) crystallized type A zeolite during a kinetic study at 100°C, dried at 120°C and calcined at 350°C. Hydrothermal crystallization of zeolite A was undertaken for a kinetic study was carried at 50, 70, and 90°C, washed and dried at 300°C for 3 hours (Hu and Lee, 1990).

The ultimate values of the rate constants obtained may be inflated or underestimated due to further reactions during the product thermal treatment. The best method for preserving reaction conditions of a quenched study is by the freeze-drying method. This method preserves reaction stages under investigations and eliminates further chemical reactions.

3.4 General Theory of Crystal Growth and Dissolution

A plausible mechanism for the formation of hydroceramic on the atomic scale involves interfacial transport of ions via the parent phases, adhesion of the ions to the surface, mobility of ions on the surface, and attachment of ions to kinks, steps and edges (Lasaga, 1981; Lasaga, 1998). The slowest of the steps always control the overall growth reaction. The reverse of the aforementioned sequence is applicable to dissolution mechanisms.

Berner (1978) proposed the use of microscopic examination of the surface morphology of partially dissolved crystals to elucidate the rate-controlling mechanisms. A smoothly dissolved crystal surface is an indication of transport-controlled mechanism; owing to the indiscriminately fast removal of materials from the entire crystal surface. Surface-controlled dissolution reaction is characterized by slow dissolution dictated by the differences in the surface energy of the crystal. Highly ordered and flat sections of crystals normally possess low energy while sharp

points, edges, or grain boundaries have higher energies. Lasaga (1998) concluded that both transport and surface mechanisms occur in series.

The value of the calculated activation energy from crystal growth or dissolution experiments can be used to determine the rate-controlling mechanisms of a reaction system under investigation (Lasaga 1984; Lasaga 1998; Lasaga et al.; 1994; Berner 1978). The activation energy of a diffusion-controlling mechanism is ~5 kcal/mole, an equivalent of the energy of a hydrogen bond. Activation energy greater than 5 kcal/mole is an indication of surface-controlling mechanisms. The activation energy of the surface-controlled dissolution of silicate minerals in aqueous media was approximately 62.7 kJ/mole, a function of surface topography, crystal structure, defect, or impurities (Lasaga, 1994).

3.5 Mechanisms of Zeolite Transformation

Numerous kinetic studies have been carried out to rationalize crystallization and dissolution mechanisms of zeolites. The controlling mechanism during crystallization and/or dissolution as a function of time can be explained based on the medium (liquid or solid) in which the transformation is taking place and the calculated activation energy of crystal formation/dissolution. The physical states of the reactants medium will shed some light on the atomic processes during zeolite crystallization in hydroceramics. The range of calculated activation energy from the rate of crystal

formation/dissolution of a material can be used as an indication of whether the controlling reaction mechanism is diffusion- or surface-reaction controlled.

Type A zeolite or the transformation of type A zeolite to hydroxysodalite has generally been used as a model to monitor the hydrothermal reaction kinetics of zeolites and the rate-limiting mechanisms are then postulated. The use of type A zeolite arises from the ease of synthesis at low temperatures, its simple structure (Kerr, 1966; Walton et al., 2001) and nonoverlapping of Bragg reflections between hydrxysodalite (Walton et al., 2001).

Several methods have been employed to determine the rate-controlling mechanism during zeolite crystallization. Kerr (1966) postulated that the kinetics of zeolite A crystallization was by (i) deposition of some dissolved sodiumalumino species on the crystal surface, (ii) crystallization increases with alkali-activation concentration, (iii) the rate of change is proportional to the amount of crystalline phases already formed, (iv) the reaction obeys a first-order kinetics. The rate-determining mechanism was ascribed to be the rapid dissolution of the amorphous species, not a direct solid-state transformation, to soluble species followed by nucleation and crystallization.

Autocalalytic nucleation theory has been used to explain the nucleation mechanisms of type A zeolites. Subotic et al., (1980) and Barrer, (1982), Kerr (1966) propounded this theory based on the data of Zhdanov (1971). The mechanism states that there exist at an early times the presence of microcrystalline domains, contained in the

amorphous gel phase. It was assumed that the autocatalytic nucleation sites were evenly distributed in the gel phase, which are released and activated (onset of growth) as a result of gel dissolution. In other words, an autocatalytic nucleation can be defined as an induction period of nucleation, which is immediatedly followed by a rapid crystal growth stage. Several studies have been conducted to reinforce this theory (Subotic and Graovac, 1985; Bronic et al., 1987; Subotic 1989; Katovic, 1989; Subotic and Bronic, 1993). Ciric (1968) studied the kinetics of zeolite A crystallization at 100°C by varying NaOH. Water-sorption method was used to calculate the percent of crystalline phase in search of concrete evidence to support Kerr's (1966) autocatalytic hypothesis.

Mathematical analysis of the crystal mass have also been undertaken to prove the correctness of the theory of the autocatalytic nucleation mechanisms (Warzyworda and Thompson, 1989; Gonthier et al., 1993; Meise and Schwochow, 1973; Kacirek and Lechert, 1975; Kacirek and Lechert, 1977).

Other theories have been used to explain zeolite crystallization mechanisms. A direct transformation of amorphous gel into crystalline phases via solid-state reaction or by surface nucleation and short-range ion migration (Rocha et al., 1991; Bodart et al., 1986; Dewaele et al., 1985) have been proposed. Another school of thought proposes homogeneous nucleation and growth from the dissolved species, with the gel as a medium for supplying reactant to the liquid. Engelhardt et al., (1983) and Engelhardt et al., (1985). Zhdanov (1971) postulated that the crystallization of

zeolites involved homogeneous nucleation and growth via the available dissolved nutrients in solution.

Combination mechanisms involving concurrent operations of solid-state and aqueous transformation of zeolite crystallization (Bodart, 1985) has been invoked. Analytical methods have been used to provide mechanistic and structural evidences for the crystallization mechanisms of zeolite A from gels to crystals. Various characterization techniques such as solid-state NMR, XRD, TG-DTA-DTG and SEM were used as an evidence for the combination processes (Bodart, 1986; Deruane, 1981; Dewaele, 1985).

3.6 Mechanisms of Hydroceramic Formation

The mechanisms in operation during hydroceramic transformation and dissolution are similar to those of zeolites. Zeolite crystallization in hydroceramic is a combination of dynamic equilibria among the amorphous solid phases (metakaolinite), the coexisting aqueous solution (NaOH, CsCl and $Sr(NO_3)_2$), and the resulting crystalline phases. The chemical and physical transformations involved in these processes are dissolution/precipitation of the starting solid material, nonaqueous reactions between the gel and the zeolite materials and finally, crystallization of the crystalline phases. All these chemical and physical transformations include the breaking (depolymerization) of chemical bonds and the formation (polymerization) of new chemical bonds. The transformations involve polymerization/depolymerization of

silicoaluminate species and the formation of polysilicate anions and silanol groups (Bodart et al., 1986).

Several reaction mechanisms can be used to explain zeolite crystallization in hydroceramic waste form. Solid and aqueous media syntheses can be used to explain hydroceramic synthesis because it involves a mixture of both liquid and solid reactants. These transformations occurred macroscopically and on a molecular level. Strontium, cesium and sodium ions were available as cations in aqueous phase because their solid precursors were dissolved in distilled water. Metakaolinite is an amorphous solid that is activated by the alkali solution. During the activation, aluminum and silicon ions were released into solution due to the dissolution of metakaolinite. The various ions involved in solution were combined as dictated by temperature, solution pH, processing time, thermodynamics/kinetics and other experimental conditions to form numerous nuclei resulting in polycrystalline zeolites. During these physical and chemical processes, the breaking of chemical bonds such Na-O-H (NaOH), Sr-O-N-H [$Sr(NO_3)_2$], Cs-Cl (CsCl), Al-Si-O-H [$(Al_2Si_2O_5(OH)_4$] take place. The formation/rearrangements of the new bonds to form zeolites involves a combination of various cations and anions or the structural rearrangement of metakaolinite to achieve a thermodynamic stability.

When the solid-state process is in operation, diffusion through solid may be the governing mechanism. In this case, alkali and alkaline ions must migrate via through solid metakaolinite and combine with aluminum and silicon to form zeolites. The

end results of these processes may lead to ion exchange, isomorphic substitution, an/or simply a combination of cations and anions to maintain electroneutrality which may lead to nucleation and growth of respective zeolites.

3.7 Evaluation of Process Variables

The effects of several processing variables on the hydration rate and stability of hydroceramic waste forms were investigated. Details are given below.

3.7.1 Effects of Precuring Samples on Hydroceramic Synthesis

The reason that a pre-curing process was usually carried out at a low temperature (<100°C) prior to processing of the zeolite containing waste form was to promote the formation of a gel containing oligomers of Al-O-Si bonds required for the formation of zeolite (Yoshida and Inoue, 1986). Further heating of the gel will lead to the nucleation of a particular zeolite phase as a function of the template used. In this instance, the solvated sodium ion served as the template. Polymerization of the oligomers result in the formation of a three-dimensional aluminosilicate crystalline network (Barrer, 1982). Hydroceramic was precured at 90°C for 24-hours to test the effect on the samples prepared at 200°C (Figure 3.23). Both cured and uncured samples were treated at 200°C for 24 hours. There was very little differece between the concentration of the equivalent sodium released during the PCT test for precured and uncured samples from 1-12 hours. After 12-hour processing time, the equivalent

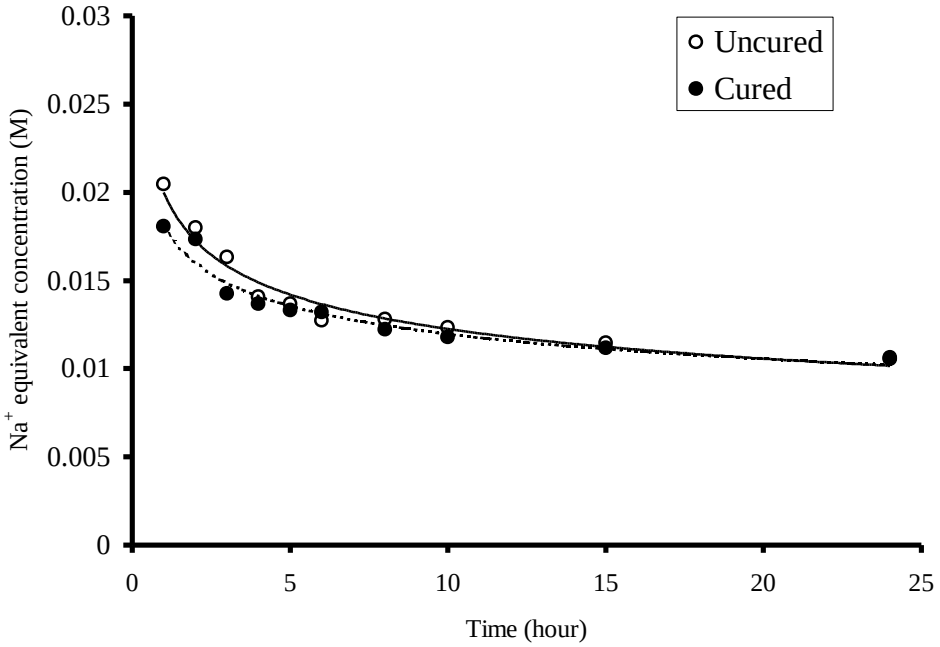

Figure 3.23. Concentration-time plot of hydroceramic. Comparison between uncured and precured at 90°C for 24 hours of hydroceramic samples synthesized at 200°C at various times.

sodium concentration is the same. Figure 3.24 compared the pH plots of both samples. The figure mimics similar trends, as that of concentration-time graph with very little numerical difference between the cured and uncured samples. Because of these observations, subsequent samples were processed without undergoing any precuring process.

3.7.2 Stability of the Crystalline Phases in Hydroceramic Waste Form

Type A zeolite formed at temperatures >100°C and processing times longer than 24 hours formed hydroceramic waste forms showing an unusual stability. The XRD diffraction patterns of the hydroceramic host waste form showed that only type A zeolite and quartz phases formed at 75-150°C for 1-500 hours and Na-P1 type zeolite and quartz phases crystallized at 175-200°C for 1-60 hours.

Walton et al., (2001) observed that low-water content and high NaOH solution resulted in the temporary formation of zeolite A but hydroxysodalite (Breck, 1984; Vaungh, 1995; Rees and Chandrasekar, 1993) was the stable end-product upon continued heating. The conversion to zeolite P at temperature greater than 100°C within a short time has been observed (Breck, 1984).

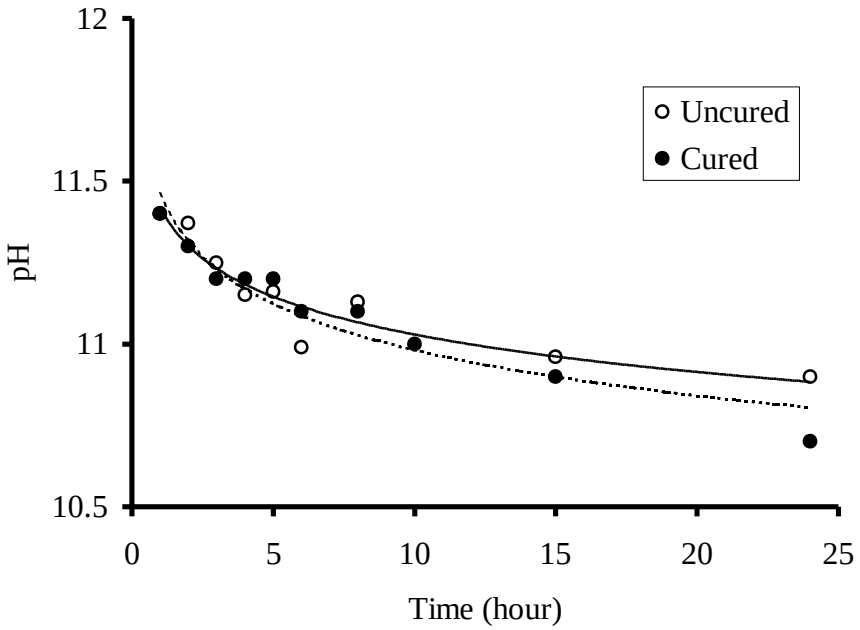

Figure 3.24. pH-time plot of hydroceramic host waste form. Comparison between uncured and precured at 90°C for 24 hours of hydroceramic samples synthesized at 200°C at various times.

3.7.3 Effects of Varying Reactants

The effect of the reactants on the crystallization of the zeolitic phases formed in hydroceramics was investigated at 125°C for 64 hours by the elimination of a reactant component from the original formulation while keeping sodium and metakaolinite constant. Samples were divided into two categories of vermiculite and nonvermiculite containing samples. The XRD patterns of both categories revealed that in all cases, only type A zeolite and quartz phases were formed (Figures 3.25 and 3.26). In fact, the new samples with each reactant taken out were more crystalline than the samples processed from the original hydroceramic host formulation probably because the absence of any one of the reactants leads to the increase in the water content.

3.7.4 Effect of Water

Since the effect of varying reactant-components did not result in any new phase or transform into other phases, the only component left uninvestigated was water. The effect of varying amount of water was tested on the original composition of hydroceramic waste form. The amount of extra water added was varied and the water content of the sodium hydroxide solution was kept constant (Table 3.3). Three samples containing 5 and 15 times more water than the initial hydroceramic host formulation were prepared and synthesized following the procedures outlined in chapter II at 125°C for 120 hours. Hardness of the samples decreases with increasing

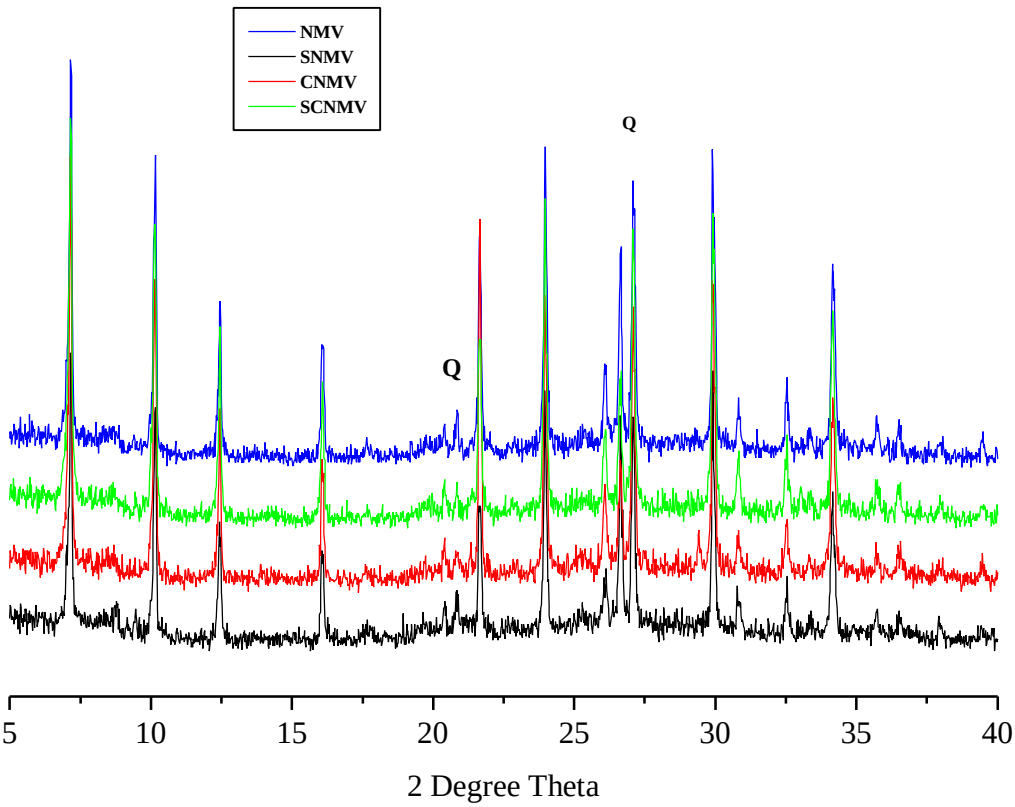

Figure 3.25. X-ray diffraction patterns of vermiculite-based hydroceramic host waste form processed at 125°C for 64 hours. In the legend letter codes, C = cesium, M = metakolinite, N = sodium hydroxide, S = strontium and V = vermiculite. Letter Q represents quartz phase two-major peaks and the remaining unmarked peaks belong to the type A zeolite.

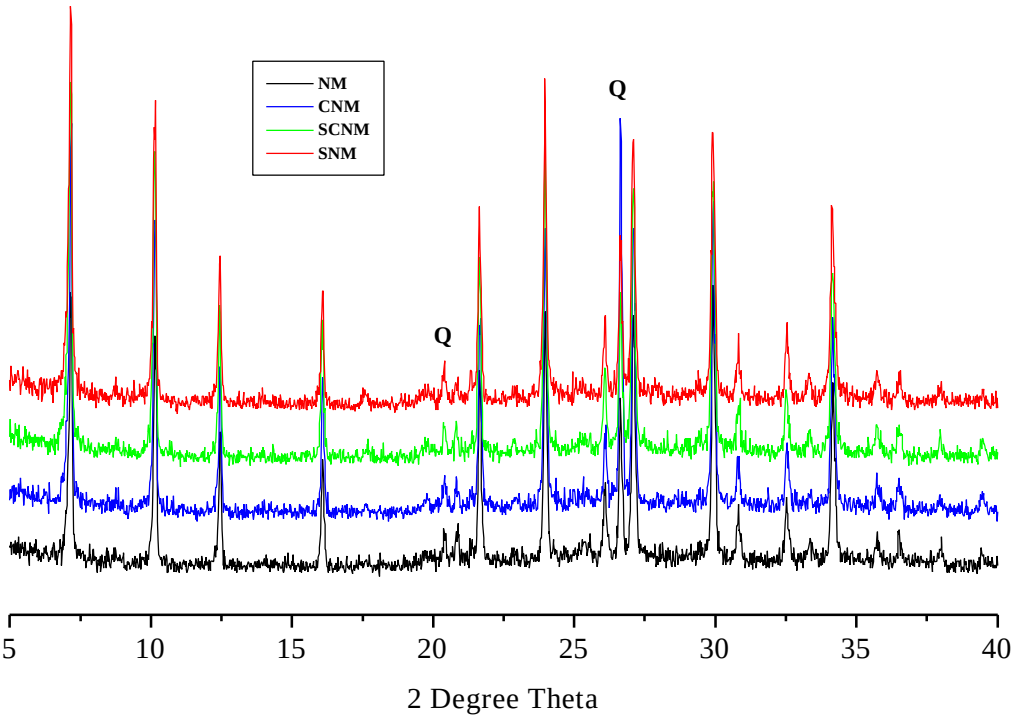

Figure 3.26. X-ray diffraction patterns of nonvermiculite-based hydroceramic host waste form processed at 125°C for 64 hours. In the legend letter codes, C = cesium, M = metakolinite and N = sodium hydroxide. Letter Q represents quartz phase two-major peaks and the remaining unmarked peaks belong to the type A zeolite.

Table 3.3 The formulation used in probing the effect of water on the crystallization of hydroceramic waste form.

Component (g)	**Hydroceramic Host**		
	HC125^{o}C120hrs 1X	**HC125^{o}C120hrs 5X**	**HC125^{o}C120hrs 15X**
Calcined Clay	4.33	4.33	4.33
Vermiculite	0.43	0.43	0.43
Sr(NO3)2	0.0225	0.0225	0.0225
CsCl	0.0225	0.0225	0.0225
37.5 wt% NaOH (9.375 M)	2.60	2.60	2.60
Distilled water	0.167	0.835	2.505

water content. The sample with 15x water content was so soft that very little effort was needed to scrape it out of the hydrothermal Teflon container. X-ray spectra of the samples only showed the presence of type A zeolite and quartz phases (Figure 3.27). Similar experiments were simultaneously conducted for hydroceramic host containing zirconia calcine and fluorinel blend calcine simulated wastes. Results will be discussed in subsequent chapters.

3.8 Recommendations

The combined results of the hydration reaction kinetics and analytical data of the hydroceramic host waste forms were used to establish processing limits. The recommended processing temperature is 200°C for 8 hours and 100% relative humidity.

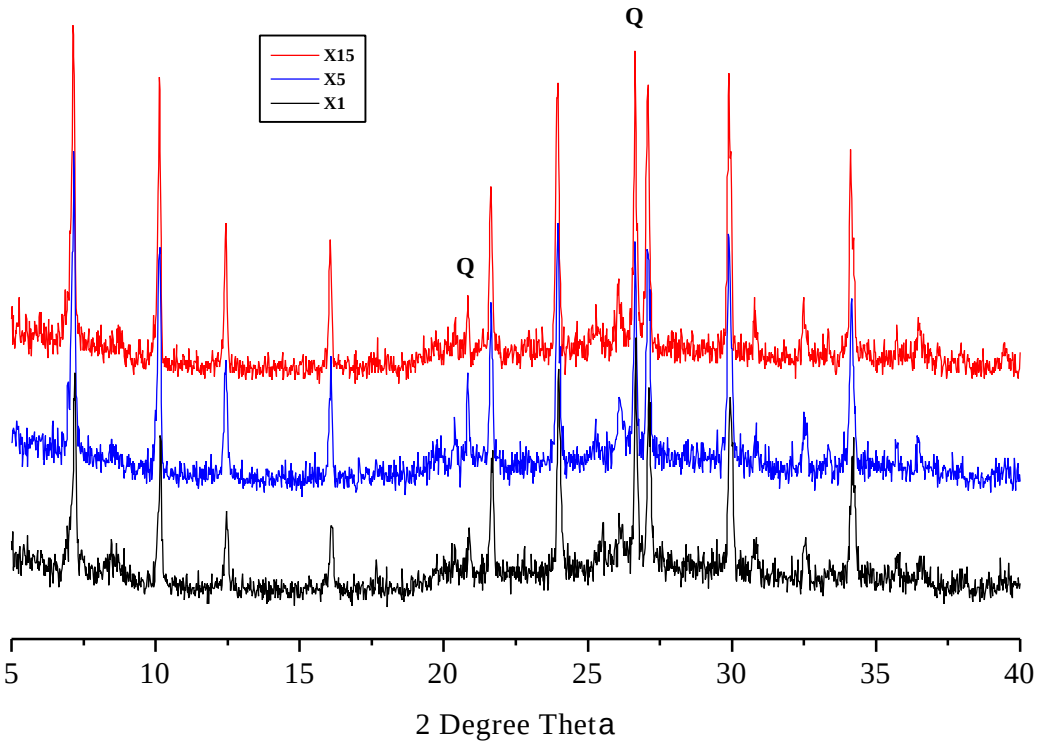

Figure 3.27. X-ray diffraction patterns of hydroceramic host waste form processed at 125°C for 120 hours. In the legend letter codes, X = factor representing the quantity of extra distilled water added to sample. Letter Q represents quartz phase two-major peaks and the remaining unmarked peaks belong to the type A zeolite.

CHAPTER IV

RESULTS OF SYNTHESIS, CHARACTERIZATION AND KINETICS OF HYDROCERAMIC HOST MIXED WITH 30 WEIGHT PERCENT SOLID OF ZIRCONIA SIMULATED CALCINED RADIOACTIVE WASTE

CHAPTER IV

RESULTS OF SYNTHESIS, CHARACTERIZATION AND KINETICS OF HYDROCERAMIC HOST MIXED WITH 30 WEIGHT PERCENT SOLID OF ZIRCONIA SIMULATED CALCINED RADIOACTIVE WASTE

4.0 Introduction

The conductivity and the pH of the "as collected" PCT test solutions were measured and plotted against time to show the overall electrical contributions of all the dissolved ions. Except for the cesium concentration that was determined by the Atomic Absorption Spectrometry (AAS), the relative concentrations of the major cations and anions in the PCT test solutions were determined via Atomic Emission Plasma (AEP) and Ion Chromatography (IC), as functions of time and temperatures. The range of concentrations for RCRA metals (Cr and Cd), anions (SO_4^{2-}, NO_3^-, F and Cl) and surrogate radionuclides (Cs and Sr) were extracted from the analytical results to compare their ranges of concentrations within the samples from each temperature. The retaining capabilities of the synthesized waste forms for the RCRA metals, anions and surrogate radionuclides were measured against the reference samples at all temperatures. Sodium concentration as a function of time was used to interpret the hydration kinetics of the hydroceramic host containing 30 weight percent waste loading of zirconia calcine simulated radioactive waste.

4.1 Results

4.1.1 Conductivity and pH Measurements

The conductivities and the pHs of the "as collected" PCT test solutions were measured and plotted together on double y-axes graphs as functions of the processing time (Figures 4.1-4.7). The conductivity and the pH values of the reference sample were 12.285 mS/cm and 12.30, respectively. These values were not included in the plots because correlations among samples belonging to the same temperature and/or different temperatures may be obscured. The plots of conductivity and pH showed the same exponential decreasing trend before reaching steady states as the processing times and temperatures increase from 75-200°C for all the hydrothermally processed samples. A steady state is defined as when the numerical value of the dependent variable such as concentration or pH remains constant. The samples processed at 175 and 200°C display slight relative increasing (Figures 4.6-4.7) exponential trends before approaching steady states.

The differences in the conductivity values between the reference sample and the processed samples for all temperatures ranged from 6-11 mS/cm. Differences in the conductivity values between the first and the last sample for all temperatures ranged from 0.50 to 2.50 mS/cm. These differences became less pronounced as the processing temperatures increased from 70-200°C, an indication of progressive chemical reactions. Approximately one pH unit difference separated the first sample

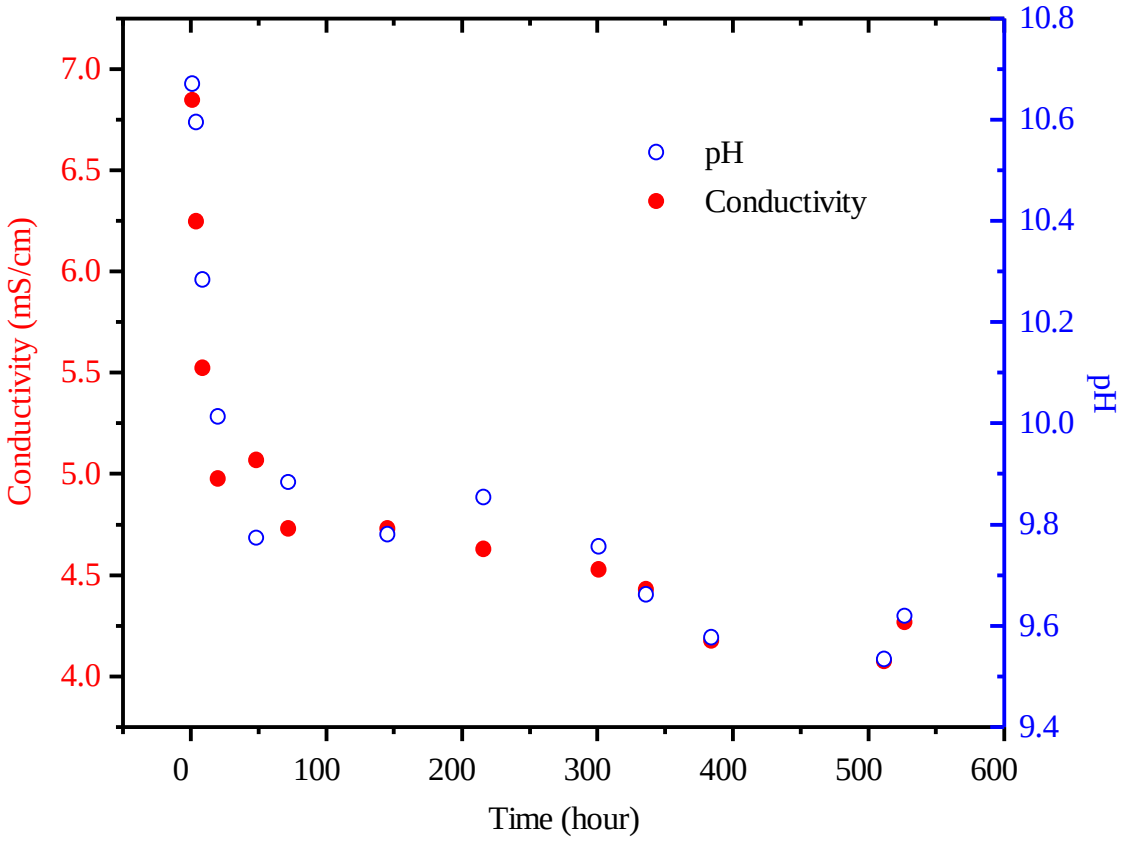

Figure 4.1. Conductivity-pH-time plot of hydroceramic host mixed with 30 weight percent of zirconia calcined simulated radioactive waste and hydrothermally autoclaved at 75°C as a function processing time.

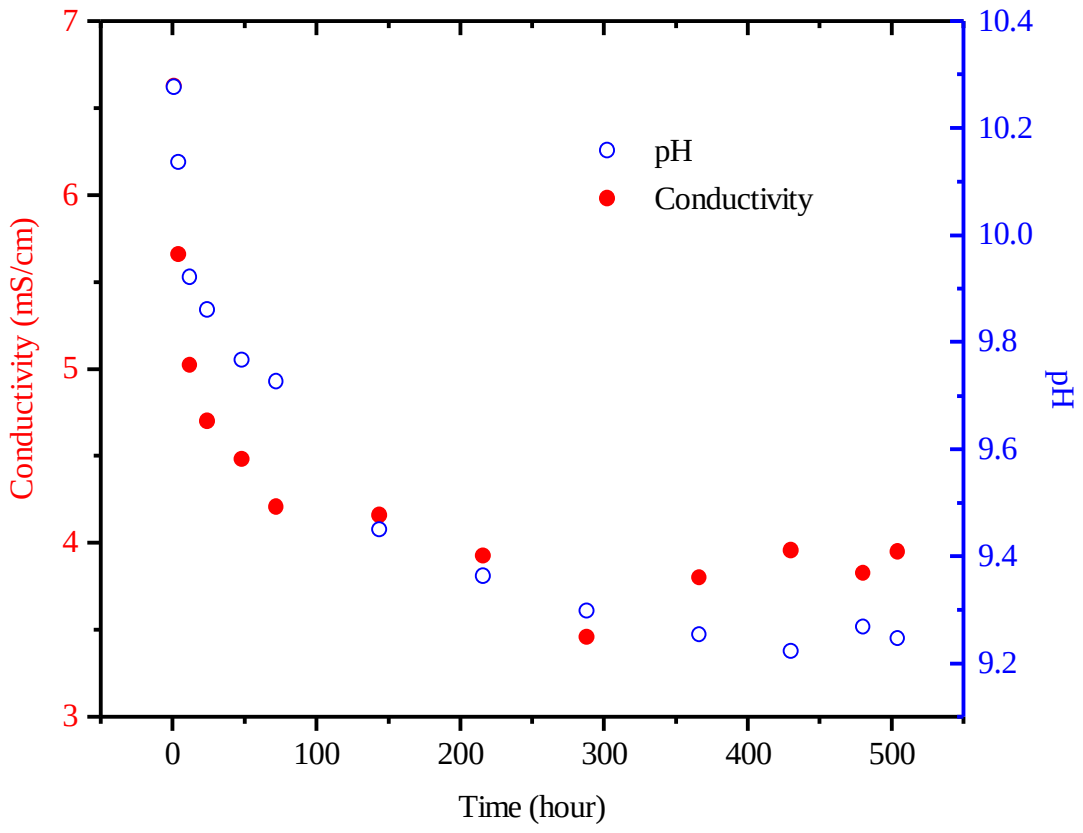

Figure 4.2. Conductivity-pH-time plot of hydroceramic host mixed with 30 weight percent of zirconia calcined simulated radioactive waste and hydrothermally autoclaved at 85°C as a function processing time.

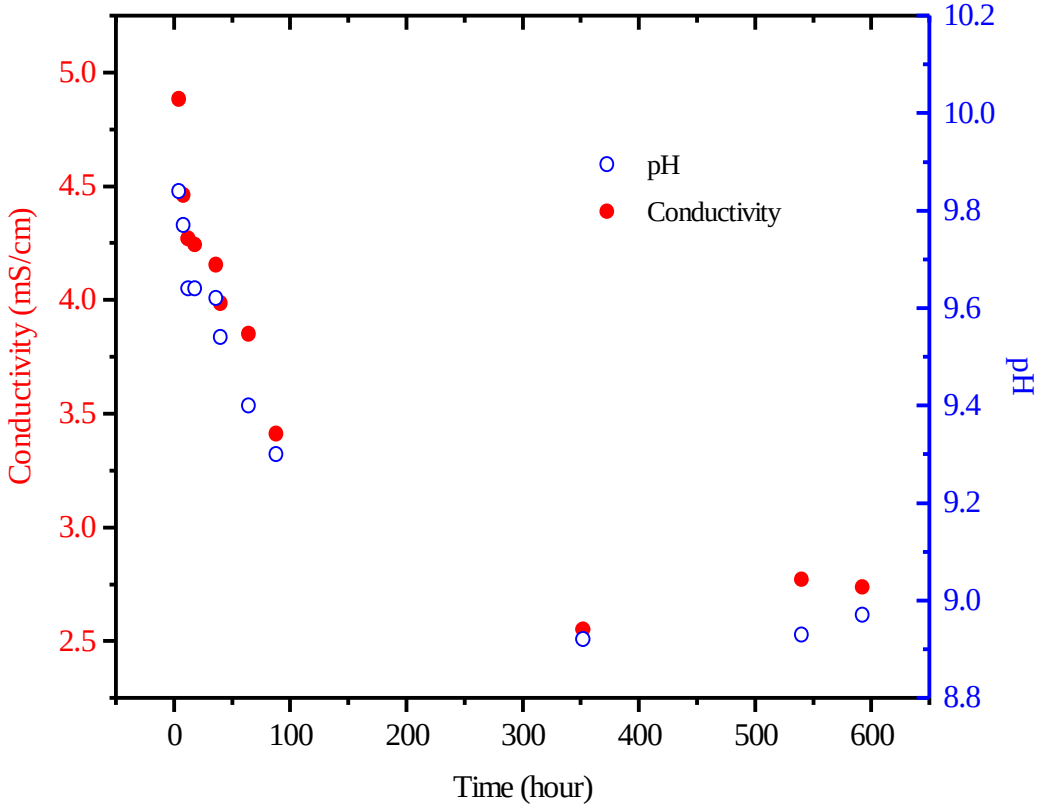

Figure 4.3. Conductivity-pH-time plot of hydroceramic host mixed with 30 weight percent of zirconia calcined simulated radioactive waste and hydrothermally autoclaved at 95°C as a function processing time.

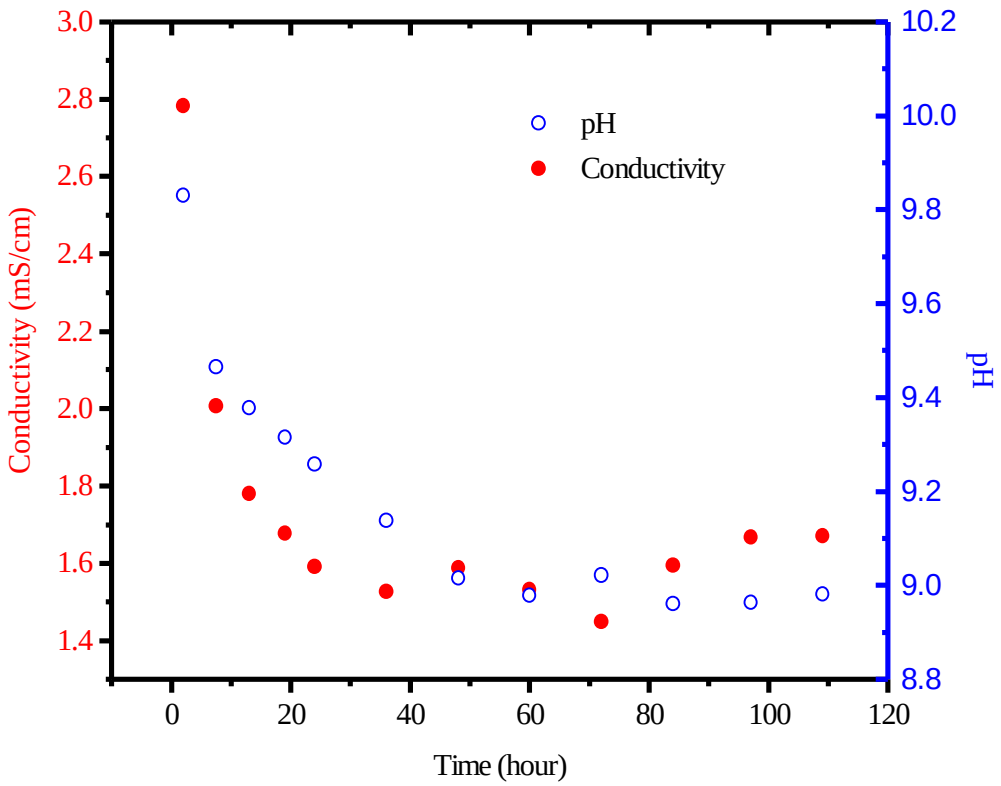

Figure 4.4. Conductivity-pH-time plot of hydroceramic host mixed with 30 weight percent of zirconia calcined simulated radioactive waste and hydrothermally autoclaved at 125°C as a function processing time.

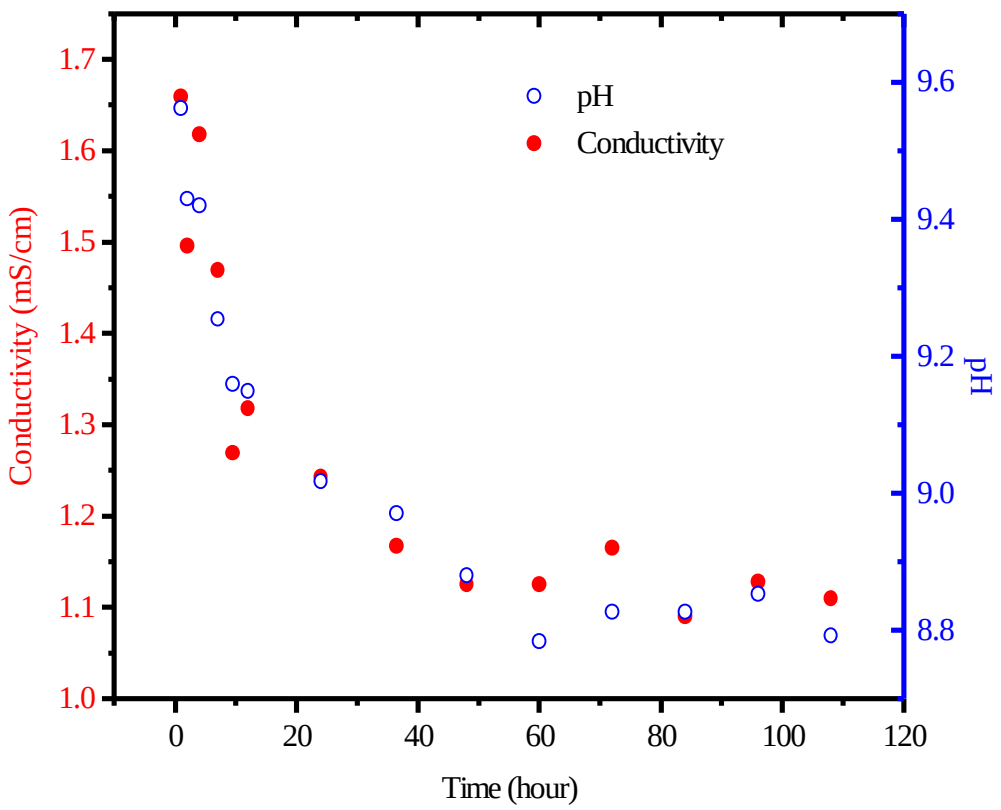

Figure 4.5. Conductivity-pH-time plot of hydroceramic host mixed with 30 weight percent of zirconia calcined simulated radioactive waste and hydrothermally autoclaved at 150°C as a function processing time.

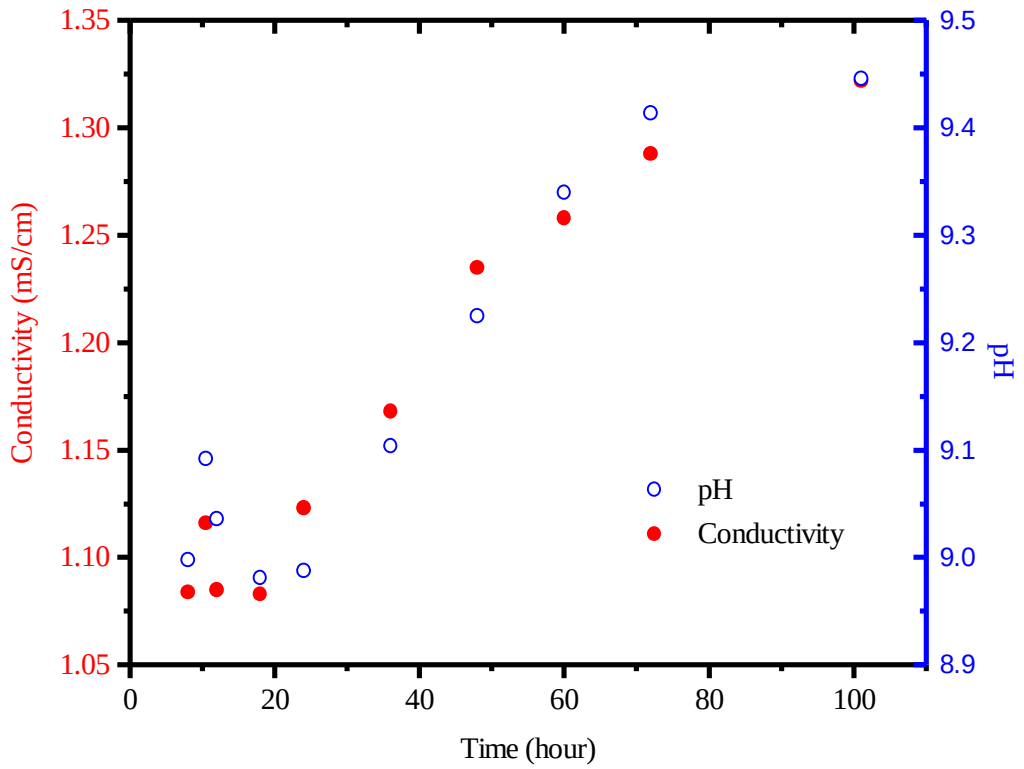

Figure 4.6. Conductivity-pH-time plot of hydroceramic host mixed with 30 weight percent of zirconia calcined simulated radioactive waste and hydrothermally autoclaved at 175°C as a function processing time.

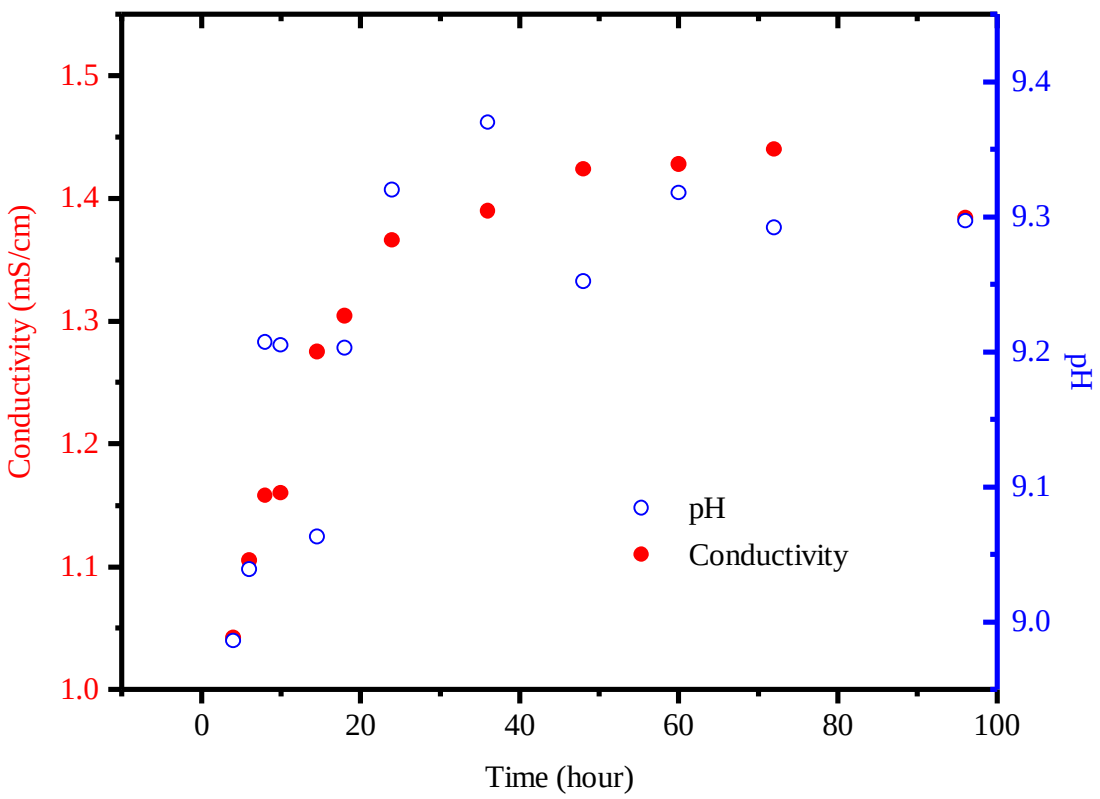

Figure 4.7. Conductivity-pH-time plot of hydroceramic host mixed with 30 weight percent of zirconia calcined simulated radioactive waste and hydrothermally autoclaved at 200°C as a function processing time.

processed at the shortest time and the last sample processed at the longest time for all temperatures.

4.1.2 Chemical Analysis

Results of the chemical analysis of the PCT test solutions conducted at 90°C for 24 hours for the major cations and anions are shown in Tables 4.1-4.7 Appendix C. The overall trend in most cases are similar, the concentrations of the ions decrease as the processing temperature increases. The reference sample ion concentrations were in most cases higher than the concentrations of the processed samples.

4.1.2.1 Chromium Results

The range of retaining capabilities, the lowest and the maximum chromium concentration measured from waste forms processed at 75, 85 and 95°C are similar (27-45 mg/L). The measured relative concentrations of chromium dramatically decrease from 125 mg/L for the reference sample to 0.06 mg/L for samples processed at 150-200°C. The chromium retaining potential of the 125°C samples at processing time above 48 hours showed less than halve of the measured concentration of the sample processed at 2 hours (Table 4.8). The chromium fixation of the 150 and 200°C samples were slightly better than the 175°C samples. Considering the high chromium concentrations measured from the reference waste form, the overall chromium retaining capability of the waste forms are very encouraging at all temperatures. The 75-125°C waste forms retained from 4x to 10x of the reference

Table 4.8. Ranges of concentrations of selected ions for each temperature summarized from tables 4.1-4.7 in comparison with the reference sample (room temperature). The maximum processing time for each temperature are indicated below the temperature.

Reference Ion Concentration (mg/L)	75°C 527 hrs	85°C 504 hrs	95°C 592 hrs	125°C 109 hrs	150°C 108 hrs	175°C 101 hrs	200°C 96 hrs
Sr (0.04)	0.02-0.07	0.02-0.05	0.02-0.09	0.02-0.03	0.02-0.15	0.03-0.15	0.02-0.10
Cs (15)	0.02-6.70	0.02-3.40	<0.02	<0.02	<0.02	<0.02	<0.02
Cr (125)	34-37	30-45	27-40	11.5-37	0.08-31	0.13-0.26	0.06-0.32
NO_3^- (1130)	105-120	90-120	90-125	70-90	67-75	67-75	70-80
SO_4^{2-} (480)	940-1240	850-1090	470-880	95-270	23-68	30-100	38-100
F (62)	75-125	90-160	90-110	85-105	85-125	75-85	75-80
Cl (95)	40-44	35-43	41-45	42-51	43-51	45-48	40-49

sample, and 150-200°C released final minimal concentrations of ?0.1 mg/L, which meets the maximum concentration level (MCL) and maximum concentration level goal (MCLG) of 1.0 mg/L (total chromium) set by the USEPA Drinking Water Regulations and Health Advisories for Inorganics (USEPA, 1996).

4.1.3 Anions

4.1.3.1 Results of Nitrate and Sulfate

The measured nitrate concentrations for the samples processed at 75, 85, 95, 125, 150, 175 and 200°C are lower by one order of magnitude (~120 mg/L) to over a factor of 16 (~70 mg/L) than the reference sample (1130 mg/L). The nitrate fixing potentials of the waste forms fall into two categories: waste forms synthesized at 75, 85 and 95°C released from 90-125 mg/L and 150-200°C samples leached 70-90 mg/L (table 4.8). The measured lowest concentration level in the 150-200°C samples is ~7x above the MCL for nitrate (USEPA, 1996). Nitrate fixing potentials of the waste forms are good judging from the large concentration released by the reference waste form.

The analytical results of sulfate concentrations with respect to the reference sample showed two distinctive trends. Waste forms synthesized at 75, 85 and 95°C released equal or more sulfate (480-1240 mg/L) concentration than the reference unautoclaved sample (480 mg/L). Conversely, the 150, 175 and 200°C waste forms dissolved more than half (270 mg/L) to more than twenty times (23 mg/L) less than the concentration

of the reference waste form. It can be concluded that the waste forms synthesized from 75, 85 and 95°C are not suitable for sulfate retention. On the other hand, the resulting waste forms from 150, 175 and 200°C temperatures are excellent in fixing sulfate, the concentrations released were much less than the MCL and MCLG limits of 500 mg/L (USEPA, 1996).

4.1.3.2 Results of Fluoride and Chloride

Fluoride concentrations for all samples at all temperatures showed increased concentrations relative to the reference sample concentration (62 mg/L). Fluoride concentrations increased by a factor of 0.25 to ~2 for samples from 75-95°C and 0.25 to 0.67 for 125-200°C samples. CaF_2 is considered a refractory compound with very low solubility in water. The question then, is why is there an increase in the fluoride ion concentrations during the PCT tests? Is CaF_2 the source of fluoride ion? To answer these questions, CaF_2 ion solubility in water at room temperature (25°C) and 90°C are compared.

CaF_2 ion solubility constant, Kso, in water at 25°C is $5x10^{-11}$ (Snoeyink and Jenkins, 1980). This corresponds to 36.2 mg/L of dissolved fluoride ion. van't Hoff (Equation 4.1) relation was used to determine the effect of the temperature on the CaF_2 solubility at 90°C, assuming equilibrium conditions (Snoeyink and Jenkins, 1980). The CaF_2 K_{so} at 90°C in water is $4.07x10^{-49}$. The concentration of fluoride ion released in water at K_{so} 90°C is $6.35x10^{-44}$ mg/L. CaF_2 displays a retrograde

solubility, the higher the temperature, the lower the solubility. From this calculation, it can be inferred that increasing fluoride ion concentrations with temperature observed from the chemical analysis of the PCT solutions may be attributed to the undersaturation of the fluoride ion in solution at temperature greater than room temperature, $K_{so,90} < K_{so,25}$ (Stumm and Morgan, 1981). Calcium fluoride is expected to be more insoluble in water during the PCT test; and therefore it did not the contribute to the concentration of fluoride.

$$\ln \frac{k_{so,90}}{k_{so,25}} ? \frac{? H^{o}}{R} \left(\frac{1}{T_{25}} ? \frac{1}{T_{90}}\right) \qquad (4.1)$$

where $k_{so,25}$ and $k_{so,90}$ are the solubility constant at 25 and 90°C, T is the temperature (^{o}K), ? H^{o} is the standard enthalpy change value (kJ/mol) and R is the universal gas constant.

The fluoride immobilizing potentials of the waste forms synthesized at 75-95°C range from poor to fair for the 125-200°C.

The capability of immobilizing chloride ions by the synthesized hydroceramic host mixed with simulated radioactive waste at all temperatures showed a similar retention capability of 40% to approximately 50% relative to the reference sample (95 mg/L).

Fluoride and chloride ion immobilization can be improved by the formation of cancrinite $(Na,Ca)_{7-8}[(AlO_2)_6(SiO_2)]_6(NO_3,SO_4,F,Cl,CO_3)_{1..5-2,}1-5(H_2O)$ in the waste forms via structural incorporation.

4.1.4 Results of Surrogate Strontium and Cesium Radionuclides

Considering the high concentration of cesium measured from the reference sample (15 mg/L), the retention potentials of all the waste forms for every temperature investigated (75-200°C) are all capable of immobilizing cesium (^{137}Cs) radionuclide from the INEEL calcined high-level radioactive wastes. Chemical analyses of the waste forms processed at 75 and 85°C showed that after 145 and 72 hours of processing time, cesium concentration was below detection level (<0.02 mg/L). Cesium concentrations released during the 24-hour PCT test for the waste forms processed at 95-200°C were below detection level for all the samples even as early as 1 hour.

Strontium concentrations released by the waste forms were very small compared to the reference sample (0.04 mg/L). The interpretations of the strontium concentration results are not straightforward because of intra- and inter-sample concentration fluctuations. Sometimes the concentration measured was below detection level (<0.02 mg/L) or randomly above the reference concentration. The fluctuation in the concentrations can be ascribed to experimental and analytical errors. Extra precautions must be exercised during sample preparations and chemical analyses.

4.1.5 XRD Results

Five x-ray diffraction patterns representing samples from 75-200°C are displayed in Figures 4.8-4.14. The x-ray diffraction patterns showed type A zeolite ($Na_{96}Al_{96}Si_{96}O_{384}.216H_2O$), hydroxysodalite ($Na_4Al_3Si_3O_{12}(OH)$, a combination of both and persistent crystalline phases from the reactants: quartz, calcium fluoride and zirconia. Only type A zeolite crystallized from samples processed at 75-95°C (Figures 4.8-4.10), a combination of type A plus hydroxysodalite formed at 125-150°C (figures 4.11-4.12) and only hydroxysodalite at 175-200°C (Figures 4.13-4.14). The major difference is that the peak intensities of type A zeolite phase formed from samples synthesized from 75-95°C resulted in as much as ~4x the intensities of samples processed from 125-150°C. Dramatic reduction in the peak intensities of samples processed at 125-150°C may be due to the formation of zeolite A that is mostly favorable at ?100°C and transformation to or the formation of hydroxysodalite. The unusual stability of type A zeolite at >100°C may be enhanced by the complex interaction mechanisms between the waste and the host formulations.

Routine computerized peak match using peak positions that matched in both intensity and location (d-spacing or 2?^{o}) with the JCPDS files showed a slight shifting of the peak positions to the left. The reason may be due to solid solution between sodium and cesium, the incorporation of cesium in place of sodium into the structure of zeolite A. Cesium (1.84 Å) has a larger ionic radius than sodium (1.12 Å) (Prewitt,

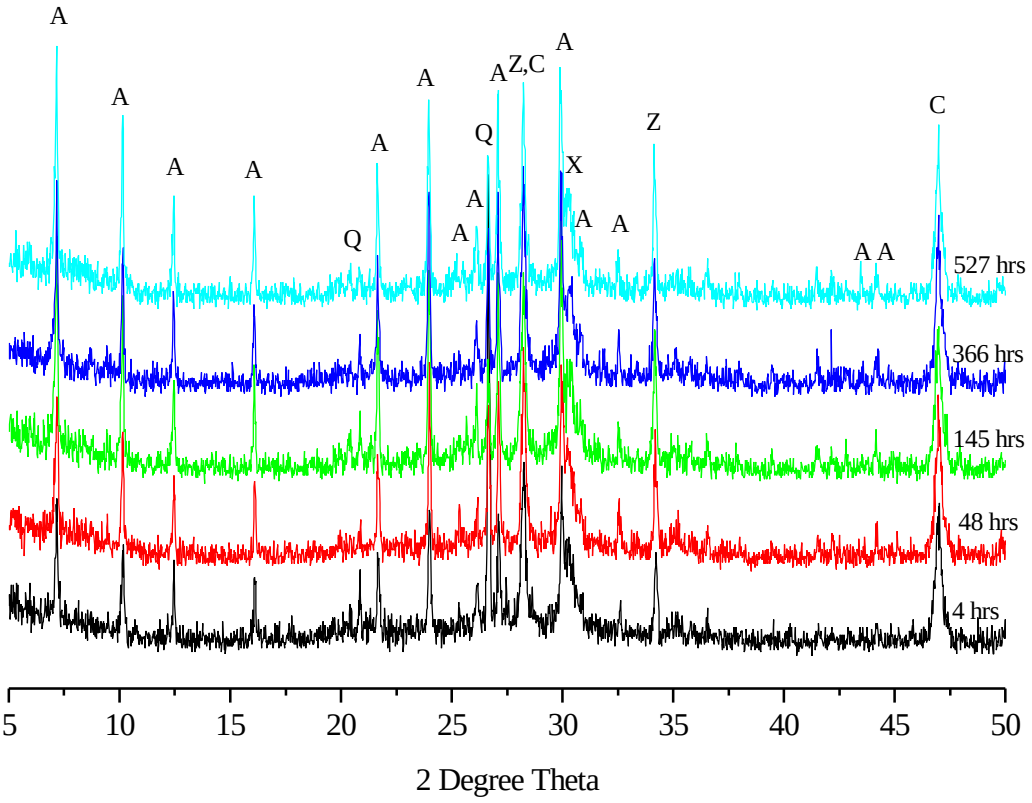

Figure 4.8. Representative XRD patterns of hydroceramic host mixed with 30 (solid) weight percent of simulated zirconia calcined radioactive waste hydrothermally synthesized at 75°C at various time intervals. A = type A zeolite ($Na_{96}Al_{96}Si_{96}O_{384}.2H_2O$, 39-0222); Z = zirconia (ZrO_2, 37-1484); C = calcium fluoride (CaF_2, 35-0816); Q = (SiO_2, 46-1045); and x unidentified poorly crystalline phase, possibly calcium compounds.

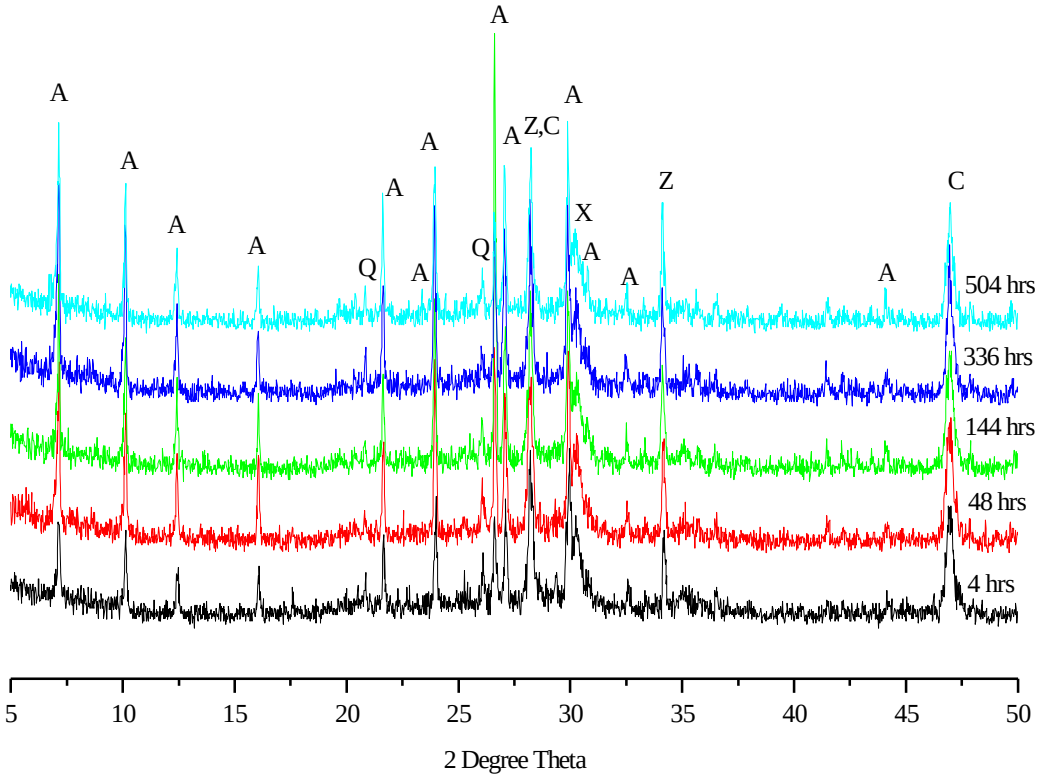

Figure 4.9. Representative XRD patterns of hydroceramic host mixed with 30 (solid) weight percent of simulated zirconia calcined radioactive waste hydrothermally synthesized at 85°C at various time intervals. A = type A zeolite ($Na_{96}Al_{96}Si_{96}O_{384}.2H_2O$, 39-0222); Z = zirconia (ZrO_2, 37-1484); C = calcium fluoride (CaF_2, 35-0816); Q = (SiO_2, 46-1045); and x unidentified poorly crystalline phase, possibly calcium compounds.

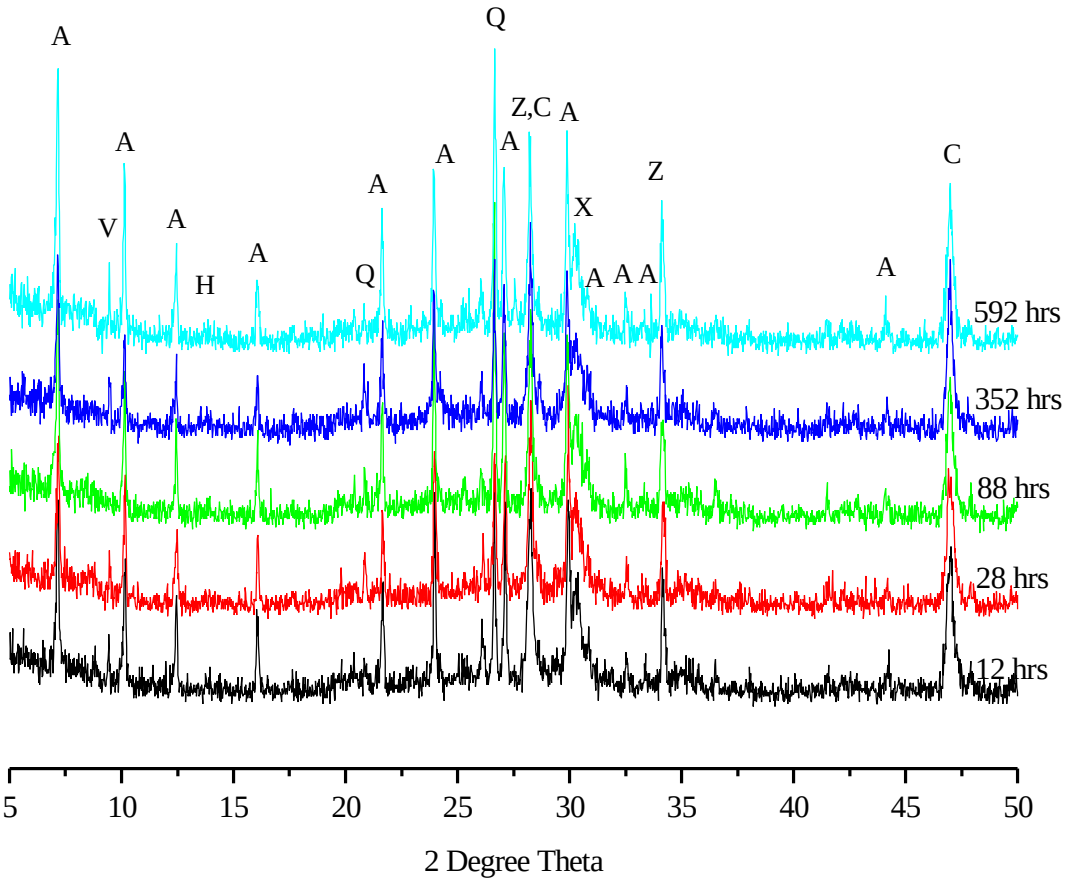

Figure 4.10. Representative XRD patterns of hydroceramic host mixed with 30 (solid) weight percent of simulated zirconia calcined radioactive waste hydrothermally synthesized at 95°C at various time intervals. A = type A zeolite ($Na_{96}Al_{96}Si_{96}O_{384}.2H_2O$, 39-0222); H = hydroxysodalite ($Na_4Al_3Si_3O_{12}(OH)$, 11-0401); Z = zirconia (ZrO_2, 37-1484); C = calcium fluoride (CaF_2, 35-0816); Q = (SiO_2, 46-1045); V = unreacted vermiculite and X = unidentified poorly crystalline phase, possibly calcium compounds.

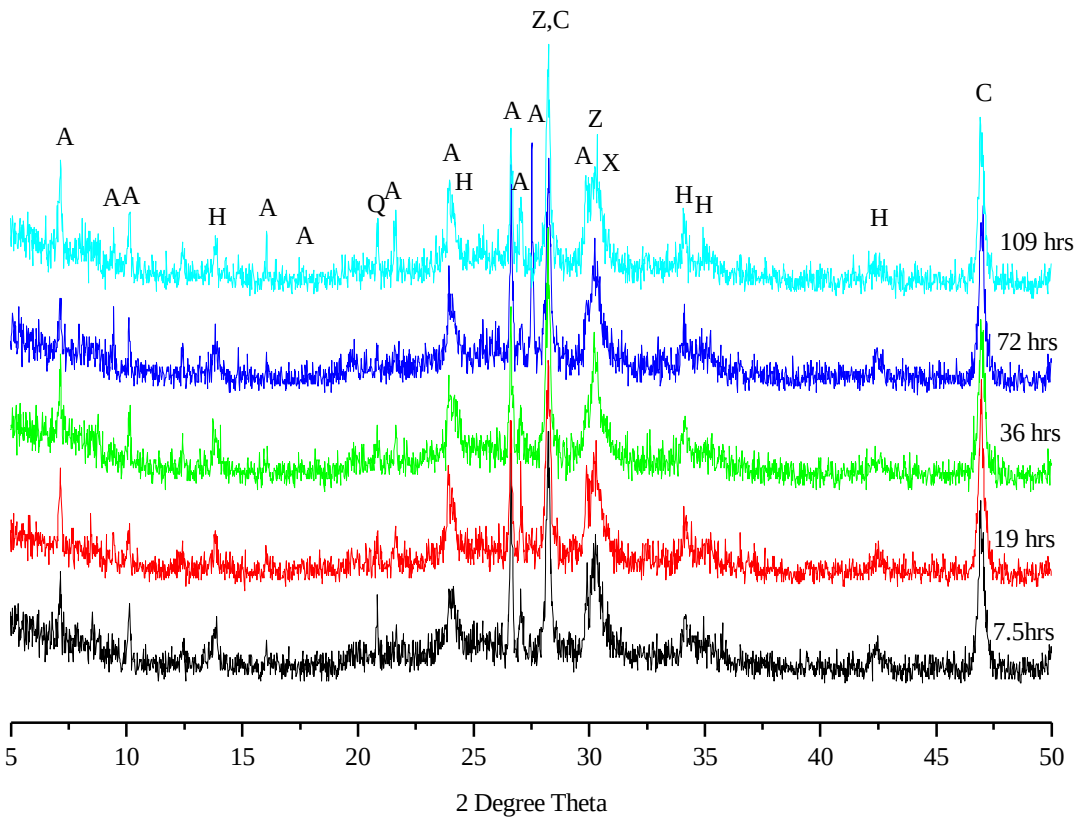

Figure 4.11. Representative XRD patterns of hydroceramic host mixed with 30 (solid) weight percent of simulated zirconia calcined radioactive waste hydrothermally synthesized at 125°C at various time intervals. A = type A zeolite ($NA_{96}Al_{96}Si_{96}O_{384}.2H_2O$, 39-0222); H = hydroxysodalite ($Na_4Al_3Si_3O_{12}(OH)$, 11-0401); Z = zirconia (ZrO_2, 37-1484); C = calcium fluoride (CaF_2, 35-0816); Q = (SiO_2, 46-1045); and x unidentified poorly crystalline phase, possibly calcium compounds.

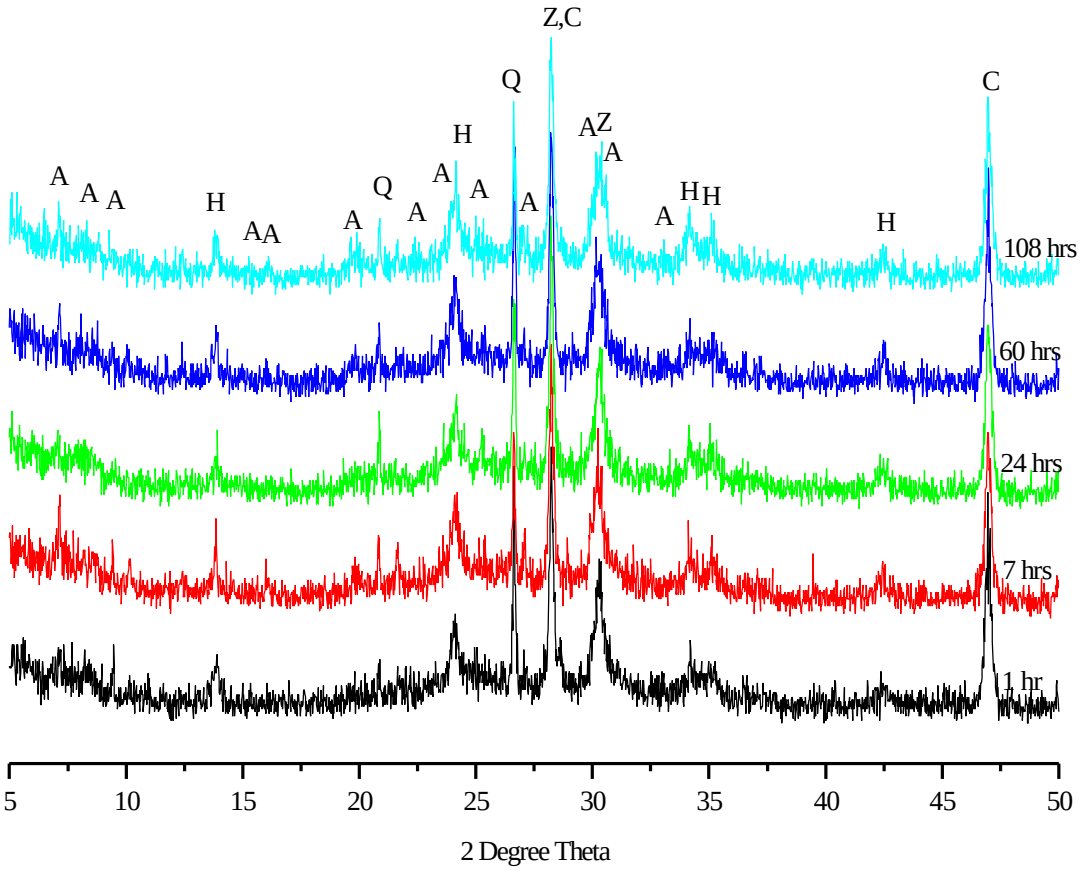

Figure 4.12. Representative XRD patterns of hydroceramic host mixed with 30 (solid) weight percent of simulated zirconia calcined radioactive waste hydrothermally synthesized at 150°C at various time intervals. A = type A zeolite ($NA_{96}Al_{96}Si_{96}O_{384}.2H_2O$, 39-0222); H = hydroxysodalite ($Na_4Al_3Si_3O_{12}(OH)$, 11-0401); Z = zirconia (ZrO_2, 37-1484); C = calcium fluoride (CaF_2, 35-0816); Q = (SiO_2, 46-1045); and x unidentified poorly crystalline phase, possibly calcium compounds.

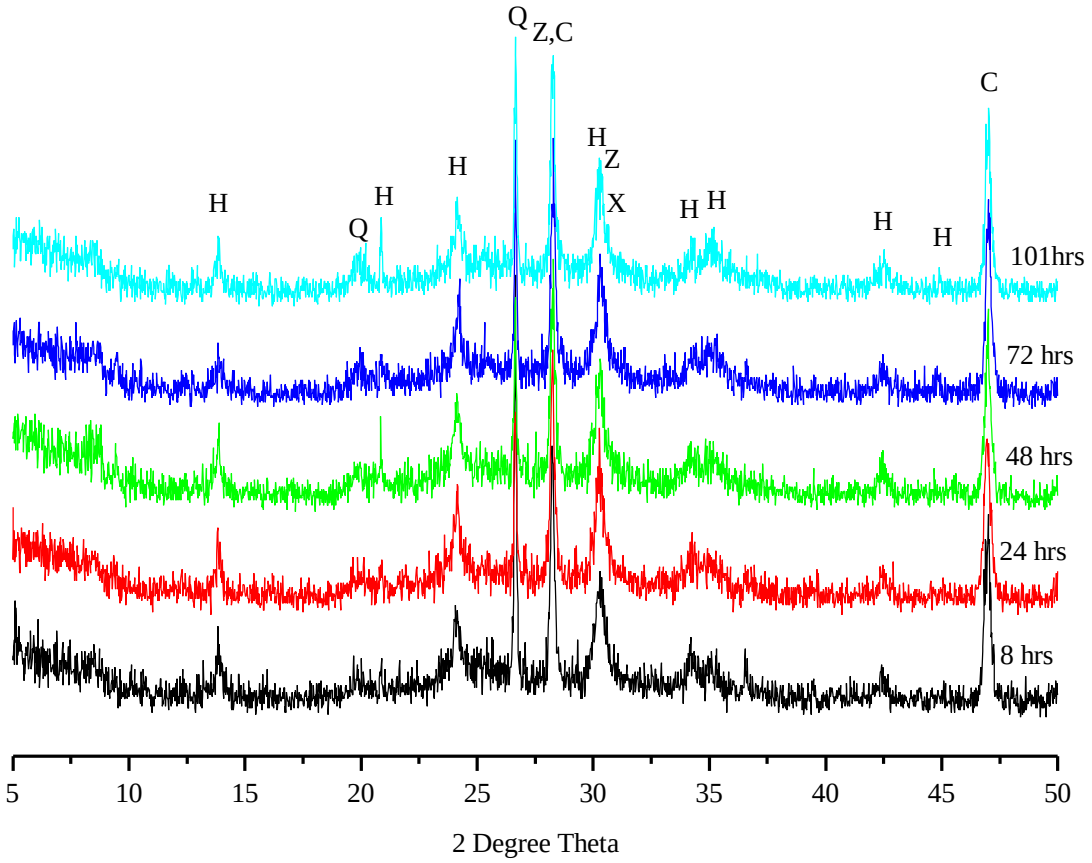

Figure 4.13. Representative XRD patterns of hydroceramic host mixed with 30 (solid) weight percent of simulated zirconia calcined radioactive waste hydrothermally synthesized at 175°C at various time intervals. H = hydroxysodalite ($Na_4Al_3Si_3O_{12}(OH)$, 11-0401); Z = zirconia (ZrO_2, 37-1484); C = calcium fluoride (CaF_2, 35-0816); Q = (SiO_2, 46-1045); and X = unidentified poorly crystalline phase, possibly calcium compound.

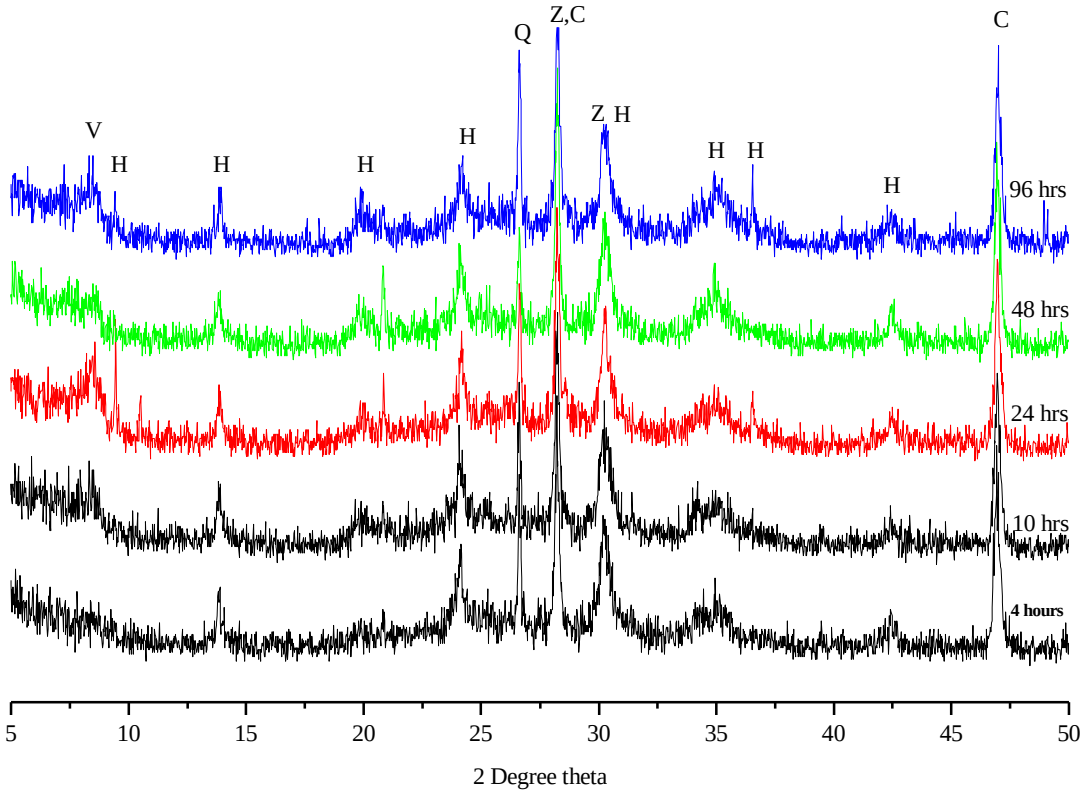

Figure 4.14. Representative XRD patterns of hydroceramic host mixed with 30 (solid) weight percent of simulated zirconia calcined radioactive waste hydrothermally synthesized at 200°C at various time intervals. H = hydroxysodalite ($Na_4Al_3Si_3O_{12}(OH)$, 11-0401); Z = zirconia (ZrO_2, 37-1484); C = calcium fluoride (CaF_2, 35-0816); Q = (SiO_2, 46-1045); and V unidentified crystalline phase, possibly unreacted vermiculite.

1976) and cesium incorporation may cause peak positions to shift to lower angles (2?) or higher d-spacing (Å). Other contributing factor to the shifting in the intensities is preferred crystallographic orientations in clay and vermiculite resulting from packing of the powder during sample preparations (Cullity and Stock, 2001) and possibly misalignment of the diffractometer.

.

4.2 Hydration Kinetics

Similar to the hydroceramic host waste forms, sodium ion was used as a surrogate ion to monitor the chemical durability of the host mixed with 30 weight percent of solid simulated radioactive waste. The reasons for choosing sodium are two fold: sodium release rate into solution during the PCT test was one of the fasted and sodium is part of the structures of intended aluminosilicate phases to be formed in the waste forms. The concentrations of sodium ion analyzed from samples at each temperature were graphically displayed as a function of time (Figures 4.15-4.21) in order to estimate individual temperature rate constant and the overall activation energy. Based on the assumption that the hydration of the waste forms obeyed a first-order kinetic's law, a nonlinear least square equation (Equation 3.1) was used to estimate the initial and steady state concentrations of the sodium ion at long time (days, months…) and the rate constants (Table 4.9). The influence of temperature on the hydration rates of hydroceramic host mixed with simulated radioactive waste were computed from the natural logarithm of the rate constants as a function of the reciprocal temperature for type A zeolite formed at 75-95°C (Figure 4.22). There is an excellent correlation

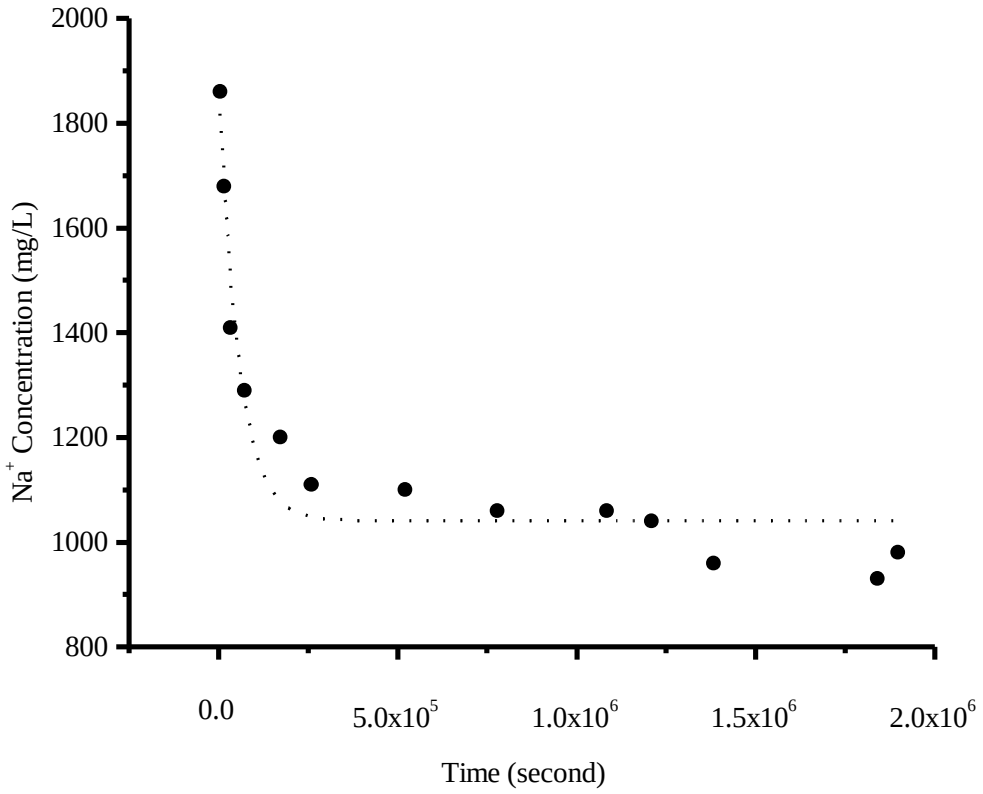

Figure 4.15. Sodium concentration as a function of time of hydroceramic host mixed with 30 weight percent of zirconia calcined simulated radioactive waste and hydrothermally autoclaved at 75°C.

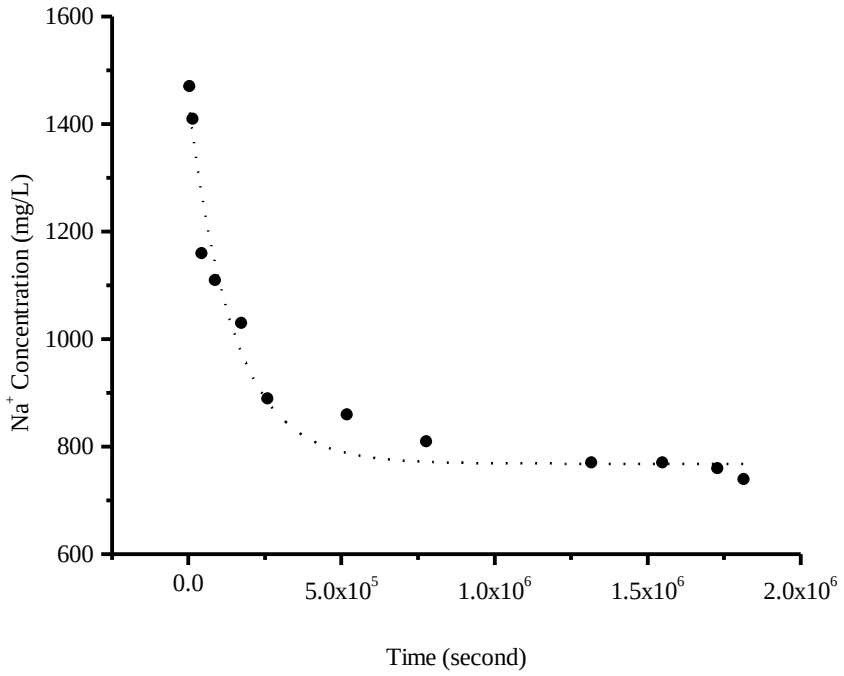

Figure 4.16. Sodium concentration as a function of time of hydroceramic host mixed with 30 weight percent of zirconia calcined simulated radioactive waste and hydrothermally autoclaved at 85°C.

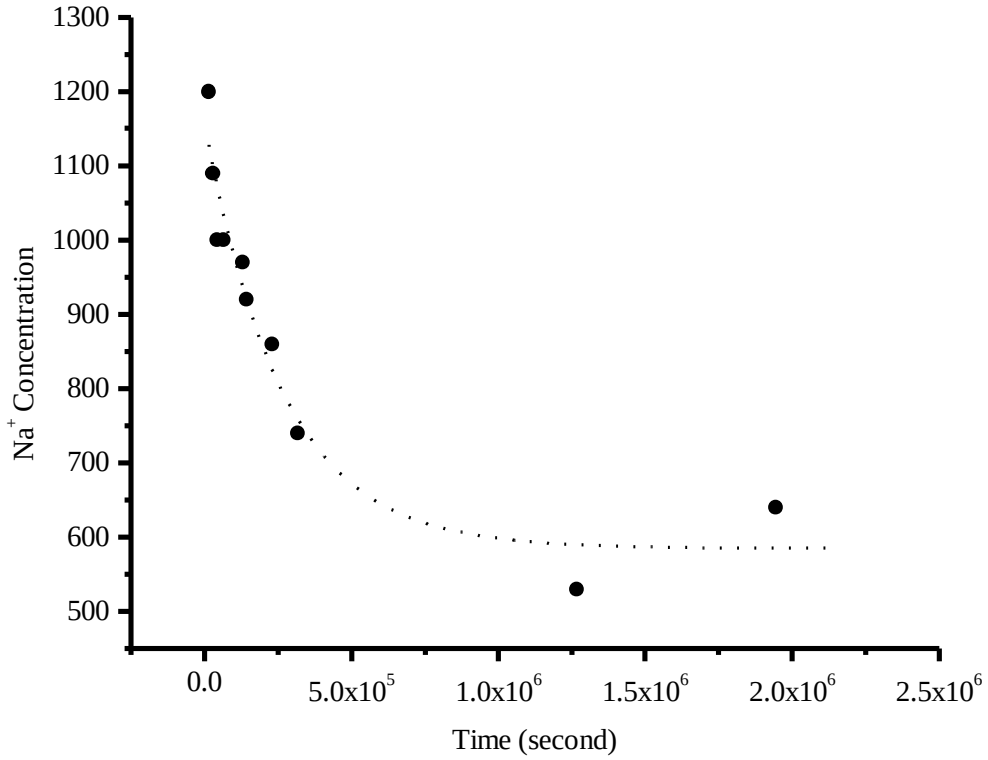

Figure 4.17. Sodium concentration as a function of time of hydroceramic host mixed with 30 weight percent of zirconia calcined simulated radioactive waste and hydrothermally autoclaved at 95°C.

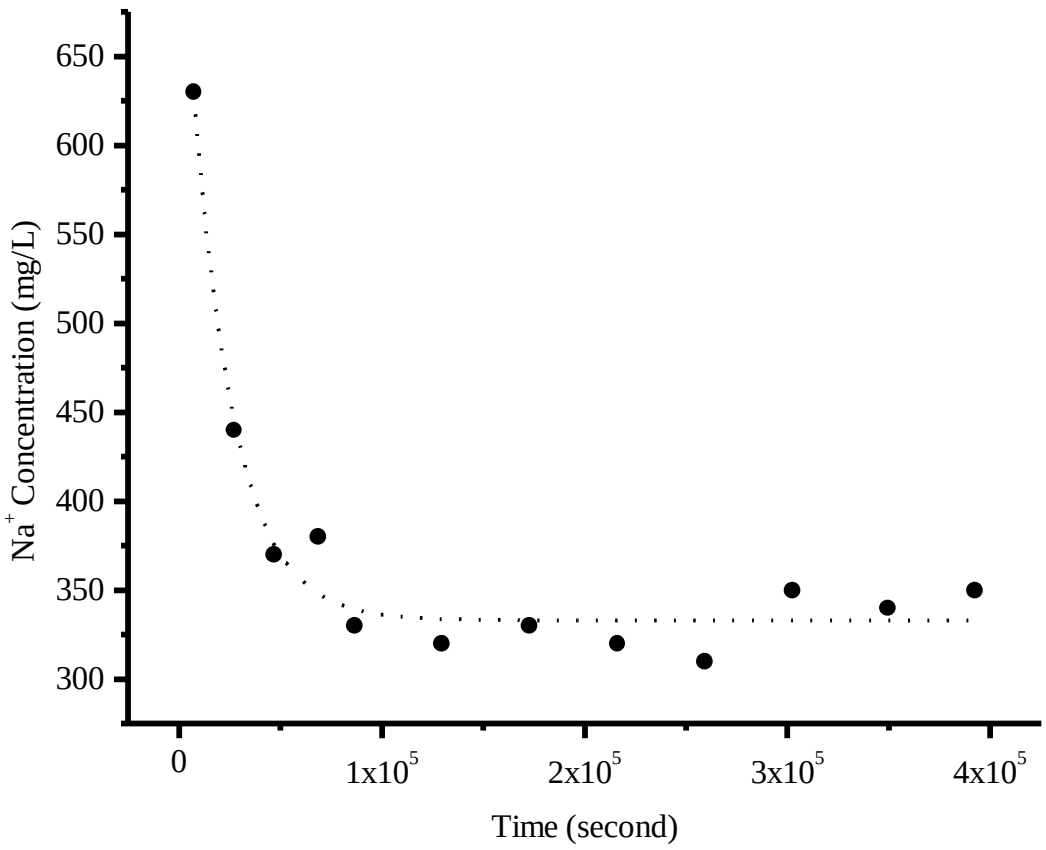

Figure 4.18. Sodium concentration as a function of time of hydroceramic host mixed with 30 weight percent of zirconia calcined simulated radioactive waste and hydrothermally autoclaved at 125°C.

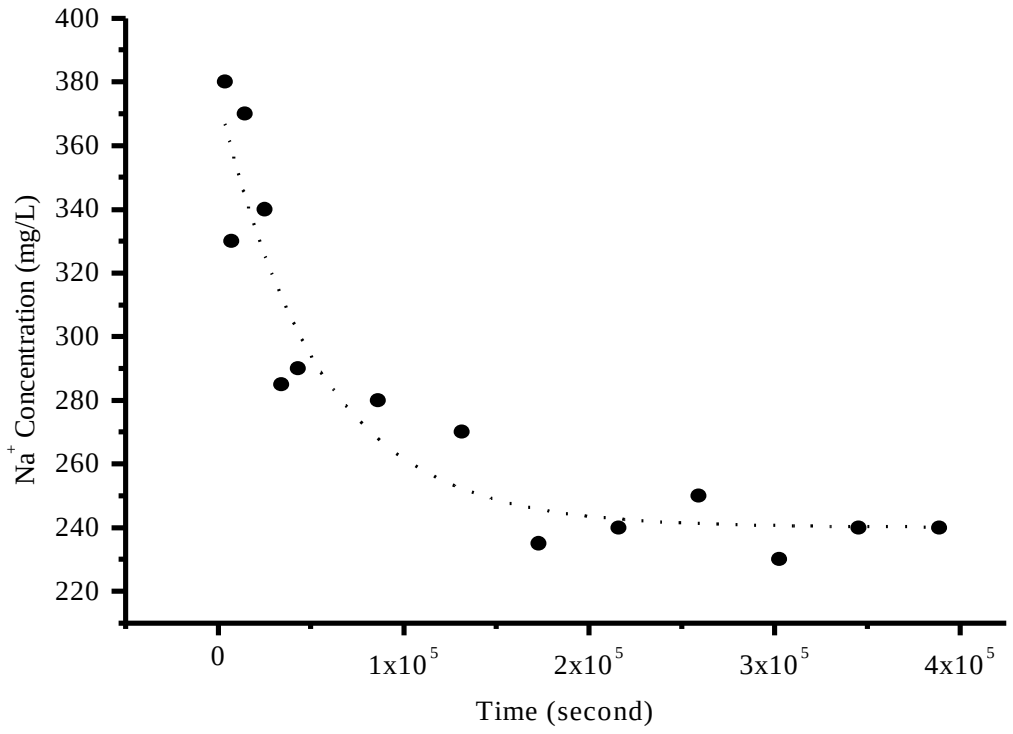

Figure 4.19. Sodium concentration as a function of time of hydroceramic host mixed with 30 weight percent of zirconia calcined simulated radioactive waste and hydrothermally autoclaved at 150°C.

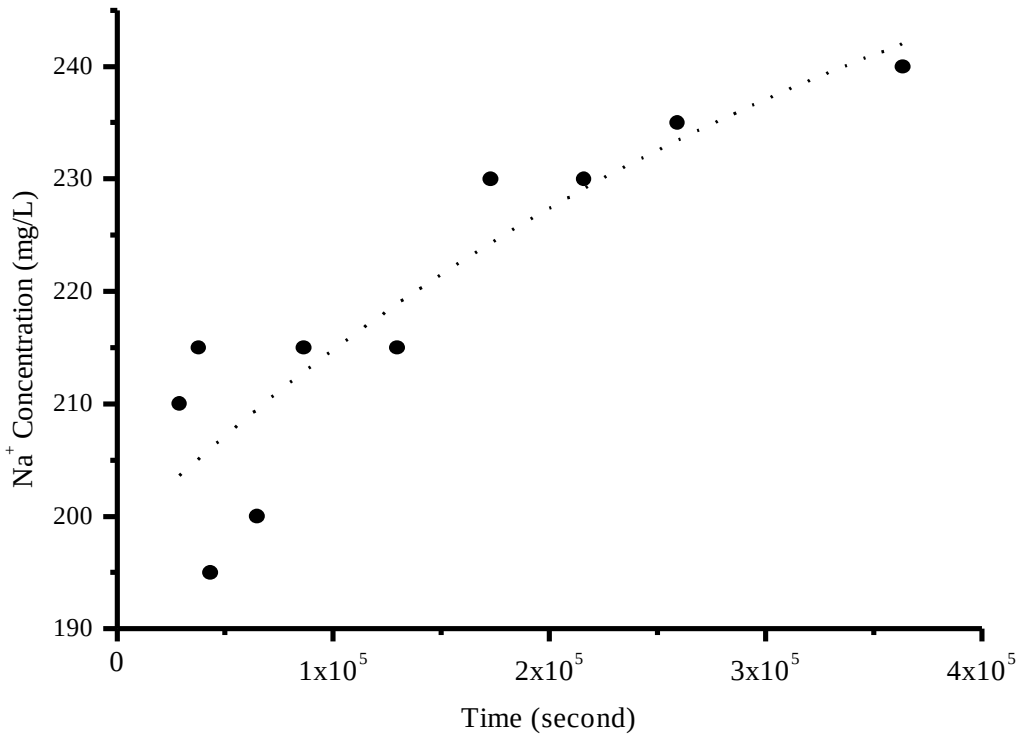

Figure 4.20. Sodium concentration as a function of time of hydroceramic host mixed with 30 weight percent of zirconia calcined simulated radioactive waste and hydrothermally autoclaved at 175°C.

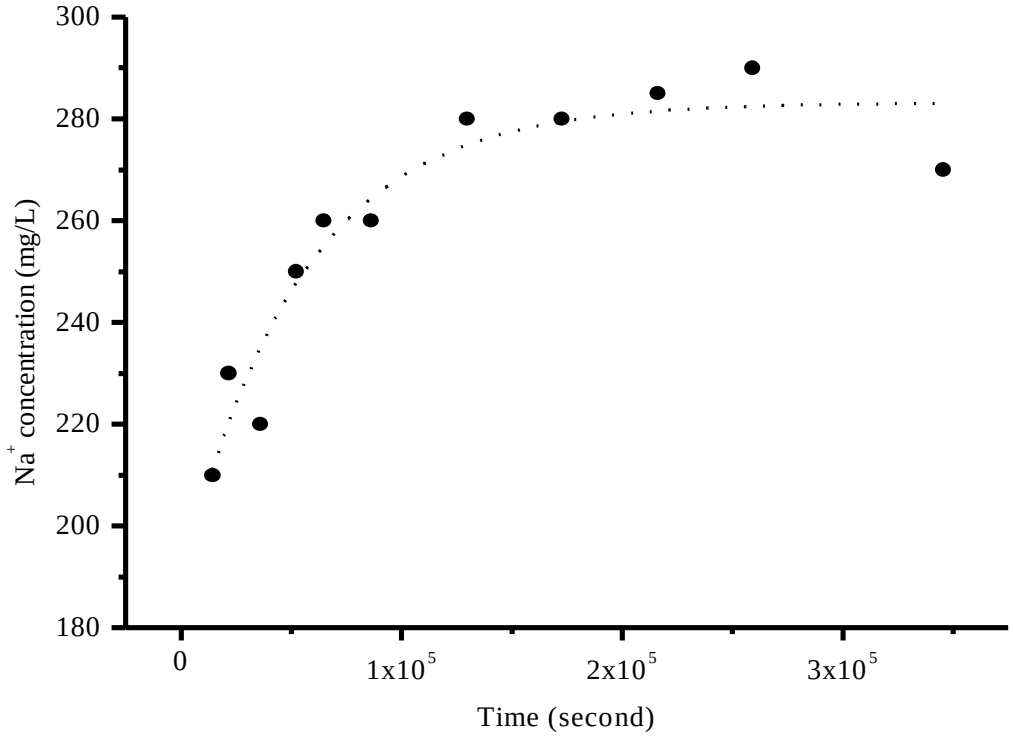

Figure 4.21. Sodium concentration as a function of time of hydroceramic host mixed with 30 weight percent of zirconia calcined simulated radioactive waste and hydrothermally autoclaved at 200°C.

Table 4.9. Summary of the rate constant calculations for the first-order hydration kinetics of hydroceramic host mixed with 30 weight percent of zirconia simulated calcined solid waste.

Temperature	Parameter		
	y_o (mg/L)	$y_?$ (mg/L)	K (s^{-1})
75°C	3058.551 ± 202.05	1200 ± 69.365	$2.40 \times 10^{-4} \pm 8.0 \times 10^{-5}$
85°C	3091.946 ± 214.88	860.27 ± 91.01	$3.60 \times 10^{-4} \pm 1.1 \times 10^{-4}$
95°C	3101.051 ± 240.67	860.27 ± 91.01	4.0×10^{-4}
125°C	3105.17 ± 69.15	365.813 ± 20.016	5.0×10^{-4}
150°C	3099.93 ± 44.84	276.324 ± 12.51	$9.10 \times 10^{-4} \pm 1.2 \times 10^{-5}$
175°C	3100 ± 0	218.50 ± 4.475	2.94×10^{-3}
200°C	3100 ± 27.33	257.727 ± 27.33	3.5×10^{-3}

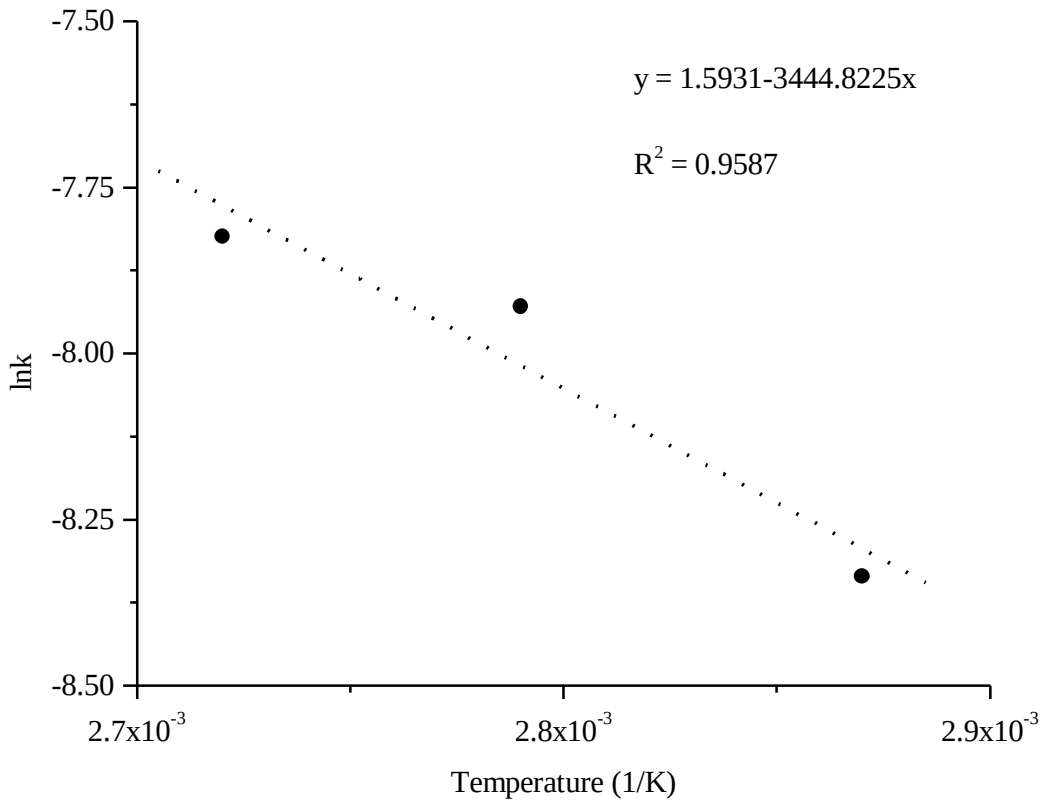

Figure 4.22. Linear plot of the rate constant of the hydroceramic host mixed with 30 weight percent of zirconia calcined simulated radioactive waste hydrothermally synthesized at 75-95°C and at various reaction times.

among the rate constants as indicated by the closeness of the value of the merit of linear regression analysis to unity. From the slope of the line, the activation energy for the type A zeolite formation in the 75, 85 and 95°C samples was calculated to be 28.642 kJ/mole (6.852 kcal/mol). The rate constants for the type A and hydroxysodalite crystallization in the 125°C and 150°C samples were estimated to be $5x10^{-4}$/s and $9.1x10^{-4}$/s, respectively. The overall activation energy for the formation of hydroxysodalite in the 175 and 200°C samples was 12.081 kJ/mol (2.89 kcal/mol). The value of the calculated activation energy for the type A zeolite crystallization in host mixed with 30 weight percent zirconia blend is 56% higher than that calculated for the formation of type A zeolite in hydroceramic host synthesized at the 75-150°C. The moderate overall activation energy (14-80 kJ/mol) for the nucleation and growth of zeolite A and hydroxysodalite in hydroceramic host mixed with simulated waste implies that the controlling mechanism is mass transfer, diffusion controlled (Lasaga, 1998; Lasaga et al., 1994; Berner, 1978).

4.3 SEM

Figures 4.23 and 4.24 show the representative SEM images of unreacted calcium fluoride in the matrix of type A zeolite and the euhedral cubes of type A zeolite formed as white granules on both the surface and the matrix of monolithic product.

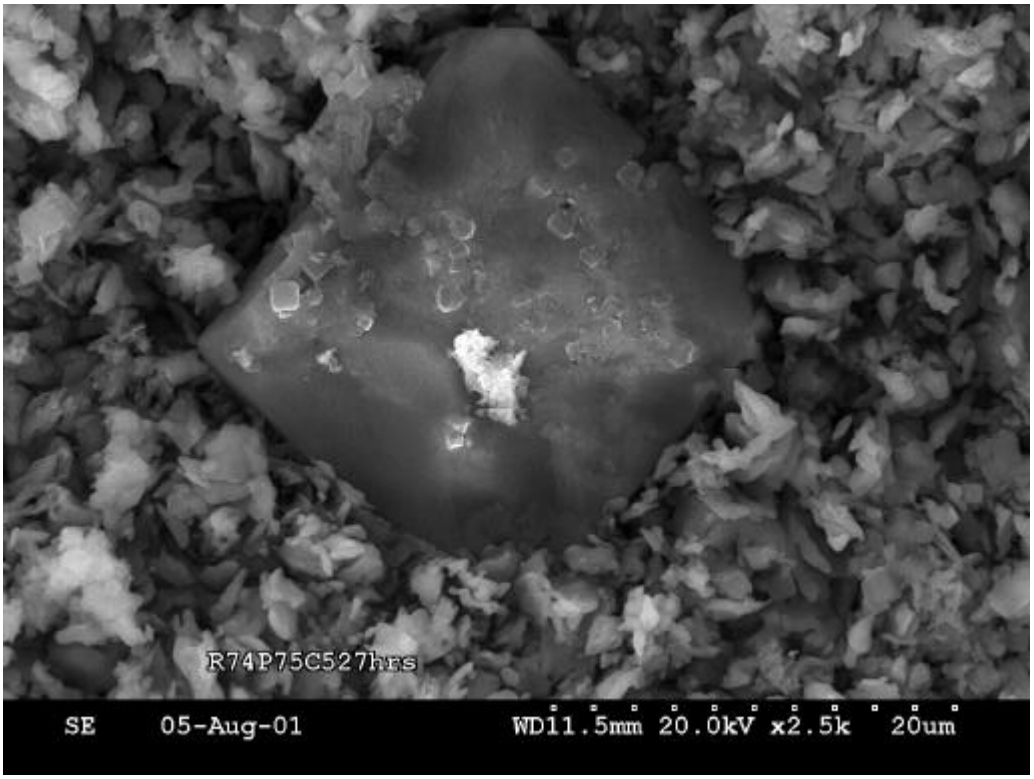

Figure 4.23 SEM of euhedral cubes of unreacted CaF_2 crystal in the matrix of type A zeolite in hydroceramic host mixed with 30 weight percent solid of simulated zirconia calcine radioactive waste and hydrothermally processed at 75°C for 527 hours.

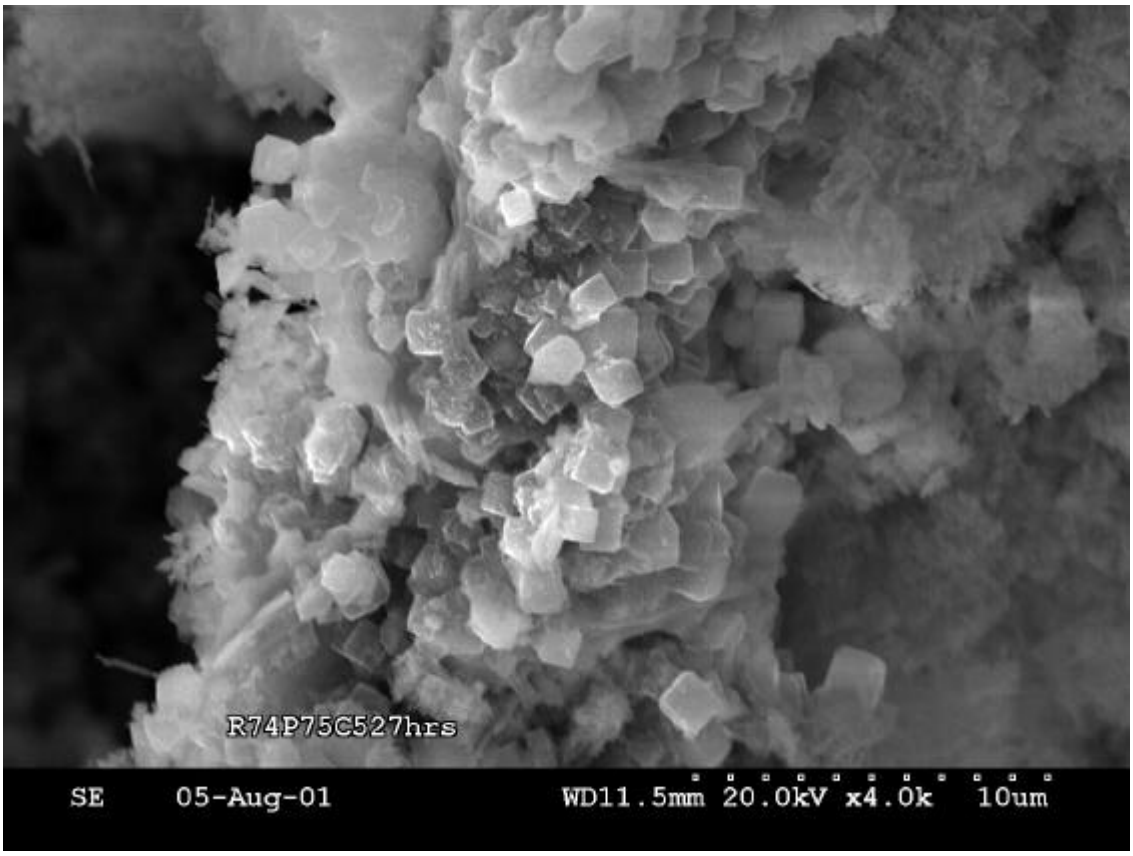

Figure 4.24 SEM of euhedral cubes of type A zeolite crystallized in hydroceramic mixed with 30 weight percent solid of simulated zirconia calcine radioactive waste and hydrothermally processed at 75°C for 527 hours.

4.4 Evaluation of Process Variables

The effects of water on the hydration kinetics and on the interactions of the resulting products during the PCT tests on the hydroceramic host plus simulated zirconia blend were investigated. The results of these experiments can be used to determine the appropriate amount of water needed that will result in the desired chemical and physical of the final products. Also, the effect of water intrusion in the saturated zone can be predicted.

4.4.1 Effect of Water

The XRD of the effects of adding 1x, 5x and 15x the amount of water to the green body of hydroceramic mixed with 30 weight percent simulated zirconia blend radioactive waste and processed at 125°C and 120 hours are shown in Figure 4.25. The XRD spectra in comparison with an untreated sample did not show any noticeable difference in the hydration rate or the crystalline phases that were already formed. There is a one-to-one match in the peak positions and the intensities of type A zeolite that co-crystallized with hydroxysodalite.

The only major difference observed was that as the amount of water content increased, the slurry for the green body became less viscous. The final products stuck to the bottom of the hydrothermal reaction vessels and had to be chipped off before they could be removed. Their hardness decreased slightly as the water content increased.

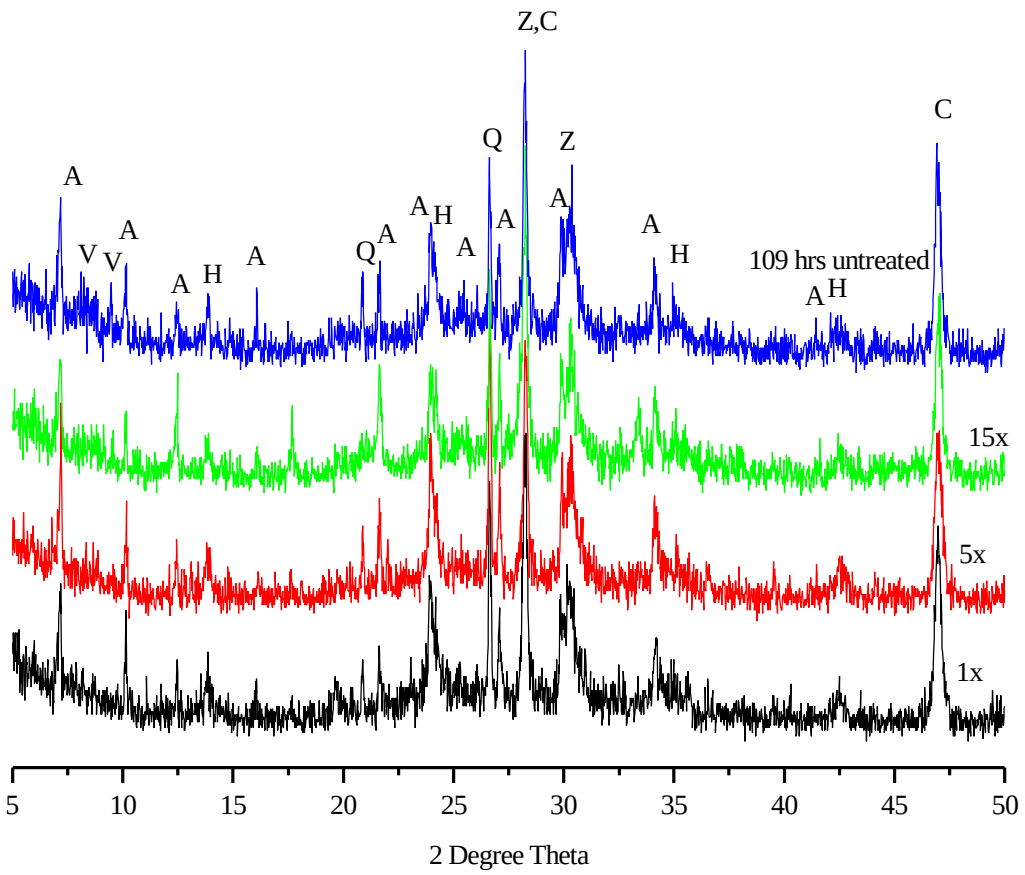

Figure 4.25. XRD patterns showing the effect of varying water content in comparison with an untreated sample of hydroceramic host mixed with 30 (solid) weight percent of simulated zirconia radioactive waste hydrothermally processed at 125°C for 120 hours. X represents the factor of water added to each sample; A = type A zeolite ($NA_{96}Al_{96}Si_{96}O_{384}.2H_2O$, 39-0222); H = hydroxysodalite ($Na_4Al_3Si_3O_{12}(OH)$, 11-0401); Z = zirconia (ZrO_2, 37-1484); C = calcium fluoride (CaF_2, 35-0816); Q = (SiO_2, 46-1045); V = unreacted vermiculite.

4.4.2 PCT Test Residues

The XRD of some selected PCT test residues for 75, 125 and 200°C samples are shown in Figures 4.26-4.28. In all cases, the spectra showed that the >75 µm <150 µm particle sizes totally immersed in water at 90°C for 24 hours did not result in the loss of waste form integrity via chemical reactions in comparison with an untreated sample. The crystalline structures of type A zeolite formed at 75°C, zeolite A plus hydroxysodalite at 125°C and hydroxysodalite at 200°C remained intact even at short processing times.

4.5 Recommendations

A recommended temperature suitable for the hydrothermal processing of the waste forms was based on the results obtained from different characterization techniques and the time (hours) the crystallization of the phases in the final products reached a steady-state. Also, a steady-state corresponds to the time when leachability of ions from samples attained constant values. In other words, the release rates of the ions are at their minimum.

The low-temperature range from 75-95°C may not be suitable to process the INEEL zirconia high-level radioactive waste because of their inability to immobilize chromium, nitrate and sulfate effectively as their higher temperature counterparts.

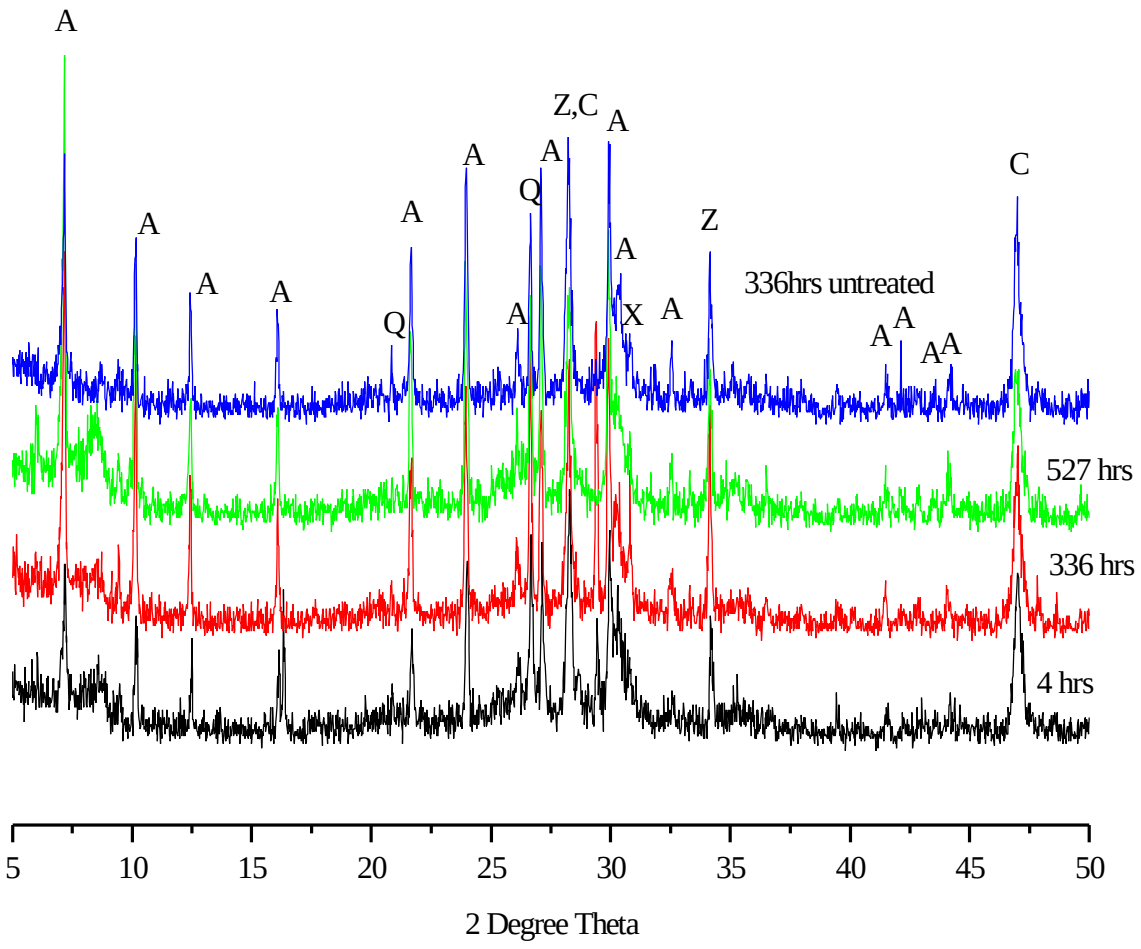

Figure 4.26. XRD patterns of selected PCT test residues compared with an untreated hydroceramic host mixed with 30 (solid) weight percent simulated zirconia radioactive waste hydrothermally synthesized at 75°C at various time intervals. A = type A zeolite ($NA_{96}Al_{96}Si_{96}O_{384}.2H_2O$, 39-0222); Z = zirconia (ZrO_2, 37-1484); C = calcium fluoride (CaF_2, 35-0816); Q = (SiO_2, 46-1045); x = unidentified poorly crystalline phase, possibly calcium compounds.

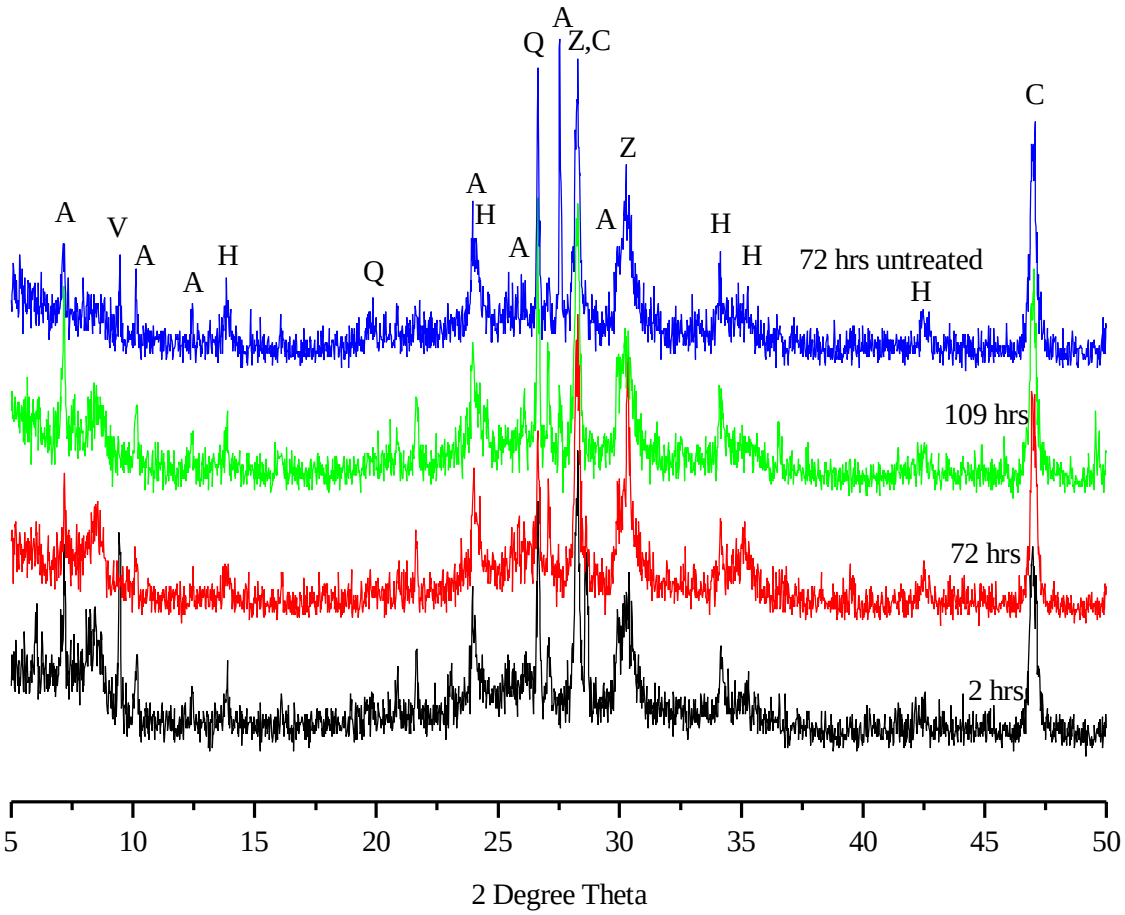

Figure 4.27. XRD patterns of selected PCT test residues compared with an untreated hydroceramic host mixed with 30 (solid) weight percent simulated zirconia radioactive waste hydrothermally synthesized at 125°C at various time intervals. A = type A zeolite ($NA_{96}Al_{96}Si_{96}O_{384}.2H_2O$, 39-0222); Q = quartz ($SiO_2$, 46-1045); H = hydroxysodalite ($Na_4Al_3Si_3O_{12}(OH)$, 11-0401); Z = zirconia (ZrO_2, 37-1484); C = calcium fluoride (CaF_2, 35-0816); and V unidentified crystalline phase, possibly vermiculite.

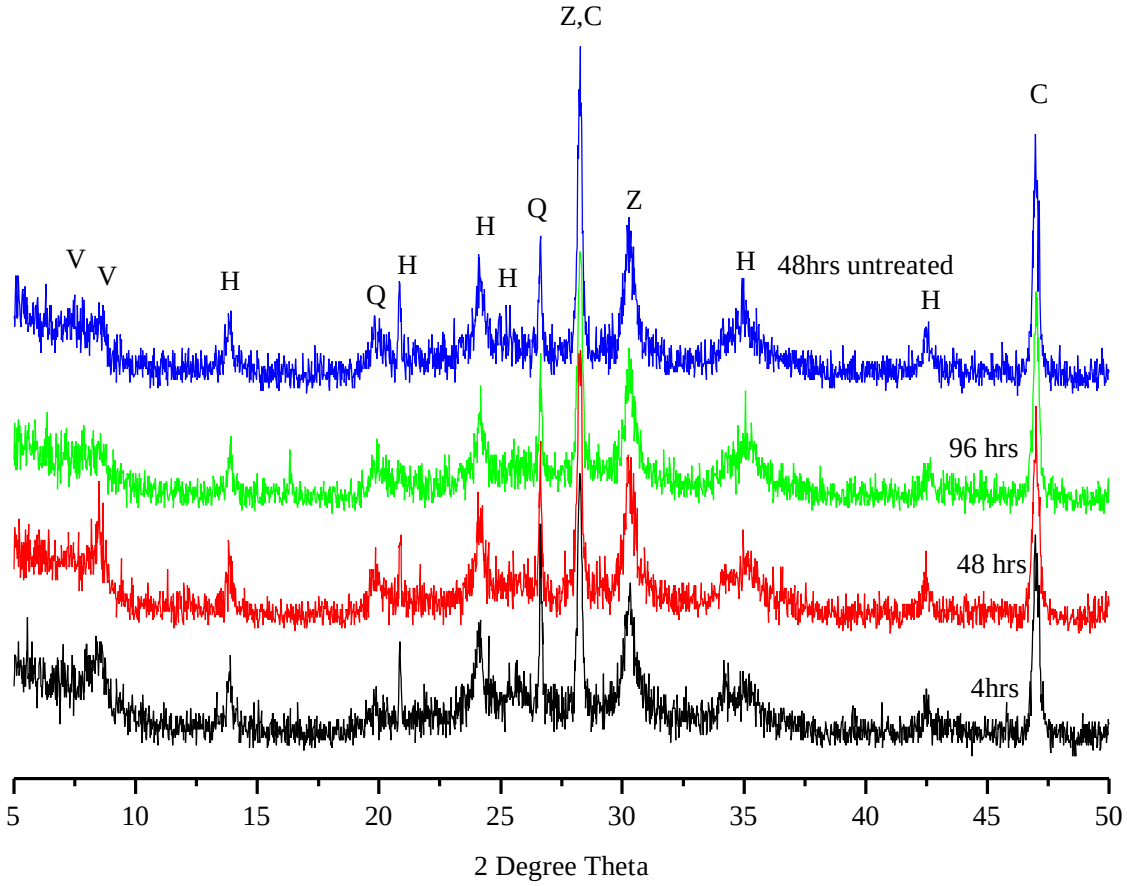

Figure 4.28. XRD patterns of selected PCT test residues compared with an untreated hydroceramic host mixed with 30 (solid) weight percent simulated zirconia radioactive waste hydrothermally synthesized at 200°C at various time intervals. Q = quartz (SiO2, 46-1045); H = hydroxysodalite ($Na_4Al_3Si_3O_{12}(OH)$, 11-0401); Z = zirconia (ZrO_2, 37-1484); C = calcium fluoride (CaF_2, 35-0816); and V unidentified crystalline phase, possibly vermiculite.

For these temperature ranges, it takes ~200 hours to reach a steady-state where the sodium concentration released during the PCT tests were 1100, 800 and 600 mg/L.

The 125°C reached a steady-state at ~36 hours with sodium concentration released amounted to 320 mg/L. At 36 hours this processing temperature immobilized surrogate radionuclides (^{90}Sr and ^{137}Cs) below the detection level of <0.02 mg/L, sulfate >3x below the USEPA Drinking Water standard, nitrate at 16x less than the reference sample and chromium 25x above the MCL of 1 mg/L. Although the 125°C samples reached a steady-state faster than 75-95°C samples the 125°C temperature will not be a recommended temperature because of its inability to immobilize chromium.

The most suitable temperature range for immobilizing the constituents of zirconia calcine high-level radioactive waste is between 150-200°C. The 150°C samples reached a steady-state at ~48 hours and 175 and 200°C at 24 hours. This temperature range can potentially fix sulfate, nitrate, chloride, chromium, cesium, strontium ions and the rest of the cations listed in Tables 4.1-4.7, Appendix C simultaneously. The 175 and 200°C sample performance during the PCT test were approximately the same. Overall, 175°C temperature is recommended as the appropriate processing temperature for the zirconia waste forms given the short processing time of 24 hours to synthesize a durable final product.

CHAPTER V

RESULTS OF SYNTHESIS, CHARACTERIZATION AND KINETICS OF HYDROCERAMIC HOST MIXED WITH 30 WEIGHT PERCENT SOLID OF FLUORINEL BLEND CALCINED SIMULATED RADIOACTIVE WASTE

CHAPTER V

RESULTS OF SYNTHESIS, CHARACTERIZATION AND KINETICS OF HYDROCERAMIC HOST MIXED WITH 30 WEIGHT PERCENT SOLID OF FLUORINEL BLEND CALCINED SIMULATED RADIOACTIVE WASTE

5.0 Introduction

The as prepared solutions of the PCT test performed at 90°C for 24 hours were collected and analyzed for their specific conductance and pH. The solutions were analyzed by the AAS, AEP and IC to determine the concentrations of the major cations and anions. The tabulated concentration data were used to gauge the retention capabilities of toxic metals (Cr and Cd), surrogate radionuclides (Cs and Sr) and anions (SO_4^{-2}, NO_3^-, F^- and Cl^-). Analytical techniques were used to identify crystalline phases and their morphologies in the final products. Sodium concentrations were used as a surrogate ion to interpret the kinetics of the hydration of hydroceramic host mixed with 30 (solid) weight percent of fluorinel blend calcine simulated radioactive waste.

5.1 Results

5.1.1 Conductivity and pH Measurements

The conductivity and the pH of the PCT test solutions were measured and plotted on a double axes graph as a function of the processing time for each sample belonging to

each of the seven temperature categories (Figures 5.1-5.7). The conductivity and the pH values of the reference sample were 11.73 mS/cm and 10.31, respectively. These values were not included in the plots of the conductivity-pH-time plots of the processed samples because of the large numerical differences between the reference and the processed samples. The difference may obscure inter- and intra-sample correlations. The conductivity value of the PCT test solution of the reference sample was unusually high. It was as much as 3x higher than the conductivity of the 1-hour sample processed at 75°C and 20x the steady state conductivity value at 200°C at 40 hours.

5.1.2 Chemical Analysis

The concentrations of the major ions as functions of time for each sample are tabulated in the Tables 5.1-5.7, Appendix D. Except for sulfate, chloride and fluoride, the concentrations of the ions in the reference sample solution are many factors higher than those samples processed above room temperatures. Generally, the concentrations of the ions decrease as the temperature and time increase for most cations and anions.

5.1.2.1 Chromium Results

The analytical concentrations of chromium obtained for all the samples at all temperatures were much less than the reference sample (155 mg/L). The chromium

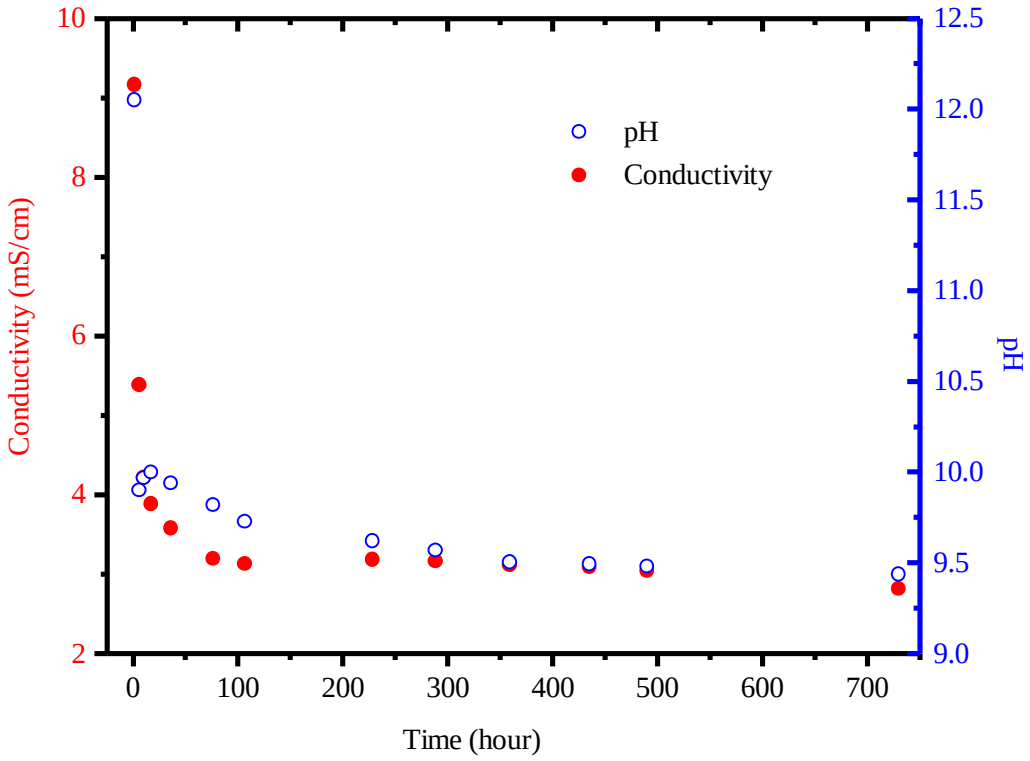

Figure 5.1. Conductivity-pH-time plot of hydroceramic host mixed with 30 weight percent of fluorinel blend calcined simulated radioactive waste and hydrothermally autoclaved at 75°C as a function of processing time.

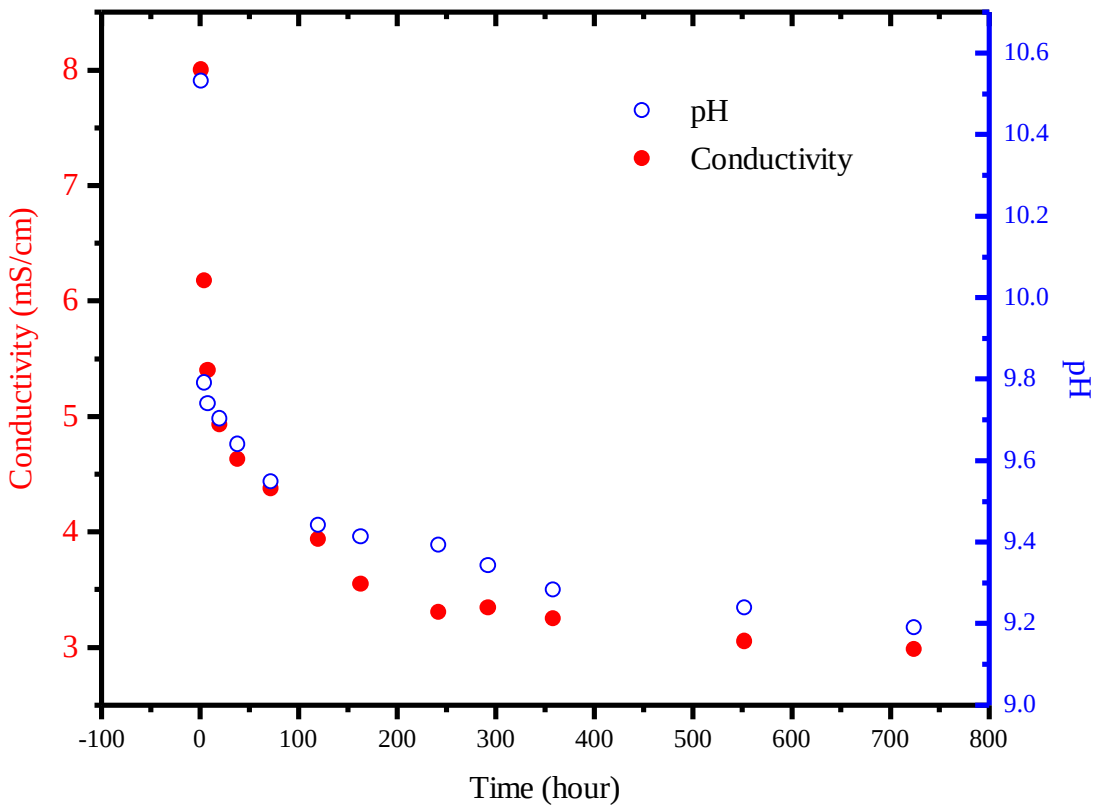

Figure 5.2. Conductivity-pH-time plot of hydroceramic host mixed with 30 weight percent of fluorinel blend calcined simulated radioactive waste and hydrothermally autoclaved at 85°C as a function of processing time.

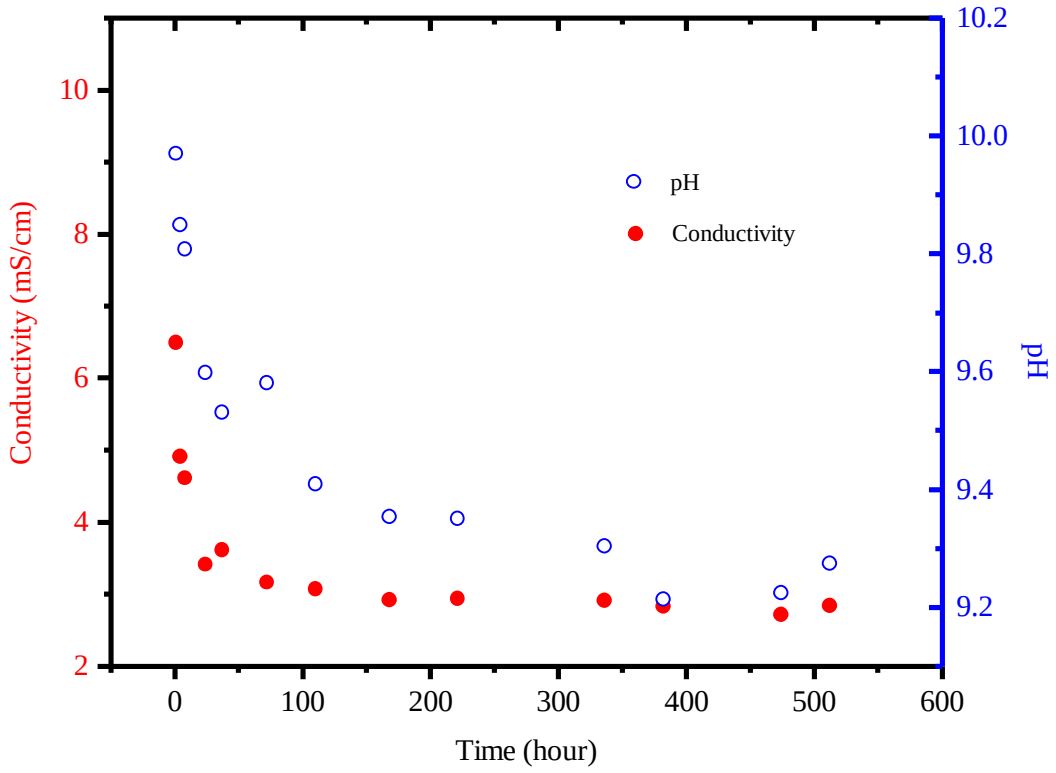

Figure 5.3. Conductivity-pH-time plot of hydroceramic host mixed with 30 weight percent of fluorinel blend calcined simulated radioactive waste and hydrothermally autoclaved at 95°C as a function of processing time.

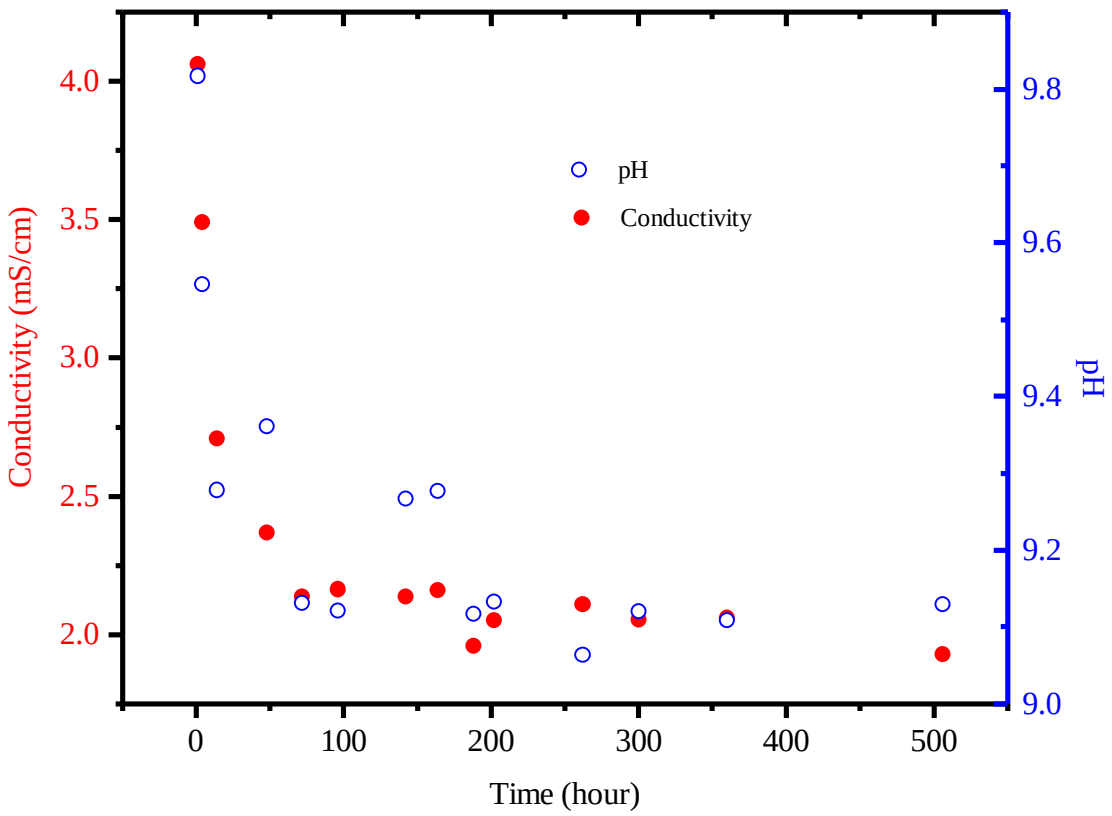

Figure 5.4. Conductivity-pH-time plot of hydroceramic host mixed with 30 weight percent of fluorinel blend calcined simulated radioactive waste and hydrothermally autoclaved at 125°C as a function of processing time.

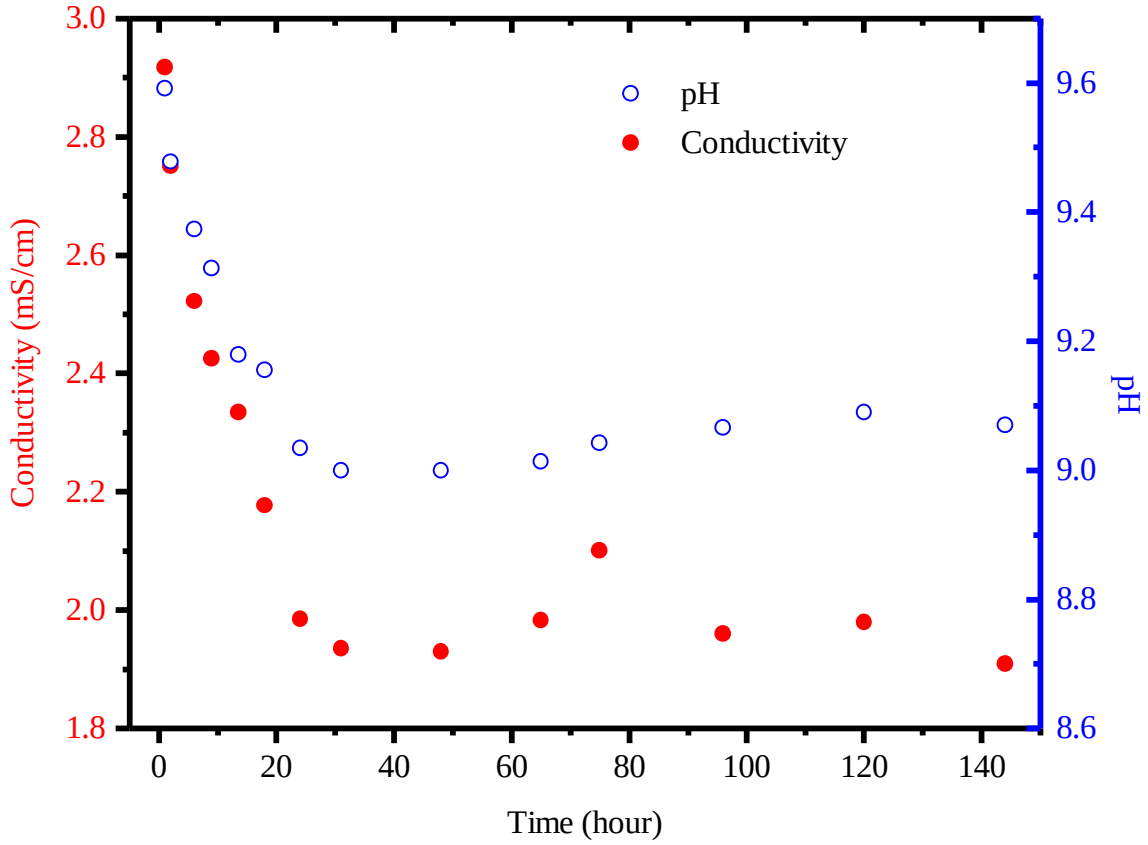

Figure 5.5. Conductivity-pH-time plot of hydroceramic host mixed with 30 weight percent of fluorinel blend calcined simulated radioactive waste and hydrothermally autoclaved at 150°C as a function of processing time.

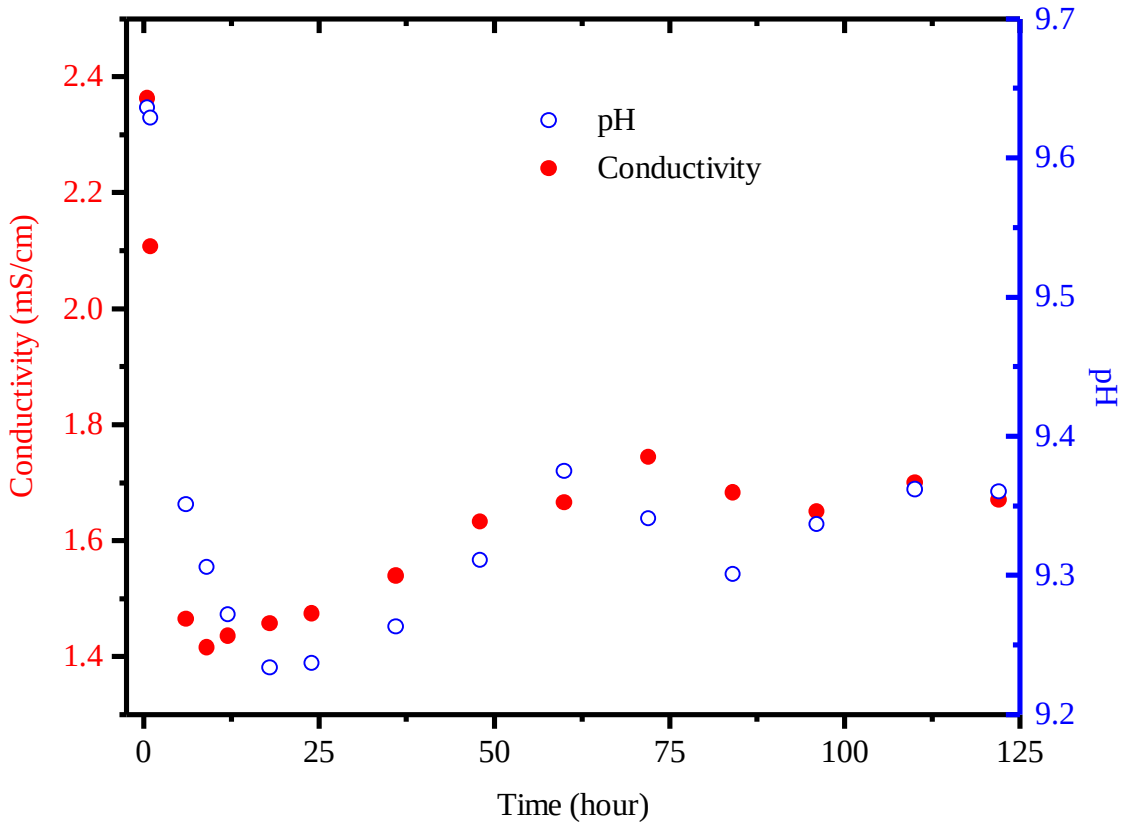

Figure 5.6. Conductivity-pH-time plot of hydroceramic host mixed with 30 weight percent of fluorinel blend calcined simulated radioactive waste and hydrothermally autoclaved at 175°C as a function of processing time.

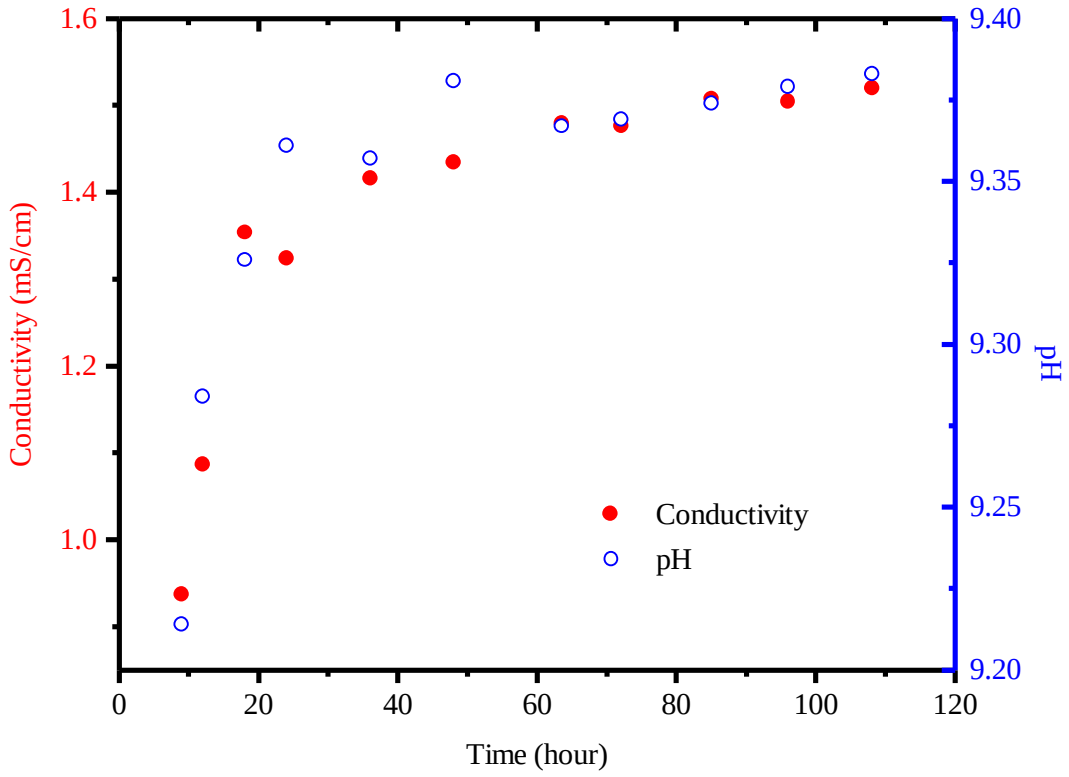

Figure 5.7. Conductivity-pH-time plot of hydroceramic host mixed with 30 weight percent of fluorinel blend calcined simulated radioactive waste and hydrothermally autoclaved at 200°C as a function of processing time.

concentrations measured were taken as total chromium ion (Cr^{III} + Cr^{VI}). No attempt was made to distinguish between Cr^{III} and Cr^{VI}. The release rate of chromium for samples processed at 75°C was approximately half (60-75 mg/L) of the sample reference concentration. The retention capabilities of chromium for the 75°C samples were much better than the 85-125°C samples. At 85-125°C, chromium concentrations released during the PCT tests (95-130 mg/L) were as much as 1.50x lower and less than half the maximum chromium concentrations for the 75°C samples. The chromium concentrations released for the 150°C samples were nearly constant (95-110 mg/L) for the first 24-hour processing times. Thereafter, the concentration decreased to ~60 mg/L. The time when the chromium concentrations reached steady state also corresponded to the processing time when the conductivity and the pH values simultaneously reached steady states. At 175°C processing temperature, chromium concentrations released during the PCT tests dropped from 80 mg/L at 0.50 hour to less than 1 mg/L after 6 hours of processing times. The 175°C and 200°C samples showed the lowest chromium concentrations (0.35-0.57 mg/L) released into solution during the PCT tests in samples processed at greater than 48 hours. Samples processed from 9 hours and longer for the 175°C and at ? 24 hours at 200°C meet the maximum concentration level (MCL) and maximum concentration level goal (MCLG) of 1.0 mg/L total chromium set by the USEPA drinking Water Regulations and Health Advisories for Inorganics (USEPA, 1996).

5.1.3 Anions

5.1.3.1 Nitrate and Sulfate

The analytical nitrate concentrations from the processed samples for samples at all temperatures were lower by a factor >0.50 to 4x less than the concentration of the reference sample (1310 mg/L). The concentration ranges from 440 to 870 mg/L for the 75-95°C samples. The 125°C samples released between 900-500 mg/L from 1-72 hours processing time and ~300mg/L at >72 hours. During the PCT tests, all the 150°C and 175°C samples released approximately a constant concentration of ~340-370 mg/L and ~300 mg/L, respectively. Similarly, the nitrate concentrations released from all the 200°C samples only amounted to ~340 mg/L. All the samples processed within the temperatures of interest showed nitrate concentrations above the USEPA limit of 10 mg/L (USEPA, 1996).

The overall concentration ranges of sulfate ion measured from the PCT test solutions for the processed samples from 75-200°C showed variability in trends compared with the reference sample (215 mg/L). Sulfate concentrations for the 75°C samples ranged from 300-770 mg/L, an increase of approximately 85-555 mg/L over the reference sample. Sulfate concentration in the 85°C samples showed a dramatic decrease from 225 mg/L for the 1 hour sample to ~40 mg/L at 200 hours, where a steady state is reached. The sulfate concentrations of the 95°C samples decreased from 130 to 50 mg/L within 8 hours of processing times and remained 7-11 mg/L afterward. The 20

mg/L measured at 37 and 382 hours can be regarded as outliers and may be associated with sample preparations and analysis (Table 5.3, Appendix D). Except for the 1-hour processed sample with sulfate concentration of ~15 mg/L, the 125°C samples sulfate concentration amounted to ~5 mg/L from 4 to 506 hours of processing. The sulfate concentrations measured (5-10 mg/L) for the 150°C samples fall within the 125°C ranges. The 175 and 200°C samples showed an increasing trend in the measured sulfate concentrations (0.3-10 mg/L) and (5.60-20 mg/L). These increasing trends in sulfate concentrations with time supported the increasing trend in the conductivity and the pH values (Figures 5.6 and 5.7) before a steady state was reached.

All the samples except the 75°C samples processed at below 36 hours retained sulfate ion very well below the 500 mg/L USEPA established limit (USEPA, 1996).

5.1.3.2 Fluoride and Chloride

Except for the 75°C samples, the fluoride concentrations released during the 24-hour PCT test were several orders of magnitude higher than the reference concentration (0.74 mg/L). The 75°C samples were not analyzed for their fluoride concentrations because their PCT test solutions were stabilized with HCl acid. HCl acid contains some amount of fluoride ions. For the 85°C samples, the fluoride concentration released for the first sample processed in 1 hour was 48 mg/L and 95-70 mg/L between 4 to 724 hours. The 1-hour sample at 95°C released 140 mg/L of fluoride

and a decreasing concentration of 115-95 mg/L at over 500 processing hours. The 125°C sample displayed three concentration ranges: 75 mg/L for the 1 hour sample, 50 mg/L for samples processed between 4 to 164 hours and 40 mg/L at >164 hours. The 150 and 175°C displayed gradual decrease in fluoride concentrations, 57-43 and 80-54 mg/L over their processing ranges of temperatures. An average of 55 mg/L constant fluoride concentration was measured for all the samples processed at 200°C. Fluoride concentrations measured from the processed samples were higher than that obtained from the reference sample. Calcium fluoride dissolution during the PCT test did not contribute to the fluoride concentrations observed in excess of the reference sample. As pointed out in Chapter 4.1.3.2, CaF_2 solubility products and their corresponding fluoride concentrations at room temperature (25°C) are higher than that at 90°C. Calcium fluoride ion solubility product at 90°C is 4.07×10^{-12} and at 25°C, 5.0×10^{-11}. Since calcium fluoride concentration at 90°C was less than that at 25°C, calcium fluoride was not the major source of fluoride released into solution during the PCT test.

Chloride concentrations measured from 85-200°C samples exceeded that of the reference sample (40 mg/L) by factors of 0.5x-3x. The 85°C samples released a constant concentration of approximately 100 mg/L. For the 95°C for the 1-hour sample, 120 mg/L of chloride ion was measured and ~100 mg/L from the samples processed from 4-512 hours. The 125 and 150°C samples displayed a narrow range of decreasing fluoride concentration of 105-80 mg/L. Only 20 mg/L separated the

highest and the lowest measured concentration for the 175°C samples. All the 200°C samples released an average of 70 mg/L.

5.1.4 Surrogate Strontium and Cesium Radionuclides

The measured strontium concentrations at all temperatures were much less than the reference concentrations (0.26 mg/L) (Tables 5.1-5.7, Appendix D). The 75°C sample processed in 1 hour yielded less than half (0.11 mg/L) the reference concentration; 6x to 9x beyond 1 hour and below detection limits (<0.02 mg/L) of the AAS instrument for samples processed at 734 hours. All the samples processed at 85,125 and 175°C released strontium concentrations below the detection limit (<0.02 mg/L) of the instrument. Between 1 to 14 hours processing time, the 150°C samples' strontium concentrations were below detection limit. Thereafter, only 0.03-0.04 mg/L were measured for the rest of the sample processed at over 14 hours. The 200°C sample displayed an opposite trend of the 150°C samples. Strontium concentrations measured were 0.09-0.04 mg/L from 1-72 hours of processing and below detection level after 72 hours.

In all cases, the measured cesium concentrations varied as functions of time and processing temperatures. The cesium concentrations for the 75°C samples decreased from 10 to 1.30 mg/L within 1-288 hours and increased slightly by 3 mg/L from >288 hours to 730 hours. The 85, 95, and 175°C samples showed decreasing measured cesium concentrations of 15-1.50, 10-2.10 and 4-1.40 mg/L. Excluding the 1-hour

sample at 125°C, all the samples processed at 125, 150 and 200°C displayed cesium concentrations below detection limit.

The waste forms performance for the retention of strontium and cesium surrogate radionuclide ions were excellent compared with the reference samples. Their retentions can be credited to the high exchange capacity of vermiculite for cesium and ion exchange between sodium and cesium ions.

5.1.5 XRD Results

The x-ray powder diffraction patterns of some representative samples are shown in figures 5.8-5.14. Type A zeolite, hydroxysodalite and a mixture of both crystalline phases were detected in addition to the persistent calcium fluoride, ziconia and quartz phases, the latter three phases originating from the reactants. Type A zeolite crystallized in the 75-95°C samples with traces of hydroxysodalite in the 95°C samples (Figure 5.8-5.10). The 125 and 150°C XRD patterns showed type A zeolite and hydroxysodalite mixed phases (Figures 5.11-5.12) and 157-200°C showed mainly hydroxysodalite (Figures 5.13-5.14).

5.2 Interpretation of Kinetics Data as a Function Temperature

The release of sodium into solutions from the processed samples during the PCT tests in the processed samples as a function of time is shown in the appendix, Figures 5.15-

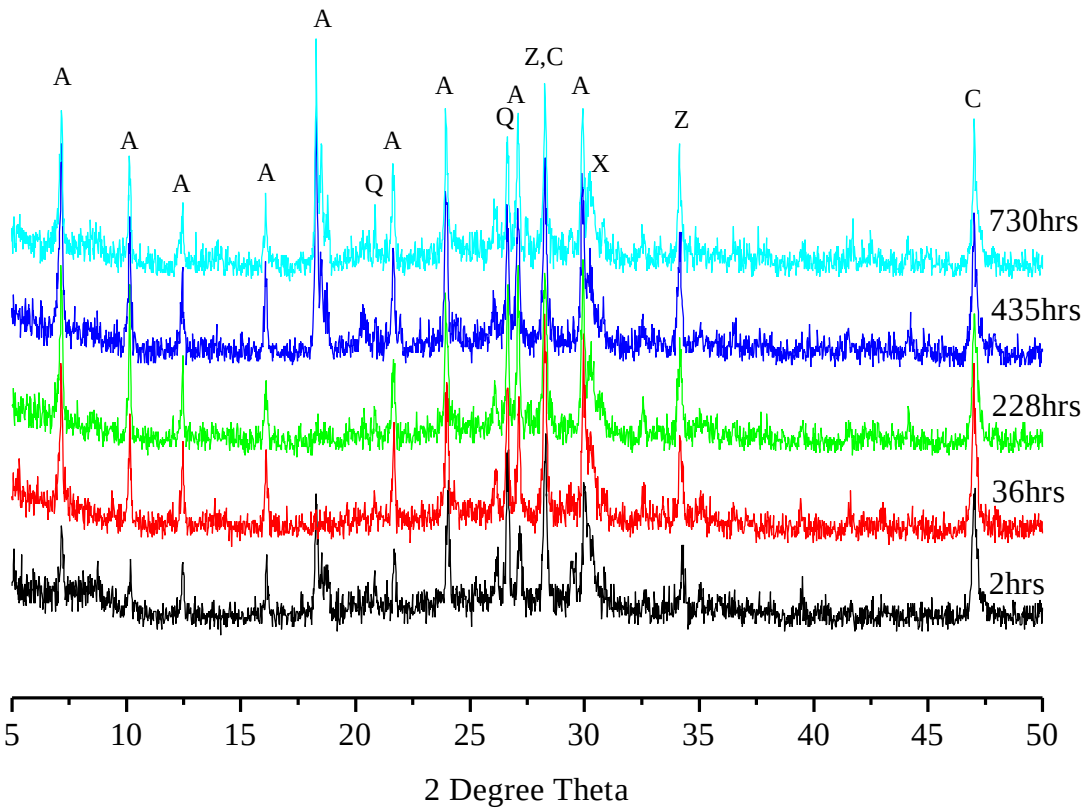

Figure 5.8 Representative XRD patterns of hydroceramic host mixed with 30 (solid) weight percent of simulated fluorinel blend calcined simulated radioactive waste hydrothermally synthesized at 75°C at various time intervals. A = type A zeolite ($NA_{96}Al_{96}Si_{96}O_{384}.2H_2O$, 39-0222); Z = zirconia (ZrO_2, 37-1484); C = calcium fluoride (CaF_2, 35-0816); Q = (SiO_2, 46-1045); and x unidentified poorly crystalline phase, possibly calcium compounds.

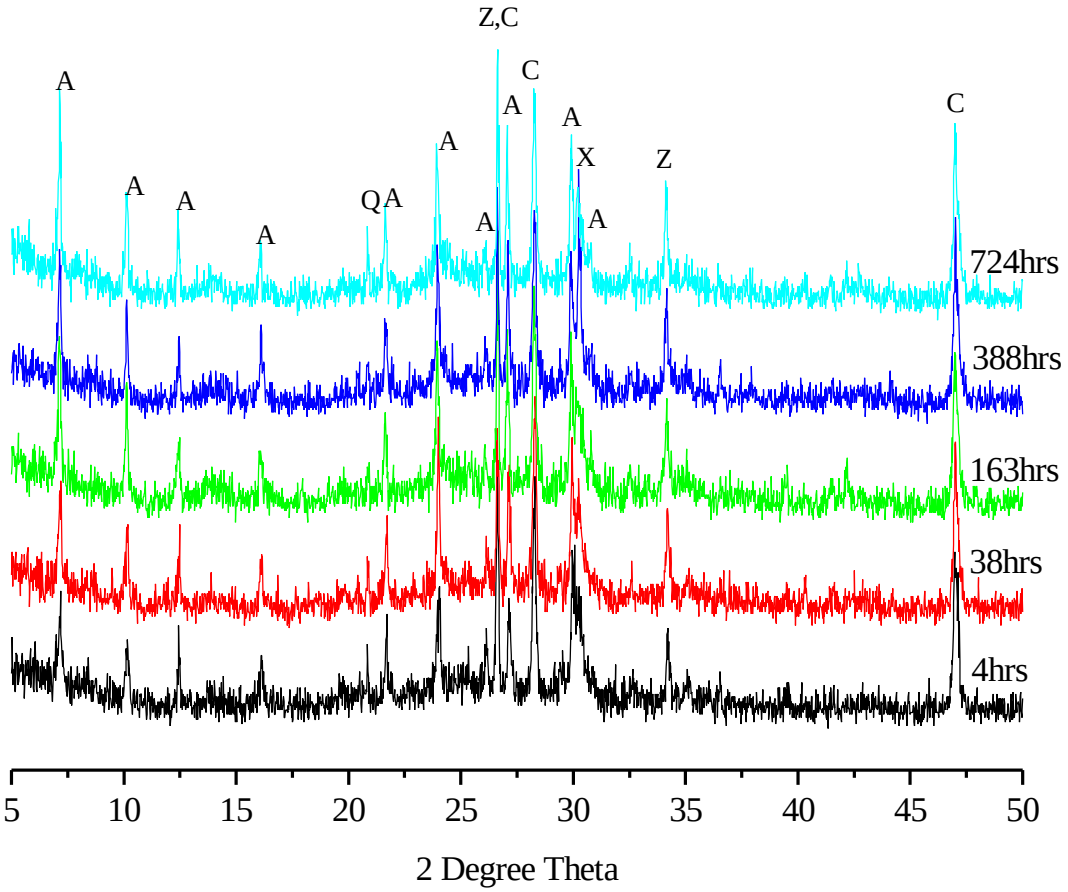

Figure 5.9 Representative XRD patterns of hydroceramic host mixed with 30 (solid) weight percent of simulated fluorinel blend calcined simulated radioactive waste hydrothermally synthesized at 85°C at various time intervals. A = type A zeolite ($NA_{96}Al_{96}Si_{96}O_{384}.2H_2O$, 39-0222); Z = zirconia (ZrO_2, 37-1484); C = calcium fluoride (CaF_2, 35-0816); Q = (SiO_2, 46-1045); and x unidentified poorly crystalline phase, possibly calcium compounds.

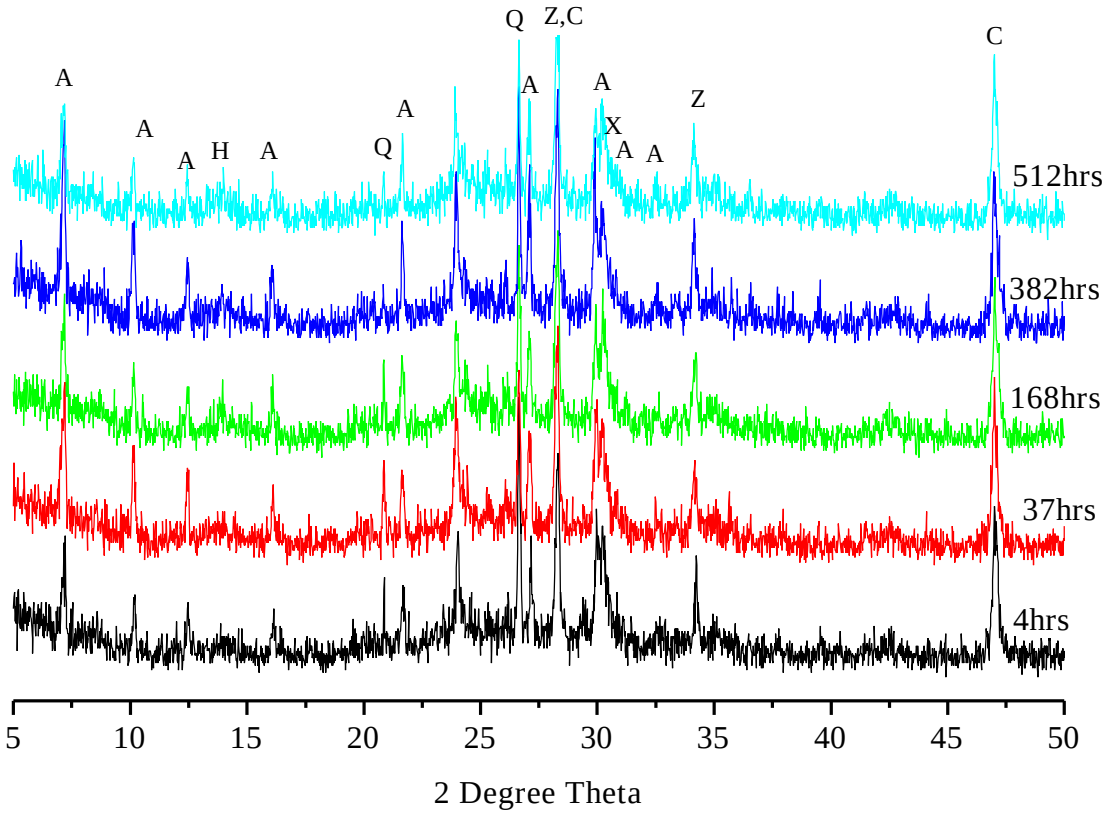

Figure 5.10 Representative XRD patterns of hydroceramic host mixed with 30 (solid) weight percent of simulated fluorinel blend calcined simulated radioactive waste hydrothermally synthesized at 95°C at various time intervals. A = type A zeolite ($NA_{96}Al_{96}Si_{96}O_{384}.2H_2O$, 39-0222); Z = zirconia (ZrO_2, 37-1484); C = calcium fluoride (CaF_2, 35-0816); Q = (SiO_2, 46-1045); H = hydroxysodalite ($Na_4Al_3Si_3O_{12}(OH)$, 11-0401) and x unidentified poorly crystalline phase, possibly calcium compounds.

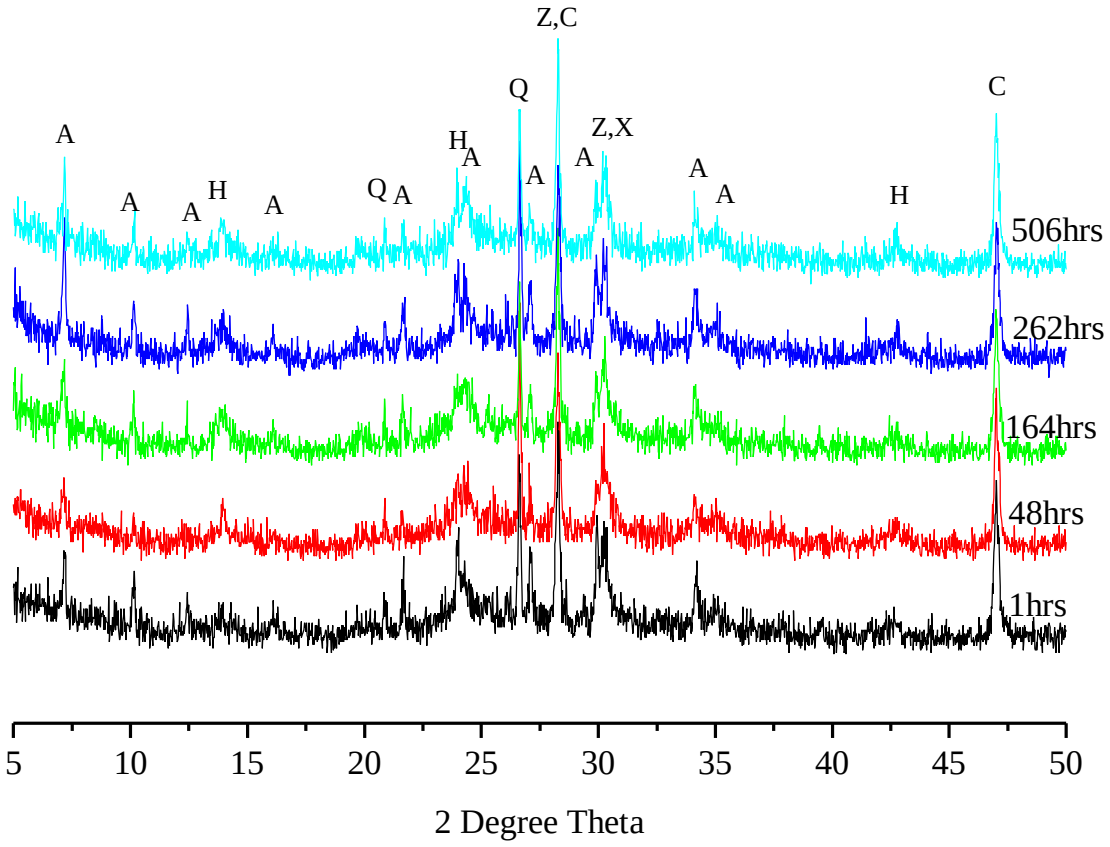

Figure 5.11 Representative XRD patterns of hydroceramic host mixed with 30 (solid) weight percent of simulated fluorinel blend calcined simulated radioactive waste hydrothermally synthesized at 125°C at various time intervals. A = type A zeolite ($NA_{96}Al_{96}Si_{96}O_{384}.2H_2O$, 39-0222); Z = zirconia (ZrO_2, 37-1484); C = calcium fluoride (CaF_2, 35-0816); Q = (SiO_2, 46-1045); H = hydroxysodalite ($Na_4Al_3Si_3O_{12}(OH)$, 11-0401) and x unidentified poorly crystalline phase, possibly calcium compounds.

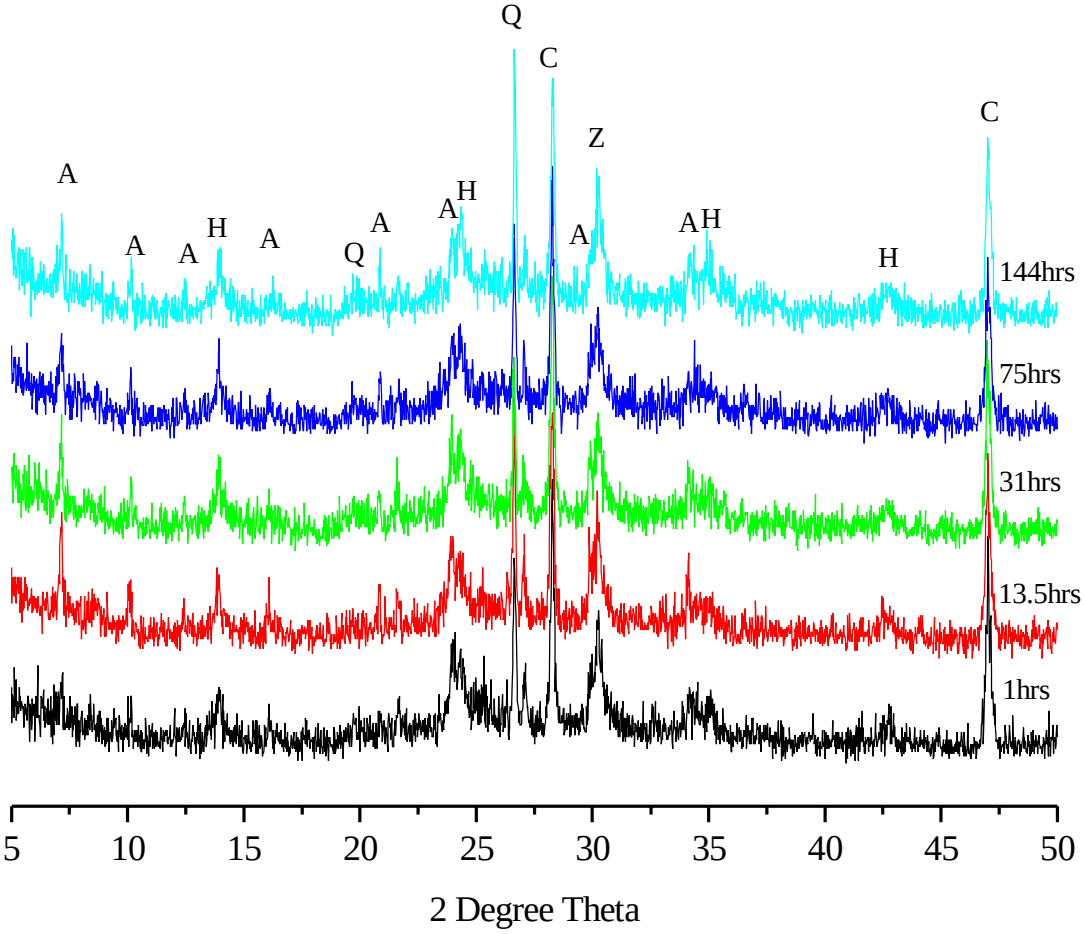

Figure 5.12 Representative XRD patterns of hydroceramic host mixed with 30 (solid) weight percent of simulated fluorinel blend calcined simulated radioactive waste hydrothermally synthesized at 150°C at various time intervals. A = type A zeolite ($NA_{96}Al_{96}Si_{96}O_{384}.2H_2O$, 39-0222); Z = zirconia (ZrO_2, 37-1484); C = calcium fluoride (CaF_2, 35-0816); Q = (SiO_2, 46-1045); H = hydroxysodalite ($Na_4Al_3Si_3O_{12}(OH)$, 11-0401) and x unidentified poorly crystalline phase, possibly calcium compounds.

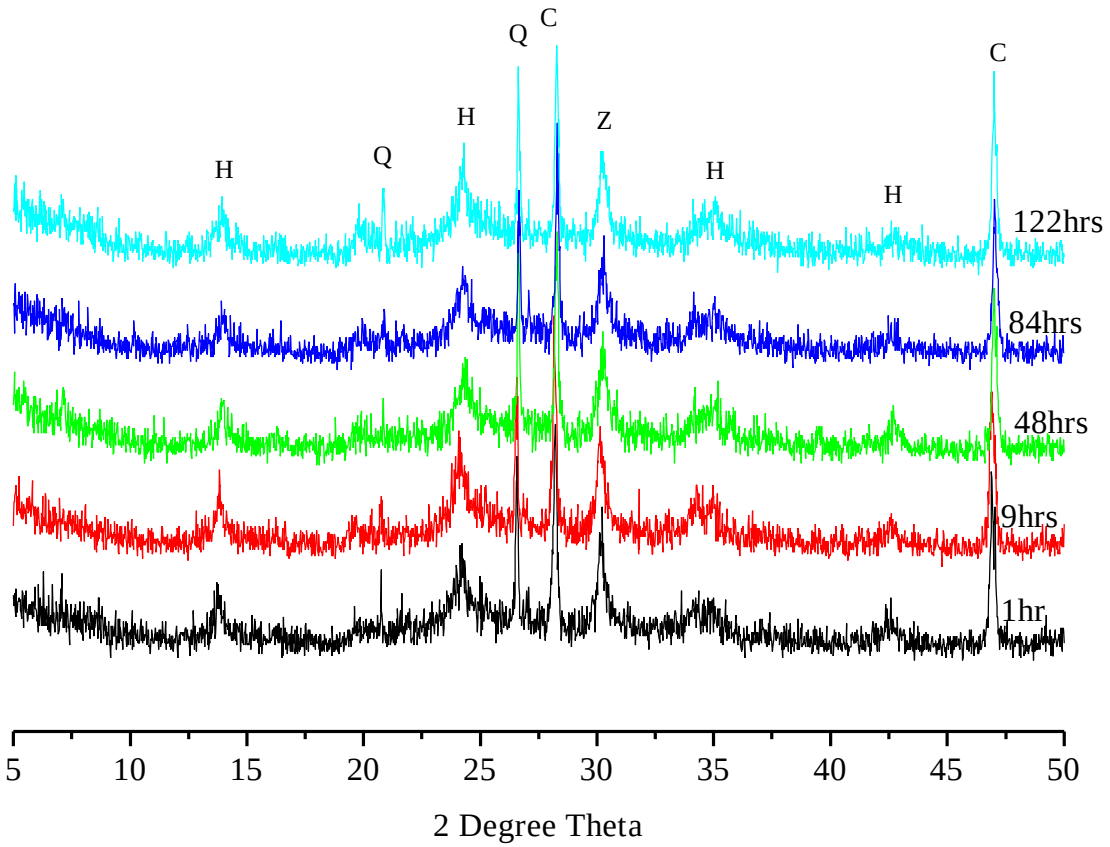

Figure 5.13 Representative XRD patterns of hydroceramic host mixed with 30 (solid) weight percent of simulated fluorinel blend calcined simulated radioactive waste hydrothermally synthesized at 175°C at various time intervals. Z = zirconia (ZrO_2, 37-1484); C = calcium fluoride (CaF_2, 35-0816); Q = (SiO_2, 46-1045); H = hydroxysodalite ($Na_4Al_3Si_3O_{12}(OH)$, 11-0401) and x unidentified poorly crystalline phase, possibly calcium compounds.

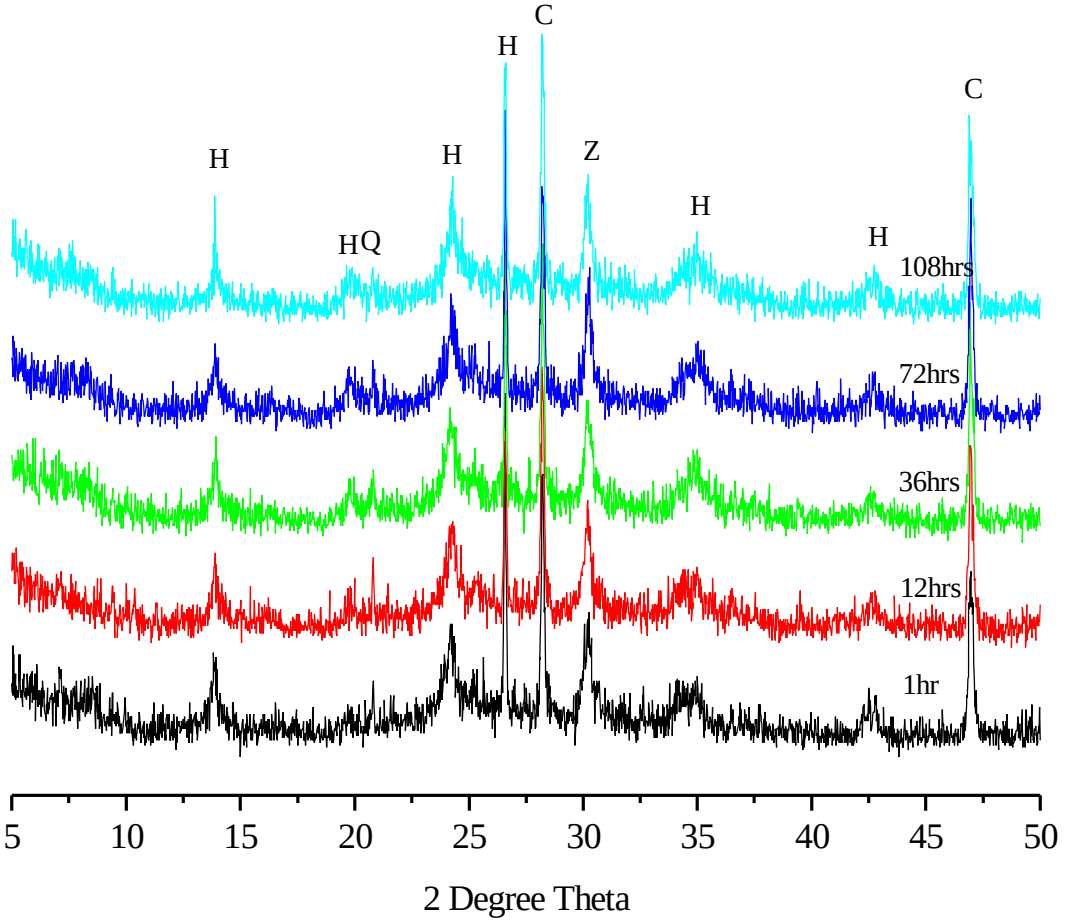

Figure 5.14 Representative XRD patterns of hydroceramic host mixed with 30 (solid) weight percent of simulated fluorinel blend calcined simulated radioactive waste hydrothermally synthesized at 200°C at various time intervals. A = type A zeolite($NA_{96}Al_{96}Si_{96}O_{384}.2H_2O$, 39-0222); Z = zirconia (ZrO_2, 37-1484); C = calcium fluoride (CaF_2, 35-0816); Q = (SiO_2, 46-1045); H = hydroxysodalite ($Na_4Al_3Si_3O_{12}(OH)$, 11-0401) and x unidentified poorly crystalline phase, possibly calcium compounds.

5.21. It should be noted that sodium concentration for the reference sample (3881 mg/L) was not included in all the plots for clarity sake. However, it was included as the initial sodium concentration at time zero, in all of the kinetic calculations. The three-parameter equation (Equation 3.1) was used to calculate the rate constants, assuming a first-order reaction kinetics and the results are summarized in Table 5.8.

The linear overall activation energy for the type A zeolite formed at 75-95°C (Figure 5.22) was estimated to be 49.57 kJ/mol (11.86 kcal/mol). This value of activation energy is 3x higher than that calculated for type A zeolite formation in hydroceramic host (75-150°C), Chapter III. The rate constants for the 125 and 150°C with the formation of a mixture of type A and hydroxysodalite were 5.50×10^{-4}/s and 7.80×10^{-4}/s. The represented estimated activation energy for the formation of hydroxysodalite in 175 and 200°C samples was 6.16 kJ/mol (1.95 kcal/mol). In all cases, mass transfer is the controlling mechanisms owing to the low values of activation energies (Lasaga, 1998; Lasaga et al., 1994; Berner, 1978).

5.3 Evaluation of the Effect of Water on the Hydration of the Host Mixed with Simulated Fluorinel Blend Calcine Waste

The effects of water on the hydration kinetics and on the interactions of the resulting products during the PCT tests on the hydroceramic host plus 30 weight percent simulated fluorinel blend calcine were investigated. The experiment can be used to determine the appropriate amount of water needed that will result in the desired

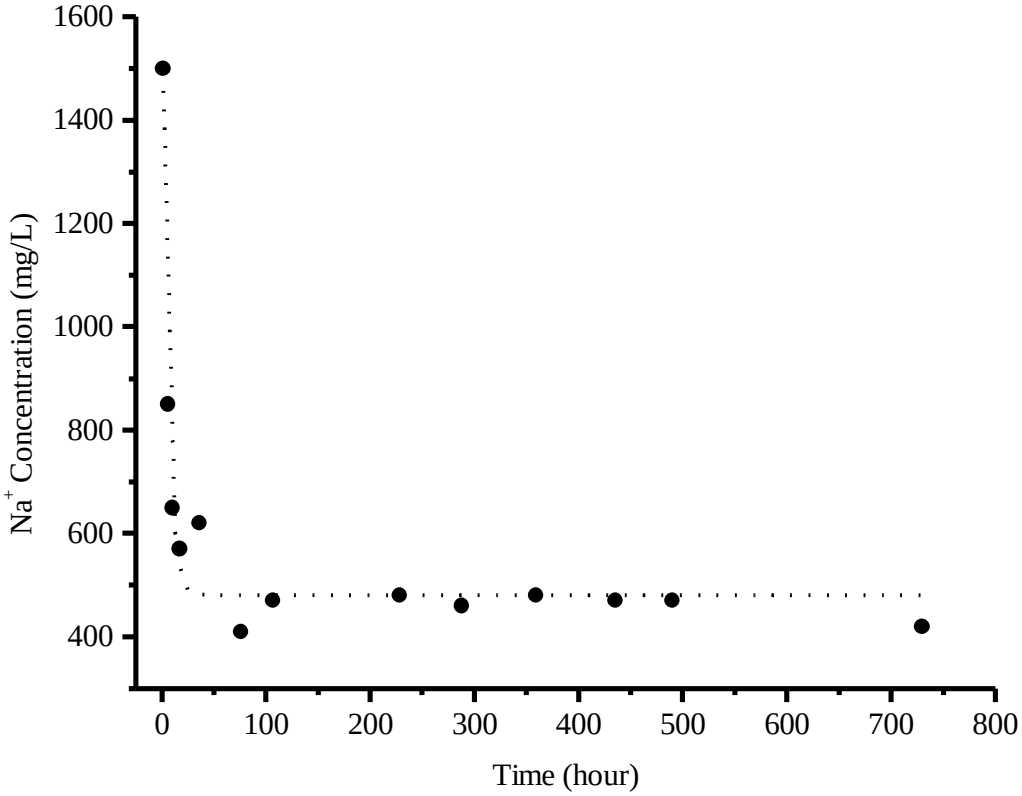

Figure 5.15 Sodium concentration as a function of time of hydroceramic host mixed with 30 weight percent of fluorinel blend calcined simulated radioactive waste and hydrothermally autoclaved at 75°C.

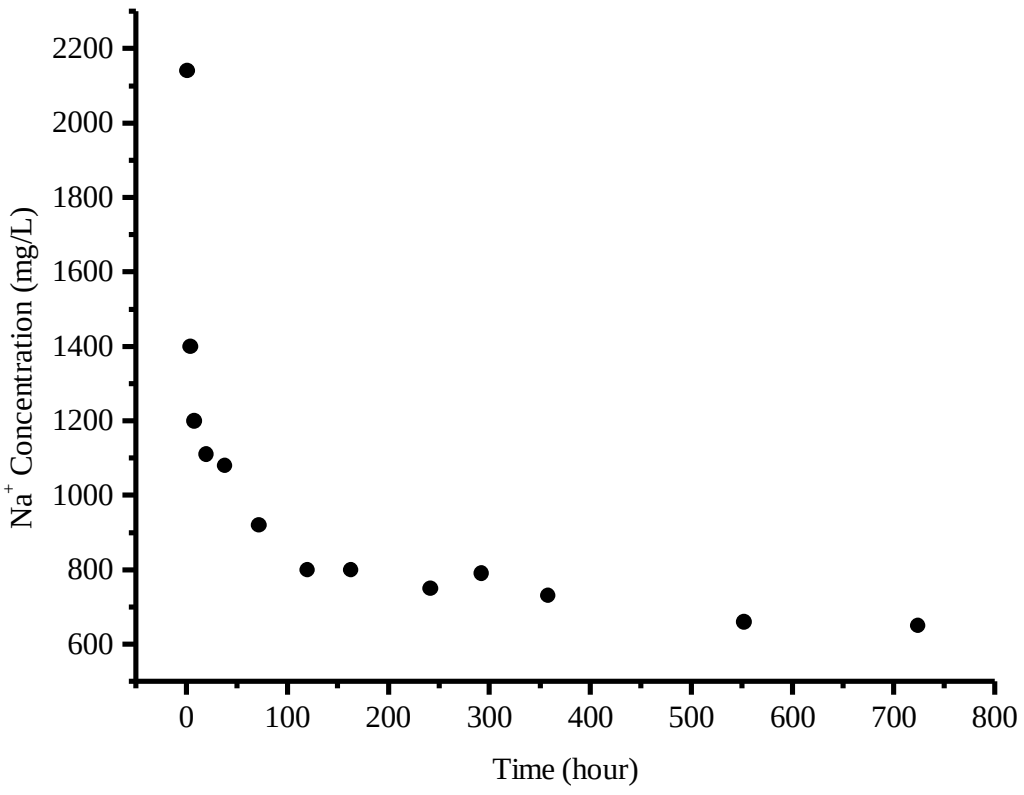

Figure 5.16 Sodium concentration as a function of time of hydroceramic host mixed with 30 weight percent of fluorinel blend calcined simulated radioactive waste and hydrothermally autoclaved at 85°C.

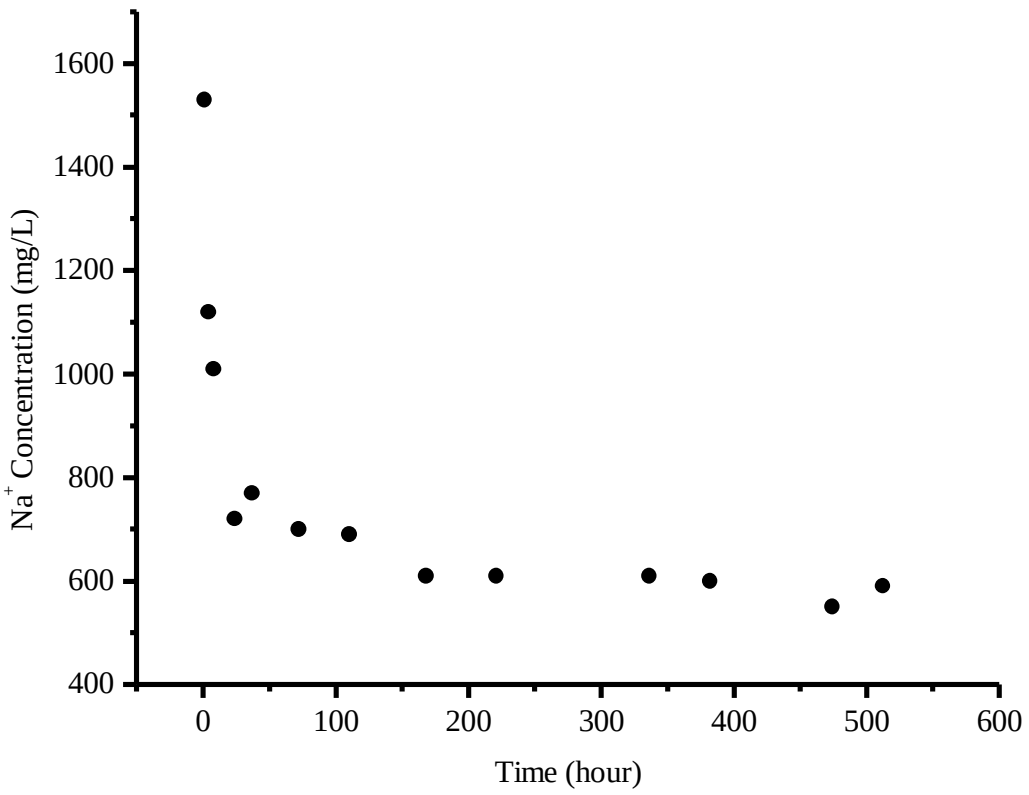

Figure 5.17 Sodium concentration as a function of time of hydroceramic host mixed with 30 weight percent of fluorinel blend calcined simulated radioactive waste and hydrothermally autoclaved at 95°C.

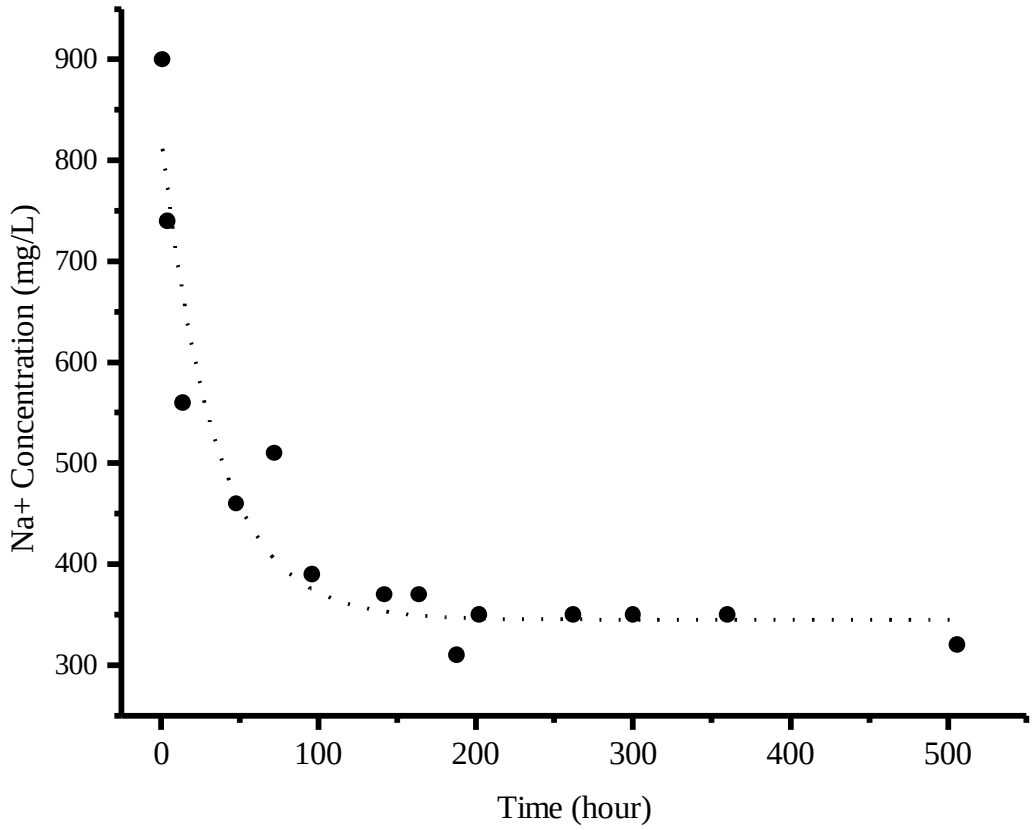

Figure 5.18 Sodium concentration as a function of time of hydroceramic host mixed with 30 weight percent of fluorinel blend calcined simulated radioactive waste and hydrothermally autoclaved at 125°C.

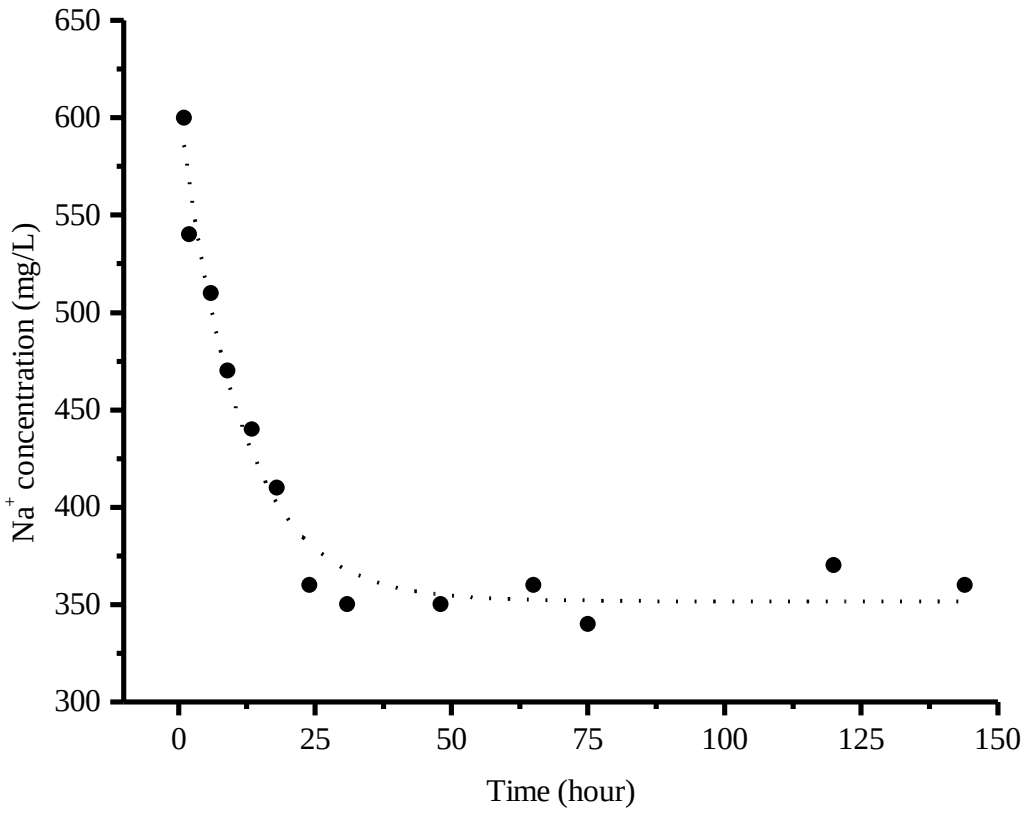

Figure 5.19 Sodium concentration as a function of time of hydroceramic host mixed with 30 weight percent of fluorinel blend calcined simulated radioactive waste and hydrothermally autoclaved at 150°C.

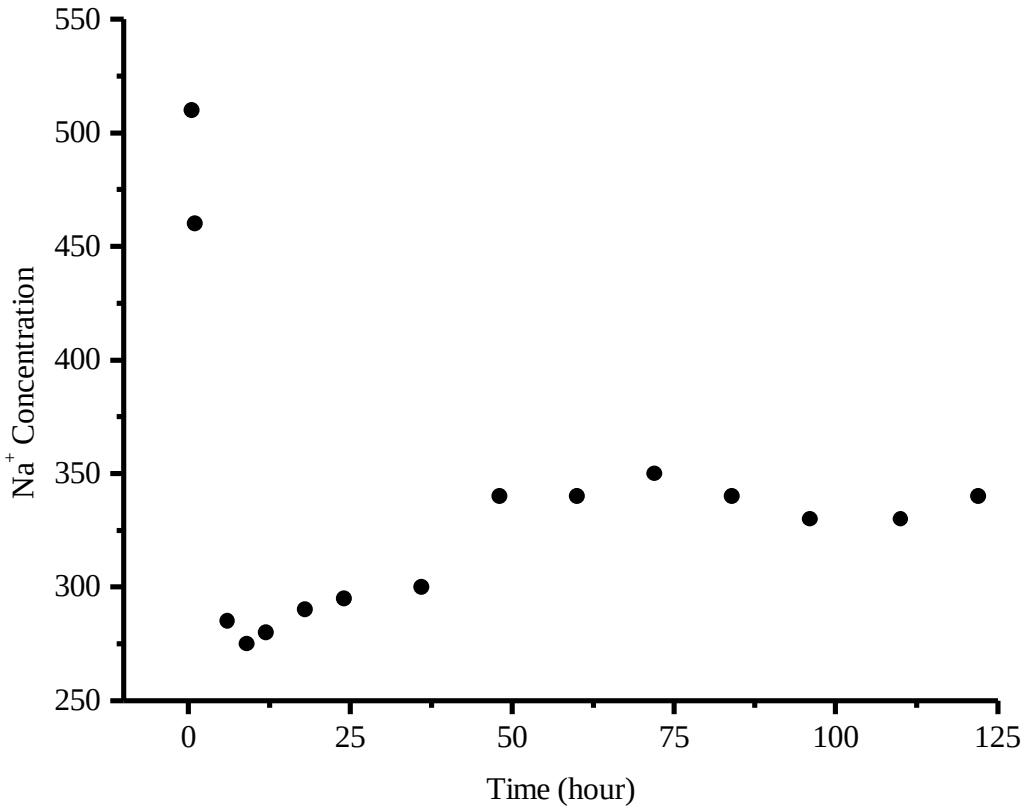

Figure 5.20 Sodium concentration as a function of time of hydroceramic host mixed with 30 weight percent of fluorinel blend calcined simulated radioactive waste and hydrothermally autoclaved at 175°C.

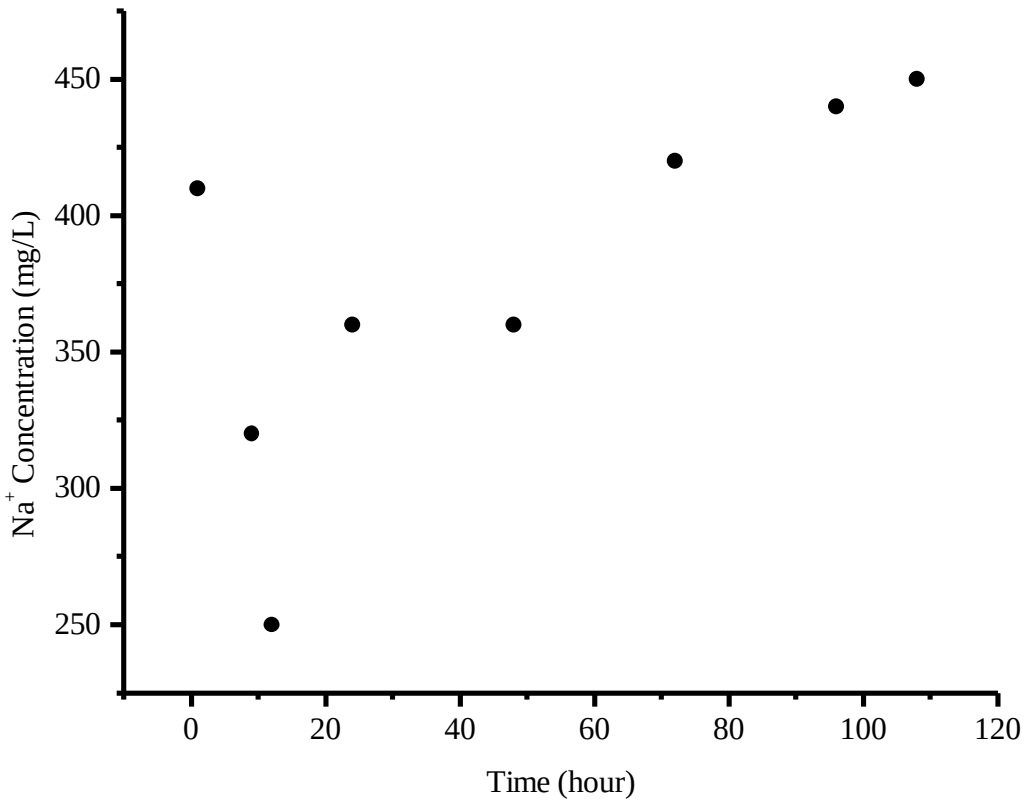

Figure 5.21 Sodium concentration as a function of time of hydroceramic host mixed with 30 weight percent of fluorinel blend calcined simulated radioactive waste and hydrothermally autoclaved at 200°C.

Table 5.8 Summary of the rate constant calculations for the first-order hydration kinetics of hydroceramic host mixed with 30 weight percent of fluorinel blend simulated calcined solid waste.

Temperature	Parameter		
	y_o (mg/L)	$y_?$ (mg/L)	K (s^{-1})
75°C	3483.60 ± 225.39	488.744 ± 75.18	1.50×10^{-4}
85°C	3834.73 ± 213.82	883.78 ± 64.24	$2 \times 10^{-4} \pm 4 \times 10^{-5}$
95°C	3893.99 ± 173.78	711.654 ± 50.43	$3.70 \times 10^{-4} \pm 6.0 \times 10^{-5}$
125°C	3880.633 ± 121.92	417.35 ± 33.84	$5.5 \times 10^{-4} \pm 7.0 \times 10^{-5}$
150°C	3899.54 ± 64.14	401.71 ± 17.95	$7.8 \times 10^{-4} \pm 9.0 \times 10^{-5}$
175°C	3899.61 ± 44.69	323.583 ± 12.04	$1.60 \times 10^{-3} \pm 1.3 \times 10^{-4}$
200°C	3900 ± 67.81	376.25 ± 23.975	1.80×10^{-3}

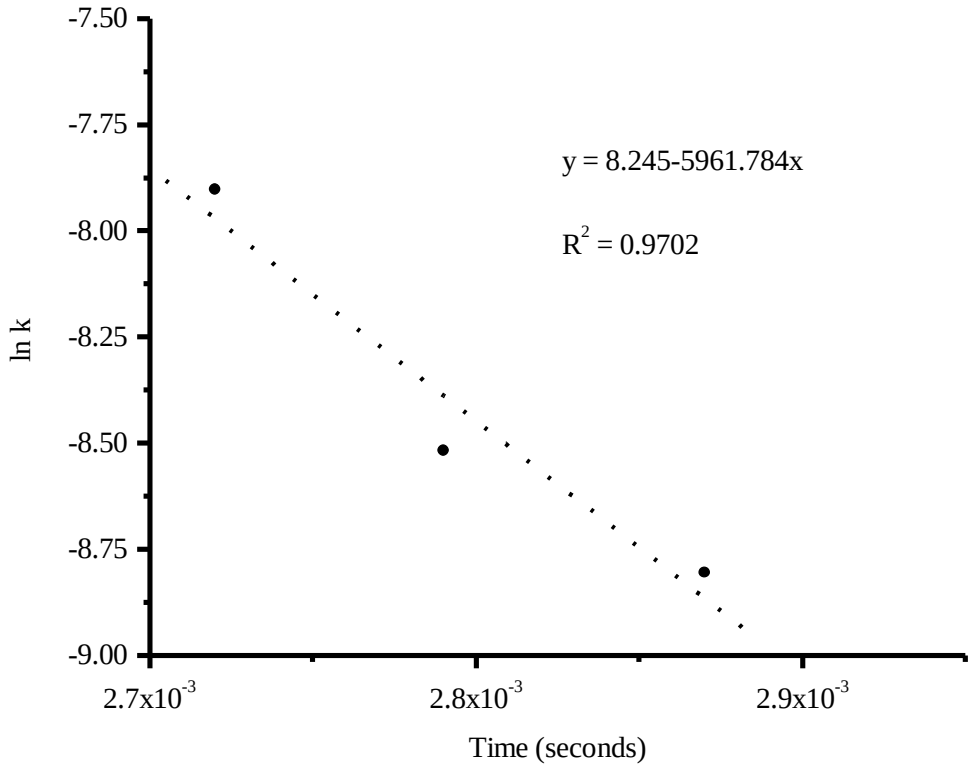

Figure 5.22. Linear plot of the rate constant of the hydroceramic host mixed with 30 weight percent of fluorinel blend calcined simulated radioactive waste hydrothermally synthesized at 75-95°C and at various reaction times.

chemical and physical properties of the final products. The effects of complete immersing particle sizes >75 ?m to <150 ?m in water and heated at 90°C, analogous to groundwater intrusion in the saturated zone with the radiation temperature of 90°C can be obtained from the PCT test residues.

5.3.1 Effect of Water on the Synthesis of Host-Waste Form

The XRD patterns showing the effect of the addition of 1x, 5x and 15x water to the hydroceramic host containing 30 solid weight percent of fluorinel blend calcined and processed at 125°C for 120 hours are shown in Figure 5.23. Type A zeolite and hydroxysodalite crystallized in all the three samples, similar to Figure 5.11. The figure shows that the degree of crystallinity is higher for 5x and 15x water containing samples. The addition of excess water accelerates crystallinity but at the expense of hardness. The more the water content increased, the softer was the end product.

5.3.2 PCT Test Residues

The XRD patterns of the PCT residues of the three randomly selected samples representing 75, 150 and 200°C are shown in Figures 5.24-5.26. The XRD patterns showed that the PCT test conditions, sample (75-150?m) to water ratio of 1:10 did not alter the crystalline phases of the synthesized waste forms. The 75°C samples retained type A zeolite, a mixture of type A zeolite and hydroxysodalite in 150°C and only hydroxysodalite in the 200°C representative samples.

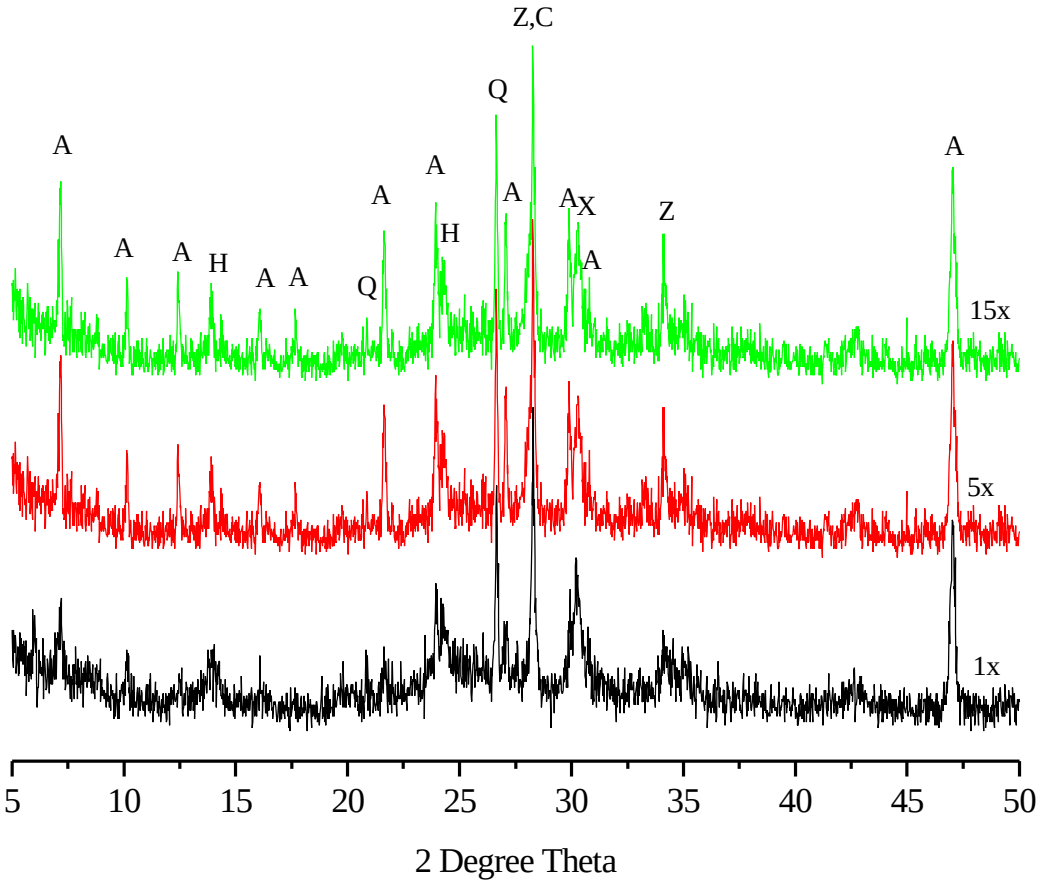

Figure 5.23 XRD patterns showing the effect of varying water content of hydroceramic host mixed with 30 (solid) weight percent of simulated fluorinel blend calcined radioactive waste hydrothermally processed at 125°C for 120 hours. X represents the factor of water added to each sample. A = type A zeolite ($NA_{96}Al_{96}Si_{96}O_{384}.2H_2O$, 39-0222); Z = zirconia (ZrO_2, 37-1484); C = calcium fluoride (CaF_2, 35-0816); Q = (SiO_2, 46-1045); and x unidentified poorly crystalline phase, possibly calcium compounds.

5.4 Recommendations

From the characterization results and chemical analysis data, 2000°C at 100% relative humidity at ~8-10 hours are the most suitable processing conditions to complete the batch process within one working shift. However, the data support allow the autogenious heat from the radioactive decay drive the curing process which could take several weeks to reach completion. This latter option eliminates a complete operational step, one which involved slightly elevated pressure, and only requires insulated storage.

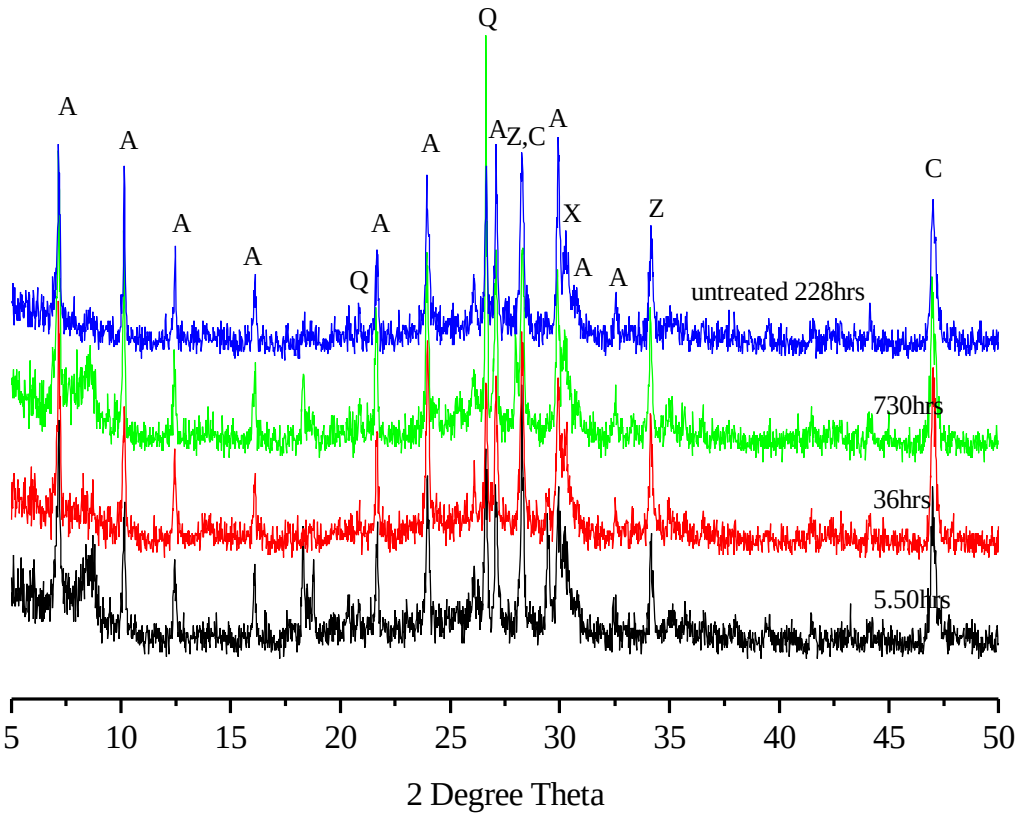

Figure 5.24. XRD patterns of selected PCT test residues compared with an untreated hydroceramic host mixed with 30 (solid) weight percent simulated fluorinel blend calcined radioactive waste hydrothermally synthesized at 75°C at various time intervals. A = type A zeolite ($NA_{96}Al_{96}Si_{96}O_{384}.2H_2O$, 39-0222); Z = zirconia (ZrO_2, 37-1484); C = calcium fluoride (CaF_2, 35-0816); Q = (SiO_2, 46-1045); and x unidentified poorly crystalline phase, possibly calcium compounds.

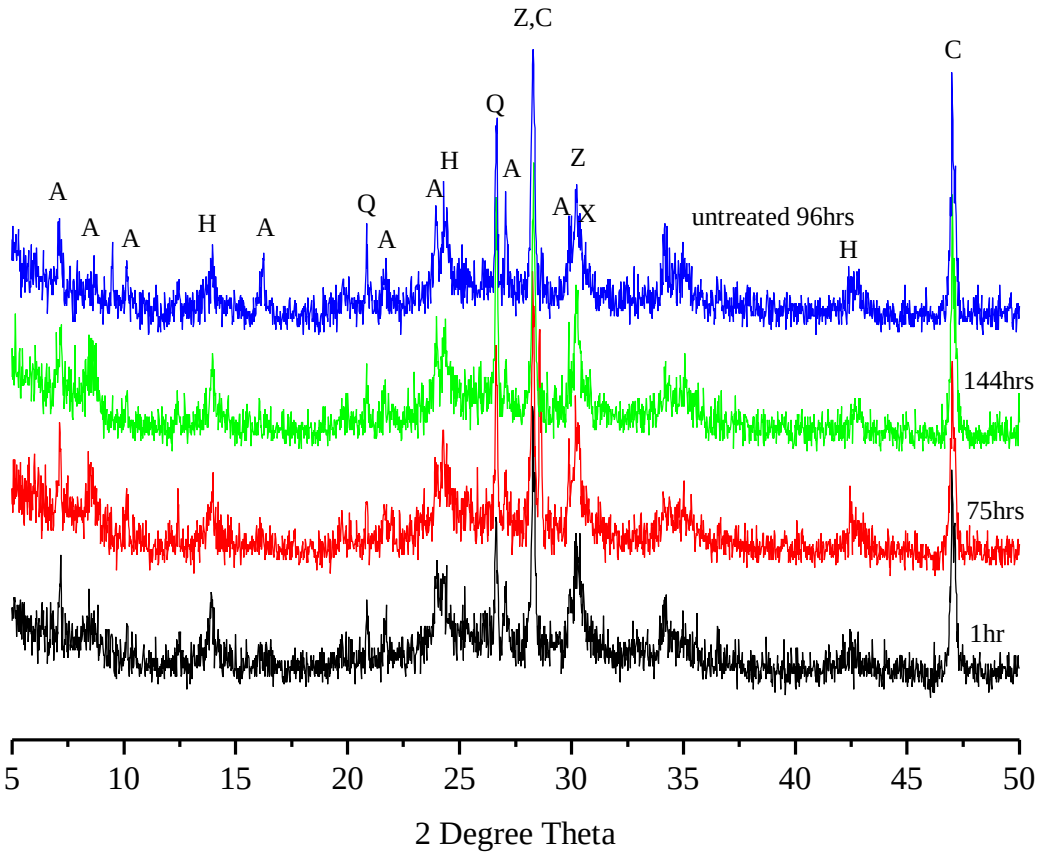

Figure 5.25. XRD patterns of selected PCT test residues compared with an untreated hydroceramic host mixed with 30 (solid) weight percent simulated fluorinel blend calcined radioactive waste hydrothermally synthesized at 150°C at various time intervals. A = type A zeolite ($NA_{96}Al_{96}Si_{96}O_{384}.2H_2O$, 39-0222); Z = zirconia (ZrO_2, 37-1484); C = calcium fluoride (CaF_2, 35-0816); Q = (SiO_2, 46-1045); and x unidentified poorly crystalline phase, possibly calcium compounds.

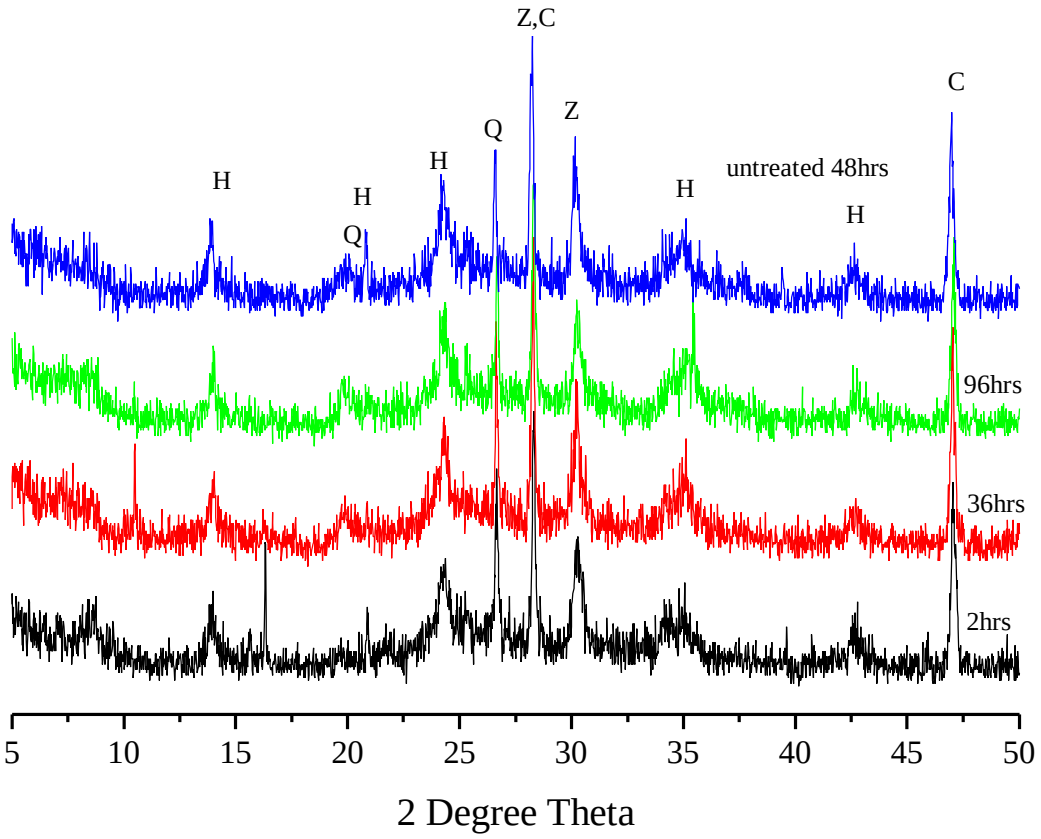

Figure 5.26. XRD patterns of selected PCT test residues compared with an untreated hydroceramic host mixed with 30 (solid) weight percent simulated fluorinel blend calcined radioactive waste hydrothermally synthesized at 200°C at various time intervals. A = type A zeolite ($NA_{96}Al_{96}Si_{96}O_{384}.2H_2O$, 39-0222); Z = zirconia (ZrO_2, 37-1484); C = calcium fluoride (CaF_2, 35-0816); Q = (SiO_2, 46-1045); and x unidentified poorly crystalline phase, possibly calcium compounds.

CHAPTER VI

SUMMARY, CONCLUSION AND FUTRE WORK

CHAPTER VI

SUMMARY, CONCLUSION AND FUTURE WORK

6.0 Summary

The objective of this study was to establish appropriate formulations that will result in optimal chemical durability and excellent physical properties in hydroceramic host waste-forms for the INEEL calcined high-level radioactive wastes; elucidate the hydration kinetics of the host and host-waste forms; and use the combined kinetics and analytical data as functions of temperature and time to establish processing limits. To meet this objective, a hydroceramic waste form based on common soda lime glass formulation was established. Twenty pozzolanic materials from various sources with different degree of chemical reactivity including fly ashes, silica fume, alumina, blast furnace slag, and natural pozzolans were used in this study. Each pozzolan or a combination pozzolans was mixed with vermiculite, cesium chloride, strontium nitrate and was activated by a solution of sodium hydroxide. The formulations were in turn processed hydrothermally with or without simulated calcined wastes. The pozzolanic materials and other reactants were screened for ease of processing, chemical reactivity and chemical durability (low leachability of ions) using PCT tests and physical properties. Finally, a combination of Troy clay (metakaolinite, a natural pozzolan) thermally altered, cesium chloride, strontium nitrate and sodium hydroxide

that satisfied glass composition, chemical durability and physical properties was chosen as the hydroceramic host waste form formulation.

Following the establishment of the hydroceramic host formulation, a systematic study of chemical durability (leachability) and hydration kinetics were undertaken as functions of temperature (75-200°C) and various time intervals.

XRD patterns of the hydroceramic host revealed type A zeolite and quartz in the samples processed at 75-150°C; while NaP1 and quartz were the two major phases formed in the 175-200°C samples. The plots of the maximum intensity of the type A zeolite (hkl, 2 0 0) and NaP1 (hkl, 3 0 1/3) as a function of the processing time, showed that the crystallizations of the crystalline phases followed a two-stage processes: the kinetic part characterized by an exponential increase type curve and a steady stage region typified by a horizontal line. The steady stage region was defined as the region where the intensity of the chosen peak approached a constant numerical value. The kinetic part of the curve suggested reacting stages and the steady stage part implies the end of reaction. These crystallization curves were the mirror images of the conductivity-pH-sodium versus time plots. SEM photomicrographs of the host product showed euhedra cubes of type A zeolite and NaP1 in support of the XRD patterns.

Another study similar to the host was carried out on at a constant 30 weight (solid) percent loading of simulated fluorinel blend calcine and zirconia calcine high-level

radioactive wastes mixed with the host formulation, maintaining glass compositional regions.

The XRD patterns of the host mixed with 30 weight percent loading of simulated fluorinel blend calcined and zirconia calcine radioactive wastes showed the same crystalline phases at the same temperatures. Type A zeolite formed at 75-95°C with traces of hydroxysodalite in the 95°C samples. Mixed phases of type A zeolite and hydroxysodalite crystallized at 125-150°C and hydroxysodalite at 175-200°C. Calcium fluoride and zirconia crystalline phases from the two wastes and quartz from the clay reactants were also revealed in addition to the crystalline phases formed in the host-waste XRD.

Modified PCT tests of the hydroceramic host and the host-containing wastes were carried out at 90°C for 24 hours. The conductivity, pH measurements and chemical analysis were used to gauge the waste forms chemical durability from their leachability as a function of processing time and temperature. Conductivity is the electrical response of the total ions present in a solution. The higher the numerical values of the conductivity measured, the more the total dissolved ions present and vice versa. The conductivity and pH of the “as prepared” PCT test solutions for the host waste forms showed an exponential decreasing trend with increasing processing time and temperature. The conductivity (7.95 mS/cm) and the pH (13.08) of the reference sample were higher than the processed samples (Figures 3.1-3.7). Sodium concentration was used as the equivalent concentration for the total dissolved ions in

the host. Sodium transient concentrations were estimated from the conductivity data and verified by the chemical analysis results. The plots of equivalent sodium concentration versus time plots followed the same trend as the conductivity-pH-time plots.

Similar exponentially decreasing trends were obtained for the conductivity-pH-time plots of the PCT test solutions from the host waste form mixed with fluorinel blend and zirconia simulated wastes. The host mixed with fluorinel blend calcine and zirconia calcine conductivity-pH-time plots of the processed samples at 75-150°C showed decreasing exponential trend, similar to that of hydrocramic host. The 175 and 200°C showed decreasing trend from ~1 hour processing time to 20 hours and then increase before reaching a steady-state at ~60 hours.

The measured transient concentrations of sodium in all samples were used as a control to interpret the hydration kinetics of the host and host-waste products. Sodium was chosen because it is an integral structural constituent of the zeolite phases formed. The reactions were assumed to follow, a first-order reaction kinetics. A nonlinear least square equation was used to estimate sodium concentrations at initial, expanded time length or when the reaction reached a steady state (constant concentration). Activation energies were calculated for the predominant type A zeolite, hydroxysodalite and NaP1 phases formed at certain temperature ranges. Rate constants were calculated for a particular temperature in which type A zeolite co-crystallized with hydroxysodalite in hydroceramic host mixed with fluorinel blend

and zirconia blend calcines. Table 6.1 summarizes the results of calculated rate constants and estimated activation energies for the phases formed in all the three waste forms. Different mechanisms governed by the chemistry of the formulations were in operation during the processing of the hydroceramic host and host mixed with fluorinel blend calcine and zirconia calcine wastes. This was evident from the crystallization of type A zeolite within different temperature ranges, the presence or absence of mixed phases and different phases at 175-200°C. Results showed that the activation energies for the formation of type A zeolite increased 3x in hydroceramic host mixed with fluorinel blend calcine and ~2x in zirconia calcine compared with the activation energy of the host. Type A zeolite formed at 75-150°C in the host and at 75-95°C in both wastes mixed with the host. The slower reaction rates of the host-waste during processing may be ascribed to the additional complexity introduced by the waste into the chemistry of the formulation. Hydroxysodalite mixed with type A zeolite crystallized at 125-150°C in host mixed with both wastes, whereas type A zeolite formed in the host at this temperature range. Finally, at 175-200°C, NaP1 crystallized in the host and hydroxysodalite formed in the host mixed with each waste.

The effects of several processing variables on the synthesis of hydroceramic waste forms and their effects on the chemical durability of the final products were investigated. The systematic elimination of a reactant one at a time from the hydroceramic host formulation resulted in excess water in the formulation especially vermiculite. The XRD patterns of samples with missing reactants showed that the

Table 6.1 Summary of the hydration kinetic results for the hydroceramic host and host mixed with 30 weight percent of simulated fluorinel blend and zirconia calcined wastes.

Waste Form	Temperature	Crystalline phase formed	Rate Constant	Activation Energy
Hydroceramic Host	75-150 ^{o}C	Type A zeolite	-	16.10 kJ/mol
	175-200 ^{o}C	NaP1	-	13.03 kJ/mol
Host mixed with 30wt% Fluorinel Blend Calcine	75-95 ^{o}C	Type A zeolite	-	49.57 kJ/mol
	125 ^{o}C	Type A zeolite + hydroxysodalite	5.5×10^{-4}/s	-
	150 ^{o}C	Type A zeolite + hydroxysodalite	7.8×10^{-4}/s	-
	175-200 ^{o}C	Hydroxysodalite	-	6.16 kJ/mol
Host mixed with 30wt% Zirconia Calcine	75-95 ^{o}C	Type A zeolite	-	28.642 kJ/mol
	125 ^{o}C	Type A zeolite + hydroxysodalite	5×10^{-4}/s	-
	150 ^{o}C	Type A zeolite + hydroxysodalite	9.1×10^{-4}/s	-
	175-200 ^{o}C	Hydroxysodalite	-	12.081 kJ/mol

crystallization increased in comparison with a sample processed normally. However, increasing crystallization did not result in the formation of a new phase.

Although the effect of adding extra water to the host-waste formulation resulted in the ease of poring a sample into the autoclave container, it decreased physical strength of the final product, increased rate of reaction, and increased crystallization of the zeolite phases. Increased crystallization with increased water content may be credited to water serving as a mineralizer, the more the water quantity the easier it is for the ions to migrate. However, with less water in the green body, transportation of chemical species will be difficult and the chemical reaction may be terminated earlier because the available water in the green body will turn into steam and escape into the vessel space. Increasing water content by 5x and 15x resulted in a physically weak hydroceramic that was easily crumbled between two fingers.

The XRD of the representative PCT residues showed that the chemistry of the already formed phases were not affected, even at low processing time and temperature.

6.1 Conclusion

A hydroceramic nuclear waste form was developed especially to address the immobilization of the reprocessing wastes from the Idaho National Engineering and Environmental Laboratory (INEEL) has been demonstrated to possess superior chemical and mechanincal properties. Furthermore, the processing requirements of

hydroceramic waste forms are simple, less costly and offer greater safety to INEEL personnel than other waste form preparation systems.

The objective of this research was two fold. The initial phase of the study was to systematically survey the suitability of readily available pozzolanic additions as raw materials for hydroceramic formulations in order to identify a source material that would be compatible with the established processing requirements for the waste form that is, no excessive water demand, proper mineralogical composition of the waste form, low leachability, waste loadings greater than 20 weight percent calcine and also readily available to INEEL in large quantities once the pozzolan(s) selection was made. Pozzolanic materials are normally finely divided substances that contain either glassy or crystalline sources of silica that are chemically reactive enough to combine with lime and water at room temperature to form cementitious material. The primary objective of the research program was to establish the final processing parameters for the preparation of hydroceramic waste forms form INEEL wastes i.e., the rate at which hydroceramic is formed, the phases that formed and the optimum temperature needed to minimize leachability.

Initial experimentations were conducted with several aluminosilicate pozzolanic materials. A total of 20 pozzolanic materials were surveyed. These included a number of different fly ash sample, natural and thermally altered clays, reactive aluminas and even finely ground bottle glass. The survey resulted in the selection of a natural, thermally altered clay (metakaolinite) that has found extensive use in the manufacture of blended Portland cement and currently mined in Troy Idaho.

A host matix formulation was initially developed using Troy metakaolinite, vermiculite, $Sr(NO_3)_2$, CsCl and NaOH and all processing parameters and chemical and mineralogical characterization was conducted on these samples. Once developed, the host matrix was used to subsequently prepare waste forms based on fluorinel and zirconia simulated calcines supplied by INEEL. A waste loading study was conducted in order to determine the maximum loading that could be sustained and still exibit the leaching characteristics and mechanical properties of the laboratory specimens. The host matrix samples and the two waste forms were processed at 75, 85, 95, 125, 150, 175 and 200°C at 100% relative humidity for times often exceeding 500 hours. Two sets of mineralogy were observed for the "host" samples and "waste loaded" samples. The host samples crystallized upon hydration to a zeolite calssified as Type A in the temperature range of 75 to 150°C and to another zeolite classifed as NaP1 from 175 to 200°C. Both sample sets contained minor amount of quartz derived from the meta-kaolin used as the pozzolan. In the waste form specimens, a mixture of predominantly Type A zeolite and minor hydroxysodalite were observed between 75 and 95°C. These gradually transformed into a mixture of hydroxysodalite with minor Type A zeolite between 125 and 150°C which in turn transformed to hydroxysodalite above 175-200°C. In all samples, minor to trace amounts of quartz from the meta-kaolin were detected.

The waste loading study optimized the hydroceramic waste form at 30% by weight for both fluorinel and zirconia waste calcines.

The conductivity, pH and concentrations of sodium measured and plotted as a function of processing times of the solutions obtained form the Product Consistency Test (PCT) decrease exponentially with time until steady states were reached.

The hydration rate studies conducted as a function of time and temperature determined that both the "host" matrix formulation and the fluorinel and zirconia waste loaded formulations followed a first-order kinetic reaction that can be summarized as follows:

From the characterization results and chemical analysis data, 2000°C at 100% relative humidity at ~8-10 hours are the most suitable processing conditions to complete the batch process within one working shift. However, the data support allow the autogenious heat from the radioactive decay drive the curing process which could take several weeks to reach completion. This latter option eliminates a complete operational step, one which involved slightly elevated pressure, and only requires insulated storage.

6.2 Suggestion for Future Work

Further investigation into hydroceramic waste forms should include detailed studies aimed at thermal and radiation stability as a function of temperature and time. This study would help determine the susceptibility of hydroceramic waste forms to an accumlation of radiolytically product gases from the pore water.

Means of porosity reduction in the final product should be included in the process route to increase density and lessen dissolution rates. Vibration or extrusion of kneaded paste under high pressure before autoclaving or using hydrothermal hot pressing techniques to decrease porosity may improve durability and high resistance to leachability.

Subjecting hydroceramic waste forms to different physical, chemical and biological conditions and quantify their effects as well as leaching of hydroceramic waste forms should be conducted under flow conditions, anoxic and in liquids other than water. Investigating the long-term effects of microbes on the chemical and physical properties of hydroceramics should also be considered and studied.

Other characterization methods that reflect burial conditions of hydroceramic waste forms involving large monoliths of a few meters needs to be carried out. The particle size range of the PCT tests conducted in this study gives no insight into long-term leaching behavior, where diffusion may give way to other controlling mechanisms, of large waste forms.

Hydroceramic waste form products should be vitrified and compare their physical properties and chemical durabilities with that of the EA benchmark glass. A cost analysis should be conducted that would reflect the effectiveness of hydroceramic

solidification, taking into consideration of the volume increase on shipping versus vitrification.

REFERENCES

Achar, B. N. N., Brindley, G. W. and Sharp, J. H. (1966) Kinetics and mechanism of dehydroxylation processes. III. Applications and limitations of dynamic methods. Proceddings of the International Clay Conference, Jerusalem, 1, 67-73.

Admixtures and ground slag for concrete (1990) Transportation research circular no. 365 (December) Washington: Transportation Research Board, National Research Council.

Amon, M., Dobeic, M., Sneath, R. W., Phillips, V. R., Misselbrook, T. H. and Pain, B. F. (1997) Farm-scale study on the use of clinoptilolite zeolite and De-Odorase for reducing odour and ammonia emissions from boiler houses. Bioresource Technology, vol.16, no. 3, 229-237.

Amor, J. N. and Farris, T. S. (1994) Simultaneous exchange and extrusion of metal exchanged zeolites. Applied Catalysis A: General, vol. 114, L187-L190.

Bergaya, F., Dion, P., Alcover, J. F., Clinard, C. and Tchoubar, D. (1996) TEM study of kaolinite thermal decomposition by controlled-rate thermal analysis. Journal of Materials Science, vol. 31, 5069-5075.

ASTM C 618-89 (1999) Standard specification for fly ash and raw or calcined natural pozzolan for use as a mineral admixture in Portland Concrete. Annual Book of ASTM Standards vol. 4, no. 2.

ASTM C 305-94 (1999) Standard Practice for Mechanical Mixing of Hydraulic Cement Pastes and Mortars of Plastic Consistency. Annual Book of ASTM Standards vol. 4, no. 1.

ASTM C 989-97b (1999) Standard Specification for Ground Granulated Blast-Furnace Slag for in Concrete and Mortals. Annual Book of ASTM Standards vol. 4, no. 2.

ASTM C 1220-98 (1999) Standard test method for static leaching of monolithic waste forms for disposal of radioactive waste. Annual Book of ASTM Standards, Nuclear, Solar, and Geothermal Energy, vol. 12, no. 1.

ASTM C 1285-97 (1999) Standard test methods for determining chemical durability of nuclear, hazardous, and mixed waste glasses: The Product Consistency Test (PCT) In: Annual Book of ASTM Standards vol. 12, no. 1.

ASTM E 1908-97 (1999) Standard guide for sample selection of debirs waste from building renovation or lead abatement project for toxicity characteristic

leaching procedure (TCLP) testing for leachable lead (Pb). Annual Book of ASTM Standards, Construction, vol. 4, no. 11.

Avrami, M. (1939) Kinetics of phase change. I. General theory. Journal of Chemical Physics, vol. 7, 1103-1112.

Avrami, M. (1940) Kinetics of phase change. II. Transformation-time relations for random distribution of nuclei. Journal of Chemical Physics, vol. 8, 212-224.

Avrami, M. (1941) Kinetics of phase change. III. Granulation, phase change, and microstructure. Journal of Chemical Physics, vol. 9, 117-184.

Bajt, S., Clark, S. B. Sutton, S. R., Rivers, M. L. and Smith, J. V. (1993) Syncrotron x-ray microprobe determination of cjromate content using x-ray absorption near-edge structure. Analytical Chemistry, vol. 65, 1800-1804.

Barnes, M. W., Scheetz, B. E., Wakeley. L. D., Atkinson, S. D. and Roy, D. M. (1982) Materials Research Society Symposia Proceedings, vol. 6, 147-154.

Barney, G. S. (1976) Fixation of radioactive wastes by hydrothermal reactions with clays. Advances in Chemistry #153, p108-125. American Chemical Society.

Barrer, R. M. (1978) Zeolites and Clay Minerals as Sorbents and Molecular Sieves. Academic Press, New York.

Barrer, R. M. (1982) Hydrothermal Chemistry of Zeolites. Academic Press, New York, New York.

Baxter, S. G. and Berghauser, D. C. (1986) Selection and performance of the natural zeolite clinoptilotite in British nuclear fuel's site ion exchange effluent plant , Sixep. Waste Management 1986. Waste Isolation in the U.S., Technical Programs and Public Education, Proceedings of the Symposium, Volume 2 p347-356. High-Level Waste, Tucson AZ, U.S.A.,.

Bell, A. T., McCormick, A. V., Hendricks, W. M. and Radke, C. J. (1986) Applications of NMR spectroscopy in the study of zeolite synthesis. Chemistry Express, vol.1, no. 12, 687-689.

Bernadzikowski, T. A., Allender, J. S., Stone, J. A., Gordon, D. E., Gould, T. H. and Westberry, C. F. (1983) High-level nuclear waste form performance evaluation. Ceramic Bulletin, vol.62, no. 12, 1364-1368 &1390.

Berner, U., Jacobsen, J. and McKinley, I. G. (1987) NEA/Nagra Workshop on Near-field Assessment of Repositories for Low and Medium Level Waste, November, 1987, Baden, Switzerland.

Bibler, N. E. (1978) Radiolytic Gas Production from Concrete Containing Savannah River Plant Waste. Report No. DP-1464, Savannah River Laboratory, Aiken, SC.

Bragg, L. and Claringbull, G. F. (1965) Crystal Structures of Minerals, Bell and Sons, London.

Breck, D. W. (1984) Zeolite Molecular Sieves. Krieger Publishing Company, Malabar, FL.

Brindley, G. W. and Nakahira, M. (1957) Role of water vapour in the dehydroxylation of clay minerals. Clay Miner., vol. 3 114-119.

Brown, G. (1961) X-ray Identification and Crystal Structures of Clay Minerals, p.132. Mineralogical Society, London.

Brownell, L. E, Kindle, C. H. and Theis, T. L. (1973) Review of Literature Pertinent to the Aqueous Conversion of Radionuclides to Insoluble Silicates with Selected References and Bibliography (Revised), 1973.

Burns, R. H. (1971) Solidification of low and intermediate level wastes, Atomic Energy Review, Vol. 9, 547-599.

Colombo, P. and Neilson, R. M. (1977) Some techniques for the solidification of some radioactive wastes in concrete. Nuclear Technology, vol. 32, 30-38.

Conner, J. R. (1990) Chemical Fixation and Solidification of Hazardous Waste. Van Nostrand Reinhold, New York.

Ciric, J. (1968) Kinetics of zeolite A crystallization. Journal of Colloid and Interface Science, vol. 28, no. 2, 315-324.

Cullity, B. D. and S. R. Stock (2001) Elements of X-ray Diffraction, 3rd edition, Prentice Hall, NJ.

Davidovits, J., Comrie, D. C., Paterson, J. H. and Ritcey, D. J. (1990) Geopolymeric concretes for environmental rpotection. Concrete International, vol. 12, no. 7, 30-40.

DeLaguna, L. R., Tamura, T., Weeren, H. O., Stuxness, E. G., McClain, W. C. and Sexton, R. C. (1968) ORNL-4259, Oak Ridge National Laboratory.

Dion, P., Alcover, J. F. and Bergaya, F. (1995) ^{27}Al ans ^{29}Si MAS NMR of kaolinie thermal decomposition by controlled rate thermal analysis. Journal of the American Ceramic Society, vol. 78, no 11, 2940-2944.

Dion, P., Alcover, J. F., Clinard, C. and Tchoubar, D. (1996) TEM study of kaoline thermal transformation by controlled-rate thermal analysis. Journal of Materials Science, vol. 31, no. 19, 5069-5075.

Dion, P., Alcover, J. F., Bergaya, F., Ortega, A., Llewellyn, P. L. and Rouquerol, F. (1998) Kinetic study by controlled-transformaton rate thermal analysis of the dehydroxylation of kaolinite. Clay Minerals, vol. 33, no. 2, 269-276

Dole, L,. Rogers, G., Morgan, M., Stinton, D., Kessler, J. and Moore, J. (1983) Cement Based-Radioactive Waste Hosts Formed Under Elevated Temperature and Pressures (FUETAP Concretes) for Savannah River Plant High-level Defense Waste. Report No. ORNL/TM-8579 (Oakridge National Laboratory, Oakridge, TN).

Dole, L. R., Moore, J. G., Rogers, G. C., West, G. A., Devaney, H. E., Morgan, M. T., McDaniel, E. W. and Kessler, J. H. (1982) Cementitious radioactive waste hosts formed under elevated temperatures and pressures (FUETAP concretes). In S. V. Topp Ed., vol. 6, pp. 585-593. Scientific Basis for Nuclear Waste Management, North-Holland, New York.

Fogler, H. S. (1999) Elements of Chemical Reaction Engineering, 3rd edition, Prentice Hall International Series in the Physical and Chemical Engineering Sciences, New Jersey.

Flynn, K. F., Barlleta, R. E., Jardine, L. J., and Steindler, M. J. (1979) Leach rate characterizations of solid radioactive waste forms. In G. J. McCarthy Ed., vol. 1, pp. 149-155. Scientific Basis for Nuclear Waste Management, New York Plenum Press.

Glasser, F. P. (1992) Progress in the immobilization of radioactive wastes in cement. Cement and Concrete Research, vol.22, 201-216.

Glasser, F. P. and Atkins, M. (1994) Cements in radioactive waste disposal. Materials Research Society Bulletin, vol. 19, 33-38.

Glasser, F. P., Rahman, A. A., Crawford, R. W., McCulloch, C. E. and Angus, M. (1982) Immobilization and Leaching Mechanisms of Radwaste Cement-based Matrices. Report DOE-RW-82-108, p. 106.

Gonthier, S. Gora, L. Guray, I. And Thompson, R. W. (1993) Further comments on the role of autocalaytic nucleation in hydrothermal Zeolite syntheseses. Zeolites, vol. 13, 414-418.

Gougar-Dunzik, M. L (1997) A Vitrifiable Cement Wasste Form for the Disposal of Spent Nuclear Fuel Reprocessing Waste. MS Thesis, The Pennsylvania State University, University Park, PA.

Gougar-Dunzik, M. L., Siemer, D. D. and Scheetz, B. E. (1996) Disposal of I.N.E.L. spent nuclear fuel reprocessing waste using glass-forming cement. Proceeding of the Embedded Topical Meeting on DOE Spent Nuclear Fuel & Fissile Material Management, Reno, NV, June 16-20, 1996, 359-365.

Gougar-Dunzik, M. L., Siemer, D. D. and Scheetz, B. E. (1998) A novel waste form for disposal of spent-nuclear-fuel reprocessing waste: A vitrifiable cement. Nuclear Technology, vol. 125, 93-103.

Gottardi, G. (1978) Mineralogy and crystal chemistry of zeolites. In L. B. Sand and F. A. Mumpton Eds., p31-44. Natural Zeolites: Occurrence, Properties, Use. Pergamon Press Inc., New York.

Grosskurth, K. P. (1991) Materials Research Society, vol., 179, 273-281.

Grutzeck, M. W. and Siemer, D. D. (1997) Zeolites synthesized from Class F ash and sodium aluminate slurry. Journal of the American Ceramic Society, vol. 80, no. 9, 2449-2453.

Haggerty, D. B. (1983) Radioactive waste stabilization: Aspects of solid-state molecular engineering and applied geochemistry. Annual Review Earth Planetry Science, vol. 11, 133-163.

Hancock, J. D. and Sharp, J. H. (1972) Methods of comparing solid-state kinetic data and its application to the decomposition of kaolinite, brucite, and BaCO3. Journal of the American Ceramic Society, vol. 55, 74-77.

Hench, L. L. (1995) The 70's: From selection of alternative waste forms to evaluation of storage system variables. In V. Jain and R. Palmer, Eds., vol. 61, 129-137. Environmental Issues and Waste Management Technologies in the Ceramic and Nuclear Industries, The American Ceramic Society, Westerville, OH.

Hinczak, I. (1990) Alternative cements- The blue circle experience in: Onoda Pacific Conference, vol. 1, 1-21.

Holt, J. B., Cutler, I. B. and Wadsworth, M. E. (1962) Rate of thermal dehydration of kaolinite in vacuum. Journal of the American Ceramic Society, vol. 45, 133-136.

Horvath, I. (1985) Kinetics and compensation effect in kaolinite dehydroxylation. Thermichimica Acta, vol. 85, 193-198.

Hu, H. C. and Lee, T. G. (1990) Synthesis kinetics of zeolite A. Industrial Engineering Chemistry Research, vol. 29, 749-754.

Izumida, T., Kawamura, F., Chino, K and Kibuchi, M. (1987) Nucler Technology, vol., 78, 185-190.

Jantzen, C. M (1984) Radioactive waste-Portland cement systems: II, Leaching characteristics. Journal of the American Chemical Society, vol. 67, no. 10, 674-678.

Jantzen, C. M., Bibler, N. E., Beam, D. C., Crawford, C. L. and Picket, M. A. (1993) Characterization of the Defense Waste Processing Facility (DWF) Environmental Assessment (EA) Glass Standard reference Material, Revision 1, June 1993.

Jantzen, C. M., Glasser, F. P. and Lachowski, E. E. (1984) Radioactive waste-Portland cement systems: I, Radionuclide distribution. Journal of the American Chemical Society, vol. 67, no. 10, 668-673.

Jiang, W., Wu, X. and Roy, D. M. (1993) Alkali-activated fly ash-slag cement based nuclear waste forms. In C. G. Interrante and R. T. Pabalan Eds., vol. 294, p. 255-260. Scientific Basis for Nuclear Waste Management, MRS, Pittsburgh, PA.

Johnson, M. L. (1992) Review: Why, when, and how biochemists should use least squares. Analytical Biochemistry, vol. 206, 215-225.

Johnson, M. L. and Faunt, L. M. (1992) Methods in Enzymology, vol. 210, 1

Johnson, M. L. and Frasier, S. G. (1985) Methods in Enzymology, vol. 117, 301

Johnson, G. M., Lee, Y., Tripathi, A. and Parise, J. B. (1999) Structural studies of hydrated germanium X-type zeolite via Rietveld analysis of synchrotron powder diffraction data. Microporous and Mesoporous Materials, vol. 31,no.1, 195-204.

Kacirek, H. and Lechert, H. (1977) Kinetic studies of the growth of zeolites of the faujasite and Na-A type. In Ed. J. R. Katzer, Eds., p244. Molecular Sieve II. American Chemical Society Symposium Series 40. American Chemical Society, Washington, DC.

Kacirek, H. and Lechert, H. (1975) Investigation on the growth of the zeolite type NaY. Journal of physical Chemistry, vol. 79, no. 15, 1589.

Katovic, A., Subotic, B., Smit, I., Despotovic, L. J .A. and Curic, M., (1989) American Chemical Society Symposium Series 398. In M. L. Occcelli and H. E. Robson, Eds., p.124. American Chemical Society, Washington, DC.

Katz, S. (1980) The reaction of hydrogen and oxygen in the presence of concretes incorporating simulated waste. In C. J. M. Northrup Eds., vol. 2 , 585-592. Scientific Basis for Nuclear Waste Mangement, Plenum Press, New York.

Kazanjian, A. R. and Killion, M. E. (1981) Radiolytic gas generation from sludge, CRD 81-025 (Rockwell International, Rocky Flats, Colorado.

Kerr, G. T. (1966) Chemistry of crystalline aluminsilicate. I. Factors affecting the formation of Zeolite A. The Journal of Physical Chemistry, vol. 70, no. 4, 1047-1050.

Kissinger, H. E. (1957) Reaction kinetics in differential thermal analysis. Anal. Chem. Vol 29, 1702-1705.

Kline, C and Hurlbut, C. S. (1993) Manual of Mineralogy, 21st edition, John Wiley and Sons, New York.

Klinowski, J. (1989) Solid-state NMR studies of zeolite catalysts. Colloids and Surfaces, vol. 36, no.2, 133-154.

Koelliker, J. K., Hellickson, M. L., Miner, J. R. and Nakaue, H. S. (1978) Improving poultry house environments with zeolite. American Society of Agricultural Engineers, Pap ASAE for Summer Meet, June 27-30 1978, p.18, ASAE, St Joseph, Mich, Logan, U.S.A., UT.

Kopac, T., Kaymakci, E., and Kopac, M (1998)Dyna mic adsorption of SO_2 on zeolite molecular sieves. Chemical Engineering Communications, vol.164, 99-109.

Kobayashi, J. (1978) Pollution by cadmium and the itai-itai disease in Japan. In Toxicity of Heavy Metals in the Environment. F. W.Oehme Ed., pp 199-260. Marcel Dekker, Inc., New York.

Lachman, I. M. and Williams, J. L. (1991) Extruded monolithic catalyst support. Symposium on Catalyst Suuports: Chemistry, Forming and Characteristics. Presented before the Division of Petroleum Chemistry, Inc. American Chemical Society, New York Meeting, August25-30, 1991, 535-543.

Laidler, K. J. (1987) Chemical Kinetics, 3rd edition, Harper Collins Publishers Inc., New York.

Lamberger, P. H. and Rogers, M. L. (1981) Tritium Waste Control. Report ML-2844 Monsanto Research Corp., Miamisburg, OH.

Langton, C. A. (1987) Slag-based saltstone formulations. MRS Scientific Basis for Nuclear Waste Management XI, M. J. Apted and R. E. Westerman, Eds., 61-72.

Langton, C. A. and Roy, D. M. (1980a) Longevity of Borehole and Shaft Sealing Materials. 2. Characterization of Cement-Based Ancient Building Materials, Report ONWI-202, The Pennsylvania State University, University Park, PA.

Langton, C. A. and Roy, D. M. (1981) Longevity of Borehole and Shaft Sealing Materials: II. Characterization of Cement-Based Ancient Building Materials. Topical Report Office of Naval Waste Isolation, Battel, (ONWI-202), October.

Langton, C. A , Dukes, M. D. and Simmons, R. V. (1983) MRS Scientific Basis for Nuclear Waste Management VIII, McVay, Eds., 575-582.

Lasaga, A.C. and Kirjpatrick, R. J. Eds. (1981) Kinetics of Geochemical Processes. Review in Mineralogy, vol. 8., Mineralogical Society of America, Washington D. C.

Lasaga, A. C. (1984) Chemical kinetics of water-rock interactions. Journal of Geophysical Research, vol. 89, no. B6, 4009-4025.

Lasaga, A. C. (1998) Kinetic Theory in Earth Sciences, Priceton University Press.

Lasaga, A. C., Soler, J. M., Ganor, J. Burch, T. E., and Nagy, K. L. (1994) Chemical weathering rate laws and global geochemical cycles. Geochimical et Cosmochimica Acta, vol. 58, 2361-2386.

Lee, J. F., Bajt, S., Clark, S. B., Lamble, G. M., Langton, C. A. and Oji, L. (1995) Chromium speciation in hazardous, cement-based waste forms. Physica B, vols. 208 & 209, 577-578.

Levenspiel, O. (1999) Chemical Reaction Engineering, 3rd edition, Wiley, New York.

Lewis, D. W. (1981) History of slag cements. Paper presented at University of Alabama Slag Cement Seminar, American Slag Association MF 186-6, April, 1981.

Li, Y. Y., Perera, S. P. and Crttenden, D. B. (1998) Zeolite monoliths for air separation Part1: Manufacture and Chracterization. Institute of Chemical Engineers Trans IchemE, vol. 76, Part A, 921-930.

Lutze, W. and Ewing, R. C. (1988) Radioactive Waste Forms for the Future, North-Holland, New York.

Macedo, P. B., Tran, D. C., Simmons, J. H., Saleh, M., Barkatt, A., Simmons, C. J., Lagakos, N. and DeWitt, E. (1979) Ceramic Nuclear Waste Management. In T. D. Chikalia and J. E. Mendel, Eds., p321. USDOE CONF-790420, Technical Information Center, Cincinnati, OH.

Malek, R. I. A., Licastro, P. H., Roy, D. M. and Langton, C. A. (1986) Slag cement-low level radioactive waste forms at Savannah River Plant. Ceramic Bulletin, vol. 65, 1578-1583.

Malhotra, V. M. (1986) Superplasticizers and other chemical admixtures in concrete, vol. 91. American Concrete Institute, Special publication, Detroit, MI.

Malhotra, V. M. (1987) Properties of fresh and hardened concrete incorporating ground granulated blast furnace slag. In V. M. Malhota, Ed., Supplementary Cementing Materials for Concrete, 291-331. Ottawa, Canadian Government Publishing Center.

Mann, N. R. and Todd, T. A. (2000) Crossflow testing of INEEL radioactive and nonradioactive waste slurries. Chemical Engineering Journal, vol. 80, Issues 1-3, 237-244.

McDaniel, E. W. and Delzer, D. B. (1988) FUETAP concretes. In W. Lutze and R.C. Ewing Eds., Radioactive waste forms for the future, 233-334.

McEvoy, J. E. (1969) US Patent Application No. 3,450,645.

McFarlane, H. F., Goff, K. M., Felicione, F. S., Dwight, C. C. and Barber, D. B. (1997) Hot demonstrations of nuclear-waste processing technologies. JOM vol. 49, no.7, 14-21, 83.

Mehta, P. K. (1980) Performance test for sulfate resistance and alkali-silica reactivity of hydraulic cements In: ASTM STP 691: Durability of building materials and components, vol. 21, 336-345.

Mehta, P. K. (1983) Pozzolanic and cementitious by-products as mineral admixture for concrete. In V. M. Malhotra, Ed., The use of fly ash, silica fume, slag and other mineral by-products in concrete, p1-46. A practical review ACI special publication SP-79, American Concrete Institute, Detroit.

Meise, W. and Schwochow, F. E. (1973) Kinetic studies on the formation of zeolite A. In W. M. Meier and J. B. Uytterhoven, Eds., Molecular Sieve p.169. Advances in Chemistry 121. American Chemical Society, Washington, DC.

Ming, D. W. and Mumpton, F. A. (1989) Zeolite in soils In) Dixon, J. B. and S. B. Weed, Eds., Minerals in Soil Environments 873-911. Soil Science Society of America, Madison, WI, U.S.A.

Morgan, M. T., McDaniel, E. W., Moore, J. G. Devaney, H. E. and Dole, L. R. (1983) Strontium leachability of hydrofracture grouts for sludge slurries. MRS Scientific Basis for Nuclear Waste Mangement VI, vol. 15., 235-242.

Moore, J. G. (1981) A Survey of Concrete Waste Forms, Alternative Nuclear Waste Forms and Interaction in Geologic Media, ORNL CONF-8005107, Gatlinburg, TN, 194-216 (1981).

Moore, J. G., Goodbee, H. W. and Kibbey, A. H. (1977) Leach behavior of hydrofracture grout incorporating radioactive wastes. Nuclear Technology, vol. 32, 39-52.

Moore, J. G., Rogers, G. C., Paehler, J. H. and Devaney, H. E. (1982) FUETAP (Formed Under Elevated Temperature and Pressures) concrete as host for radioactive wastes. MRS Scientific Basis for Nucearl Waste Management, vol. 6, 585-593.

Murray, P. and White, J. (1949) Kinetics of the thermal dehydration of clays. Transaction of British Ceramic Society, vol. 48, 187-200.

Newman, A. C. D. editor (1987) Chemistry of Clay Minerals, Mineralogical Society of England Monograph, no. 6, Oxford university Press, New York.

Nogawa, K. (1984) Cadmium. In J. O.Nriagu (Ed.), Changing Metal Cycles and Human Health, pp. 275-284, Springer-Verlag, New York.

Nogawa, K., Honda, R., Kodo, T., Tsuritani, I., and Yamada, Y. (1987) Limits to protect people eationg cadmium in rice, based on epidemiological studies. Trace Subs. Environm. Health, vol. 21, 431-439.

Odoj, R., Hilpert, K., and Gerads, H. (1979) Investigation of the volatility of cesium from aluminosilicates by mass spectrometry. In G. J. McCarthy, Ed., MRS Scientific Basis for Nuclear Waste Management, vol. 1, pp. 227-229, New York Plenum Press.

Omega Engineering Inc., (1989) The pH and Conductivity Handbook vol. 27, Stanford, CT.

Pellegrino, C., Ito, T., Gabelica, J. B. and Derouane, E.G. (1990) Characterization of zeolite Nu-10 by ^{129}Xe NMR spectroscopy. Applied Catalysis, vol. 6, no. 1, L1-L7.

Pilter, Z., Szabo, S., Hasznos-nezdei, M. and Pallai-Varsanyi, E. (2000) X-ray diffraction study of the effect of microwave treatment of zeolite Na-A. Microporous and Mesoporous Materials, vol.40, nos.1-3, 257-262.

Rees, L. V. C. and Chandrasekhar (1993) Formation of Zeolite from the system Na_2O-Al_2O_3-SiO_2-H_2O in alkaline medium (pH > 10). Zeolites, vol. 13, 524-533.

Redfern, S. A. T. (1987) The kinetics of dehydroxylation of kaolinite. Clay Miner., vol. 22, 447-456.

Ringwood, A. E., Kesson, S. E., Reeve , K. D., Levins, D. M. and Ramm, E. J. (1988) Synroc. In W. Lutze and R.C. Ewing Eds., Radioactive waste forms for the future, 233-334.

Roy, D. M. (1978) Cement based nuclear waste solidification forms. Proc. Conf. on High-level Radioactive Waste Forms, L. Casey, Ed., U. S. Nuclear Regulatory Commission (December 18-21, 1978), Denver, CO, p. 479-516, NUREG/CP-0005.

Roy, D. M. (1978) High-Level Radioactive Waste Forms. Symposium Proceedings, NUREG/CP-0005, 438-508.

Roy, D. M. (1990) Cementitious Material in Nuclear Waste Management, Cements Research Progress 1988, 261-292, 1990.

Roy, D. M. and Burns, F. L. (1982) Recent Advances in Repository Seal Materials. Scientific Basis for Nuclear Waste Management, W. L. Lutze Ed. vol.11, 631-640. Symposium Proceedings, MRS, North-Holland, NY.

Roy, D. M. and Gouda, G. R. (1978) High-level radioactive waste incorporation into (Special) cements. Nuclear Technology, vol. 40, 214-219.

Roy, D. M., Scheetz, B. E., Wakeley, L. D. and Atkinson, S. D. (1980) DOE/ET/41900-1 Rockwell International, Energy Systems Group, 1980.

Roy, D. M., Scheetz, B. E., Wakeley, L. D. and Barnes, M. W. (1982) Nuclear and Chemical Waste Management, vol. 3, 35-42.

Roy, D. M. and Scheetz, B. E. (1993) Chemistry and microstructure of Solidified Waste Forms. Lewis Publishers, CRC Press, Inc., Boca Raton, FL.

Scheetz, B. E., Silsbee, M. R. and Roy, D. M. (1993) Proceedings of the INDO-US Workshops on Durability of Concrete Structres, Bangladore, India, p. 1-17, 1993.

Scheetz, B. E., Roy, D. M., Tanner, C., Barnes, M. W., Grutzeck, M. W. and Atkinson, S. D. (1985) Ceramic Bulletin, vol. 64, no. 5, 687-690.

Schoeny, R. (1996) Use of Genetic Toxicology Data in U. S. EPA Risk Assessment: The Mercury Study Report as an Example. Environmental Health Perspectives, vol. 104 (suppl. 3), 663-673.

Severin, D. and Gupta, A. K. (1999) Composition analysis of petroleum waxes by zeolite molecular sieve-GCMS. Petroleum Science and Technology, vol. 17, no.9, 967-980.

Shannon, R. D. (1976) Revised effective ionic radii and systematic studies of interatomic distances in halides and chalcogenides. Acta Crystallographica, A22, 751-757.

Sharp, J. H., Brinkley, G. W. and Archar, B. N. N. (1966) Numerical data for some commonly used solid-state reaction equations. Journal of the American Ceramic Society, vol. 49, 379-382.

Siemer, D. D. (1995) Hot isostatically pressed concrete as a radwaste form. In Jain J. and Palmer, R Eds., Environmental Issues and Waste Management Technologies in the Ceramic and Nuclear Industries, vol. 61, 657-664. Ceramic Transactions, American Ceramic Society, Westerville, OH.

Siemer, D. D., Grutzeck, M. W. and Scheetz, B. E. (2000) Comparison of materials for making hydroceramic waste forms. In Gregory T. Chandler and Xiangdong Feng, Eds., Environmental Issues and Waste Management Technologies in the Ceramic and Nuclear Industries V, Ceramic Transactions, vol. 107, 161-167.

Siemer, D. D., Grutzeck, M. W., Roy, D. M and Scheetz, B. E. (1998) Zeolite waste forms synthesized from sodium bearing waste and metakaolinite. Waste Management Proceedings, March 1-5, 1998, Tucson, AZ.

Shimizu, S., Kiyozumi, Y., Maeda, K., Mizukami, F., Pal-Borbely, G., Milhayi, R. M. and Beyer, H. K. (1996) Transformation of intercalated layered silicates to zeolites in the solid state. Advanced Materials, vol. 8, no. 9, 759-762.

Spark, D. L. (1995) Inorganic soil components. In Environmental Soil Chemistry, p.23-53, Academic Press, New York.

Srinivasan, A. and Grutzeck, M. W. (1999) Adsorption of SO_2 by zeolites synthesized from fly ash. Environmental Science and Technology, vol. 33, no. 9, 1464-1469.

Stone, J. A. (1977) Evaluation of Concrete as a Matrix for Solidification of Savannah River Plant Wastes. Report No. DP-148 (Savannah River Laboratory, Aiken, SC).

Stone, J. A., Goforth, S. T. and Smith, P. K. (1979) Preliminary Evaluation of Alternative Forms for Immobilization of Savannah River Plant High-level Waste. The U. S. Department of Energy, DE-AC09-76SR0001.

Subotic, B. and Bronic, J. (1993) In Proceddings of the 9th International Conference on Zeolites. R. von Ballmoos, J. B. Higgins and M. M. J. Treacy Eds., p. 321, Butterworth-Heinemann, Boston.

Sylvester, P. and Clearfield, A. (1998) Removal of strontium and cesium from simulated Hanford groundwater using inorganic ion exchange materials. Solvent Extraction and Ion Exchange, vol. 16, no. 6, 1527-1539.

Szostak, R. (1998) Molecular Sieves, second edition. Blackie Academic and Professional, New York.

Taylor, H. F., (1997) Cement Chemistry, 2nd edition, Thomas Telford, London.

Toussaint, F., Fripiat, J. J. and Gastuche, M. C. (1963) Dehydroxyaltion of kaolinite. I. Kinetics. Journal of physical Chemistry, vol. 67, 26-30.

Tsuchiya, K. (1978) Cadmium Studies in Japan: A Review. Elsevier/NorthHolland Biomedical Press, pp. 376, New York.

U. S. EPA (1985a) National Primary and Secondary Drinking Water Regulations; Synthetic Organic Chemicals, Inorganic Chemicals and Microorganisms. Federal Register, vol. 50, 46936-47022.

U. S. EPA (1991e) National Primary and Secondary Drinking Water Regulations; Synthetic Organic Chemicals and Inorganic Chemicals; Monitoring for Unregulated Contaminants; National Primary Drinking Water Regualtions Implementation; National Secondary Drinking Water Regulations. FederalRegister, vol. 56, 3526-3599.

Virtanen, J. (1983) Freeze-thaw resistance of concrete containing blast-furnace slag, fly ash or condensed silica fume. In: V. M. Malhotra Ed., ACI Special Publication SP-79: The use of fly ash, silical fume, slag and other mineral by-products in concrete, 923-942, Detroit American Concrete Institute.

Walton, R.I., Millange, F., O'Hare, D., Davies, A. T., Sankar, G. and Catlow, C. R. A. (2001) In situ energy-dispersive X-ray diffraction study of the hydrothermal ceystallization of zeolite A. 1. Influence of reaction conditions and transformation into sodalite. Journal of Physical Chemistry B. vol.105, no.1, 1089.

Wilson, A. D. and Nilchoson, J. W. (1993) Acid-base Cements. Cambridge University Press.

Xi, Y., Siemer, D. D. and Scheetz, B. E. (1995) Leachability of blended cement wasteform for Cd^{2+} and Na^{+} rich liquid waste, 701-708 . In Environmental Issues and Waste Management Technologies in the Ceramic and Nuclear Industries. Ceramic Transactions, vol. 61, Jain J. and Palmer, R editors, American Ceramic Society, Westerville, OH.

Xuequan, W., Sheng, Y, Xiaodong, S., Mingshu, T. and Liji, Y. (1991) Alkali-activated cement based radioactive waste forms. Cement and Concrete Research, vol. 21, 16-20.

Yamasaki, N., Yanagisawa, K., Kanahara, S., Nishioka, M., Matsuoka, K. Yamazaki, J. (1984) Immobilization of radioactive wastes in hydrothermal synthetic rock: Lithification of silica powder. Journal of Nuclear Science Technology, vol. 21, no. 1, 71-73.

Yanagisawa, K., Kanahara, S., Nishioka, M., Matsuoka, K. and Yamazaki, N. (1984) Immobilization of radioactive wastes in hydrothermal synthetic rock: Hydrothermal synthesis of pollucite. Journal of Nuclear Science Technology, vol. 21, no. 7, 558-560.

Yang, J., Xie, D., Yelon, W. B. and Newsam, J. M. (1988) Aluminum-gallium substitution in zeolite Li-A(BW). Journal of Physical Chemistry, vol. 92, no. 12, 3586-3588.

Yoshida, A. and Inoue, K (1986) Formation of Faujasite-type zeolite from ground Shirasu Volcanic glass. Zeolites, vol. 6,467-373.

Zhdanov, S. P., (1971) Some problems of zeolite crystallization. In R. F. Gould, Ed., Advances in Chemistry Series 101, p.20. American Chemical Society, Washington, DC.

APPENDIX A

QBASIC COMPUTER PROGRAM CODES

Computer program called QBASIC used in calculating the oxides in the hydroceramic host or host mixed with fluorinel blend and zriconia formulations, refererence in Chapter II: (Darryl D. Siemer, Idaho National Engineering and Environmental Laboratories, Idaho Falls, ID).

```
10 REM "11compo...15dec99 reflects increased % NO3 in run 17 calcine 7.8 vs5.9
20 REM "calc.s composition & dHYD (based on HSC oxide hydration values)&Non
Bonded Oxygen NBO calc.
30 REM "adds NaALx solution to possible ingredients" & adjusts JBFA comp.
40 REM this version lumps MgO with CaO & Fe2O3 with Al2O3 (line 581)
REM Cs/Sr soln contains 0.058, 0.097, 0.078, & 0.025 g. C2O, SrO, nitrate, & Cl pr
cc
41 CLS
42 INPUT "indicate if you want a description printed (y/n) & if so enter one ", g$, h$
46 IF g$ = "y" THEN PRINT h$
INPUT "are wts really in grains "; k$
60 DIM newtroy(20), act3(20), srs(20), cc(20), mont(20), al2(20), zr2(20), zr22(20),
zr33(20), bent(20), pao(20), tox2(20), A(100), B(100), C(100), al(100), bl(100),
zr(100), t(100), S(100), ALL(100), NA(20), CS(100), SR(100), L(25), HMAT(25),
SEC(25), SEC51(25), TRU(25), NASI(25), V(25), SOI(25), JBFA(25), NAOH(25),
troy(25), naohhh(25), zr208(25), tox(25), meta(25)
70 REM "data ignores minor oxides...15 components only
80 PRINT "matrix order is
Al2O3,B2O3,CdO,CaO,CaF2,Cr2O3,Cs2O,Fe2O3,water,K2O,MgO,Na2O,SiO2,SrO
,ZrO2..fifteen components and two 'wild cards"
PRINT "          first the cements"
110 INPUT "grams SECAR 51 "; SECAR51
120 INPUT "grams SECAR 71 is"; SECAR
130 INPUT "grams OPC is"; OPC
INPUT "grams ceramicrete is "; cc
140 INPUT "grams BFS is"; BFS: REM BFS data is Penn state's
PRINT "           next the waste stuff"
INPUT "grams #44 SRS liquid simulant (d=1.467)"; srs: IF k$ = "y" THEN srs =
15.4 * srs
REM simulant is 11.5M NaOH, 1.49 M NaNO3 & 0.69 M CsCl, dens.=1.4
INPUT "milliliters of 2008 AD flowsheet SBW"; TRUEX: TRU = .0863 * TRUEX
INPUT "milliliters of SBW (JAM-08-94)"; LI: LIWT = LI * 8.519999E-02
INPUT "grams #1027 alumina calcine is "; al2
INPUT "grams #64 zirconia calcine is "; zr2
IF zr2 > 0 THEN INPUT "was it fines y/n "; x$: IF x$ = "y" THEN zr22 = zr2 AND
zr2 = 0
INPUT "grams #74 zirconia calcine is "; zr: REM next data is ours
IF zr > 0 THEN INPUT "was it fines y/n "; y$: IF y$ = "y" THEN zr33 = zr: zr = 0
INPUT "grams 2008 AD Zr LLW calcine is "; zr3
INPUT "grams run #17 Zr/Na blend"; bl
IF bl > 0 THEN INPUT "was it fines y/n "; z$: IF z$ = "y" THEN bl2 = bl: bl = 0
```

```
INPUT "grams #20 blend calcine is "; al: REM data is ours
PRINT "          next the pozzolans & other matrix formers"
180  INPUT "grams hobby or indian red pottery clay is "; clay
185  INPUT "grams englehard metakaolin is "; meta
187 INPUT "grams new Troy clay is "; newtroy
190 INPUT "grams Troy clay is "; troy: IF srcs > 0 THEN troy = troy + .395 * srcs
INPUT "grams dry basis bentonite (spec. tested was 11% water)"; bent
200 INPUT "grams INEL soil"; SOIL
210 INPUT "grams vermiculite is"; verm
INPUT "grams Montour fly ash ...class F"; mont
INPUT "grams jim bridger fly ash ", jb
230 INPUT "grams silica"; SILICA
240 INPUT "grams added alumina"; ALUM
PRINT "next the activators"
250 INPUT "grams added 3.22 sodium silicate soln (38% solids) "; nas
260 INPUT "grams added Red Devil lye (94% NaOH)"; NAO

INPUT "grams MWG/Palomo's #3 activator (.186 g Naoh to 1 g water glass ", act3
270 INPUT "wt added 25% NaOH (SpG=1.224) is "; naohh
275 INPUT "wt added 37.5% NaOH (1.348 sp g) is ", naohhh
277 IF k$ = "y" THEN naohh = naohh * 15.4
   IF k$ = "y" THEN naohhh = naohhh * 15.4
allnaoh = .25 * naohh + .375 * naohhh + .94 * NAO + .159 * act3
INPUT "grams additional potassium oxide is"; K2O
PRINT "              next the other stuff"
INPUT "g NaNO3"; nano3
INPUT "grams of p. 9 tox mix "; tox
INPUT "grams of toxmix#2 is "; tox2
INPUT "g 60% sodium sulfide is "; na2s
INPUT "g FeS is "; fes
INPUT "grams jan2999 'SrCs'-clay mix is  "; srcs

INPUT "grams extra B2O3 (mw=69.8) is ", b2o3
290 INPUT "grams extra cesium oxide"; CSO
300 INPUT "grams extra strontium oxide"; SrO
310 INPUT "grams additional lime as CaO"; LIME
320 INPUT "grams added water is"; h
330 INPUT "identify any additional substance & its wt"; C$, STUFF
340 INPUT "identify any additional substance & its wt"; E$, STUFF2
IF clay = 0 THEN clay = .0000000001#
troy = troy + .7 * tox
DATA 0,0,0,0,0,0,.063,0,0,0,0,.197,0,.059,0
FOR I = 0 TO 14: READ tox2(I): tox2(I) = tox2(I) * tox2: NEXT
350 total = b2o3 + newtroy + act3 + srs + cc + fes + nano3 + mont + al2 + zr22 +
zr33 + sim + bent + .605 * srcs + na2s + tox2 + SECAR51 + pao + meta + SECAR +
OPC + BFS + al + zr + bl + clay + SILICA + ALUM + NAO + CSO + K2O + SrO +
```

```
h + STUFF + STUFF2 + LIWT + LIME + TRU + nas + verm + SOIL + jb + naohh +
troy + naohhh + zr2 + .3 * tox + zr3
DATA 0,0,0,0,0,0,0,0,.102,.267,.229,0,0,0,0
FOR I = 0 TO 14: READ cc(I): cc(I) = cc(I) * cc: NEXT
400 DATA .711,0,0,.271,0,0,0,.0024,.0035,.00035,.0036,.0031,.007,.00015,0
410 FOR I = 0 TO 14: READ SEC(I): SEC(I) = SEC(I) * SECAR: NEXT
420 DATA .508,0,0,.359,0,0,0,.0237,.026,.0028,.0046,.0007,.0343,.0005,0
430 FOR I = 0 TO 14: READ SEC51(I): SEC51(I) = SEC51(I) * SECAR51: NEXT
460 DATA .042,.0001,0,.65,0,.0001,0,.027,.01,.011,.02,.0017,.191,.0010,.0004
470 FOR I = 0 TO 14: READ A(I): A(I) = A(I) * OPC: NEXT
500 DATA .073,.0002,0,.410,0,.0001,0,.0034,0,.0047,.103,.0036,.34,.0006,.001
510 FOR I = 0 TO 14: READ B(I): B(I) = B(I) * BFS: NEXT
520 DATA .201,0,0,.0945,0,0,0,.0722,.0046,.02,.011,.02,.592,0,0
530 FOR I = 0 TO 14: READ JBFA(I): JBFA(I) = JBFA(I) * jb: NEXT
540 DATA .401,.042,.019,.07,.262,.009,0,.007,0,.009,0,.049,0,.001,.129
550 FOR I = 0 TO 14: READ al(I): al(I) = al(I) * al: NEXT: REM #20 Zr blend
DATA .139,0,0,.064,0,0,0,.048,0,.012,.051,.017,.662,0,0
FOR I = 0 TO 14: READ SOI(I): SOI(I) = SOI(I) * SOIL: NEXT
  REM wastes
DATA .0139,0,0,0,0,0,.0024,0,.54,0,0,.317,0,0,0
FOR I = 0 TO 14: READ srs(I): srs(I) = srs(I) * srs: NEXT
DATA .33,.0065,.0003,.03,.006,.0053,.0001,.023,0,.08,0,.457,0,0,0
FOR I = 0 TO 14: READ L(I): L(I) = L(I) * LIWT: NEXT
DATA .301,.0057,.0036,.015,.0185,.0021,.0008,.0155,0,.0904,0,.545,0,0,.00063
FOR I = 0 TO 14: READ TRU(I): TRU(I) = TRU(I) * TRU: NEXT

DATA .70,.004,0,.011,.034,.002,0,.002,0,.003,0,.074,0,0,0
FOR I = 0 TO 14: READ al2(I): al2(I) = al2(I) * al2: NEXT: REM #1027
REM
Al2O3,B2O3,CdO,CaO,CaF2,Cr2O3,Cs2O,Fe2O3,water,K2O,MgO,Na2O,SiO2,SrO
,ZrO2..fifte
DATA .183,.003,0,.174,.383,.007,0,.001,0,.008,0,.034,0,.002,.202
FOR I = 0 TO 14: READ zr2(I): zr2(I) = zr2(I) * zr2: NEXT: REM 64
DATA .183,.003,0,.174,.383,.007,0,.001,0,.008,0,.034,0,.002,.202
FOR I = 0 TO 14: READ zr22(I): zr22(I) = zr22(I) * zr22: NEXT: REM 64 fines

552 DATA .32,0,.0106,0,.42,.0038,.021,0,0,0,0,.054,0,.009,.09
FOR I = 0 TO 14: READ pao(I): pao(I) = pao(I) * pao: NEXT
DATA .222,.037,0,.095,.378,.006,.005,.001,0,0,0,.006,0,.009,.235
FOR I = 0 TO 14: READ zr(I): zr(I) = zr(I) * zr: NEXT: REM #74
DATA .222,.037,0,.095,.378,.006,.0095,.001,0,0,0,.006,0,.009,.235
FOR I = 0 TO 14: READ zr33(I): zr33(I) = zr33(I) * zr33: NEXT: REM #74 fines
zr33
DATA .202,.019,.025,.0,.409,.006,.005,.003,0,.0087,0,.0782,0,.009,.233
FOR I = 0 TO 14: READ zr208(I): zr208(I) = zr208(I) * zr3: NEXT
DATA .118,.034,.059,.102,.4,.016,0,.005,0,.011,0,.053,0,.001,.197
```

```
FOR I = 0 TO 14: READ bl(I): bl(I) = bl(I) * bl: NEXT: REM #17
  REM pozzolans
DATA .216,0,0,.0011,0,0,0,.020,.001,.012,.019,.014,.718,0,0
FOR I = 0 TO 14: READ C(I): C(I) = C(I) * clay: NEXT
DATA .404,0,0,.0014,0,0,0,.0036,.0093,.0014,.00046,.0052,.573,0,0
FOR I = 0 TO 14: READ meta(I): meta(I) = meta(I) * meta: NEXT
DATA .353,0,0,.013,0,0,0,.03,.02,.006,0,.001,.557,0,0
FOR I = 0 TO 14: READ newtroy(I): newtroy(I) = newtroy(I) * newtroy: NEXT
REM
Al2O3,B2O3,CdO,CaO,CaF2,Cr2O3,Cs2O,Fe2O3,water,K2O,MgO,Na2O,SiO2,SrO
,ZrO2..fifte

DATA .305,0,0,.026,0,0,0,.03,.02,.006,0,0,.613,0,0
FOR I = 0 TO 14: READ troy(I): troy(I) = troy(I) * troy: NEXT
DATA .109,0,0,0,0,0,0,.253,.08,0,.171,.001,.383,0,0
FOR I = 0 TO 14: READ V(I): V(I) = V(I) * verm: NEXT
DATA .298,0,0,.0098,0,0,0,.11,0,.018,.0076,0,.527,.0008,0
FOR I = 0 TO 14: READ mont(I): mont(I) = mont(I) * mont: NEXT
DATA .193,0,0,.008,0,0,0,.027,0,.004,.0191,.029,.72,0,0
FOR I = 0 TO 14: READ bent(I): bent(I) = bent(I) * bent: NEXT
DATA 0,0,0,0,0,0,0,0,0,0,0,0,1,0,0
FOR I = 0 TO 14: READ S(I): S(I) = S(I) * SILICA: NEXT
DATA 0,0,0,0,0,0,0,0,.62,0,0,.090,.289,0,0
FOR I = 0 TO 14: READ NASI(I): NASI(I) = NASI(I) * nas: NEXT
DATA 1,0,0,0,0,0,0,0,0,0,0,0,0,0,0
FOR I = 0 TO 14: READ ALL(I): ALL(I) = ALL(I) * ALUM: NEXT
DATA 0,0,0,0,0,0,0,0,0.2715,0,0,.7285,0,0,0
710 FOR I = 0 TO 14: READ NA(I): NA(I) = NA(I) * NAO: NEXT
720 DATA 0,0,0,0,0,0,0,0,.803,0,0,.197,0,0,0
730 FOR I = 0 TO 14: READ NAOH(I): NAOH(I) = NAOH(I) * naohh: NEXT
732 DATA 0,0,0,0,0,0,0,0,.71,0,0,.29,0,0,0
735 FOR I = 0 TO 14: READ naohhh(I): naohhh(I) = naohhh(I) * naohhh: NEXT
DATA  0,0,0,0,0,0,0,0,.562,0,0,.1965,.242,0,0
FOR I = 0 TO 14: READ act3(I): act3(I) = act3(I) * act3: NEXT
740 DATA 0,0,0,0,0,0,1,0,0,0,0,0,0,0,0
750 FOR I = 0 TO 14: READ CS(I): CS(I) = CS(I) * CSO: NEXT
760 DATA 0,0,0,0,0,0,0,0,0,0,0,0,0,1,0
770 FOR I = 0 TO 14: READ SR(I): SR(I) = SR(I) * SrO: NEXT
780 DATA 0,0,0,0,0,0,0,0,1,0,0,0,0,0,0
790 FOR I = 0 TO 14: READ HMAT(I): HMAT(I) = HMAT(I) * h: NEXT
CdO = tox * .114 * .033
800 FOR I = 0 TO 14: t(I) = newtroy(I) + act3(I) + srs(I) + cc(I) + mont(I) + al2(I) +
zr2(I) + zr22(I) + bent(I) + pao(I) + tox2(I) + SEC51(I) + meta(I) + SEC(I) + A(I) +
B(I) + C(I) + S(I) + al(I) + zr(I) + zr33(I) + bl(I) + ALL(I) + NA(I) + NAOH(I) +
naohhh(I) + CS(I) + SR(I) + L(I) + HMAT(I) + TRU(I) + NASI(I) + V(I) + SOI(I) +
JBFA(I) + troy(I) + zr208(I): NEXT
```

```
810 t(3) = t(3) + LIME: t(11) = t(11) + .477 * na2s + (31 / 85) * nano3
t(6) = t(6) + sim * .0069: t(8) = t(8) + .647 * sim: t(11) = t(11) + sim * .287
t(2) = t(2) + CdO:  t(6) = t(6) + .244 * srcs: t(13) = t(13) + .152 * srcs: t(1) = t(1) +
b2o3
820 t(9) = t(9) + K2O: t(7) = t(7) + .9 * fes: t(11) = t(11) + .354 * na2s * tox2: t(8) =
t(8) + .4 * na2s
h20 = t(8)
830 FOR I = 0 TO 14: tot = tot + t(I): NEXT
840 TRUETOT = tot + STUFF + STUFF2: drytot = TRUETOT - t(8)
850 GOTO 1310
860 FOR I = 0 TO 14: t(I) = t(I) / total: NEXT
870 PRINT "% Al2O3 is ", 100 * t(0), "% B2O3 is", 100 * t(1)
880 PRINT "% CdO is ", 100 * t(2), "%CaO is", 100 * t(3)
890 PRINT "% CaF2 is ", 100 * t(4), "% Cs2O is", 100 * t(6)
900 PRINT "% Cr2O3 is ", 100 * t(5), "% Fe2O3 is", 100 * t(7)
910 PRINT "% K2O is ", 100 * t(9), "% MgO is", 100 * t(10)
920 PRINT "% Na2O is ", 100 * t(11), "% SiO2 is", 100 * t(12)
930 PRINT "% SrO is ", 100 * t(13), "% water is", 100 * h20 / total
940 PRINT "% ZrO2 is ", 100 * t(14), "% of"; C$; " is", 100 * STUFF / TRUETOT
950 PRINT "% of "; E$; "is ", 100 * STUFF2 / TRUETOT, "% sulfide is "; 24.6 *
na2s / total + 36 * fes / total
960 IF TRU > 0 THEN PRINT "% of Pb0, NiO, P2O5, & SO4 are"; 100 * TRU *
.0024 / TRUETOT; 100 * .0014 / TRUETOT; 100 * TRU * .007 / TRUETOT; 100 *
TRU * .042 / TRUETOT
f = tox / total
IF tox > 0 THEN PRINT "% of As,Ba,Ag, Cd, Cr, Pb, & Hg from TOXMIX#1 are "
IF tox > 0 THEN PRINT f * 2.8; f * 3.36; f * 1.35; f * 3.3; f * 2.99; f * 2.19; f * 3.33
965 IF tox2 > 0 THEN PRINT "% As, Se, Pb, Cd,Cr, and Ag from TOXMIX#2 are ";
3 * tox2 / total

zrtot = zr + zr2 + zr22 + zr33 + zr3: bltot = bl + al + bl2
PRINT "% nitrate & Cl from SrCs, Calcines, TOXMIX's, NaNO3, & SIM  is "; (srs *
4.9 + al2 * 11 + zr22 * 15.1 + bl2 * 8.7 + zr33 * .6 + srcs * 18.3 + 2.95 * tox + al *
4.5 + bl * 7.8 + 32 * tox2 + zr2 * 5.1 + sim * 6.7 + 100 * (62 / 85) * nano3) / total;
"and "; (srcs * 6.2 + 4.1 * tox + 3.8 * tox2 + .175 * sim) / total
IF srs > 0 THEN PRINT "percent nitrite is "; .049 * srs * 100 / total

IF (zr + zr33 + bl + bl2 + al2) > 0 THEN PRINT " % sulfate from calcines is ", ((bl +
bl2) * 2.32 + (zr + zr33) * 3.5) + al2 * 4 / total
IF pao > 0 THEN PRINT "% nitrate from Pao's calcine is "; 10 * pao / total
IF pao > 0 THEN PRINT "% lead and mercury for it are "; .15 * pao / total; "and";
.56 * pao / total

IF cc > 0 THEN PRINT "% P205 from ceramicrete is "; 40.2 * cc / total
970 PRINT "g:SBW ASH  "; "2008 TRUEX ASH  "; "AL CALCINE   "; "ZR
CALCINE   "; "FL-blend CALCINE"
```

```
980 PRINT SPC(5); LIWT; SPC(6); TRU; SPC(8); al2; SPC(11); zrtot; SPC(13);
bltot
PRINT "total, zrtot and bltot are", total, zrtot, bltot

990 PRINT "total weight is "; total; "g, fraction dry solids is "; 1 - (h20 / total);
"fraction dry stuff that's waste is"; (LIWT + TRU + al2 + zrtot + bltot + CSO + SrO +
.31 * srs) / (total * (1 - h20 / total))

1000 PRINT "g: water  "; "SECAR51      "; "SECAR71   "; "BFS     "; "OPC     ";
"NaOH": GOTO 1020
1010 PRINT h + .8 * naohh; SECAR51; SECAR; BFS; OPC; allnaoh
1020 PRINT SPC(1); h + .62 * naohh; SPC(5); SECAR51; SPC(10); SECAR71;
SPC(4); BFS; SPC(5); OPC; SPC(4); NAO + .197 * naohh
clay = clay + troy + meta + bent + newtroy
1030 PRINT "g: silica", "clay", "vermiculite", "soil", "flyash"
1040 PRINT SILICA, clay, verm, SOIL, jb + mont

1050 PRINT "ratio of water:cement = "; (TRUETOT - drytot) / (SECAR51 + cc +
SECAR + BFS + OPC + 1E-08)
1060 R1 = (t(11) / 31 + t(9) / 47) + 1E-08: R2 = t(3) / 56 + t(10) / 40: R3 = t(0) / 51 +
t(7) / 79.9
1070 PRINT "atomic ratios of M2O/MO/M2O3/SiO2 are "; 1; ":"; R2 / R1; ":"; R3 /
R1; ":"; t(12) / 60 / R1
PRINT "# of non-bridging oxygens are "; 2 * R - 4; "and dG hyd is "; DHYD; "
Kcal/mole"

1080 INPUT "printout y/n"; D$
1090 IF D$ = "n" THEN END
 IF g$ = "y" THEN LPRINT
 IF g$ = "y" THEN LPRINT h$

LPRINT "g:SBW ASH  "; "2008 TRUEX ASH  "; "AL CALCINE   "; "ZR
CALCINE   "; "FL-blend CALCINE"
LPRINT SPC(5); LIWT; SPC(6); TRU; SPC(8); al2; SPC(11); zrtot; SPC(13); bltot
LPRINT "total weight is "; total; "g, fraction dry solids is "; drytot / TRUETOT;
"fraction dry stuff that's waste is"; (LIWT + TRU + zrtot + bltot + al2 + CSO + SrO) /
(total - total * t(8))
1130 LPRINT "g: water", "SECAR51", "SECAR 71", "BFS", "OPC"
1140 LPRINT h + .8 * naohh, SECAR51, SECAR, BFS, OPC
1150 LPRINT "g: silica", "clay", "vermiculite", "NaOH", "INEL soil", "flyash"
1160 LPRINT SILICA, clay, verm, allnaoh, SOIL, jb + mont
1170 LPRINT "ratio of water:cement = "; (TRUETOT - drytot) / (SECAR51 +
SECAR + BFS + OPC + 1E-08)
1180 LPRINT "% Al2O3 is ", 100 * t(0), "% B2O3 is", 100 * t(1)
1190 LPRINT "% CdO is ", 100 * t(2), "%CaO is", 100 * t(3)
1200 LPRINT "% CaF2 is ", 100 * t(4), "% Cs2O is", 100 * t(6)
```

```
1210 LPRINT "% Cr2O3 is ", 100 * t(5), "% Fe2O3 is", 100 * t(7)
1220 LPRINT "% K2O is ", 100 * t(9), "% MgO is", 100 * t(10)
1230 LPRINT "% Na2O is ", 100 * t(11), "% SiO2 is", 100 * t(12)
1240 LPRINT "% SrO is ", 100 * t(13), "% water is", 100 * h20 / total
1250 LPRINT "% ZrO2 is ", 100 * t(14), "% of "; C$; " is", 100 * STUFF /
TRUETOT
1260 LPRINT "% of "; E$; " is ", 100 * STUFF2 / TRUETOT, "% sulfide is ", (24.6
* na2s + 36 * fes) / total
1270 IF TRU > 0 THEN LPRINT "% of Pb0, NiO, P2O5, & SO4 are"; 100 * TRU *
.0024 / total; 100 * TRU * .0014 / total; 100 * TRU * .007 / total; 100 * TRU * .042 /
total
DATA .298,0,0,.0098,0,0,0,.11,0,.018,.0076,0,.527,.0008,0
FOR I = 0 TO 14: READ mont(I): mont(I) = mont(I) * mont: NEXT

IF tox > 0 THEN LPRINT "% of As,Ba,Ag, Cd, Cr, Pb, & Hg from TOXMIX#1 are "
IF tox > 0 THEN LPRINT f * 2.8; f * 3.36; f * 1.35; f * 3.3; f * 2.99; f * 2.19; f *
3.33
IF pao > 0 THEN LPRINT "% nitrate from Pao's calcine is "; 10 * pao / total
IF pao > 0 THEN LPRINT "% lead and mercury for it are "; .15 * pao / total; "and";
.56 * pao / total
IF cc > 0 THEN LPRINT "% P205 from ceramicrete is "; 40.2 * cc / total
1275 IF tox2 > 0 THEN LPRINT "% As, Se, Pb, Cd,Cr, and Ag from TOXMIX#2
are "; 3 * tox2 / total
LPRINT "% nitrate & Cl from SrCs, Calcines, TOXMIX's, NaNO3, & SIM  is "; (srs
* 4.9 + al2 * 11 + zr22 * 15.1 + bl2 * 8.7 + zr33 * .6 + srcs * 18.3 + 2.95 * tox + al *
4.5 + bl * 7.8 + 32 * tox2 + zr2 * 5.1 + sim * 6.7 + 100 * (62 / 85) * nano3) / total;
"and "; (srcs * 6.2 + 4.1 * tox + 3.8 * tox2 + .175 * sim) / total
IF srs > 0 THEN LPRINT "percent nitrite is "; .049 * srs * 100 / total
IF (zr + zr33 + bl + bl2) > 0 THEN LPRINT " % sulfate from calcines is ", ((bl + bl2)
* 2.32 + (zr + zr33) * 3.5) / total
1280 LPRINT "atomic ratios of M2O/MO/M2O3/SiO2 are "; 1; ":"; R2 / R1; ":"; R3 /
R1; ":"; t(12) / 60 / R1
1290 LPRINT "# of non-bridging oxygens are "; 2 * R - 4; "and dG hyd is "; DHYD;
" Kcal/mole"
1300 END
1310 TOTH = t(0) / 102 + t(1) / 69.6 + t(3) / 56 + t(6) / 286 + t(9) / 94.2 + t(10) / 40.3
+ t(11) / 62 + t(12) / 60: REM SiO2 & Al203 dG hydration data from Jantzen,et al, J
Non Cyst Sol., 67(1984)p.207, oxide hydration data from HSC calcn. using 1000
moles H2O/mole
1320 DHYD = t(0) * 3.04 / 102 - t(1) * 9.93 / 69.6 - t(3) * 6.591 / 56 - t(6) * 84.42 /
286 - t(9) * 76.73001 / 94.2 + t(10) * 8.743 / 40.3 - t(11) * 53.09 / 62 + t(12) * 5.59 /
60: DHYD = DHYD / TOTH
1330 PRINT "hydration energy of glass formers is "; DHYD; "kcal/mole"
1340 R = (3 * t(0) / 102 + 3 * t(1) / 69.6 + t(3) / 56 + t(6) / 286 + t(9) / 94.2 + t(10) /
40.3 + t(11) / 62 + 2 * t(12) / 60) / (2 * t(0) / 102 + t(12) / 60): REM NBO calcn from
WINCO-1133, p. 13
```

```
1350 PRINT "non bonded oxygens of glass makers are ", 2 * R - 4
1360 GOTO 860
```

APPENDIX B

DERIVATION OF EQUATION 3.1 USED TO CALCULATE RATE CONSTANTS FOR HYDROCERAMIC WASTE FORMS

Derivation of Equation 3.1

$$\frac{dy}{dt} = -k(y - y_{\infty}) \quad (1)$$

$$\frac{dy}{y - y_{\infty}} = -k\,dt \quad (2)$$

$$\frac{dy}{y - y_{\infty}} = -k\,dt \quad (3)$$

$$\frac{d(y - y_{\infty} + y_{\infty})}{y - y_{\infty}} = -k\,dt \quad (4)$$

$$\frac{d(y - y_{\infty}) + y_{\infty}}{y - y_{\infty}} = -k\,dt \quad (5)$$

where $y = (y - y_{\infty}) + y_{\infty}$

$$dy = d(y - y_{\infty}) + dy_{\infty}$$

and dy_{∞} is a constant = 0

$$\frac{d(y - y_{\infty})}{y - y_{\infty}} = -k\,dt \quad (6)$$

integrate to obtain

$$\ln(y - y_{\infty}) = -kt + C \quad (7)$$

At t = 0 and y = y_o,

$$\ln(y - y_{\infty}) = -kt + \ln(y_0 - y_{\infty}) \quad (8)$$

$$\frac{y - y_{\infty}}{y_o - y_{\infty}} = e^{(-kt)} \quad (9)$$

solve for y in equation (9) to finally obtain

$$y \;?\; y_{?} \;?\; (y_{0} \;?\; y_{?})e^{?kt} \quad (10)$$

APPENDIX C

CHEMICAL ANALYSIS OF THE PCT TEST SOLUTIONS FOR HYDROCERAMIC MIXEI SIMULATED ZIRCONIA CALCINE HIGH-LEVEL RADIOACTIVE WASTI

mg/L	Reference 25°C	1 Hr	4 Hrs	9 Hrs	20 Hrs	48 Hrs	72 Hrs	145 Hrs	216 Hrs	301 Hrs	336 Hrs	38 Hr
AI	700	160	135	125	120	67	80	66	60	25.7	35	18.
B	165	90	95	95	90	90	90	85	90	85	80	75
Ca	1.37	0.32	0.30	2.52	2.49	1.74	2.98	3.41	2.18	1.92	2.09	1.1
Cr	125	37	38	36	34	37	36	36	36	36	35	37
Cs	15	6.70	4.90	5.20	3.40	2.20	1.90	1.60	<0.2	<0.2	<0.2	0.6
Fe	<0.02	0.92	0.51	0.48	0.290	0.12	0.27	0.59	N/A	N/A	N/A	N/A
K	75	10.10	10.60	10.40	9.50	9.50	9.60	8.40	7.10	8.10	7.80	10.
Mg	0.02	<0.02	<0.02	0.12	0.13	0.12	0.22	0.22	0.12	0.05	0.11	0.0
Na	3100	1860	1680	1410	1290	1200	1110	1100	1060	1060	1040	960
Si	10.10	2.44	1.63	3.57	3.10	1.39	2.97	2.73	2.91	2.84	2.95	1.6
Sr	0.04	<0.02	<0.02	0.06	0.06	0.04	0.06	0.07	0.04	0.04	0.04	0.0
F	62	120	95	100	125	110	105	100	85	85	80	80
Cl	95	43	44	42	40	42	42	40	42	40	39	42
NO2	4.70	2.10	1.80	1.60	0.50	0.50	0.60	0.70	0.5	0.5	0.40	0.9
NO^-_3	1130	115	120	115	115	120	115	115	115	115	110	110
PO_4^{3-}	<0.1	<0.1	<0.1	<0.1	<0.1	<0.1	<0.1	<0.1	<0.1	<0.1	<0.1	<0.
SO_4^{2-}	480	1040	1240	1110	1160	1180	1040	1080	1050	1060	1060	960

Table 4.1. Concentration of the major species in the 24-hour PCT test solution at va Hydroceramic with 30 weight percent solid waste loading of zirconia calcine simulated radioact 75°C.

Mg/L	Reference 25°C	1 Hr	4 Hr	12 Hrs	24 Hrs	48 Hrs	72 Hrs	144 Hrs	216 Hrs	288 Hrs	366 Hrs	
Al	700	110	105	80	75	58	70	44	23.40	28.90	22.80	2
B	165	100	100	95	90	85	85	80	80	66	75	7
Ca	1.37	1.77	0.31	1.42	2.27	2.40	3.29	3.303	2.74	2.26	2.47	3
Cr	125	45	46	43	42	39	37	38	35	29.20	32	3
Cs	15	3.40	5.10	3.30	1.10	1.60	0.60	<0.20	<0.20	<0.20	<0.20	<
Fe	<0.02	0.18	0.05	0.03	0.03	0.04	0.03	0.03	0.04	0.02	0.03	0
K	75	10.50	11.60	10.80	9.50	8.90	9.10	8.90	7.90	6.0	6.6	6
Mg	0.02	0.07	0.04	0.10	0.08	0.09	0.20	0.13	0.21	0.41	0.23	0
Na	3100	1470	1410	1160	1110	1030	890	860	810	690	770	7
Si	10.10	4.50	1.41	1.24	1.58	1.50	2.93	2.82	2.20	3.01	2.55	2
Sr	0.04	0.04	<0.02	0.03	0.04	0.04	0.05	0.05	0.05	0.04	0.04	0
Zr	N/A	<0.02	<0.02	<0.02	<0.02	0.09	0.07	0.09	0.11	0.06	0.08	0
F	62	160	125	110	100	95	90	85	105	100	110	1
CI	95	43	43	41	43	40	39	41	40	35	39	4
NO_2	4.70	0.040	0.50	0.60	0.60	0.50	2.10	0.60	0.50	0.40	0.50	0
NO^-_3	1130	120	120	115	120	115	105	115	110	90	105	1
$PO^{-3}4$	<0.1	<0.01	<0.01	<0.01	<0.01	<0.01	<0.01	<0.01	<0.01	<0.01	<0.01	<
SO^{-2}_4	480	1070	1070	980	980	950	850	930	1050	870	1030	1

Table 4.2. Concentration of the major species in the 24-hour PCT test-solution at various processi with 30 weight percent solid waste loading of zirconia calcine simulated radioactive waste synthesized a

Mg/L	Reference 25°C	4 Hr	8 Hrs	12 Hrs	18 Hrs	36 Hrs	40 Hrs	64 Hrs	88 Hrs	352 Hrs	540 Hrs
Al	700	130	120	95	90	85	70	48	41	12	15.5
B	165	90	95	90	90	90	90	85	75	58	63
Ca	1.37	0.85	1.26	0.55	1.20	1.27	1.17	1.42	1.35	1.50	1.40
Cr	125	39	37	34	39	35	35	37	34	26.90	30
Cs	15	<0.02	<0.02	<0.02	<0.02	<0.02	<0.02	<0.02	<0.02	<0.02	<0.0
K	75	10.70	8.80	10.4	10.80	9.50	9.10	9.50	7.60	5.2	5.4
Mg	0.02	0.11	0.19	0.05	0.17	0.08	0.08	0.11	0.15	0.16	0.17
Na	3100	1200	1090	1000	1000	970	920	860	7.40	530	640
Si	10.10	3.03	3.38	4.61	3.56	3.17	3.43	3.61	3.60	3.03	2.62
Sr	0.04	0.02	0.03	<0.02	0.03	0.04	0.03	0.04	0.04	0.09	0.05
F	62	110	105	105	105	105	105	105	105	100	100
CI	95	45	44	41	42	42	41	45	44	42	43
NO_2	4.70	1.10	1	1.20	1.10	1	1.1	1.80	1.2	1.70	1.70
NO^-_3	1130	125	120	120	120	115	115	115	105	90	95
$PO^{-3}4$	<0.1	<0.1	<0.1	<0.1	<0.1	<0.1	<0.1	<0.1	<0.1	<0.1	<0.1
SO^{-2}_4	480	880	710	690	700	700	690	720	630	470	540

Table 4.3. Concentration of the major species in the 24-hour PCT test-solution at va Hydroceramic with 30 weight percent solid waste loading of zirconia calcine simulated radioact 95°C.

Mg/L	Reference 25°C	2 Hr	7.5 Hrs	13 Hrs	19 Hrs	24 Hrs	36 Hrs	48 Hrs	60 Hrs	72 Hrs	84 Hrs
Al	700	45	14	7.20	9.70	9.1	8.90	8.50	8.30	8.90	7.10
B	165	54	44	40	42	38	38	40	40	38	42
Ca	1.37	0.14	0.26	0.19	0.31	0.71	0.53	0.84	0.18	0.53	0.49
Cr	125	37	35	29.60	31	25.80	24.90	17.40	14.70	11.8	11.5
Cs	15	<0.2	<0.2	<0.2	<0.2	<0.2	<0.2	<0.2	<0.2	<0.2	<0.2
K	75	4.60	3.02	2.65	2.78	2.31	2.15	2.21	2.09	1.91	2.11
Mg	0.02	0.05	0.11	0.06	0.07	0.13	0.12	0.12	0.02	0.10	0.11
Na	3100	630	440	370	380	330	320	330	320	310	350
Si	10.10	1.36	1.0	1.29	3.55	3.81	3.11	4.40	2.43	5.10	3.26
Sr	0.04	<0.02	<0.02	<0.02	<0.02	0.03	0.03	0.05	<0.02	0.03	0.02
F	62	100	105	105	105	95	90	90	85	90	95
CI	95	47	48	44	46	42	46	45	46	47	46
NO_2	4.70	0.60	0.70	0.60	0.60	0.50	0.30	0.30	0.40	0.40	0.40
NO^-_3	1130	90	80	70	75	70	70	75	75	70	75
$PO^{-3}4$	<0.1	<0.1	<0.1	<0.1	<0.1	<0.1	<0.1	<0.1	<0.1	<0.1	<0.1
SO^{-2}_4	480	270	110	105	105	95	90	150	145	95	150

Table 4.4. Concentration of the major species in the 24-hour PCT test-solution at va Hydroceramic with 30 weight percent solid waste loading of zirconia calcine simulated radioact 125°C.

Mg/L	Reference 25°C	1 Hr	2 Hrs	4 Hrs	7 Hrs	9.5 Hrs	12 Hrs	24 Hrs	36.5 Hrs	48 Hrs	60 Hrs	72 Hrs
Al	700	11.70	7.50	20.60	6.50	6.20	5.60	14.20	17.50	12.20	12.20	11.60
B	165	36	33	36	37	30	32	32	31	31	33	33
Ca	1.37	0.31	0.60	0.15	0.67	0.38	0.08	0.90	1.97	1.74	1.43	1.08
Cd	N/A	<0.02	<0.02	<0.02	<0.02	<0.02	<0.02	<0.02	<0.02	<0.02	<0.02	<0.02
Cr	125	31	21.60	28.40	21.30	7.80	10	4.30	1.50	0.17	0.13	0.08
Cs	15	<0.2	<0.2	<0.2	<0.2	<0.2	<0.2	<0.2	<0.2	<0.2	<0.2	<0.2
Fe	<0.02	<0.02	<0.02	0.04	0.08	0.87	0.56	0.49	0.56	0.38	0.31	0.32
K	75	3.10	2.20	2.50	2.16	1.75	1.89	1.73	1.60	1.42	1.08	1.46
Mg	0.02	0.11	0.26	0.18	o.o8	0.29	0.07	0.14	0.27	0.44	0.24	0.15
Na	3100	380	330	370	340	285	290	280	270	235	240	250
Si	10.10	2.58	3.39	0.80	5	1.83	1.36	5.70	11.30	11	7.80	8.30
Sr	0.04	<0.02	0.02	<0.02	0.05	<0.02	<0.02	0.07	0.15	0.11	0.10	0.09
Zr	N/A	0.08	<0.02	<0.02	<0.02	0.44	0.03	<0.02	<0.02	<0.02	<0.02	<0.02
F	62	125	120	125	125	105	105	105	105	95	90	90
CI	95	51	56	56	48	47	49	49	45	43	46	44
NO_2	4.70	0.40	1	0.3	0.20	0.20	0.20	0.30	0.8	0.30	0.10	0.20
NO^-_3	1130	75	75	75	75	70	70	70	65	67	70	70
$PO^{-3}4$	<0.1	<0.1	<0.1	<0.1	<0.1	<0.1	<0.1	<0.1	<0.1	<0.1	<0.1	<0.1
SO^{-2}_4	480	39	27.50	38	40	22.90	23.40	28.50	30	48	57	68

Table 4.5. Concentration of the major species in the 24 -hour PCT test-solution at various processi with 30 weight percent solid waste loading of zirconia calcine simulated radioactive waste synthesized a

Table

Mg/L	Reference 25°C	8 Hr	10.5 Hr	12 Hrs	18 Hrs	24 Hrs	36 Hrs	48 Hrs	60 Hrs	72 Hrs
Al	700	6.20	5.10	6.80	6.20	8.90	6.10	6.40	7.50	7
B	165	30	31	29.30	29.10	29.70	28	28.10	26.20	26.90
Ca	1.37	1.51	0.48	1.67	1.31	1.60	1.27	1.41	1.42	1.66
Cr	125	0.20	0.26	0.20	0.19	0.18	0.17	0.16	0.16	0.15
Cs	15	<0.2	<0.2	<0.2	<0.2	<0.2	<0.2	<0.2	<0.2	<0.2
K	75	1.27	1.26	1.27	1.18	1.20	1.18	1.20	1.07	1.08
Mg	0.02	0.21	0.13	0.22	0.18	0.30	0.18	0.21	0.21	0.22
Na	3100	210	215	195	200	215	215	230	230	235
Si	10.10	9.30	3.70	10.20	9.70	10	8.60	9.90	9.30	9.40
Sr	0.04	0.12	0.03	0.13	0.11	0.12	0.11	0.12	0.12	0.13
F	62	80	85	85	75	75	75	75	75	75
CI	95	48	46	46	46	45	45	45	46	45
NO_2	4.70	0.30	0.70	0.80	0.80	0.90	0.60	0.80	0.70	0.40
NO^-_3	1130	70	67	69	70	69	70	70	75	70
$PO^{-3}4$	<0.1	<0.1	<0.1	<0.1	<0.1	<0.1	<0.1	<0.1	<0.1	<0.1
SO^{-2}_4	480	38	30	36	48	62	80	90	95	90

Concentration of the major species in the 24 -hour PCT test-solution at various processi
with 30 weight percent solid waste loading of zirconia calcine simulated radioactive waste synth

Mg/L	Reference 25°C	4 Hr	6 Hr	8 Hrs	10 Hrs	14.5 Hrs	18 Hrs	24 Hrs	36 Hrs	48 Hrs	60 Hrs	72 Hrs	96 Hr
Al	700	9.50	10.10	8.70	2.34	8.60	10.30	10.20	10.10	10.80	10.90	11.20	4.5
B	165	31	31	29.40	30	31	31	33	35	36	35	37	37
Ca	1.37	0.66	2.20	0.85	0.23	0.96	0.88	1.24	1.15	1.06	1.12	0.90	0.1
Cr	125	0.21	0.32	0.13	0.16	0.14	0.14	0.15	0.13	0.09	0.08	0.07	0.0
Cs	15	<0.2	<0.2	<0.2	<0.2	<0.2	<0.2	<0.2	<0.2	<0.2	<0.2	<0.2	<0.
K	75	1.05	1.20	1.03	0.85	1.14	1.12	1	0.87	0.86	0.89	0.77	0.6
Mg	0.02	0.07	0.11	0.10	<0.20	0.10	0.08	0.11	0.08	0.09	0.11	0.06	0.0
Na	3100	210	230	390	220	250	260	260	280	280	285	290	27(
Si	10.10	7.80	7.80	8.10	5.40	8.70	8.90	9.40	7.90	7.20	7.40	7.10	4.2
Sr	0.04	0.06	0.06	0.06	<0.02	0.07	0.08	0.10	0.09	0.07	0.08	0.07	0.0
F	62	75	80	85	85	90	85	85	85	85	80	80	80
CI	95	49	45	41	40	41	41	41	41	43	42	43	43
NO_2	4.70	0.60	0.20	1.10	0.20	0.40	0.80	0.40	0.60	0.50	0.40	0.80	0.2
NO^-_3	1130	75	75	70	70	75	75	75	75	80	75	75	80
$PO^{-3}4$	<0.1	<0.1	<0.1	<0.1	<0.1	<0.1	<0.1	<0.1	<0.1	<0.1	<0.1	<0.1	<0.
SO^{-2}_4	480	38	53	59	66	80	80	90	100	100	100	100	100

Table 4.7. Concentration of the major species in the 24-hour PCT test-solution at various processin with 30 weight percent solid waste loading of zirconia calcine simulated radioactive waste synthesized a

APPENDIX D

CHEMICAL ANALYSIS OF THE PCT TEST SOLUTIONS FOR HYDROCERAMIC MIXEI SIMULATED FLUORINEL BLEND CALCINE HIGH-LEVEL RADIOACTIVE W

mg/L	Reference 25°C	1 Hr	5.5 Hrs	10 Hrs	17 Hrs	36 Hrs	76 Hrs	106.5 Hrs	228 Hrs	288 Hrs	359 Hrs	4 H
Al	1850	630	49	54	43	39	29.2	26.7	24.4	25.3	30	20
B	145	75	64	63	60	58	54	53	54	54	55	55
Ca	4.20	5.2	1.33	1.84	1.70	1.70	1.15	1.21	1.60	1.83	4.13	1.
Cd	<0.02	0.2	0.05	0.06	0.05	0.07	0.03	0.03	0.07	0.06	0.33	0.
Cr	155	75	75	70	67	67	63	60	45	63	63	63
Cs	42	10.1	3.9	3.3	2.6	2.4	2.7	1.8	1.4	1.3	4.3	2.
Fe	1.36	0.51	<0.02	0.03	0.04	0.03	<0.02	<0.02	0.06	0.28	0.51	0.
K	175	33	20.4	12.8	13.1	12.9	10.6	11.1	10.1	11.2	14.1	11
Mg	0.09	0.25	0.09	0.11	0.10	0.10	0.08	0.09	0.10	0.10	0.31	0.
Na	3900	1500	850	650	570	620	410	470	480	460	480	47
Si	24.2	10.4	3.06	3.90	3.17	2.88	2.53	2.78	4.10	4.50	9.20	2.
Sr	0.26	0.11	0.04	0.04	0.04	0.04	0.03	0.03	0.04	0.04	0.12	0.
Zr	0.06	<0.05	<0.05	0.15	0.07	0.24	0.26	0.37	0.38	0.39	1.71	0.
NO^-_3	1310	630	590	540	530	480	440	450	490	470	480	48
SO_4^{2-}	215	770	630	540	460	350	290	320	400	380	420	40

Table 5.1. Concentrations of the major species in the PCT test solutions conducted at 90 °C for 24 host mixed with 30 weight percent solid waste loading of fluorinel blend calcined simulated radioactiv synthesized at 75°C.

Mg/L	Reference 25°C	1 Hr	4 Hrs	8 Hrs	20 Hrs	38 Hrs	72 Hrs	120 Hrs	163 Hrs	242 Hrs	292 Hrs	3 H
Al	1850	520	105	85	75	67	57	42	43	24	25.5	1
B	145	155	115	110	110	110	110	100	95	85	85	8
Ca	4.2	0.68	1.90	1.23	1.16	0.98	0.67	0.53	0.49	0.55	0.91	0
Cd	<0.02	0.08	0.20	0.02	<0.02	0.11	0.04	0.05	<0.02	<0.02	<0.02	<
Cr	155	125	125	125	125	120	115	120	120	120	120	1
Cs	42	14.8	9.4	8.3	5.6	6.7	6.9	3.3	5.90	4.50	4.70	3
Fe	1.36	0.14	0.04	<0.02	<0.02	0.13	0.04	0.04	0.03	<0.02	<0.02	<
K	175	45	32	26.9	24.1	22.9	21.0	17.8	15.1	13.6	14.2	1
Mg	0.09	0.02	0.08	0.13	0.04	<0.02	<0.02	<0.02	<0.02	0.04	0.10	0
Na	3900	2140	1400	1200	1110	1080	920	800	800	750	790	7
Si	24.20	4.8	4.5	2.88	2.41	2.02	1.53	1.72	2.31	2.88	3.41	3
Sr	0.26	<0.02	0.03	<0.02	<0.02	<0.02	<0.02	<0.02	<0.02	<0.02	<0.02	<
Zr	0.06	<0.05	0.04	0.61	0.47	0.87	0.82	0.55	0.41	0.44	0.61	0
F	0.74	48	95	85	75	75	75	75	75	80	80	7
CI	40	115	105	105	115	105	105	105	100	100	100	1
NO_2	0.90	2.2	1.8	1.9	1.8	1.6	1.6	1.8	1.6	1.9	1.6	1
NO^-_3	1310	870	790	770	730	710	700	670	600	550	560	5
$PO^{-3}4$	<0.1	<0.2	<0.2	<0.2	<0.2	<0.2	<0.2	<0.2	<0.2	<0.2	<0.2	<
SO^{-2}_4	215	225	155	125	95	90	100	66	44	30	45	4

Table 5.2. Concentrations of the major species in the PCT test solutions conducted at 90 °C for 24 host mixed with 30 weight percent solid waste loading of fluorinel blend calcined simulated radioacti synthesized at 85°C.

Mg/L	Reference 25°C	1 Hr	4 Hrs	8 Hrs	24 Hrs	37 Hrs	72 Hrs	110 Hrs	168 Hrs	221 Hrs	336 Hrs	3 H
Al	1850	120	115	100	58	46	41	27.70	22.40	23.10	22.20	1
B	145	120	120	115	90	100	85	85	80	80	80	8
Ca	4.2	0.97	0.57	0.73	0.36	0.40	0.22	0.38	0.25	0.23	0.24	0
Cd	<0.02	0.02	<0.02	<0.02	<0.02	<0.02	<0.02	<0.02	0.04	<0.02	0.02	<
Cr	155	120	115	120	115	115	105	110	105	105	105	9
Cs	42	10.9	8.1	5.4	4.2	5.1	4.1	3.0	2.90	3.90	4.40	2
Fe	1.36	<0.02	<0.02	<0.02	<0.02	<0.02	<0.02	<0.02	<0.02	<0.02	<0.02	<
K	175	37	28.2	26.4	19.8	20.90	17.60	15.20	15.10	15.40	13.50	1
Mg	0.09	0.04	<0.02	<0.02	<0.02	<0.02	<0.02	<0.02	<0.02	<0.02	<0.02	<
Na	3900	1530	1120	1010	720	770	700	690	610	610	610	6
Si	24.20	3.44	2.03	2.21	2.51	1.69	2.13	2.95	1.90	1.80	1.98	1
Sr	0.26	<0.02	<0.02	<0.02	<0.02	<0.02	<0.02	<0.02	<0.02	<0.02	<0.02	<
Zr	0.06	0.49	0.43	0.43	0.13	<0.05	<0.05	<0.05	0.07	0.05	<0.05	0
F	0.74	140	115	110	105	105	110	105	100	100	100	9
CI	40	120	105	105	105	100	95	100	95	95	95	9
NO_2	0.90	2.20	1.8	2.3	1.8	5.4	1.8	2.3	1.80	1.90	1.90	1
NO^-_3	1310	770	670	660	470	570	420	460	450	450	460	4
$PO^{-3}4$	<0.1	<0.02	<0.02	<0.02	<0.02	<0.02	<0.02	<0.02	<0.02	<0.02	<0.02	<
SO^{-2}_4	215	130	55	49	7.0	21.6	6.9	8.1	9.5	9.80	11	2

Table 5.3. Concentrations of the major species in the PCT test solutions conducted at Hydroceramic host mixed with 30 weight percent solid waste loading of fluorinel blend calcin waste hydrothermally synthesized at 95°C.

Mg/L	Reference 25°C	1 Hr	4 Hrs	14 Hrs	48 Hrs	72 Hrs	96 Hrs	142 Hrs	164 Hrs	188 Hrs	202 Hrs	262 Hrs
Al	1850	110	51	28.40	36	34	22.50	36	27.70	7.50	19.60	8.10
B	145	100	85	66	53	45	49	52	47	43	47	48
Ca	4.2	1.07	0.39	0.46	0.73	0.37	0.46	1.17	0.66	0.59	1.25	0.81
Cd	<0.02	0.03	0.03	0.13	<0.02	0.26	0.17	<0.02	0.05	0.09	<0.02	<0.02
Cr	155	130	120	110	100	105	105	105	110	95	100	105
Cs	42	3.10	<0.2	<0.2	<0.2	<0.2	<0.2	<0.2	<0.2	<0.2	<0.2	<0.2
Fe	1.36	<0.02	<0.02	0.18	<0.02	0.18	0.14	0.08	0.09	0.09	0.09	<0.02
K	175	35	27.70	19.10	14	13.60	11.90	11.90	10.70	9.80	8	9
Mg	0.09	0.08	0.04	0.13	0.17	0.09	0.23	0.13	0.09	0.15	0.32	0.41
Na	3900	900	740	560	460	510	390	370	370	310	350	350
Si	24.20	4.20	1.60	1.94	4.30	2.45	2.49	6.70	4.30	2.50	5.10	3.19
Sr	0.26	<0.02	<0.02	<0.02	<0.02	<0.02	<0.02	0.04	<0.02	<0.02	0.02	<0.02
Zr	0.06	o.18	0.14	0.21	0.29	0.37	0.35	0.29	0.25	0.23	0.28	0.27
F	0.74	75	54	52	53	53	54	52	47	42	41	42
CI	40	95	105	95	90	85	90	85	100	85	85	85
NO_2	0.90	3.80	3.20	2.80	2.50	2	2.30	2.10	2.10	1.80	1.80	1.90
NO^-_3	1310	640	440	360	300	275	290	300	320	300	330	340
$PO^{-3}4$	<0.1	<0. 1	<0. 1	<0. 1	<0. 1	<0. 1	<0. 1	<0. 1	<0. 1	<0. 1	<0. 1	<0. 1
SO^{-2}_4	215	14.30	7.10	4.90	4.50	4.70	5.10	5	4.80	4.90	5	5.90

Table 5.4. Concentrations of the major species in the PCT test solutions conducted at Hydroceramic host mixed with 30 weight percent solid waste loading of fluorinel blend calcin waste hydrothermally synthesized at 125°C.

Mg/L	Reference 25°C	1 Hr	2 Hrs	6 Hrs	9 Hrs	13.5 Hrs	18 Hrs	24 Hrs	31 Hrs	48 Hrs	65 Hrs	75 Hrs
Al	1850	62	47	41	35	22.4	25	17.70	16.80	9.10	17.80	17.60
B	145	59	53	53	52	50	47	39	38	38	40	38
Ca	4.2	0.97	0.59	0.46	0.65	0.26	0.78	1.06	1.15	1.10	1.59	1.34
Cd	<0.02	0.02	<0.02	0.02	<0.02	0.04	<0.02	<0.02	<0.02	0.17	0.03	0.02
Cr	155	110	110	105	95	110	100	90	85	75	75	58
Cs	42	<0.02	<0.02	<0.02	<0.02	<0.02	<0.02	<0.02	<0.02	<0.02	<0.02	<0.02
Fe	1.36	<0.02	<0.02	<0.02	<0.02	<0.02	<0.02	<0.02	0.02	0.23	0.06	0.09
K	175	20.50	18	15.60	13.90	12.10	10.40	8.30	7.30	7.20	6.80	5.70
Mg	0.09	0.10	0.05	0.04	0.08	0.04	0.07	0.19	0.15	0.33	0.51	0.16
Na	3900	600	540	510	470	440	410	360	350	350	360	340
Si	24.20	5.20	4.40	4.20	4.20	3	5.30	5.60	6.20	3.71	6.30	7.10
Sr	0.26	0.02	<0.02	<0.02	<0.02	<0.02	0.03	0.03	0.04	0.02	0.04	0.04
Zr	0.06	<0.05	<0.05	<0.05	<0.05	<0.05	<0.05	<0.05	<0.05	0.25	<0.05	<0.05
F	0.74	57	55	54	53	54	51	49	49	51	48	48
CI	40	95	95	95	85	85	85	85	85	85	85	85
NO_2	0.90	2.30	2	1.90	1.70	1.50	1.10	0.90	0.90	0.70	0.80	0.70
NO^-_3	1310	370	370	390	370	370	350	330	340	340	350	340
$PO^{-3}4$	<0.1	<0.10	<0.10	<0.10	<0.10	<0.10	<0.10	<0.10	<0.10	<0.10	<0.10	<0.10
SO^{-2}_4	215	4.80	4.50	4.10	5.30	4.80	5.10	5.30	6.30	8.30	0.60	8.60

Table 4.5. Concentrations of the major species in the PCT test solutions conducted at Hydroceramic host mixed with 30 weight percent solid waste loading of fluorinel blend calcin waste hydrothermally synthesized at 150°C.

Mg/L	Reference 25°C	0.5 Hr	1 Hr	6 Hrs	9 Hrs	12 Hrs	18 Hrs	24 Hrs	36 Hrs	48 Hrs	60 Hrs	72 Hrs	84 Hrs
Al	1850	39	26.10	9.60	9.30	8.90	6.90	7.90	9.90	15.30	15.30	21.50	14.60
B	145	52	47	34	31	32	34	34	35	40	43	44	41
Ca	4.2	0.34	0.15	0.39	0.36	0.33	0.40	0.36	2.73	0.46	0.37	0.41	0.44
Cd	<0.02	0.05	0.09	0.10	0.07	0.05	0.05	0.05	0.03	0.06	0.03	0.06	0.04
Cr	155	80	59	1.12	0.98	0.86	0.70	0.72	1.14	0.59	0.53	0.46	0.49
Cs	42	4.1	4.7	1.20	4.20	2.70	0.60	1.40	2.80	2.70	1.40	2.30	2.80
Fe	1.36	<0.02	0.02	<0.02	<0.02	0.06	0.05	0.07	<0.02	0.08	0.05	<0.02	<0.02
K	175	12.30	10.60	5.30	4.70	4.70	3.88	4.60	4.80	4.70	3.73	3.83	3.27
Mg	0.09	<0.02	0.03	0.03	0.04	0.04	0.06	0.04	0.09	0.04	0.03	0.04	0.04
Na	3900	510	460	285	275	280	290	295	300	340	340	350	340
Si	24.20	3.91	0.81	5.0	4.20	5.30	5.30	5.5	2.47	5.50	4.80	3.90	4.80
Sr	0.26	<0.02	<0.02	<0.02	<0.02	<0.02	<0.02	<0.02	<0.02	<0.02	<0.02	<0.02	<0.02
Zr	0.06	0.46	0.56	0.55	0.53	1.03	0.71	0.67	0.44	0.82	0.71	<0.05	<0.05
F	0.74	80	80	65	59	62	63	63	65	66	66	68	66
CI	40	80	80	68	68	68	65	67	68	69	67	69	69
NO_2	0.90	1.20	0.50	0.50	0.80	2.1	0.50	0.40	0.30	0.30	0.50	0.50	0.50
NO^-_3	1310	290	285	260	255	265	270	280	295	320	320	330	320
$PO^{-3}4$	<0.1	<0.02	<0.02	<0.02	<0.02	<0.02	<0.02	<0.02	<0.02	<0.02	<0.02	<0.02	<0.02
SO^{-2}_4	215	0.3	4.0	4.8	4.90	6.0	6.20	6.60	10.3	9.60	10.60	10.30	9.70

Table 5.6. Concentrations of the major species in the PCT test solutions conducted at Hydroceramic host mixed with 30 weight percent solid waste loading of fluorinel blend calcine waste hydrothermally synthesized at 175°C.

Mg/L	Reference 25°C	1 Hr	9 Hrs	12 Hrs	24 Hrs	48 Hrs	72 Hrs	96 Hrs	110 Hrs
Al	1850	66	33	49	30	28.50	39	34	36
B	145	42	38	28	44	47	64	65	69
Ca	4.2	2.37	1.60	1.70	1.26	1.17	1.19	0.70	0.72
Cd	<0.02	0.41	0.32	0.41	0.20	0.18	0.21	0.11	0.12
Cr	155	12.10	1.94	1.15	0.71	0.58	0.57	0.57	0.58
Cs	42	<0.2	<0.2	<0.2	<0.2	<0.2	<0.2	<0.2	<0.2
K	1.36	10.60	7.30	4.60	5.30	5	4.60	4.9	5.20
Mg	175	0.23	0.15	0.19	0.13	<0.02	0.15	0.10	0.12
Na	3900	410	320	250	360	360	420	440	450
Si	24.20	14.30	7	8.70	10.40	7.40	6.40	5.70	4.80
Sr	0.26	0.09	0.04	0.07	0.05	0.04	0.04	0.02	<0.02
F	0.74	58	52	53	49	47	53	55	56
CI	40	75	68	50	70	70	70	75	70
NO_2	0.9	0.9	0.40	0.40	0.40	0.3	0.20	0.40	0.2
NO^-_3	1310	280	280	190	320	320	340	350	340
$PO^{-3}4$	<0.1	<0.1	<0.1	<0.1	<0.1	<0.1	<0.1	<0.1	<0.1
SO^{-2}_4	215	5.60	7.60	5.70	11.20	11	16.60	19.10	21.40

Table 5.7. Concentrations of the major species in the PCT test solutions conducted at Hydroceramic host mixed with 30 weight percent solid waste loading of fluorinel blend calcin waste hydrothermally synthesized at 200°C.

APPENDIX E

BIBLIOGRAPHY OF VITRIFIABLE, HYDROCERAMIC CBC WASTE FORM

Johnson Olanrewaju, Barry Scheetz, Michael W. Grutzeck and Daryl D. Siemer, (2001) Hydration kinetics of hydroceramic waste form as a host for the INEEL calcined high-level radioactive waste. American Chemical Society, Division of Nuclear Chemistry and Technology, 222nd ACS National Meeting Chicago, IL, August 26-30.

Naveen Krishnamurthy, Johnson Olanrewaju, Michael W. Grutzeck, Stephen Kwan, Daryl D. Siemer and Barry E. Scheetz, (2001) Hydroceramic Waste Forms: An alternate to Glass for SBW. American Chemical Society, Division of Nuclear Chemistry and Technology, 222nd ACS National Meeting Chicago, IL, August 26-30.

Barry E. Scheetz, Michael W. Grutzeck, Johnson Olanrewaju and Darryl D. Siemer, (2000) Development of hydroceramic waste form. 8th International Conference on Nuclear Engineering, Baltimore, MD, April 2-6.

Siemer, D. D., J. Olanrewaju, B. Scheetz, N. Krishnamurthy and M. Grutzeck, (2000) Development of Hydroceramic Waste Forms. Ceramic Transactions proceedings, 2000 Amer. Ceram. Mtg. St. Loius, MO.

Siemer, D. D., J. Olanrewaju, B. Scheetz and M. Grutzeck, (2000) Development of Hydroceramic Waste Forms for INEEL Calcined Waste. Ceramic Transactions Proceedings, 2000 Amer. Ceram. Soc. Mtg. St. Louis, MO.

D. D.Siemer, M. W. Grutzeck and B. E. Scheetz, (1999) Comparison of Materials for making hydroceramic waste forms. Ceramic Transactions, vol. 93.

Siemer, D. D., M. L. D. Gougar, M. W. Grutzeck, D. M. Roy and B. E. Scheetz, (in Press) Preliminary Formulations Studies for a "Hydroceramic" Alternative Waste Form for INEEL HLW. American Nuclear Society.

Gougar, M. L. D., D. D. Siemer and B. E. Scheetz (1999) A novel Waste form for Disposal of Spent-Nuclear-Fuel Reprocessing Waste: A Vitrifiable Cement. Neclear Technology, vol. 125, No.1, 93-103.

Siemer, D. D., M. W. Grutzeck, D. M. Roy and B. E. Scheetz, (1998) Zeolite Waste Forms Synthesized from SBW and Metakaolinte. Waste Management '98, Tucson, AZ CD-ROM.

Gougar, M. L. D., (1997) A Vitrifiable Cement Waste Form for Disposal of Spent Nuclear Fuel Reprocessing Waste. MS Thesis in Environmental Pollution Control, The Pennsylvania State University, University Park, PA.

Michael W. Grutzeck and Darryl D. Siemer, (1997) Zeolites synthesized from Class F fly ash and sodium aluminate slurry, Journal of the American Ceramic Society, vol. 80, No. 9, 2449-2453.

Siemer, Darryl D., Barry E. Scheetz, CliffOrcutt and Mary Lou Gougar, (1996) Hot Isostatic Press (HIP) Vitrification of Radwaste Concretes. Glass as a Waste Form and Vitrification Technology: Summary of an International Workshop, National Academy Press, Washinton, D. C.

Gougar, M. L. D., Duane Siemer and Barry E. Scheetz, (1996) Vitrifiable Concrete for Disposal of Spent Nuclear Fuel Reprocessing Waste at I.N.E.L. Proceedings of the Embeded Topical Meeting on DOE Spent Nuclear Fuel and Fissile Material Management, American Nuclear Society, Reno, NV p. 359-366.

Siemer, D. D., Roy, D. M., Grutzeck, M. W., Gougar, M. L. D. and Scheetz, B. E., (1996) PCT Leach Tests of Isostatically Pressed (HIPped) Zeolitic Concretes. Proceedings of the Materials Research Society Annual Meeting Symposium II, Scientific Basis for Nuclear Waste Management XX.

Gougar, M. L. D., D. D. Siemer and B. E. Scheetz, (1995) Vitrifiable Concrete for Disposal of Spent Nuclear Fuel Reprocessing Waste at I. N. E. L. Proceedings of the Materials Research Society Annual Meeting Symposium on the Scientific Basis for Nuclear waste Management XIX.

Siemer, D. D., B. E. Scheetz and M. L. D. Gougar, (1995) Hot Isostatic Press (HIP) vitrification of Radwaste Concretes. Proceedings of the Materials Research Society Annual Meeting Symposium on the Scientific Basis for Nuclear Waste Management XIX.